

VALUE-ADDED PRODUCTS FROM CHICKEN FEATHER FIBERS AND PROTEIN

Except where reference is made to the work of others, the work described in dissertation is my own or was done in collaboration with my advisory committee. This thesis does not include proprietary or classified information.

Xiuling Fan

Certificate of Approval:

Peter Schwartz
Professor
Polymer and Fiber Engineering

Roy M. Broughton, Chair
Professor
Polymer and Fiber Engineering

Ann Beth Jenkins Presley
Associate Professor
Consumer Affairs

Yehia El Mogahzy
Professor
Polymer and Fiber Engineering

Joe F. Pittman
Interim Dean
Graduate School

VALUE-ADDED PRODUCTS FROM CHICKEN FEATHER FIBERS AND PROTEIN

Xiuling Fan

A Dissertation

Submitted to

the Graduate Faculty of

Auburn University

in Partial Fulfillment of the

Requirements for the

Degree of

Doctor of Philosophy

Auburn, Alabama

May 10, 2008

VALUE-ADDED PRODUCTS FROM CHICKEN FEATHER FIBERS AND PROTEIN

Xiuling Fan

Permission is granted to Auburn University to make copies of this dissertation at its discretion, upon the request of individuals or institutions and at their expense.
The author reserves all publication rights.

Signature of Author

Date of Graduation

VITA

Xiuling Fan, daughter of Zhengju Fan and Peilian Liu, was born on July 6, in Henan Province, People's Republic of China. She graduated from Wuhan Institute of Chemical Technology with a Bachelor of Engineering in Fine Chemical Engineering in 1993 and from Beijing University of Chemical Technology with a Master of Science in Polymer Materials in 1996. As she worked as a part-time researcher in Beijing University of Chemical Technology, China, she was employed as a lecturer for over 5 years in Beijing Leather Industry School, China. In January, 2002 she joined Ngee Ann Polytechnic, Singapore as a design & development officer. She entered the Graduate School at Chemical Engineering Department of Auburn University, in August, 2002, and in August, 2003, at Polymer and Fiber Engineering Department of Auburn University where she worked under the supervision of Dr. Roy M. Broughton. She married Yuhong Wang, son of Bangyin Wang and Youcong Shi.

DISSERTATION ABSTRACT

VALUE-ADDED PRODUCTS FROM CHICKEN FEATHER FIBERS AND PROTEIN

Xiuling Fan

Doctor of Philosophy, May 10, 2008
(M. S., Beijing University of Chemical Technology, 1996)
(B. A., Wuhan Institute of Chemical Technology, 1993)

274 Typed Pages

Directed by Roy M. Broughton

Worldwide poultry consumption has generated a huge amount of feather “waste” annually. Currently, the feather has a low value-being used for animal feed in the world.

The quality of fibrous air filters depend on their main component, fibers. The main physical structure of chicken feathers is barbs which can be used directly as fibers. They have small diameter, which makes them a good choice for air filtration. The main chemical structure of chicken feathers is structural fibrous protein, keratin. Therefore, chicken feathers could potentially be used for protein fiber production.

To obtain chicken feather fibers, barbs were stripped from the quills by a stripping device and separated with a blender. Some feather fibers were entangled with polyester staple fibers, and needlepunched to form a nonwoven fabric. Some feather fibers were blended with CelBond™ bi-component polyester as binder fibers, and pressed between two hot plates to produce thermobonded nonwovens. Whole chicken feathers were ground into powder and their keratin was reduced in water. The reduced keratin was salt precipitated, dried and dissolved in ionic liquid with/without bleach cotton.

The reduced chicken feather keratin ionic liquid solutions were spun into regenerated fibers through dry-jet wet spinning.

The needlepunched and thermobonded nonwovens were tested for filtration and other properties. With an increase of areal density and feather fiber composition, the air permeability of the needlepunched nonwovens decreased, and their filtration efficiency and pressure drop both increased. The case can be made that feather fibers gave fabrics better filtration at the same fabric weight, but at the expense of air permeability and pressure drop. The scrim and needlepunching process improved the filtration efficiency. Their strength depended on scrim. The hot-press process was very simple. The thermobonded nonwovens had very high air permeability. In them, there was also an inverse relation between air permeability and either pressure drop or filtration efficiency.

From these kinds of nonwovens, it is realized that feather fibers' fineness and the tree/fan-like structure of the feather does not offer a high level of performance advantages over conventional fibers. The use of feather fiber in air filtration applications must rely primarily on a favorable cost and weight differential in favor of the feather fiber.

Only after chicken feather keratin was reduced, could it dissolve well in ionic liquid. 100 % chicken feather keratin did not produce high tenacity fibers. Reduced chicken feather keratin and cellulose produced blend fibers with mechanical properties close to silk, cotton, and polyester fibers. Chemically reforming crosslinks might improve mechanical properties and the stability of the fibers to water and make them suitable for most fibrous applications. From this, it can be proposed that using chicken feathers for fiber production may be a good way to add value to chicken feather "waste".

ACKNOWLEDGEMENTS

The author Xiuling Fan would like to gratefully and sincerely thank to her advisor Dr. Roy M Broughton, for always providing the patient guidance, support, timely advice and encouragement throughout the whole graduate studies. He challenged and guided the author to a more independent thinking, and a deeper understanding of scientific work. The author also expresses her gratitude to the other members of her advisory committee, Dr. Peter Schwarz, Dr. Ann Beth Jenkins Presley, and Yehia El Mogahzy and outside reader, Dr. Hess for their interest, understanding and timely invaluable advice.

The author's appreciation also goes to Dr Gisela Buschle-Diller, David Clark, Dr. Fatma Kilinc-Balci, Steve Howard, Dr. Ramsis Farag and Jeff Thompson for their invaluable input on advice on experiments, or the setting up and operation of equipments. Bacteriological testing was done in the laboratory of Dr Robert Norton and by Kea Macklin. The friendship and support of Dr. Weijun Wang, Dr. Jaewoong Lee, David Branscomb, Dr. Guanglin Shen, Tom and Brenda Caring and many others are much appreciated and have led to many interesting and good-spirited discussions relating to this research.

Finally, and most importantly, the author would like to thank her husband Yuhong Wang for his unwavering love, understanding and quiet patience and encouragement during the author's studies. His support and encouragement was in the end what made this dissertation more smoothly.

Style manual or journal used THE ACS STYLE GUIDE: A MANUAL FOR AUTHORS
AND EDITORS

Computer software used MICROSOFT WORD 2003

TABLE OF CONTENTS

LIST OF FIGURES	xii
LIST OF TABLES	xvi
CHAPTER 1 INTRODUCTION AND LITERATURE REVIEW	1
1.1 Introduction.....	1
1.2 General information about chicken feathers.....	1
1.2.1 Chemical structure- keratin.....	3
1.2.2 Physical structure of feather fibers	7
1.2.3 Physical properties of feather fibers	8
1.2.4 Possible Applications of feather fibers	10
1.3 Extraction of feather keratin from chicken feathers	15
1.4 Review of air filters	17
1.4.1 Why use air filters.....	17
1.4.2 Filter media	19
1.4.3 Mechanism of air filtration in fabric filters.....	24
1.4.5 Evaluation of performance of air filters.....	27
1.4.6 Air filtration materials.....	36
1.4.7 Characterization of air filters	42
1.4.8 Filter media defects.....	44
1.4.9 Microorganism on air filters	46
1.4.10 Air filter market and trends.....	47
1.5 Reference	48
CHAPTER 2 PREPARATION OF FEATEHR FIBERS FOR USE IN FIBROUS PRODUCTS.....	58
2.1 Introduction.....	58
2.2 Equipments	59
2.2.1 Stripping machine	59
2.2.2 Blender	61
2.3 Experimental	62
2.3.1 Materials	62
2.3.2 Procedure	62
2.4 Results and Discussions.....	63
2.4.1 Bacterial testing results	63
2.4.2 Feather fiber (barb) separation.....	68
2.5 Conclusion	70
2.6 Reference	71

CHAPTER 3 NEEDLEPUNCHED NONWOVEN AIR FILTERS FROM CHICKEN FEATHER FIBERS	72
3.1 Introduction.....	72
3.2. Experimental.....	73
3.3.1 Materials	73
3.2.2 Equipment.....	73
3.3.3 Procedure to produce needlepunch nonwovens.....	77
3.3.4 Property testing of the needle punched nonwoven for filtration.....	79
3.4 Results and Discussion	79
3.4.1 Properties of first set of needlepunched nonwovens with thick scrim.....	79
3.4.2 Properties of needlepunched nonwovens produced by adjusted needle height and with new light scrim	87
3.5 Conclusion	135
3.6 Reference	137
CHAPTER 4 THERMOBONDED NONWOVEN AIR FILTERS FROM CHICKEN FEATEHR FIBERS	139
4.1 Introduction.....	139
4.2 Experimental.....	142
4.2.1 Preparation of thermobonded chicken feather fiber nonwovens	142
4.2.2 Property testing of the thermobonded nonwovens for filtration.....	144
4.3 Results and Discussion	145
4.3.1 Filtration properties of thermal bonded nonwovens	145
4.3.2 Tensile properties of thermal bonded nonwovens	150
4.4 Thermal bond nonwoven for heat transfer study	155
4.4.1 Manufacturing of thermal bonded nonwovens for heat transfer.....	155
4.4.2 Thermal conductivity of the thermal bonded nonwoven	155
4.5 Conclusion	157
4.6 Reference	158
CHAPTER 5 PRODUCTION OF REGENERATED CHICKEN FEATHER FIBER ...	159
5.1 Introduction.....	159
5.2 Dissolution of CF.....	163
5.2.1 Introduction.....	163
5.2.2 Experimental.....	168
5.2.3 Results and discussion	175
5.3 Production of Regenerated CF fiber	184
5.3.1 Introduction.....	184
5.3.2 Experiments	185
5.3.3 Results and Discussion	188
5.4 Conclusions.....	202
5.5 Reference	203
CHAPTER 6 PREDICTION OF AIR PERMEABILITY OF FEATHER FIBER NEEDLPUCHED NONWOVENS FOR AIR FILTRATION	206
6.1 Introduction.....	206
6.2. Analytical Models.....	206
6.3 Comparison with Experiments.....	208

6.4 Conclusion	216
6.5 Reference	216
CHAPTER 7 PREDICTION OF PENETRATION AND INITIAL FILTRATION	
EFFICIENCY OF FEATHER FIBER NONWOVENS FOR AIR FILTRATION	218
7.1 Introduction.....	218
7.2 Analytical model.....	219
7.2.1 Filtration including diffusion	219
7.2.2 Filtration including interception	221
7.2.3 Filtration including diffusion and interception	222
7.3 Calculation method and comparison with experiments.....	223
7.3.1 Known conditions of penetration measurement	223
7.3.2 Calculation of constants in the penetration equation	224
7.3.3 Calculation of penetration of CF nonwovens and comparison with Experiments	230
7.4 Conclusion	253
7.5 Reference	255

LIST OF FIGURES

Figure 1-1 Picture of feathers	3
Figure 1-2 β -keratin - the β -sheet twists gradually	4
Figure 1-3 β -sheet twists gradually.....	5
Figure 1-4 Schema of chicken feathers.....	7
Figure 1-5 Chicken feather keratin fiber structures (a) and its surface structure (b).....	8
Figure 1-6 Schematic representation for SDS–keratin complexes with a high amount of SDS added prior to dialysis	17
Figure 1-7 Sketch of punches density and depth of penetration of needlepunching	22
Figure 1-8 Different microfiltration membranes	23
Figure 1-9 Mechanism of air filtration.....	24
Figure 1-10: Cross sectional SEMs of a surface loaded media and a depth media	28
Figure 1-11 Comparison of laboratory test results to performance in real operating conditions of a synthetic filter	33
Figure 1-12 Cost breakdown of a class F7 filter.....	35
Figure 1-13 Nanofibers on a Cellulose Filter Media Substrate	41
Figure 1-14 Loading of submicron NaCl on a composite nanofiber structure	42
Figure 1-15 Media Characterization	44
Figure 1-16 Media Defects	45
Figure 2-1 Mechanism sketch of Stripping Machine.....	60
Figure 2-2 Blender sketch.....	61
Figure 2-3 Feather fibers.....	69
Figure 3-1 Mechanism sketch of Spinlab 338	74
Figure 3-2 Sketch of Vacuum box	75
Figure 3-3 Needlepunch process sketch	76
Figure 3-4 Needle Action – Schematic.....	76
Figure 3-5 Effect of areal density, mixed ratio and times of experiencing needlepunching process on air permeability (first set)	81
Figure 3-6 Filtration properties of needlepunched nonwovens (first set) compared to some commercial air filters.....	82

Figure 3-7 Relationship of air permeability with pressure drop and penetration of needle punched nonwovens (first set) compared to the commercial air filters	83
Figure 3-8 Tensile properties of needlepunched nonwovens (first set)	86
Figure 3-9 Effect of areal density and component on air permeability of new nonwovens	90
Figure 3-10 Effect of density and component on filtration efficiency of feather fiber nonwovens by adjusted needles and new scrim	98
Figure 3-11 Effect of areal density on filtration efficiency of needlepunched scrim layers nonwovens (Nd: 2/2)	99
Figure 3-12 Assumed efficiency straight line of needlepunched layers of scrim nonwovens to porosity	100
Figure 3-13 Effect of density and component on pressure drop of new feather fiber and scrim nonwovens compared to that of first set of nonwovens	103
Figure 3-14 Relationship of the pressure drop of new CF and scrim nonwovens to air Permeability	105
Figure 3-15 Relationship of filtration efficiency to air permeability of feather fiber nonwovens by adjusted needles & new scrim.....	105
Figure 3-16 Relationship of the filtration efficiency of new CF and scrim nonwovens to pressure drop.....	106
Figure 3-17 Effect of density and component on tensile strength of new CF needlepunched nonwovens and scrim layers (from 6 to 10 layers).....	107
Figure 3-18 Effect of density and component on tensile strength of feather fiber nonwovens and by adjusted needles & new scrim (Nd: 2/2).....	108
Figure 3-19 Effect of density and component on %strain at maximum load of scrim layers nonwovens and feather fiber nonwovens by adjusted needles & new scrim in both directions	109
Figure 3-20 Effect of needling density on air permeability of new CF nonwovens.....	112
Figure 3-21 Effect of composition of new CF nonwovens on the air permeability at different same needlepunching density.....	120
Figure 3-22 Effect of different needlepunching density on the filtration efficiency of new CF nonwoven	121
Figure 3-23 Filtration efficiency tendencies of new nonwovens at the same needlepunching density.....	122
Figure 3-24 Effects of needlepunching density on the pressure drop of new CF nonwovens	124

Figure 3-25 Effect of composition on the pressure drop of new CF nonwoven.....	125
Figure 3-26 Effects of areal density and needlepunching density on the thickness of new CF nonwovens.....	126
Figure 3-27 Effects of composition on the thickness of new CF nonwoven at different needlepunching density	128
Figure 3-28 Comparison of commercial air filters to needlepunched new CF nonwovens	129
Figure 3-29 Effects of needlepunching density on the maximum load of new CF Nonwovens	130
Figure 3-30 Effects of composition of new CF nonwovens on the maximum load at different needlepunching density	132
Figure 3-31 Comparison of maximum load of CF nonwovens with that of two layers of scrim and commercial air filter	133
Figure 3-32 Relationship between filtration efficiency and air permeability of new CF nonwovens	134
Figure 3-33 Relationship between filtration efficiency and pressure drop of new CF nonwovens at different needlepunching density.....	135
Figure 4-1 Mechanism sketch of hot pressing	144
Figure 4-2 Filtration property of the thermobonded nonwovens compared to some commercial air filters.....	147
Figure 4-3 Relationship between pressure drop and air permeability of the thermobonded nonwovens compared to the commercial air filters	148
Figure 4-4 Effect of the bonding time on the tensile property of the thermobonded nonwovens	151
Figure 4-5 Tensile property of CF thermal bond nonwovens (a, and b).....	152
Figure 4-6 Tensile property of CF thermal bond nonwovens.....	153
Figure 4-7 Thermal conductivity of thermal bond nonwoven	156
Figure 4-8 Thermal conductivity of thermal bond nonwovens	157
Figure 5-1 Breakage of disulfide bonds by reduction.....	160
Figure 5-2 Basic chemical structure of an ionic liquid	161
Figure 5-3 Chemical structure of BMIMCl	162
Figure 5-4 Diagram of production of regenerated CF fibers	163
Figure 5-5 Reducing disulfide bonds of CF keratin.....	164
Figure 5-6 Salt extraction diagram of protein.....	166
Figure 5-7 Breaking disulfide bonds of keratin during dissolving	167
Figure 5-8 Diagram of reducing process	170

Figure 5-9 Diagram of dissolving process	173
Figure 5-10 Sketch of SDS-PAGE	174
Figure 5-11 IL Solution of Reduced CF keratin	182
Figure 5-12 SDS-PAGE of precipitated reduced CF keratin in IL solution	183
Figure 5-13 Sketch of dry-jet wet spinning	185
Figure 5-14 Stepped godets	186
Figure 5-15 Effect of the extrusion rate on the tenacity of regenerated 100% reduced CF keratin fibers	189
Figure 5-16 Effect of cellulose content on the tenacity of regenerated CF fibers	191
Figure 5-17 Effect of draw-down on tenacity of regenerated CF fibers.....	197
Figure 5-18 Relationship of linear density to tenacity of regenerated CF keratin fibers	198
Figure 5-19 Regenerated 100% chicken feather fibers after different post treatment.....	199
Figure 5-20 CF and Cellulose blend fiber.....	200
Figure 7-1 Relationship of measured penetration to calculated penetration of CF nonwovens	252
Figure 7-2 Relationship of measured filtration efficiency to calculated filtration efficiency of CF Nonwovens	254

LIST OF TABLES

Table 1-1 Aminoacid content in keratin fiber from chicken feather	6
Table 1-2 Filter efficiency/application guidelines	32
Table 2-1 Bacteria recovered on feathers (Average count - CFU/g)	64
Table 2-2 Comparison of bacteria of commercials to feather products	67
Table 3-1 Experiment design for needlepunched nonwovens	78
Table 3-2 Air permeability of first set of needlepunched nonwovens	80
Table 3-3 Filtration properties of commercial air-filters	83
Table 3-4 Filtration properties of needlepunched nonwovens (first set, CF/PET 75/25)	84
Table 3-5 Tensile Properties of Needlepunched Nonwovens with thick scrim	85
Table 3-6 Filtration and tensile properties of new CF/PET 0/100 nonwovens	91
Table 3-7 Filtration and tensile properties of new CF/PET 33/67 nonwovens	92
Table 3-8 Filtration and tensile properties of new CF/PET 50/50 nonwovens	93
Table 3-9 Filtration and tensile properties of new CF/PET 67/33 nonwovens	94
Table 3-10 Filtration and tensile properties of new CF/PET 75/25 nonwovens	95
Table 3-11 Filtration and tensile properties of needlepunched scrim layers	96
Table 3-12 Filtration and tensile properties of new CF/PET 33/67 nonwovens needlepunched with Nd 4/4	113
Table 3-13 Filtration and tensile properties of new CF/PET 33/67 nonwovens needlepunched with Nd 1/1	114
Table 3-14 Filtration and tensile properties of new CF/PET 50/50 nonwovens needlepunched with Nd 4/4	115
Table 3-15 Filtration and tensile properties of new CF/PET 50/50 nonwovens needlepunched with Nd 1/1	116
Table 3-16 Filtration and tensile properties of new CF/PET 67/33 nonwovens needlepunched with Nd 4/4	117
Table 3-17 Filtration and tensile properties of new CF/PET 67/33 nonwovens needlepunched with Nd 1/1	118
Table 4-1 Filtration properties of thermal bond nonwovens in different density	145

Table 4-2 Filtration properties of thermal bond nonwovens in different Density	146
Table 4-3 Filtration properties of thermal bond nonwoven in different mix ratio(Control thickness: 1mm).....	149
Table 4-4 Filtration properties of thermal bonded nonwovens in different volumetric density.....	150
Table 4-5 Air permeability and tensile property of thermal bond nonwoven.....	154
Table 5-1 Recipe of dissolution of CF in 40g IL (Cellulose is bleached cotton)	172
Table 5-2 Effect of swelling time and stirring speed on production of reduced Keratin ready to spin.....	176
Table 5-3 Effect of reducing time on the production of reduced keratin.....	178
Table 5-4 Effect of reducing temperature on the production of reduced keratin.....	179
Table 5-5 Effect of urea concentration on the production of reduced keratin	180
Table 5-6 Mechanical properties of regenerated 100% CF keratin fibers	190
Table 5-7 Mechanical properties of regenerated CF keratin fibers (80%CF, 20%Cellulose, Cellulose/CF 1/4, extrusion solution Cellulose 1.5%, CF6%)	192
Table 5-8 Mechanical properties of regenerated CF keratin fibers (25%CF, 75%Cellulose, Cellulose/CF 1/3, extrusion solution Cellulose 1.6%, CF4.8%) ...	193
Table 5-9 Mechanical properties of regenerated CF keratin fibers (66.7%CF, 33.3%Cellulose, Cellulose/CF 1/2, extrusion solution Cellulose 1.75%, CF3.5%)	194
Table 5-10 Mechanical properties of regenerated CF keratin fibers (66.7%CF, 33.3%Cellulose, Cellulose/CF 1/2, extrusion solution Cellulose 1.5%, CF3.0%)	195
Table 5-11 Mechanical properties of regenerated CF keratin fibers (50%CF, 50%Cellulose, Cellulose/CF 1/1, 1extrusion solution Cellulose 2.0%, CF2.0%)	195
Table 5-12 Mechanical properties of regenerated CF keratin fibers (20%CF, 80%Cellulose, Cellulose/CF 4/1, extrusion solution Cellulose 4.8%, CF0.6%)	196
Table 5-13 Tensile Properties of regenerated CF Fibers Compared to some protein fibers	201
Table 6-1 Measured and calculated data of new 50/50 nonwoven sample (1)	209
Table 6-2 Measured and calculated data of new CF/PET 75/25 nonwovens	211
Table 6-3 Measured and calculated data of new CF/PET 67/33 nonwovens	212
Table 6-4 Measured and calculated data of new CF/PET50/50 nonwovens	213

Table 6-5 Measured and calculated data of new CF/PET 33/67 nonwovens	214
Table 6-6 Measured and calculated data of new CF/PET 0/100 nonwovens	215
Table 7-1 Measured basic physical data of CF/PET 0/100 nonwovens	225
Table 7-2 Measured basic physical data of CF/PET 75/25 nonwovens	225
Table 7-3 Measured basic physical data of CF/PET 50/50 nonwovens	226
Table 7-4 Weight of scrim, PET and CF fibers in Sample (18), (9) and (1)	227
Table 7-5 Volume fraction of fibers and diameter of nonwovens fibers in Sample (18), (9) and (1).....	228
Table 7-6 Interception parameter of Sample (18), (9) and (1).....	229
Table 7-7 Values of A and B of Sample (18), (9) and (1)	229
Table 7-8 Measured penetration of sample (18), (9) and (1).....	230
Table 7-9 Calculation results of constants of penetration equation.....	230
Table 7-10 Weight of scrim, PET and CF fibers in CF/PET 0/100 nonwovens.....	231
Table 7-11 Volume fractions of fibers and average diameter of all fibers in CF/PET 0/100 nonwovens	232
Table 7-12 Interception parameter of CF/PET 0/100 nonwovens	232
Table 7-13 Values of A and B in CF/PET 0/100 nonwovens.....	233
Table 7-14 Calculation results of the penetration of CF/PET 0/100 nonwovens	234
Table 7-15 Calculation results of the filtration efficiency of CF/PET 0/100 Nonwovens	235
Table 7-16 Measured basic physical data of CF/PET 33/67 nonwovens	236
Table 7-17 Weight of scrim, PET and CF fibers of CF/PET 33/67 nonwovens	238
Table 7-18 Volume fractions of fibers and average diameter of all fibers in CF/PET 33/67 nonwovens	238
Table 7-19 Interception parameters of CF/PET 33/67 nonwovens	239
Table 7-20 Values of A and B in CF/PET 33/67 nonwovens.....	239
Table 7-21 Calculation results of the penetration and its relative error of CF/PET 33/67 nonwovens	240
Table 7-22 Calculation results of the filtration efficiency of CF/PET33/67 Nonwovens	240
Table 7-23 Weight of scrim, PET and CF fibers of CF/PET 50/50 nonwovens	241
Table 7-24 Volume fractions of fibers and average diameter of all fibers in CF/PET 50/50 nonwovens	242
Table 7-25 Interception parameters of CF/PET 50/50 nonwovens	242
Table 7-26 Values of A and B in CF/PET 50/50 nonwovens.....	243

Table 7-27 Calculation results of the penetration and its relative error of CF/PET 50/50 nonwovens	243
Table 7-28 Calculation results of the filtration efficiency of CF/PET 50/50 nonwovens	244
Table 7-29 Measured basic physical data of CF/PET 67/33 nonwovens	245
Table 7-30 Weight of scrim, PET and CF fibers of CF/PET 67/33 nonwovens	245
Table 7-31 Volume fractions of fibers and average diameter of all fibers in CF/PET 67/33 nonwovens	246
Table 7-32 Interception parameters of CF/PET 67/33 nonwovens	246
Table 7-33 Values of A and B in CF/PET 67/33 nonwovens.....	247
Table 7-34 Calculation results of the penetration and its relative error of CF/PET 67/33 nonwovens	247
Table 7-35 Calculation results of the filtration efficiency of CF/PET 67/33 nonwovens	248
Table 7-36 Weight of scrim, PET and CF fibers in CF/PET 75/25 nonwovens.....	248
Table 7-37 Volume fractions of fibers and average diameter of all fibers in CF/PET 75/25 nonwovens	249
Table 7-38 Interception parameters of CF/PET 75/25 nonwovens	249
Table 7-39 Values of A and B in CF/PET 75/25 nonwovens.....	250
Table 7-40 Calculation results of the penetration and its relative error of CF/PET 75/25 nonwovens	250
Table 7-41 Calculation results of the filtration efficiency of CF/PET 75/25 nonwovens	251

CHAPTER 1

INTRODUCTION AND LITERATURE REVIEW

1.1 Introduction

Recognizing feather “waste” as a potential source of usable fiber studies were begun to demonstrate and develop that usefulness by making commercial products. In this study chicken feathers were used to produce air filters and regenerated keratin fibers. This literature review includes a discussion of:

General information about chicken feathers and feather fibers,

Extraction of feather keratin from chicken feathers and

Air filter review.

1.2 General information about chicken feathers

Feathers are very special structures which distinguish birds from other animals and have important physiological functions. A chicken has about 5% to 7% of its body weight in feathers so chicken feathers are an important by-product in the poultry industry. Currently, increasing poultry consumption both in the United States and abroad has produced a great amount of “waste”. Over four billion pounds of chicken feather “waste” is generated by the US poultry industry alone each year [1].

Presently, feathers might be considered as “waste” because their current uses are economically marginal and their disposal is difficult. In the previous time and sometimes

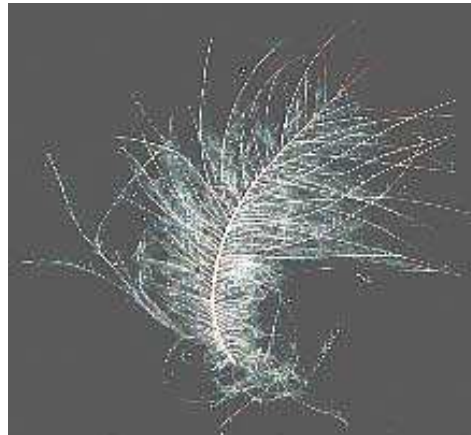
in present the feathers are cooked/ sterilized at elevated temperature and high pressure, then dried and ground to powder to be used as a feed supplement for livestock, mainly for ruminants. However, this is a fairly expensive process. The quality of the produced protein product is low, lacking some essential amino acids and having poor digestibility by animals. It sells for only about \$0.50 per kilogram. This marginal profit causes supply exceeding demand [2-4]. Disposal methods such as burning or burying are also occasionally used, but they are environmentally unfriendly. Burning feathers causes air pollution and in a landfill feathers decompose very slowly and would require a lot of land. After research for many years on their physical and chemical structures and properties, new, economically interesting applications for them are expected to be found for this large amount of chicken feathers. Presently, the chicken feather “waste” as a potential source of fibers (both original and regenerated) is being gradually recognized.

There are several kinds of feathers. The type we know best is that shown in Figure 1-1(a), and it is called a **contour feather**. The stiff, cylindrical, sharp-pointed "midrib" of the contour feather is known as the **shaft**, or **rachis** (RAY-kiss). The slender, parallel side branches arising from two sides of the shaft are **barbs**, and all the barbs considered collectively as one flat thing are known as the **vane**. Most of what we see in the Figure is the vane. If you examine a barb under the microscope you'll see that it bears minute hooked branches, kind of like VelcroTM hairs. These are **barbules**, and the barbules of adjacent barbs hook together to hold the barbs into a well organized vane. In the Figure, especially toward the vane's base, you can see that some barbs have come undone from their neighbors. The Figure 1-1(b) shows a feather-type known as a **semiplume**. Semiplumes have shafts like contour feathers, but their vanes are fluffy, not well

organized with the barbs "zipped together" as in the contour feather. The barbs of feather can be used directly as fibers.



(a)



(b)

Figure 1-1 Picture of feathers [1]

1.2.1 Chemical structure- keratin

Feathers consist of about 91% keratin, 1.3% fat, and 7.9% water [5]. Keratin is a hard protein that is also found in hair, skin, hooves and nails. Birds and reptiles have their own keratins, very different from the α -keratins in mammals. **Bird and reptile keratins** are composites made up from both fibrous and matrix components. The fibrous feather keratin can stretch approximately 6% before breaking, unlike hair α -keratin that can

stretch to twice its length. Protein chemists think that the main secondary structure in bird and reptile keratin is the **β -keratin** [6]. The **β -keratin** does not lie flat but twists gradually (Figure1-2). Each polypeptide chain in these **β -keratins** has a central helical section with less regular regions at each end. These regions contribute to the matrix component and have some -S-S- (cysteine) cross-links. **Silks** have also many β -sheets in their structures but they are different from the β -keratins because they have very few -S-S- links. These sheets are **antiparallel**, so polypeptide chains next to each other run in opposite directions and the sheets stack together in layers like a pack of playing cards (Figure1-3).

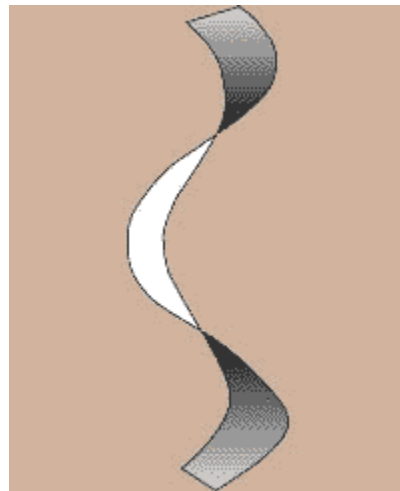


Figure 1-2 β -keratin - the β -sheet twists gradually [6]

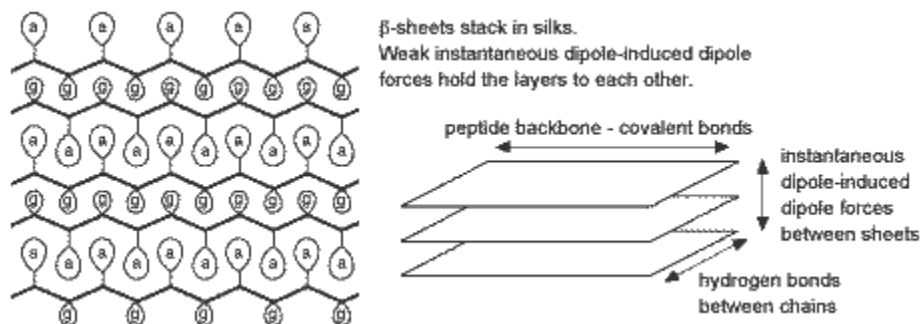


Figure 1-3 β -sheet twists gradually [6]

β -keratin contains ordered α -helix or β -sheet structures and some disordered structures. The feather has barb and quill parts. The feather barb fraction has slightly more α -helix over β -sheet structure, whose melting point is 240 °C. The quill has much more β -sheet than α -helix structure and has a melting point of 230 °C [5]. Feather keratin has an average molecular weight of about 60,500 g/mol [6], ranging from 59,000 to 65,000 Daltons [7]. Feather keratins are composed of about 20 kinds of proteins, which differ only by a few amino acids [8]. The distribution of amino acids is highly nonuniform, with the basic and acidic residues and the cysteine residues concentrated in the N- and C-terminal regions. The central portion is rich in hydrophobic residues and has a crystalline β -sheet conformation [9].

Feather keratin is a special protein. It has a high content of cysteine (7%) in the amino acid sequence [7] (see Table 1-1 [10]), and cysteine has -SH groups and causes the sulfur-sulfur (disulfide) bonding. The high content cysteine makes the keratin stable by forming network structure through joining adjacent polypeptides by disulfide cross-links. The feather keratin fiber is semi-crystalline and made up from a crystalline fiber phase

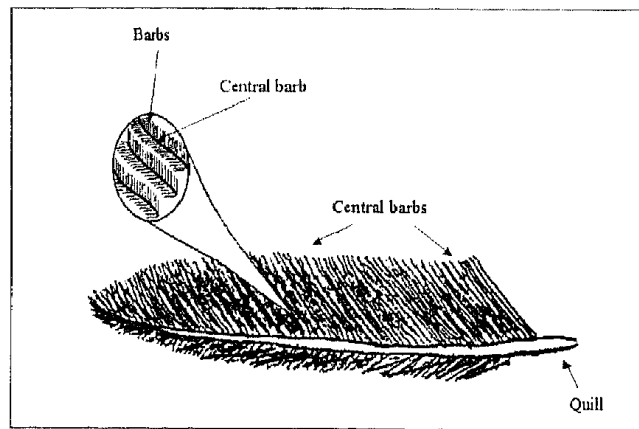
and an amorphous protein matrix phase linked to each other [35]. The crystalline phase consists of α -helical protein braided into microfibrils where the protein matrix is fixed by intermolecular interactions, especially hydrogen bonds. In protein, hydrogen bonds are many and strong.

Table 1-1 Amino acid content in keratin fiber from chicken feather [10]

Functional groups	Amino acid	Contents (as % mole)
Negatively charged	Aspartic acid	5
	Glutamic acid	7
Positively charged	Arginine	5
Conformationally special	Proline	12
	Glycine	11
Hydrophobic	Phenylalanine	4
	Alanine	4
	Cysteine	7
	Valine	9
	Isoleucine	5
	Leucine	6
	Tyrosine	1
Hydrophilic	Threonine	4
	Serine	16

1.2.2 Physical structure of feather fibers

As stated above, barbs can be used as fibers. The big part of a feather's physical structure is the barb. Just like general feathers, barbs also have branching structure and nodes along the barb shown in Figure 1-4. Feathers have a hierarchical structure beginning with the level of the central barbs which grow directly from the quill. The central bars are tiny "quill" which also grow barbs [11]. Nodes and barbs on the feather fiber are related with memory properties and improve the structural strength.



(a)



(b)

Figure 1-4 a schema of chicken feathers [11]

Figure 1-5 (a) and (b) shows surface characteristics of feather fibers. From the figure, it can be observed that these fibers are not hollow as tubes, but are filled. The cleft lines or striations along the fibers cause a certain surface roughness, which may contribute to interfacial strength in composites (one of the possible applications for these fibers). The geometric characteristics of fibers change as the sampling point goes along the fiber. Their representative sample of cylindrical solid barbs was measured at three different anatomic positions: their bases, the mean point in the stems and at the nodes. From this point, it was found that the apparent diameter of down barbs ranges from 4 to 8 μm . The feather fiber length was dependent on the time and velocity of separation process [11].

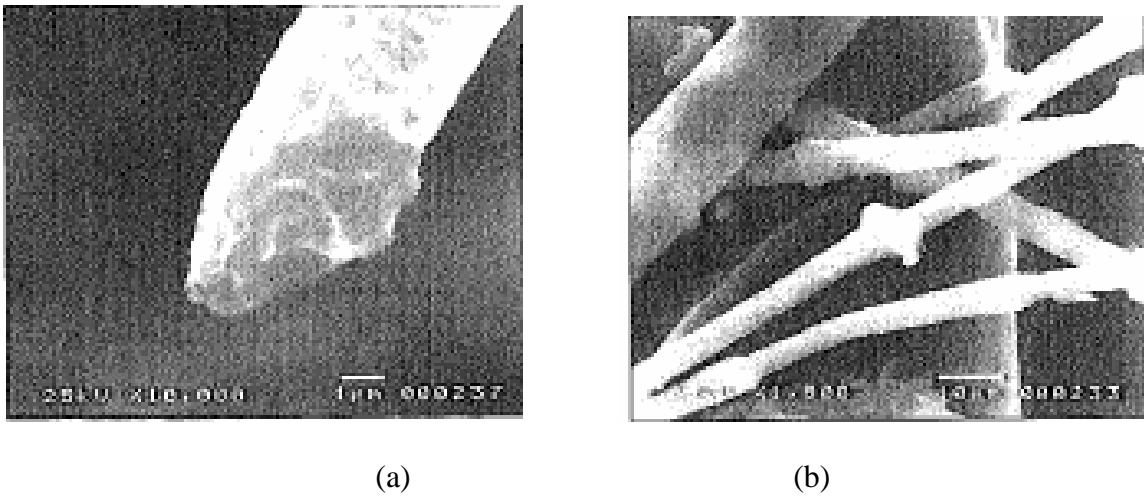


Figure 1-5 chicken feather keratin fiber structures (a) and its surface structure (b) [11]

1.2.3 Physical properties of feather fibers

In keratin protein there are both hydrophilic and hydrophobic amino acids, but 39 of the 95 amino acids are hydrophilic [12]. Serine is the most abundant amino acid and the

-OH group in each serine residue helps chicken feathers to absorb moisture from the air. Feather fiber is, therefore, hygroscopic. Chicken feather fibers and quill have a similar content of moisture, around 7%.

Fiber diameter is approximately 5-50 μm [13]. Fiber length through different processing can be different, but it can be expected to be 3-13 mm. Therefore, the fiber aspect ratio (length/diameter) can be in the range of 400-2600 [14].

Because the chicken feather fiber is not completely solid, the fiber's volume always includes both solid matter (the walls of fiber) and air (the hollow inside the fiber). The density of chicken feather fibers is always interpreted as apparent density. It is reported that density of chicken fibers is 0.89 g/cm^3 [14] and measured by displacing a known volume and weight of ethanol with an equivalent amount of fiber.

Since the chicken feather fiber is mainly made up of the structural protein keratin, its chemical durability is primarily determined by keratin. Because keratin has extensive cross-linking and strong covalent bonding within its structure, the feather fiber shows good durability and resistance to degradation. The chemical durability experiments showed that chicken feather fibers degrade rapidly in alkali environments [15], but significantly less in near-neutral and slightly acidic conditions.

The functions of a bird's feathers are highly related to their mechanical properties and their mechanical properties are related to the keratin structure. Keratin has a structure which transports forces through negligible distortion. It is reported that elasticity moduli of feather keratin ranges from 0.045 GPa to 10 GPa [16]. The Young's modulus of chicken feather fibers was found to be in the range of 3 - 50 GPa [17] and the tensile strength of oven-dried chicken feather fibers in the range of 41-130 MPa [18].

1.2.4 Possible Applications of feather fibers

Environmental concerns always [19] encourage study to replace synthetic materials with a variety of natural materials. Natural fibers have recently attracted scientists' attention because of their advantages from the environmental standpoint, but almost all the research has been focused on cellulose from vegetable sources. Currently, the keratin fiber from chicken feathers is recognized as an almost infinite source of high performance materials, but it needs further studies to demonstrate a basis for innovative technologies and useful raw materials. Economic interest about feather fiber usage has been gradually increasing.

To obtain and use the feather fiber, barbs need to be stripped from the quill. In February 1998, Agricultural Research Service chemist Walter Schmidt and his colleagues (George Gassner, Mike Line, Rolland Waters and Clayton Thomas) received a patent for a process for cleaning, chopping, and separating feather fibers from the quill of chicken feathers [19]. From it, two pounds of feathers yields about one pound of the fiber fraction and one pound of the quill fraction [20]. This patent involves the following basic steps [21]: collecting raw feathers, washing feathers in a polar water-soluble organic solvent, repeating the washing step, drying the feathers, removing fibers from feather shafts using mechanical shredding or shearing or a high speed constant flow centrifugal grinder and separating the light fibers from the heavier quills through a turbulent airflow by apparent density difference.

The unique shape, a center fiber with many branching fibers, makes feather fibers ideal for random orientation processes such as injection molding, dry mat formation, or

wetlay. Maybe these materials derived from chicken feathers could be used to improve the properties of existing composite materials, to replace non-renewable constituents, or to develop entirely new biocomposite materials with novel applications. There have been a few reports about useful products manufactured from feathers [19].

Walter Schmidt invented a technique to mix chicken feather fibers with paper and strong, less dense plastic composites to produce products such as car dashboards and boat exteriors. A fiber that can be used in lightweight, sound-deadening composite materials maybe find use in office cubicles, cars and sleeping compartments of tractor trailers [22].

The Environmental Quality Laboratory scientist also found feather fiber can take place of some of the wood pulp to make such paper products as air filters and decorative paper [23]. Because of the super fine size and shape of feather fibers, filtration may be the first commercial value for processed chicken feathers. Many filters are made from wood pulp, but feather fiber has an advantage--it is finer than wood pulp. Wood pulp fibers have a width of 10-20 microns, but feather fibers' thickness is only 5 μm . Therefore, filters produced from feather fiber will have smaller holes, causing more spores, more dust and dander to be taken away from the air and entrapped in the filter. Homes and office buildings maybe obtain the benefit of using this kind of air filter for their fine filtration, resulting in lessening allergies and sick building syndrome. Another possible use may be in vacuum filters, decreasing the amount of spores and dust that can injury asthmatic lungs. A process of making air filter paper using chicken feather fiber has been patented in China [24]. The process includes using feather fiber as major material, mixing with plant fiber at a given ratio, and making specific paper with multiple applications. Compared with existing paper-making process, this process has the

advantages of better air permeability and filterability, full reutilization of waste, less pollution to environment, reduced consumption of wood pulp, reduced cost, and high application value. Furthermore, the composite paper is able to contain only 49 % wood pulp and 51% feather fiber [25]. In one word, the chicken feather paper meets the requirement for environmental protection.

In search of a new insulation material, Dr. Roy Broughton of Auburn University in Alabama has prepared nonwoven feather-fiber materials in a different way [26]. Instead of spreading on latex after forming fiber sheets, Dr. Broughton blends synthetic fibers with the feather material and then molds the combination into 2-to-4-inch-thick sheets. When these sheets are heated, the synthetic material partially melts and holds the feather fibers in place. The resulting combination insulates well and holds its shape better than down alone does. It is found that feather insulation could prove useful in comforters and even attics and walls.

Feather fibers might be used in water filters [27]. This application might not only help solve the waste-feather problem, but it might also produce better water filters than present common filters, such as those made of activated carbon. Before the fiber was placed in a filter, it was "activated" with ultrasound to produce additional microscopic pores in the fiber's structure. The prototype of feather-fiber water filters was produced by packing the fibers into plastic columns. Tests indicated that the feather filters took contaminants away from home drinking water or industrial waste. In the laboratory experiments, it had also found that feather fiber filters filtrated nuclear byproducts such as radioactive strontium and cesium and the microstructure of feather fibers trapped these hard-to-remove contaminants [27].

In composites with thermoset polyesters, feathers were reported to increase strength by 20% and decrease weight by 50% [28]. Dweib et al. [29] used vacuum-assisted resin transfer molding to infuse feather mats along with sheets of recycled paper with soybean oil-based resin. These materials were combined with structural foam to construct sandwich beams. The beam of recycled paper and chicken feathers had a global modulus of 950 MPa and a failure load of 24.2 kN while the woven E-glass beam had a global modulus of 1580 MPa and a failure load of 39.3 kN during testing in 4-point bend. The flexural rigidity and strength of the feather/recycled paper beam were comparable to values for cedar wood.

Barone et al. studied chicken feather fibers reinforced LDPE polymer matrix [30]. From physical property testing and microscopy they found there were some interaction between the fiber and polymer without the need for coupling agents or chemical treatment of the fibers. The feather fibers could be directly incorporated into the polymer using standard thermomechanical mixing techniques. The density of the composite upon introduction of keratin feather fiber is not increased, but reduced by 2%.

Hamoush and El-Hawary [31] tried to improve concrete properties such as strength and durability by adding chicken feather fibers to the concrete. The feathers were washed, screened, and dried. Three volume fractions of chicken feathers (1, 2, and 3%) were tested. Their study showed that the feather fiber reinforced concrete was lighter in weight and stronger in flexure than ordinary Portland cement plain concrete and smaller in compressive and tensile strengths than those of plain concrete, which indicates that feathers help produce cheaper lightweight concrete. The concrete with 1% feathers had higher flexural strength after 14, 28 and 56 days and so was that with 2% feather fibers

after 56 days, which provides a possibility for the concrete used under impact loading. One disadvantage was that the flexural strength decreased when the feather content was over 2%. It was found that the pore solution in cement-based materials is strongly alkaline, with a pH of 12.5-13.5 [32]. Alkaline environments accelerate feather fiber decay. The alkaline testing conditions caused low compressive and tensile strength measurement value. Two methods (treating feathers by a water-repellent agent and impregnating feathers with a blocking agent followed by a water-repellent agent) are used to reduce the alkalinity of the matrix to prevent both short- and long-term decay, both compressive and tensile strength. The compressive, tensile and flexural strengths of concrete with treated feather were improved compared to untreated-feather-reinforced concrete.

Using chicken feather fiber was studied to separate heavy metals from water [33]. It was found that the chicken feather fiber has very good adsorbent properties and removed effectively heavy metals such as copper, lead, chromium, mercury and uranium from solutions. The solution with pH 2-8 adsorbed heavy metals best and alkaline ultrasonic treatment improved the metal uptake of the keratin fiber many times. Washing feather fibers with dilute hydrochloric acid at a pH of 1.2 could desorb 99% of adsorbed copper ions. All of the testing results showed that it is possible that the stability of feather fibers allows them usable as a biosorbent for a number of cycles after being washed by hydrochloric acid.

1.3 Extraction of feather keratin from chicken feathers

Keratin is structural fibrous protein. The wool keratin fiber has been used as textile fibers or to produce strong fibers, but chicken feather keratin has not found use. Since more than 4 million tons of chicken feathers are produced by the poultry industry worldwide [34], it seems that chicken feather is the most abundant keratinous material in the world. If chicken feather keratin is dissolved and spun as protein fiber, then chicken feathers provide a good resource of keratin.

The feather fiber is exceptionally strong and stiff [11]. Sulphur-sulphur cross-links between cysteine molecules as well as hydrogen bonds are responsible for the good stiffness and strength of keratin. Extraction of chicken feather keratin can be achieved only if the disulfide and hydrogen bonds are broken. In 1940s to 1950s a number of studies had shown that the inter-molecular cross-links in keratin can be broken to obtain a spinnable fraction, which can be processed into polymeric materials, such as filament fibers. Such new biopolymeric materials from feather keratin might find interesting applications; e.g., as packaging material, or as matrix material in fiber reinforced composites [97].

As known, there is a very close relation between the strength of fiber and length of the constituent chains. To retain the mechanical properties, protein chains need to be kept during extraction of chicken feather keratin. The key for this purpose is to rupture the -S-S- disulfide bonds only but not break the main polypeptide chain while dissolving feather keratin [36].

Currently, there are several methods to dissolve chicken feather keratin. Both reducing agents and oxidizing agents can be used to break the disulfide bonds. The most

common method is using reducing agents in alkaline solution. Goddard and Michaelis [36] worked on the extraction of the keratin of wool and chicken feathers in alkaline thioglycolate, cyanide, and sulfide, and examined the properties of the precipitates obtained by acidification of the alkaline dispersions. They suggested that alkalinity was a prerequisite for the reduction. To explain inability of reducing agents to disperse keratin in less alkaline solutions at pH 10, they hypothesized that, for the dispersion of keratin, both the disulfide groups and the salt linkages of the keratin molecule must be broken. From their work, Patterson et al. [37] found that thioglycolic acid could reduce the disulfide groups of wool over a wide pH range, but no dispersion occurred if the reduction was carried out in neutral or acid solution.

Jones and Mecham [38] studied the dispersion of feather keratin in Na₂S solutions under various experimental conditions such as temperature, time, Na₂S concentration, and ratio of keratin to Na₂S and recovered dispersed protein by acidification of the dispersion to pH 4.2 They discovered that when feathers were treated with 0.1 M Na₂S (100 ml of solution per 7.5 g of keratin) for about 2 hours at 30 °C, the maximum dispersion of feather keratin was obtained with minimal degradation. They also found [39] that protein denaturants such as urea could help keratin disperse at neutral and alkali could act as that of a dispersing agent for the reduced keratin.

Schrooyen et al. studied stabilization of solutions of feather keratins by sodium dodecyl sulfate (SDS) [39]. They extracted feather keratins from chicken feathers with aqueous solutions of urea and 2-mercaptoethanol. Removal of 2-mercaptoethanol and urea by dialysis resulted in aggregation of the keratin polypeptide chains and oxidation of the cysteine residues to form a gel. SDS was added to the keratin solution prior to dialysis

to prevent extensive aggregation of the keratin chains. It was found that higher SDS/keratin ratios (1–2 g SDS/g keratin) seemed to prevent the oxidation reaction between different keratin chains, resulting in more intramolecular disulfide bond formation (shown in Figure 1-6).

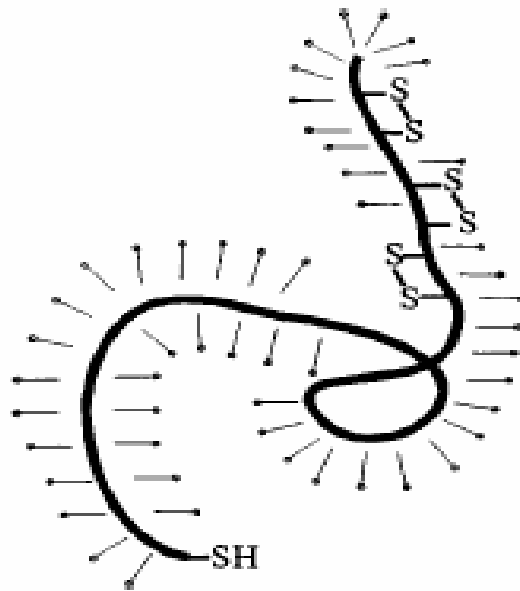


Figure 1-6 Schematic representations for SDS–keratin complexes with a high amount of SDS added prior to dialysis [39]

1.4 Review of air filters

1.4.1 Why use air filters?

Air filters are used to improve the quality of indoor air by removing harmful particles, gases or microorganisms from the atmosphere to protect sensitive manufacturing processes and components. During the past decade people have become more and more concerned about the environment and energy. As knowledge about the exterior and interior environment has increased, stricter demands for air quality in

protecting the environment are formulated to provide a healthier, more comfortable and more productive indoor climate in public areas, commercial buildings and manufacturing facilities. At the same time, manufacturing and process industries have become more and more advanced, demanding cleaner, more efficient and more economical air filtration processes. All these trends clearly have special requirements in today's air filters for air handling systems. Stricter requirements for filter performance - and increased concerns about the hygienic aspects of filter design and use - are other apparent developments. Concerns about conserving energy and reducing costs have led to new guidelines for cost and environmental analyses of filters [40].

Most air filtration applications have one common purpose – to protect against harmful airborne contaminants. In the case of breathable air filtration such as heating, ventilation and air-conditioning (HVAC) or cabin air filtration, the air filter is protecting people's health from both natural and man-made contaminants.

Depending on the field of application, there are many kinds of air filters. The most common ones are engine (automotive panel air filter, heavy duty air filter and cabin air filter), indoor air (HVAC, particulate removal, odor/gas removal) and industrial air filtration (gas turbine and dust collection filter applications).

As in many other areas, the need for best performance is also growing. Today's air filters typically demand longer lifespan to reduce material use and maintenance cost; higher strength to reduce losses during processing; greater resistance to rupture, so that systems can operate under harsher conditions and of course with finer and finer filtration removal efficiencies [41].

1.4.2 Filter media

Air filters use media to capture particles. The filter media determines the level or quality of filtration that a filter provides. Elsevier's Filter Media Handbook [42] has described the classification of filter media. There are woven fabric, nonwoven fabric, screens and meshes, membranes, and so on.

Woven media [43] Very little change has taken place in the weaving process for 40 years, but woven media have been improved in the past 40 years. These improvements are shown not only in the basic material of the yarn from which the fabric is woven, but also in the structure of the medium as used in the filter. Forty years ago, almost all woven media were made of staple fiber yarns, now a large part of woven media is woven from monofilament or multifilament 'yarns'.

Woven media are now from fibrillated tape yarns, and yarns can hold electrostatic charges, and the finished fabric probably experience one or more surface treatment processes, such as calendaring or napping. Some woven media maybe use surface coatings, or multilayer cloths may be made by lamination or multilayer weaving.

Nonwoven Media [43] Great changes have taken place in nonwovens media in the last 40 years. They are manufactured by using many different technologies [43] such as wet laid nonwovens, meltspinning webs, drylaid webs, needled felts and others. Previously, felts were mainly used as supported pads, but needlepunched felts had very little use. Needle felts then developed rapidly, as their tensile strengths and fiber shedding characteristics were improved. Surface treatments, resin and thermal bonding were applied to improve fiber retention properties; electrostatic properties were established, and the needlefelt seemed to become the medium of choice, especially for fine filtration.

Each nonwoven filtration product maybe uses one or several of these technologies in composite structures.

Wet laid Nonwovens [43] are produced by a technology, in which short cut fibers are uniformly dispersed in water first to form slurry, the slurry is transported onto a continuous moving fine mesh screen named the wire, and then a mat is formed after removing water. The nonwoven is produced by further water elimination through drying. Wet laid nonwovens are used for air filtration mainly because this manufacturing can control structure size and filtration characteristics with acceptable strength for converting. Wet laid air filtration media are applied in many fields such as HVAC, heavy duty air intake, automotive air intake, gas turbine and cabin air. This technology can use pore size gradient to produce multiple layers. These layers include mechanical filtration (a prefilter that removes most particles), electrostatic filtration (the middle layer allows high initial filtration efficiency) and the last layer/filter that allows high efficiency for all filter life. Therefore, this technology causes higher efficiencies, higher dust holding capacity, lower-pressure drop and longer life.

Dry laid Nonwovens [43] are produced by a process which disperses fibers uniformly, and deposits them onto a continuous fine mesh screen. A mat is then formed as a medium of filtration. There are two dry laid methods: carding and airlaying:

- In carding separated and aligned fibers are going through a system of cards and then are sent to or through a cross-lapper to a bonding technique.

- In airlaying, short fibers are transported by an air stream and form a randomly oriented web on a moving belt or perforated drum. Generally, airlaid webs have a lower

density and higher softness than carded webs and can use many kinds of fibers and fiber blends. Airlaid nonwovens are very common in HVAC.

One general method to bond dry laid webs is needlepunch, in which the web is punched vertically by barbed needles, with some fibers oriented in the z-direction and entangled to provide strength. Needle punched nonwovens seem to have relatively high densities, where two layers of scrim are always used to cover dry laid webs.

Punching density presents the number of stitches per square centimeter. Figure1-7 (a) shows schematically the meaning of stitches per Centimeter Square [44]. Punching density is given by [44]:

$$\text{Punching density (Stitches/cm}^2\text{)} = \frac{\text{Number of needles per cm working width}}{\text{Advance (mm)/stroke}} \times 10$$

On the other hand the “Depth of Penetration” is the length of needle that penetrates through the upper surface of the stitching plate (as shown in Figure1-7 (b)). Obviously at higher depth of penetration, more barbs go through the mat and more fibers are transported in the vertical direction [44].

L. Gardmak and L. Martensson [42] found that needlepunched nonwovens’ thickness decrease with more penetration per unit area, their density, however, increases for the first phase and then decreases. This is because of both the fiber damage and a weight decrease per unit area of about 5% for each pass through the needling machine, as there is some loss of fibers and an extension of the felt while being needled. Air permeability also

decreases with the increase of needling density. They also stated that with the increase of depth of needle penetration the consolidation of fiber in the web increases.

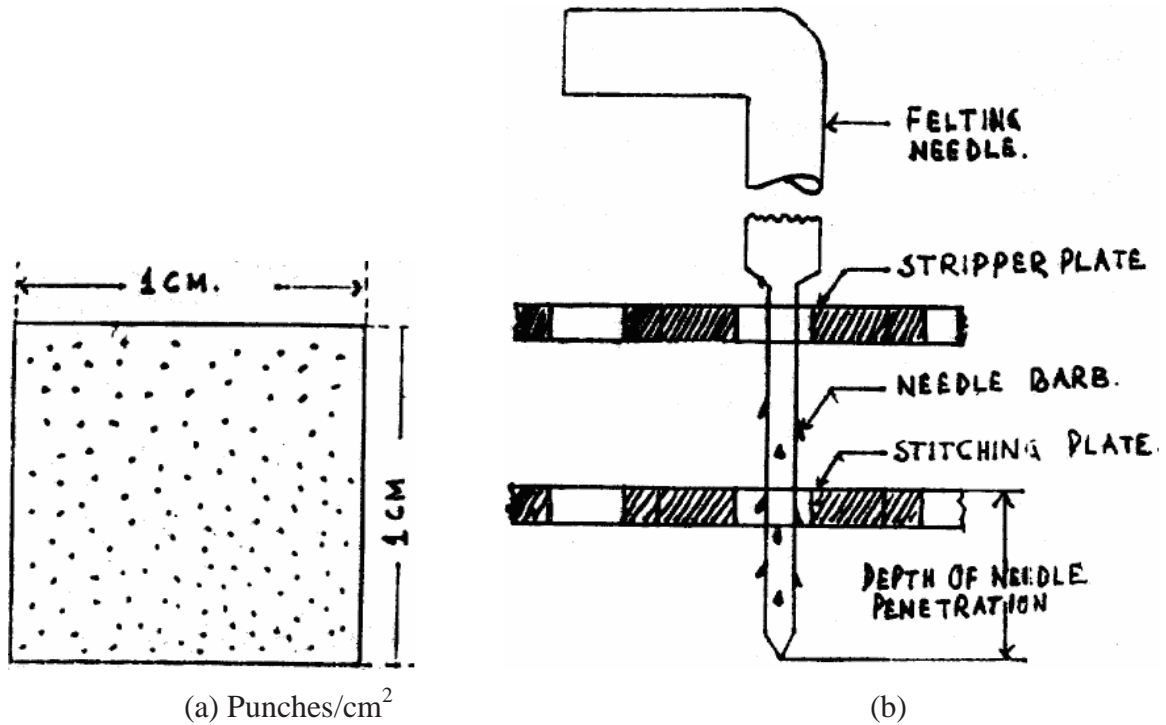
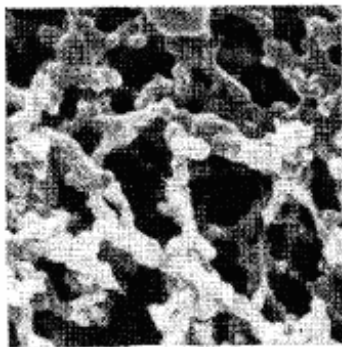


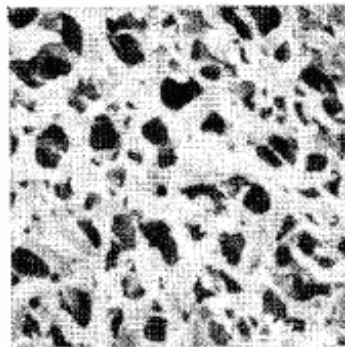
Figure1-7 Sketch of punches density and depth of penetration of needlepunching [44]

J. W. S. Hearl, M. A. I. Sultan and T. N. Choudhuri [45] found that in the amount of needling decreases the fabric weight produced from a particular web weight. This is because of the drafting and spreading of fibers during punching. In doing research on 2.2 dtex polypropylene needle punched filter fabric, P. A. Smith and G. J. I. Igwe [46] found that the needling density also affected both collection capacity and filtration efficiency. An increase in needling density leads to reduced collection capacity as might be expected, but it was unusual to find that it also causes reduced filtration efficiency.

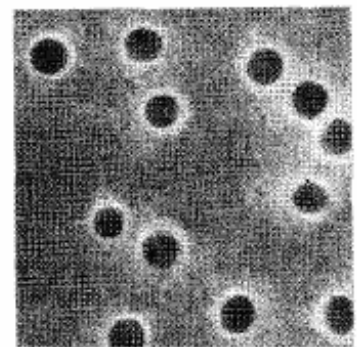
Membranes [43] are almost entirely a new kind of filter media of the past 40 years. First they were made of cellulose esters, now from a wide range of polymers. They are thin and soft, and needs support. Recently, they have been made from metal or ceramic to have stiffer or more solid structures, so that they may be applied to more abrasive, more erosive, more corrosive, and hotter processes. The need for finer filtration has led to the rapid expansion of membrane applications, and different microfiltration membranes have been produced (Figure 1-8).



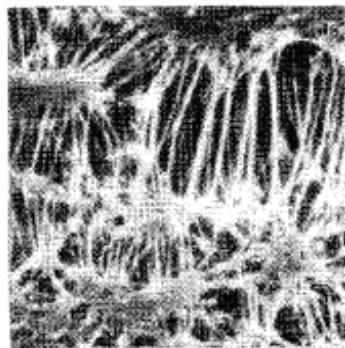
Mixed esters of cellulose membrane.



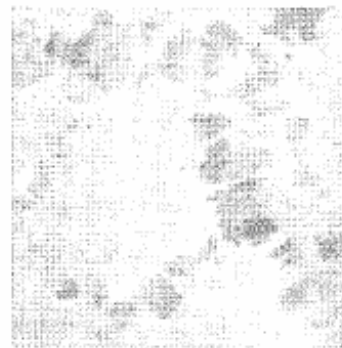
Durapore polyvinylidene difluoride membrane.



Isopore track-etched polycarbonate membrane.



Fluoropore PTFE membrane.



Solvex polypropylene membrane.

Figure 1-8 Different microfiltration membranes [42]

1.4.3 Mechanism of air filtration in fabric filters

Here the filtration mechanism of fabric filter is discussed. The fabric filter is a simple device in which dust-bearing gas is passed unidirectionally through a permeable textile medium [47]. The dust particles are arrested on the dirty gas side of the fabric, while the cleaned gas passes through the cloth and out of the collector to be either vented to atmosphere, or returned to some part of a processing operation. Technically speaking, filtration uses direct interception, inertial interception, diffusion and/or electrostatic attraction to arrest dust particles [47] [48] [49] [50] (see Figure 1-9).

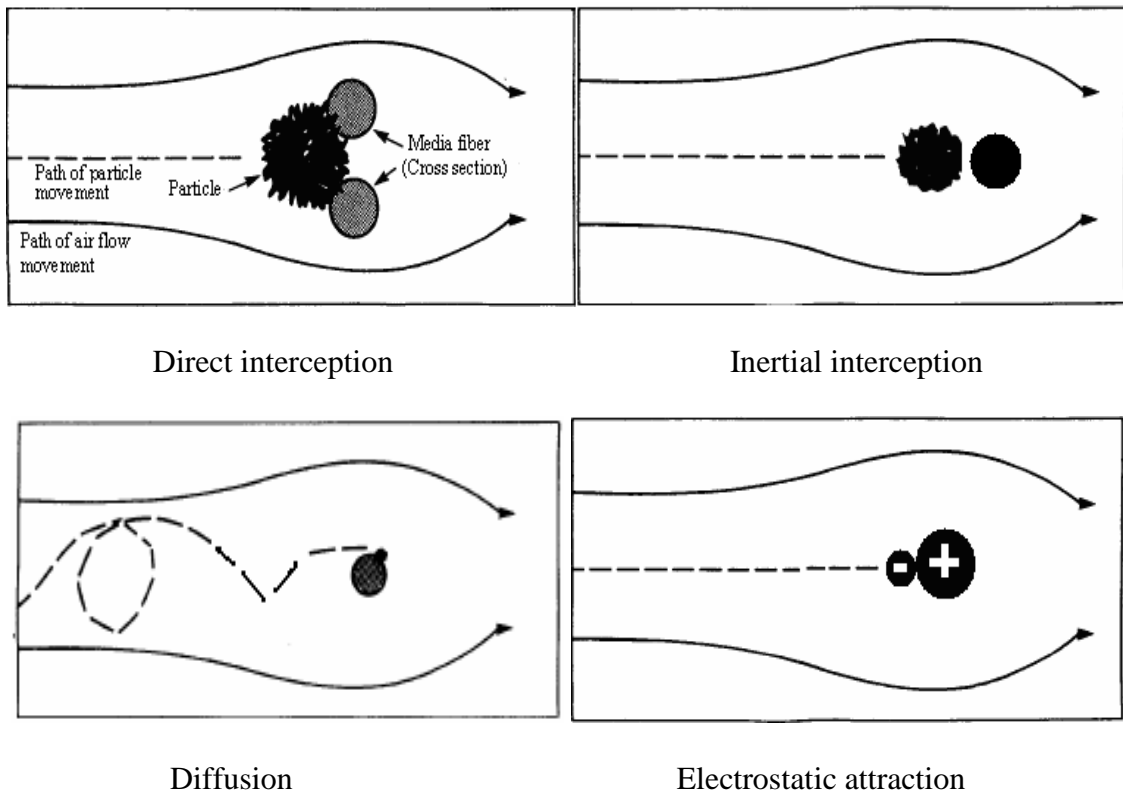


Figure 1-9 Mechanism of air filtration [47], [48], [49], [50]

Direct interception is the easiest filtration mechanism to envision (see Figure 1-9). It occurs when a moving particle is larger than the opening between fibers and cannot pass through. It is ineffective method of filtration because the vast majority of particles are far smaller than spaces between fibers.

Inertial interception or impaction occurs as the air-stream passes through a random network of fibers. Some particles will strikes onto the filter medium and be caught due to their inertia (momentum) driving them into the filter media. The compressed air-stream, because of its relatively low density and inertia, changes direction and flows around the fibers. Particles in the size range of 1.0 to 0.3 μm randomly collide with the fibers. Hence, inertial interception works to trap a high percentage of particles not trapped by direct interception. The larger the particle and the smaller the fiber, the greater is the chance of inertial interception. Conversely, the larger the fiber and the smaller the particle size, the more difficult it is for the particle to free itself from the influences of streamlines.

Diffusion [47] [48] [49] [50] occurs due to the random motion of small particles, also known as Brownian motion. They are so small in the size range of 0.1 μm or smaller that their direction and velocity are influenced by molecular collisions. They do not tend to follow the airstreams but behave more like gases than particles. These randomly moving particles collide with fibers more often than they would due to inertial impaction alone. The slower the particles move through the filter, the more opportunities there are for this to happen. As the particles traverse the flow stream, they collide with the fiber and are collected. So, this mechanism is most important for extremely small particles moving very slowly through thick filters of very fine fibers.

Electrostatic attraction [47] [48] [49] [50] is based on the principle that objects carrying opposite electrical charges are attracted to one another. Particles and fibers are charged differently. After fiber contact is made, smaller particles are retained on the fibers by a weak electrostatic force. This can be important for particles below 5 μm , and sometimes can make an otherwise poor medium perform satisfactorily.

Caking-cake formation [48] is the build up of particulate material on the filter surface. New fabric filters catch individual particles by single fibers with any combination of the above mentioned mechanisms. The particles deposit on fibers, project into the gas flow, and then act as additional sites to catch particles further. Finally, chain-like aggregates form. Studies on structure of aggregates shows that deposition mainly takes place on previously deposited particles, and then a complete matrix made up of particles forms quickly. When the matrix is set up, true surface filtration or direct interception achieves subsequent particle capture, and the filtration of filter fabric becomes negligible, and the fabric acts as a support for the matrix.

Since the resistance to gas flow increases when the cake forms and filter pressure drop is a measure of the force required to move air through the filter at a given velocity, the pressure drop needed across the filter increases. To keep the same rate of gas flow as at start-up, higher pressure drop needs to be applied, so more work is required for the driving fan. When the pressure drop attains an unacceptable level, the cake of filter fabric has to be dislodged and the pressure drop falls to an acceptable level. This new pressure drop level across the fabric will always be higher than the initial value at start-up because some of the dust particles cannot be removed by the cleaning system and have become permanently lodged in the fabric. Following the cleaning action, more particles in the gas

stream collide with particles which have remained on the fibers and new caking-cake formation process restarts. This irreversible change will gradually improve the capture of fine particles, which in turn raises the fabric filter's efficiency to near 100%.

Filter media are generally categorized as a surface loading or a depth loading type of media according to the places of capturing particle (see Figure 1-10) [51]. A surface loading media has a majority of particles stored on the surface with minimal depth penetration. A depth loading media shows minimal surface storage with particles stored throughout the depth. Changing the particle diameter can make the surface loading media a depth loading media and vice versa. The direct and inertial interception mechanisms are used by the large particles on the surface and surrounding inter-fiber space flow passages of filters, while the small particles use the diffusion mechanism in the depth of the media. Fiber diameter also has effect on the type of media since finer fibers produce more inter-fiber space. The submicron fiber layered filter has a concentration and dispersion of particles on the surface layer. The fact that the fine fiber media holds 2.5 times more mass of particulate than the submicron media at the same pressure drop shows that there are about 2.5 times more inter-fiber spaces in the fine fiber materials than in the submicron media.

1.4.5 Evaluation of performance of air filters

A lot of air filters made of different materials and applied in different fields are produced. Furthermore, new materials manufacturing capability has made significant progress in the last few years, which allows the production filtration media to have both a performance and cost advantage over traditional materials for filter manufacture. As the

filtration industry expanded, a standard method was very valuable to the product designer, filtration engineer and filter user for evaluation and prediction of performance of air filters became increasingly important.

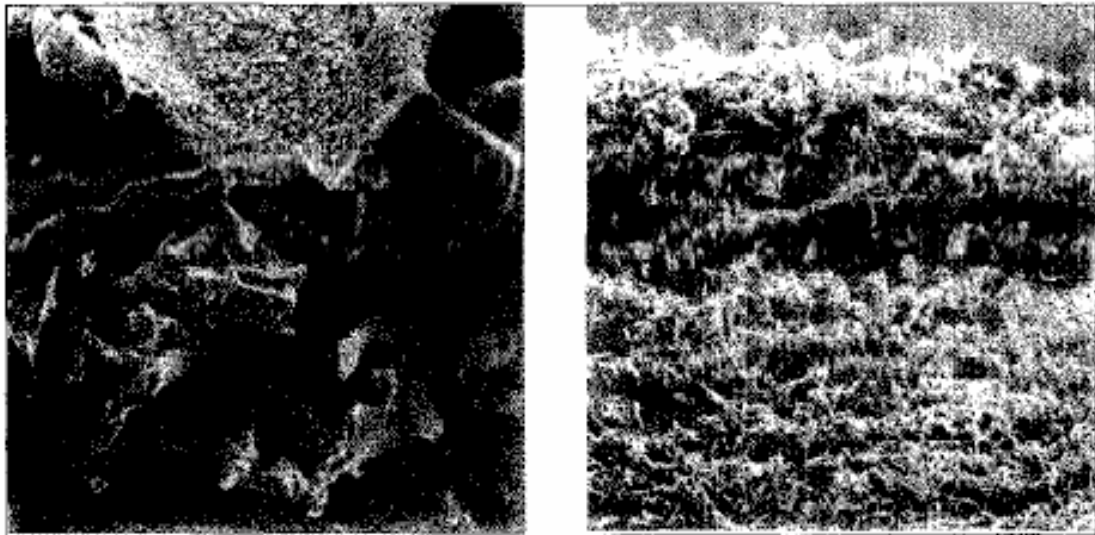


Figure 1-10: Cross sectional SEMs of a surface loaded media and a depth media [51].

The first air filter standard method was developed by the American Society of Heating, Refrigerating, and Air Conditioning Engineers (ASHRAE) in 1968 (ASHRAE 2-68). The method was updated in 1976 to address issues with the initial standard. This resulted in publication of ASHRAE 52-76. In 1992 it was improved for reducing testing time. Thus, ASHRAE 52.1-1992 was approved as the generally accepted method standard for air filter evaluation. Now, several articles have been written about evaluation of air filter [52] [53]. Generally, the major criteria for evaluating filtration media and consideration for product design are as follows: air permeability, filtration efficiency, filtration capacity (or life) and filtration cost.

Air permeability is the property which permits the passage of air when a difference in pressure exists across the boundaries of the material. Air permeability is one indication of a substance's porosity.

It is measured under carefully specified conditions, such as total pressure, partial pressure on the two sides of the specimen, temperature and relative humidity. Air Permeability ASTM D737-96 is Standard Test Method for Air Permeability of Textile Fabrics. This test method covers the measurement of the air permeability--the rate of air flow passing perpendicularly through a known area under a prescribed air pressure differential between the two surfaces of textile fabrics. It is generally expressed as air speed (volume per area per time) in SI units as $\text{cm}^3/\text{cm}^2/\text{s}$ or in customary units as $\text{ft}^3/\text{ft}^2/\text{min}$ [52], [53].

Air permeability is tested as follows [52, 53]: A circle of fabric is clamped into the tester and through the use of a vacuum; the rate of airflow is adjusted until a specified pressure difference between the two fabric surfaces (face and back) is achieved. The airflow is measured and the air permeability is calculated.

For fibrous air filters, according to Igwe and Smith finer fibers produce a lower permeability owing to greater surface area of the fibers [54]. Mahabir S. Atwal related air permeability to friction (drag) occurring between air and fibers of the fabric [55]. Hence, the resistance to the flow of air presented by a fabric is greatly influenced by fiber fineness. According to Lamb and Costanza, air permeability varies linearly with fiber diameter and hence fineness at constant fabric weight and constant fabric density [56]. Kothari and Newton investigated the role of web weight and needle penetration and needling density on air permeability and concluded air permeability is almost directly

proportional to the reciprocal of fabric weight per unit area [57]. But Dent did not agree with that theory and he emphasized fabric density and thickness [58]. Hearle and Sultant reported decrease in air permeability with increase in fabric weight with web weight but also reported a reduction in fabric weight during needling operation [59]. Clayton introduced sectional air permeability [60]. Atwal correlated fabric weight per unit area, porosity, fiber fineness, and thickness of fabric with air resistance [61].

Filtration efficiency [62] defines how well the product will remove the contaminants of interest. It is the ratio of particles trapped by a filter over the total number of particles found in the air upstream of the filter. A count of the downstream particles is often used to determine the number of particles trapped by the filter. Filter efficiency can either be based on specific particle size ranges or based on the total number of particles of all sizes. There are numerous testing procedures utilized for determining filter efficiency.

- **ASHRAE Standard 52.2-1999** [62]: This standard narrates air filtration efficiency particles in size ranges: 3 to 10 μm , 1 to 3 μm , and 0.3 to 1 μm . According to the filtration efficiency of these three size groups of particles, a Minimum Efficiency Reporting Value (MERV) between 1 and 16 is selected. A higher MERV shows greater filter efficiency and the filter is more effective to remove smaller particles

- **ASHRAE Standard 52.1-1992** [62]: This method describes air filter efficiency by using the mass of particles arrested by the filter, which makes the standard also called a weight-arrestance test. However, these tests do not show the air efficiency against the smaller particles typically found in dust, only that of relatively large particles.

ASHRAE Standard 52.2-1999 is new and more descriptive.

Different air filters have different filtration efficiency, and then have different applications (Table1-2) [63].

Dust-holding capacity (or life) is the amount of a particular dust trapped and hold before the maximum allowable back pressure or pressure drop is reached [64]. It determines the operating life of the air cleaner which is fixed mainly by some figure of tolerable resistance and shows how much dust the air filter can retain before reaching a point of air flow restriction. Higher capacity means a longer filter life. (When evaluating dust-holding capacity, it is important to compare dust-holding capacities between filters at the same final pressure drop to make accurate comparisons of projected filter life.) Capacity is generally conveyed in grams. For example, an air filter with a dust capacity of 250 grams means it will hold that much dust before cleaning or replacement is necessary [65].

Dust-holding capacity is tested by ASHRAE 52.1 and 52.2. Its measurement often uses the collection of synthetic dust. Due to using coarse dust, the dust will gather in the filter media during laboratory tests in a completely different way from that it would in real operating conditions. Figure1-11 [66] shows an example of electrostatically charged filters that have been tested in the laboratory and in real operating circumstances. According to measurements, at the same pressure drop, the filter has the higher dust holding in the laboratory than in reality. The design of the filter material and its structure completely determines agreement between the laboratory and reality. Filters with glass fiber materials often indicate the opposite properties--a higher dust-holding capacity for dust in air than that measured in lab.

Table1-2 Filter efficiency/application guidelines [63]

Filter Efficiency Rating			Application Guidelines		
MERV Rating (ASHRAE Std. S2.2)	Dust Spot Efficiency (ASHRAE Std. S2.1)	Arrestance (ASHRAE Std. S2.1)	Typical Contaminant	Typical Applications	Typical Air Filter
1	<20%	<65%	> 10.0 µm Particle Size Pollen Spanish moss Dust mites Sanding dust Spray paint dust Textile fibers Carpel fibers	Minimum filtration Residential Window air conditions	Throwaway -Disposable fiberglass or synthetic panel filter Washable -Aluminum mesh, latex coated hair, or foam panel filters Electrostatic -Self changing (passive) woven polycarbonate panel filter
2	<20%	65-70%			
3	<20%	70-75%			
4	<20%	75-80%			
5	<20%	80-85%	3.0-10.0µm Particle size Mold Spores Hair spray Fabric protector Dusting aids Cement dust Pudding mix Stuff Powdered milk	Commercial buildings Better residential Industrial workplace Paint booth inlet air	Pleated filters -Disposable, extended surface, 25 to 125 mm (1 to 5 in.) thick with cotton-polyester blend media, cardboard frame, Cartridge Filters -Graded density viscous coated cube or pocket filters, synthetic media Throwaway - Disposable fiberglass or synthetic panel filters
6	<20%	85-90%			
7	25-30%	>90%			
8	30-35%	>90%			
9	40-45%	>90%	1.0-3.0µm Particle Size Legionella Humidifier dust! Lead Dust Milled flour Coal dust Auto emissions Nebulizer drops Welding fumes	Superior residential Better commercial buildings Hospital laboratories	Bag Filters -Nonsupported (flexible) microfibre fiberglass or synthetic media, 300 to 900 mm (12 to 36 in.) deep, 6-12 pockets Box filters -Rigid style cartridge filters 150mm (6 to 12 in.) deep may use lofted (air laid) or paper (wet laid) media
10	50-55%	>95%			
11	60-65%	>95%			
12	70-75%	>95%			
13	80-90%	>98%	0.30-1.0 µm Particle Size All bacteria Droplet nuclei (sneeze) Cooking oil Most smoke Insecticide dust Copier toner Most face powder Most paint pigments	Hospital Inpatient car. General Surgery Smoking lounges Superior commercial buildings:	Bag Filters -Nonsupported (flexible) microfibre fiberglass or synthetic media, 300-900 mm (12 to 36 in.) deep, 6 to 12 pockets. Box Filters -Rigid style cartridge filters 150mm (6 to 12 in.) deep may use lofted (air laid) or paper (wet laid) media
14	90-95%	>98%			
15	>95%	n/a			
16	n/a	n/a			
n/a	n/a	n/a	≤0.30µm Particle Size Virus (unattached) Carbon dust Sea salt All combustion smoke Radon progeny	Cleanrooms Radioactive material Pharmaceutical manufacturing Carcinogenic materials Orthopedic surgery	HEPA/ULPA Filters ≥99.97% efficiency on 0.30 µm particles, IEST Type A ≥99.99% efficiency on 0.30 µm particles IEST Type C ≥99.999% efficiency on 0.10-0.20 µm particles, IEST Type D ≥99.999% efficiency on 0.10-0.20 µm particles, IEST Type F
n/a	n/a	n/a			
n/a	n/a	n/a			
n/a	n/a	n/a			

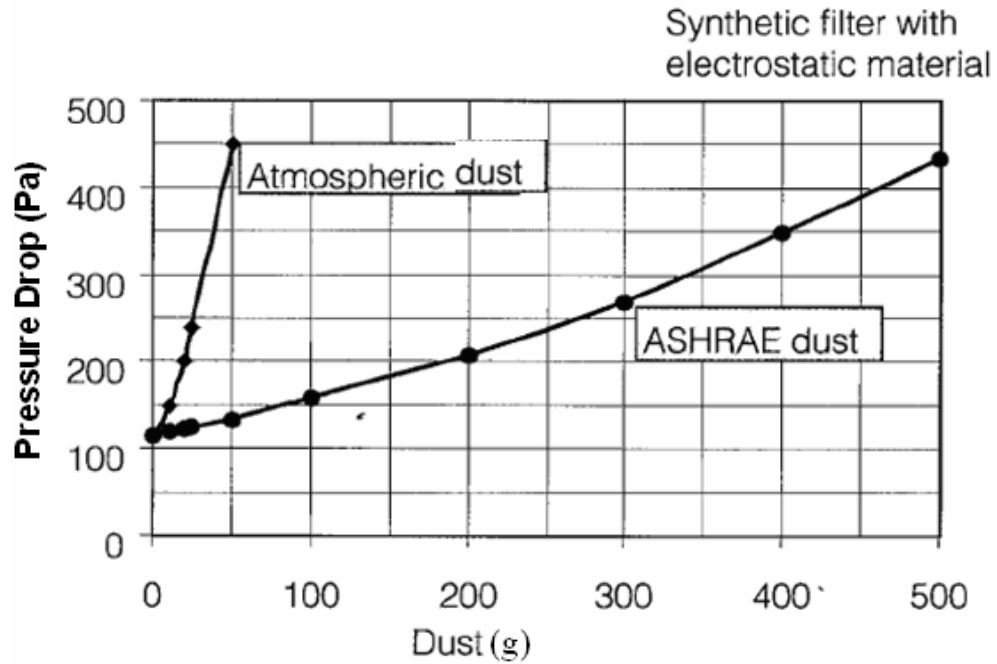


Figure 1-11 Comparison of laboratory test results to performance in real operating conditions of a synthetic filter [65]

Recent studies [67] have shown that dust holding capacity can be impacted by several parameters such as loading particle size, filter face velocity, filter packing density, filter fiber diameter, and in electrically active materials fiber charge, and particle charge. To achieve high dust-holding capacity, a fibrous filter material should be designed to have fine fiber diameters, low packing density, operate at low face velocity, and incorporate as much electrostatic interactions as possible. Thinner fibers make the media have more uniform pore size distribution and the filter has better ability to catch and retain particles [68].

Filtration cost often accounts for a large portion of the total cost in the ventilation system of a building. It can be described as the life cycle cost (LCC) [69]. LCC can be defined as follows:

$$LCC = \text{Investment} + LCC_{\text{Maintenance}} + LCC_{\text{Disposal}} + LCC_{\text{Energy}}$$

In above equation, Investment is capital costs of the filter installation when the new ventilation system was first installed (filters +frame + labor). $LCC_{\text{Maintenance}}$ and LCC_{Disposal} are total purchasing and disposal cost of an air filter. LCC_{Energy} was total running cost of energy (electricity to power the fan). It is calculated from the average pressure drop of the filters which is often taken as the mean value between initial pressure loss and final pressure loss during operation. Filter pressure drop is a measure of the force required to move air through the filter at a given velocity. Each component in the system contributes a resistance to the air flow, which results in a pressure drop across itself. The total system resistance is the sum of all the pressure drops along the air flow path (including the filter). The air filter pressure drop is a function of the velocity of the air and the filter type (medium). Pressure drop costs money. A 10 psi pressure drop requires approximately 1.5 HP or an 1100 watt increase in electrical power consumption for a compressor generating 100 scfm at 100 psig [70]. Over a 10-20 year period the overall life cycle cost is dominated by the cost of energy that can typically add up to over 80% of the total cost. The longer the period considered the larger would be the energy cost as a proportion of the total cost [71]. An example of a class F7 filter is shown in Figure 1-12 and its energy running costs account for 81% of the total cost.

Since the pressure drop across the filter directly affects energy running costs, a low pressure drop is an important element in keeping total running costs down and an effective way of optimizing the total cost of an installation. Caking is the build up of particulate material on the filter surface. Generally, when caking occurs, air permeability

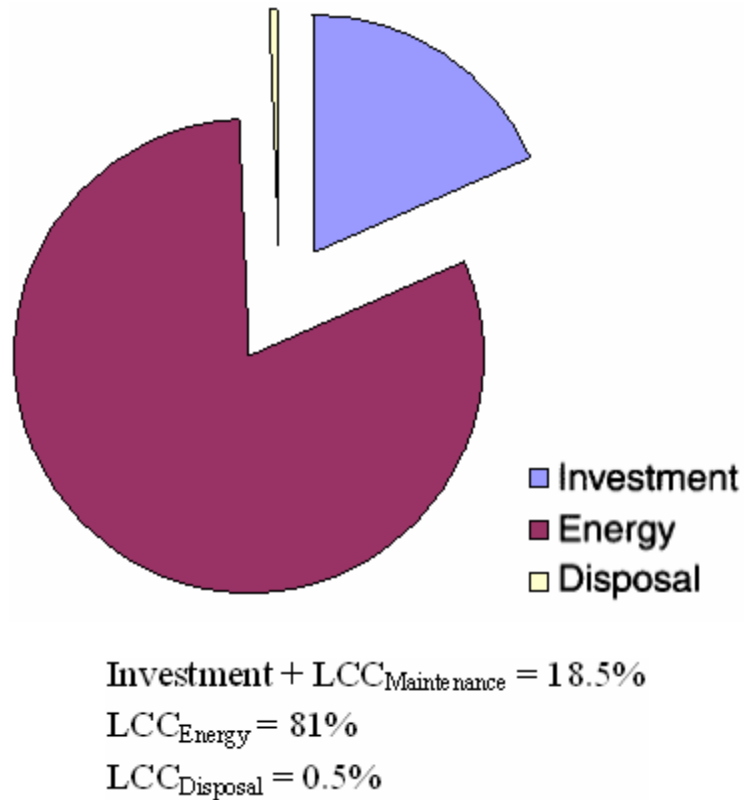


Figure 1-12 Cost breakdown of a class F7 filter [70]

decreases, dust-holding capacity increases, and pressure drop increases. But if the pressure drop increases drastically, it indicates the end of the useful lifetime of the filter. The most widely used method to measure the pressure drop across the filter is an air filter gauge [72]. Typically 1.6-1.7 inches of water is maximum pressure drop at which point testing generally stops [73]. If the pressure drop is higher than this specified value, the filter is rejected. It has been known that as filter efficiency and filter capacity increase, pressure drop also increases. One of the goals of air filtration research has been to increase holding capacity, maximize air permeability and delay the onset of caking while keeping delta P constant and low [73].

1.4.6 Air filtration materials

From the discussion above, one can conclude that a filter media determines the quality of filtration that a filter provides. The material that the filters are made of is often the most important factor that must be considered in the design of the filter if optimum performance is desired. Fibrous filters are efficient to capture submicrometer particles with a relatively small pressure drop compared to alternative dust collection devices, so they have been applied in disposable respirators, automotive cabin air filters, vacuum cleaner bags, indoor air filters, and industrial gas cleaning devices. Fibrous filter media are inexpensive and can be used without replacement for a long period of time (up to several months or years) at normal particle concentrations. Materials suitable for use as filter media include glass, polymers such as polypropylene, ceramic, and stainless steel, some of which can be used in high-temperature filtration. Over the past ten-year period there has been a considerable change in the filter media are used in ventilation applications [51]. Up until about 30 years ago, almost all such filters were based on glass fiber. Today, glass fiber only accounts for 40% of the market.

Glass fiber [74] is a common industrial fiber used at high temperatures. It has excellent tensile properties which only begin to degrade at about 288°C (550°F). Glass has poor resistance to alkalies and to strong acids such as hydrofluoric, concentrated sulfuric and hot phosphoric acids. Glass fibers also abrade at yarn intersections if the fibers are distorted by longitudinal or transverse forces. To decrease abrasion and acid/alkali degradation, glass fibers are applied in topical fields such as silicone/graphite or Teflon. Glass fabrics are generally used at low air-to-cloth ratios and need minimal shaker or reverse air forces for cake release. Glass has a high Young's modulus (the fiber

is brittle) so glass fibers are easily woven into cloth that is then cut and sewn into filter bags. In the cross machine direction (fill) some of the yarns may be texturized to improve particulate collection

Generally, glass fibers are very small and have a diameter of between 0.5-2.0 μm , which leads glass based media far weaker than synthetic media [41]. For this disadvantage, the glass fiber used in bag filters is laminated to a synthetic scrim and used together with the line of glue, which often covers the separator stitches and not only covers the needle holes, but also spreads the tensile load imposed by the separator stitches on the media when inflated in use.

In general, glass fibers are not easy to needle into nonwoven structures because needling can abrade or break scrim and/or batting fibers. Moreover, if the fibers are not crimped, a bat cannot preserve its integrity during manufacturing.

Needled glass felt has recently appeared in the market-place [74]. It is made of β -glass with about 4 μm diameter which assures high particulate collection (low penetration and low air-to-cloth ratios) and has a high Young's modulus. This glass felt is produced by lightly needling β -glass on one side to a woven glass scrim. A high temperature resistant silicone type resin is used to glue the needle glass to the scrim. Because the fabric is stiff, compared to other needled structures such as Nomex[®], cleaning could be a problem. Because of the high permeability of this glass fabric and high strength characteristics of the scrim and adhesive, bags of this material have been used for pulse jet cake removal.

Glass has high melting point, but also has a disadvantage from this [74]. If a dust laden glass bag filter have the dust in the ambient air for easy ignition, the consequent

fire burns rapidly with a very high heat and smoke generation. The dust on fibers helps the dust burn with plenty of oxygen. A bonding agent often used in glass media, phenol-formaldehyde resin, gives out a dense and acrid smoke.

Polymer air filters now take up the major air filter market [51]. This is because polymer based materials satisfy performance specifications of ventilation applications well.

The filtration efficiency of a filter is mainly determined by fiber size. Polymer fibers can be prepared in a wide range of sizes. By using different process parameters, different diameter fibers are possibly produced in range of from 0.1 μm to 100 μm [51], but the fiber diameter for a class F7 glass fiber material has very small range, and its average is 1 μm [51]. The fine diameter ensures high filtration efficiency. Polymer fibers can be made suitable for electrostatic charging and this can further improve filter efficiency. Depending on the type of polymeric materials, essentially two methods of charging materials, the triboelectric effect and the corona treatment can be used.

Using polymer fibers, it is possible to vary the fiber sizes throughout the thickness of the medium, so that dust is loaded in the interior of the medium, rather than on the surface. This gives a low pressure drop across the filter, resulting in low energy cost. Polymer based fibers combine high tensile strength and good strain resistance.

Based on energy use during manufacture and disposal, a polymer based filter material, with a plastic frame, impacts the environment least among any commercial filter currently available on the market [50]. It is reported that the polymer material itself seems able to reduce the growth or survival of microorganisms in multi-layered polymer medium [75]. Polymer based materials have the ability to be welded to ensure airtight

joints, and do not need any binder. It is also possible using polymer based filter media to produce a tailor-made filter media for a specific application.

Polymer fibers respond to fire very differently from glass fibers [74]. They have a much lower melting point than glass, so they characteristically melt away from the heat source. This property of polymer makes trapped dust encapsulated in the molten state of the media to burn. The net result is that polymer media burn with less heat and produce negligible smoke, with minimum amounts of toxic gas.

Long fibers [74, 76] produced by meltspinning are in some special applications. In spunbond processes, the melted polymer is pumped through a spinneret (die) onto a take-up system of a continuous wire. Fibers generally have diameters 7-60 μm . The webs are produced by thermal point bonding. The process of web production combined with fiber production is generally more economical than nonwoven production using staple fiber. Spunbond material is commonly used in some applications such as industrial air filtration for requirement of very high strength.

The meltblowing processes use hot air at the die tip to further extrude the fibers and produce 1-3 mm diameter fibers. These fibers produce soft, selfbonded fabrics that are usually used in HVAC and cabin filters where high performance fine filtration is required. Sometimes, meltblowing fiber based filters use a high electrostatic charge for high efficiency performances in air filtration, and for this a loss of electrostatic charge implies the loss in efficiency of the filter.

Nanofibers [77] generally refer to fibers with a diameter less than $1\mu\text{m}$. Polymeric nanofibers have been used in a number of commercial air filtration applications over the

last 20 years, and hold promise for technical benefits in an expanding field of filtration applications.

Small fibers in the submicron range, in comparison with larger ones, are well known to provide better filter efficiency at the same pressure drop. For nanometer-scale fibers, the effect of slip flow at the fiber surface has to be taken into consideration [78]. Due to the slip at the fiber surface, drag force on a fiber is smaller than that in the case of nonslip flow, which translates into lower pressure drop. On the other hand, the slip flow makes the portion of the air flowing near the fiber surface larger than that in the case of non-slip flow, which translates into more particles traveling near the fiber, resulting in higher diffusion, interception and inertial impaction efficiencies (see filtration mechanism) [79, 80]. Therefore, although smaller fiber size leads to higher pressure drop, interception and inertial impaction efficiencies will increase faster, more than compensating for the pressure drop increase. From consideration about dependence of efficiency and pressure drop on fiber sizes and effect of slip flow, small fiber sizes 0.2 to 0.3 μm are highly desired for filtration applications. Polymeric nanofibers can be produced by the electrospinning process.

Since the fibers have a small diameter, the thickness of the nanoweb can be quite small, for example, a thickness of four nanofiber diameters approaches one micron. With few mechanical properties that preclude the use of conventional web handling and filter pleating equipment, nanofiber webs can be applied onto various substrates for appropriate mechanical properties to allow pleating, filter fabrication, element handling, durability in use, and filter cleaning. Figure 1-13 shows an SEM of commercially-available nanofibers electrospun onto a cellulose substrate for air filtration [81]. The nanofiber diameter is

approximately 250 nm, compared to the substrate of cellulosic fiber, whose diameters exceeds ten microns. This composite filter media structure has been successfully pleated on high-speed rotary pleating equipment with minimal damage to the nanofiber layer. Figure 1-14 is a composite media sample that has been exposed to a submicron sodium chloride contaminant, with particles in the size range of 0.01 to 0.5 μm . The nanofibers are covered by the salt particles, while the larger substrate fiber has collected relatively few of the submicron particles [77]. Increased filtration efficiency for submicron contaminants can be achieved by nanofibers.

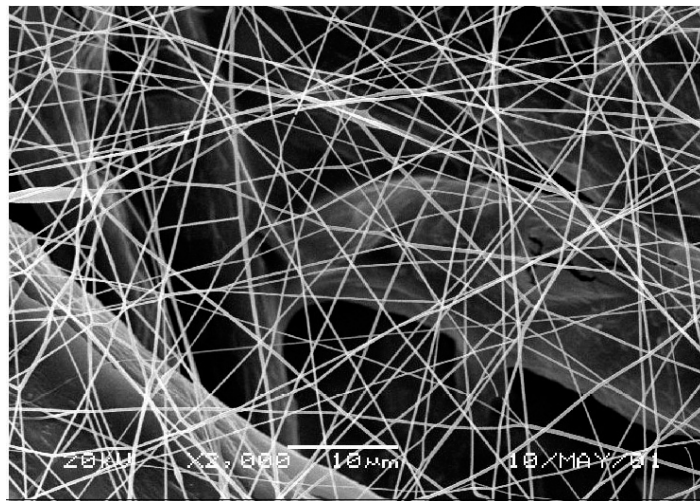


Figure1-13 Nanofibers on a Cellulose Filter Media Substrate [77]

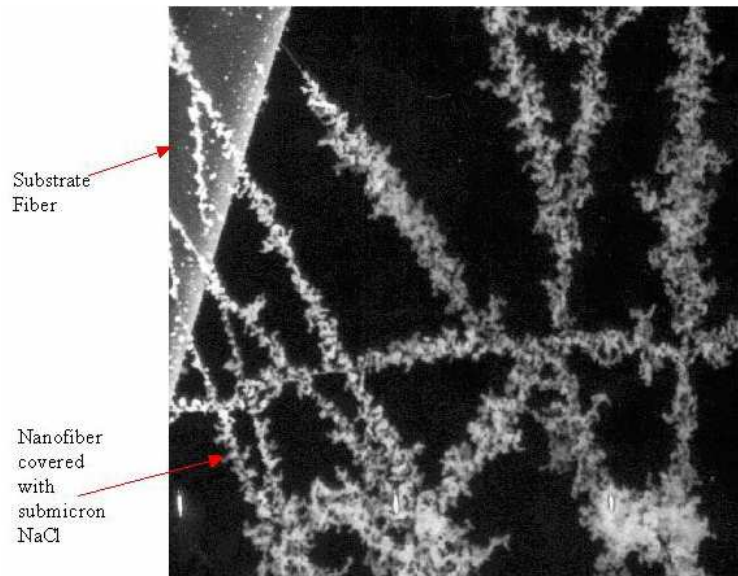


Figure1-14 Loading of submicron NaCl on a composite nanofiber structure [77]

1.4.7 Characterization of air filters

Filter Media characterization and the matching of media to the operating environment and particulate characteristics are important to understanding and optimizing media performance. [82]

There are four major criteria to evaluate filtration media permeability, filtration efficiency, filtration capacity (or life) and filtration cost, but many media parameters are important for properties of filtration media [83]. They cover from macroscopic physical parameters to microscopic filtration details. The macroscopic parameters are important for media processing and for durability in filtration application conditions. Most of them tensile strength, tear strength, burst strength, bend capability, thickness and basis weight are derived from the paper industry and are covered in Technical Association of the Pulp and Paper Industry (TAPPI) standards. The test methods for measuring parameters such as pore size, permeability, particle collection efficiency, particle loading and retention

characteristics are standardized by SAE, ASTM, IES and others. Generally, all the macroscopic measurements are decided by the media composition. Fiber type, saturate resin, manufacturing process, post treatments and uniformity criteria have impact on these macroscopic parameters.

Microscopic properties of filter media are used in media optimization of filtration performance of filters. The elementary parameters provide the most insight for a primitive look at media types and how they perform. Figure 1-15 [82] shows two basic parameters, solidity and fiber diameter. For a fibrous filter media, the media solidity describes the volumetric fraction or percentage of solids. The fiber diameter and/or knowledge of the fiber diameter distribution decide much about the filtration performance of a media. For example, the Knudsen Number (Kn , a dimensionless number defined as the ratio of the molecular mean free path length to a representative physical length scale) [82], is important to nanofiber based media. Because the diameter of nanofibers is very small, Kn becomes big and cannot be neglected, indicating slip or transition flow that will yield a significant effect on particle collection and pressure drop performance. The inter-fiber space reduces as solidity increases. For the media with small diameter, a single inter-space is smaller and the density of inter-spaces is larger than that with big diameter. What the particle sees will be different depending upon the solidity versus fiber diameter relationship and the particle diameter.

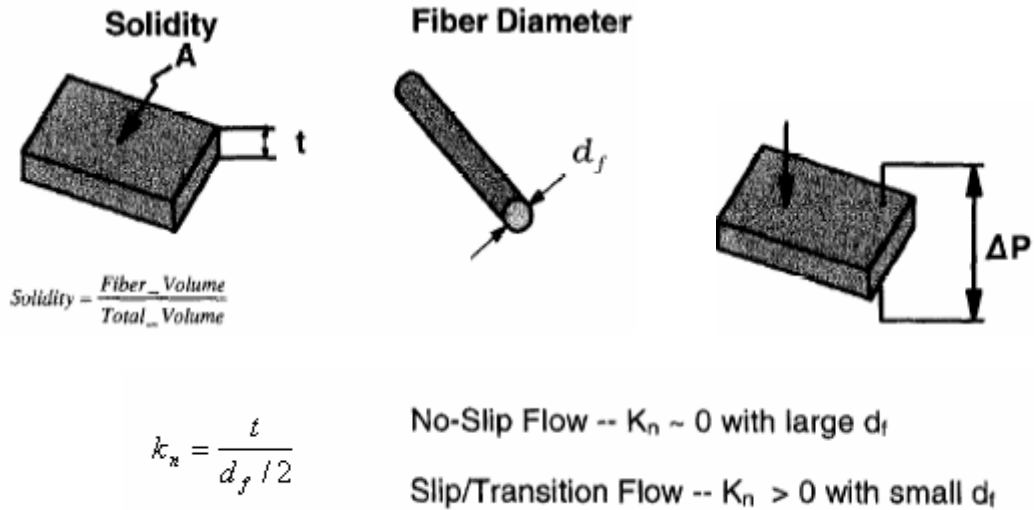


Figure1-15 Media Characterization [82]

1.4.8 Filter media defects

The ideal random structure of filter medium should have an expected statistical variation of parameters, but in fact there are defects in filter media [82], which limits media design optimization. When the raw materials experience manufacturing processes, specific ordered variation is introduced, which leads to defects. Defects range from gross defects that can be seen by naked eyes to microscopic defects that can be detected only by sophisticated apparatus.

In Figure 1-16 there are some SEM examples of defects in the medium [82]. Figure 1-16 (a) shows a poorly distributed saturating resin. The high solidity region will worsen pressure drop and particle collection. Figure 1-16 (b) illustrates a fiber defect. There is a large fiber in the circular pinhole which changed the fiber deposition pattern during manufacture. When the higher velocity air flows through the hole, it will orient the fiber

in the flow direction so this type of defect cannot be compensated. Figure 1-16 (c) and (d) show fiber diameter distribution defects. There are few if any small fibers near large fibers. This defect generally is compensated by a thick media for the lower than expected efficiency, with an increased pressure drop penalty.

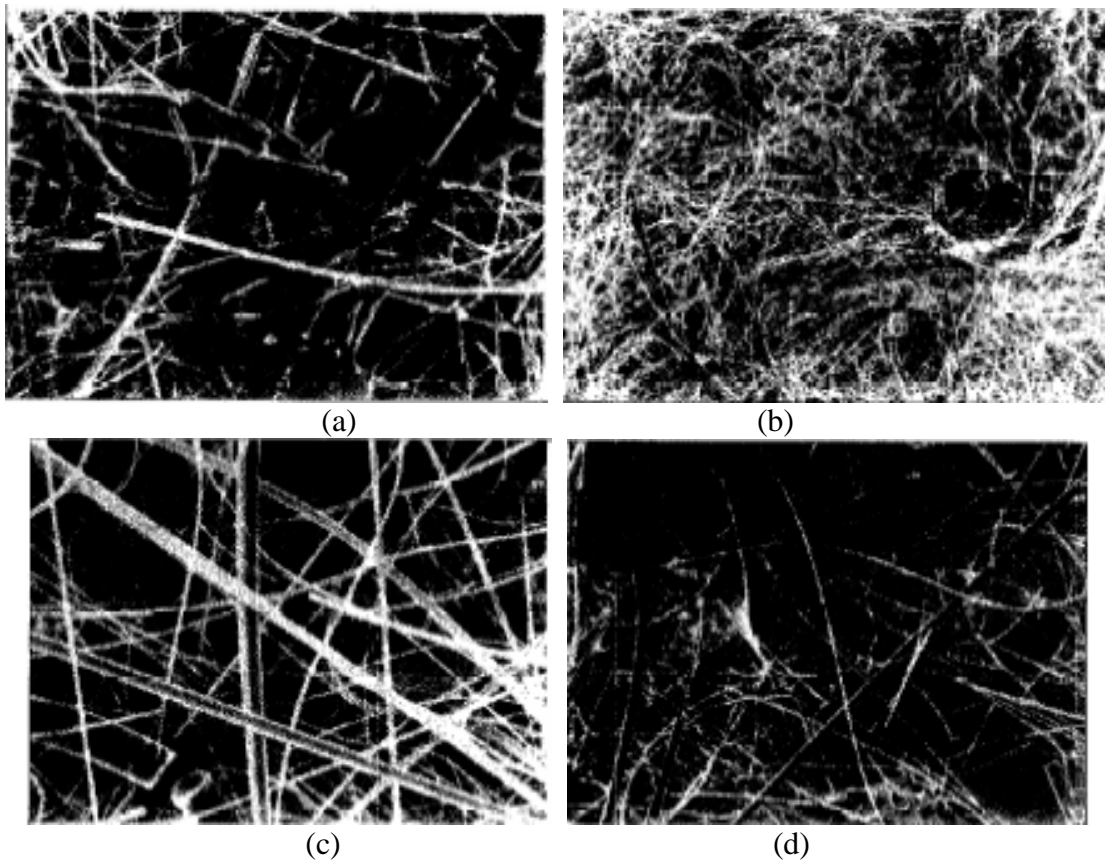


Figure 1-16: Media Defects [82]

There are many more types of defects in practice. Because of all of these defects, the media design cannot be optimized and theoretical predictions do not conform to experiments. In order to obtain realistic theoretical predictions of filtration performance, each caused detrimental effect has to be quantified.

1.4.9 Microorganism on air filters

It has been indicated that air filters have effect on the increase of microorganism concentration in air-conditioned rooms [84]. In the air, there are not only mineral and soot particles, but also bioaerosols involving plant debris, fragments of insects, skin scales and hairs of mammals, microorganisms (bacteria, fungal spores) and pollen. Air filters collect all of these particles on them. It has been shown that fiber materials did not inhibit growth of microorganism [85] [86], but, instead, microorganisms may use atmospheric dust deposited in air filters as nutrient if humidity is sufficient and filters are not exposed to an air flow [87]. For example, some research found that bacterial and mold spores collected in air filter media are able to survive over prolonged periods of time and mold growth might occur especially when humidities are high ($RH > 70\%$) and filters are not exposed to air flow [87]. At the same time, the captured microorganisms can reproduce immediately and be given out to the airflow, causing sick building syndrome [88].

Filter media can be treated with an antibacterial/antifungal coating, which does not effect on the filtration efficiency [89]. These coating chemicals inhibit the growth of mold, mildew, fungi, and bacteria in the filter media, thus keep the filter from being a potential incubator of these microorganisms. However, this treatment only kills those that would potentially grow on the filter, but cannot deal with those that are airborne and pass through the filter so that it cannot solve completely the problem that indoor levels of many air pollutants may be two to five times higher than outdoor levels.

The food industry increasingly needs air filtration equipment. Without filtration the airborne dust particles can bring bacteria, fungi and spores into the food products.

Therefore, it is necessary to eliminate these microbial contaminants [90]. Some research has been done to solve this problem. An air cleaning filter is coated with silver or an enzyme [91]. The coating converts oxygen into active oxygen and effectively sterilizes the microorganisms present in the air; and at the same time it directly hydrolyzes the cell wall of these microorganisms and destroys their cell membrane, thus killing the microorganisms.

1.4.10 Air filter market and trends

People spend as much as 90% of their time indoors so indoor air quality affects their health most [92]. It is now realized that the filtration system in a building not only protects the mechanical and electronic equipment, but more importantly, it needs to protect the people. Air is mainly cleaned by air filters [92]. Therefore, there is a very wide perspective and market for more efficient air filters.

The market of filters for cleaning air in homes, commercial buildings, and industrial plants around-the-world will rise from \$6 billion in 2005 to \$7.5 billion in 2009 [93]. The US market for air cleaners was a \$300 million business in 1998 with an expected growth rate of 10 percent per year. The average retail price for air cleaners has risen to \$100 [92]. Japan is the second largest market after the US. In the United States, of the total nonwovens market of approximately \$2 billion, filtration media represent its at least \$200-250 million [94]. One of the largest segments of nonwovens is needled felts for dust filtration, predominantly used in outside collectors or in pulse-jet filter.

The fibers used in air filters first include cotton, glass and later polymers. But polymers have disposal problem because they do not easily decompose in nature.

Recently, the fibers chosen for air filters are those existing plentifully in nature such as poultry feather and plants or grass cellulose fibers [95].

One trend of air filter media is toward needle punched felts as opposed to woven media. In the US needle punched felts are used more widely than woven media and the same is true in Europe [96]. In Japan needle punched felts account for 46% percent of the bag media market [93]. Thermobonded, molded and melt-blown nonwovens are being used for face masks. These two markets for industrial and medical uses represent converted nonwovens currently valued between \$40 million and \$50 million [96].

1.5 References

- [1] Parkinson, G. Chementator: a higher use for lowly chicken feathers. *Chem Eng* 1998; 105(3):21.
- [2] Papadopoulos, MC; El Boushy, AR; Roodbeen, AE; Ketelaars, EH; Effects of processing time and moisture content on amino acid composition and nitrogen characteristics of feather meal, *Anim Feed Sci Technol*; 14, 1986, p279–90.
- [3] Papadopoulos, MC; El Boushy, AR; Roodbeen, AE; The effect of varying autoclaving conditions and added sodium hydroxide on amino acid content and nitrogen characteristics of feather meal; *J Sci Food Agric*; 36, 1985, p1219–26.
- [4] Steiner, RJ; Kellems, RO; Church, DC; Feather and hair meals for ruminats Part IV. Effect of chemical treatments of feather and processing time on digestibility, *J Anim*

Sci; 57, 1983, p495–502.

- [5] Schmidt, WF; Line, MJ; Physical and chemical structures of poultry feather fiber fractions in fiber process development. In: TAPPI Proceedings: 1996 Nonwovens Conference; p135–140.
- [6] Fraser, RDB; MacRae, TP; Rogers, GE.; Keratins: their composition, structure, and Biosynthesis; Springfield: Charles C. Thomas Publisher; 1972, p31.
- [7] Murayama-Arai K, Takahashi R, Yokote Y, Akahane K.; Amino acid sequence of feather keratin from fowl. *Eur J Biochem* 1983; 132:501–7.
- [8] Woodin, A. M.; Molecular size, shape and aggregation of soluble feather keratin. *Biochem. J.* 57, 1954, p99- 109.
- [9] Arai, K. M.; Takahashi, R.; Yokote, Y.; Akahane, K.; Amino acid sequence of feather keratin from fowl. *Eur. J. Biochem.*; 132, 1983, 501-507.
- [10] Schmit, W.F.; Innovative feather Utilization strategies, *Proceeding Poultry Waste Management Conference*, Springdate, Arkansas, 1998
- [11] Martinez-Hernandez, Ana L.; Velasco-Santos, Carlos; De Icaza, Miguel; Castano, Victor M.; Microstructural characterisation of keratin fibres from chicken feathers; *International Journal of Environment and Pollution*; 23(2), 2005, p 162-178
- [12] Alberts, B., Bray, D., Lewis, J., Raff, M., Roberts, K., Watson, J.D.; *Molecular Biology of the Cell, 3rd Edition (1994)*, Garland Press, New York, NY
- [13] Kar, P. and Misra, M.; Use of Keratin Fiber for Separation of Heavy Metals from Water, *Journal of Chemical Technology and Biotechnology*, 79, 2004, p1313-1319

2004

- [14] Barone, J.R. and Schmidt, W.F.; Polyethylene Reinforced with Keratin Fibers Obtained from Chicken Feathers, *Composites Science and Technology* (2005), 65, 1173-181
- [15] Rock, J. W.; Barbieri, R. J.; Justice, J. M.; Kurtis, K. E.; Gentry, T. R.; Nanko, H. ; Characterization of chicken feather materials for use in biocomposites; *Proceedings of the American Society for Composites, Technical Conference* (2005), 20th, 143/1-143/15
- [16] Bonser, R.H.C. and Purslow, P.P. (1995). The Young's modulus of feather keratin. *Journal of Experimental Biology*, 198, p1029-1033.
- [17] Jeffrey, W; Koc, J. W.; Physical and mechanical properties chicken feather materials, 2006, A Thesis Presented to The Academic Faculty
- [18] Hong, C.K., Wool, R.P. (2005). Development of Bio-Based Composite Materials from Soybean Oil and Keratin Fibers. *Journal of Applied Polymer Science*, 95: p1524-1538.
- [19] <http://www.satyamag.com/feb06/schmidt.html> 07/28/06
- [20] <http://www.mcsweeneys.net/2000/06/19schmidt.html> 07/27/06
- [21] Gassner, III; George; Schmidt; Walter; Line; Michael J.; Thomas; Clayton; Waters; Rolland M.; Fiber and fiber products produced from feathers; January 6, 1998, USP 5,705,030
- [22] <http://www.ehponline.org/docs/2000/108-8/innovations.html> 07/27/06
- [23] http://www.fass.org/fasstrack/news_item.asp?news_id=269 , 11/23/06
- [24] Wang, Zhengshun, A process for making specific paper by using fowl feather.

- Faming Zhuanli Shenqing Gongkai Shuomingshu* (2005), 9 pp, CN 1570273 A
- [25] <http://www.scienceblog.com/community/older/archives/H/usda597.html> 07/28/06
- [26] Ye, Weiqin; Broughton, Roy M. Jr.; Hess, Joseph B. Chicken feather fiber: A new fiber for non-woven insulation materials, *Proceedings of the Largest International Nonwovens Technical Conference (1998)*, p7.1-7.7
- [27] http://www.phschool.com/science/science_news/articles/materials_take_wing.html
08/12/2006
- [28] Berenberg B., Natural fibers and resins turn composites green, *Compos Technol* ; 7(6); 2001; p12–6.
- [29] Dweib MA, Hu B, O_Donnell A, Shenton HW, Wool RP. All-natural composite sandwich beams for structural applications. *Compos Struct.*; 63(2); 2004; p147–57.
- [30] Barone, Justin R.; Schmidt, Walter F.; Polyethylene reinforced with keratin fibers obtained from chicken feathers, *Composites Science and Technology* 65 (2005) 173–181
- [31] Hamoush, S.A., El-Hawary, M.M. (1994). Feather fiber reinforced concrete. *Concrete International*, 16(6); p33-35
- [32] Mehta, P. K. and P. J. M. Monteiro (2006). *Concrete: Microstructure, Properties, and Materials*. Third Edition. McGraw-Hill, New York.
- [33] Kar, P.; Misra, M.; Use of keratin fiber for separation of heavy metals from water; *Journal of Chemical Technology and Biotechnology*, 79(11), November, 2004, p 1313-1319
- [34] Schmidt, W.F.; Innovative feather utilization strategies, *Proceeding Poultry*

- Waste Mnagement Conference*(1998), Springdate, Arkansas.
- [35] Nakamura, Y.; Wool fiber, *Polymeric Mterials Encyclopedia*, CRC Press, USA, Bol, 11, 1996, p8769-8776
- [36] Howitt, F. O.; Wool, silk and regenerated protein fibers-chemistry; *Review of Textile Progress* (1955), p70-90.
- [37] Goddard, David R.; Michaelis, Leonor; A study on keratin; *Journal of Biological Chemistry* (1934), 106, p605-14
- [38] Jones, C. B.; Mecham, D. K.; The dispersion of keratins I. The dispersion and degradation of certain keratins by Na₂S; *Archives of Biochemistry* (1943), 2, p209-23
- [39] Jones, Chase B.; Mecham, Dale K.; The dispersion of keratins II. Studies on the digestion of keratins by reduction in neutral solutions of protein denaturants, *Archives of Biochemistry*, 3, 1943, p193-202
- [40] Montefusco, Ahlstroms Francesca; The use of nonwovens in air filtration, *filtration and separation*, , 42(2), March 2005, p30-31
- [41] <http://www.environmental-expert.com/resultteachpressrelease.asp?cid=5122&codi=5730> 08/12/06
- [42] Derek B Purchase & Ken Sutherland. (2002.) *Handbook of Filter Media*, Elsevier Advanced Technology, 2nd Edition.
- [43] Sutherland, Ken; How filter media have evolved over the last 40 years *Filtration and Separation*, v 40, n 3, April, 2003, p 28-31
- [44] Chatterjee, K.N. et al. Polyester needle punched nonwoven dust filter for controlling air pollution (Part 4), *Man-make textile in India*, 33(8), 1990, P276-9

- [45] Hearle, J W S; Sultan, M A I; Chaudhry, T N; A study of needled fabrics part II: effects of the needling process, *Journal of textile institute*, 59 (2), 1968, p103-116
- [46] Igwe, G J I; Smith, P A; Influence of some production parameters on the characteristics of needled felts for air filtration, *Melliand Textilberichichte-International textile reports*; 14(8), 1985, p626,
- [47] Barlow, G.; Sayers, I. C., Filter fabrics for dust control, *Filtration and Separation*, v 11, n 5, Sep-Oct, 1974, p467-470
- [48] http://www.strionair.com/air_filtration_principles.asp 10/02/06
- [49]http://www.ecompressedair.com/library/compressedairfiltersbasics_p2.shtml10/02/06
- [50] www.oznet.ksu.edu/library/hous2/ncr393.pdf 10/02/06
- [51] Anon, Indoor air filtration: Why use polymer based filter media? *Filtration and Separation*, v 38, n 2, March, 2001, p 30-32
- [52] B. Dean Arnold, Nonwoven material performance in air filtration applications, *International Nonwovens Technical Conference 2001*
- [53] Ptak, T. J.; Selection and optimization of air filters; *Advances in Filtration and Separation Technology*, 15, 2002, 676-680;
- [54] Igwe, G. J. I.; Smith, P. A.; The influence of some production parameters on the characteristics of needlefelts for gas filtration; *Journal of the Textile Institute*; 77(4), 1986, p263-6
- [55] Atwal, Mahabir S.; Factors affecting the air resistance of nonwovens needle-punched fabrics; *Textile research journal*; 57(10); 1987, P574-579
- [56] Lamb, G. E. R., Costanza, P. A.; Influences of fiber geometry on the performance of nonwoven air filters, Part 2: fiber diameter and crimp frequency; *Textile Research*

- Journal*, 49(2), 1979, p79-87
- [57] Kothari, V. K., Newton, A.; The air permeability of nonwoven fabrics, *Journal of the textile institute*, 65(10), 1974, p525-531
- [58] Kent, R. W., J.; The air-permeability of non-woven fabrics; *Journal of the textile institute*, 67(6); 1967; p220
- [59] Hearle, J. W. S., Sultan, M. A. I.; A study of needled fabrics Part I: experimental methods and properties; *Journal of the textile institute*; 58(6); 1967; p251-265
- [60] Paul, Parishit; Chatterjee, K.N.; Mukherjee, A.K.; Study on air permeability of needle punched non-woven fabric; *Man made textiles in India*, 47(7), 2004, p248-251
- [61] Hearle, J. W. S., Sultan, M. A. I., A study of needled fabrics Part IV: the effects of stretch, shrinkage, and reinforcement, *Journal of textile institute*, 59, 1968, p161-182
- [62] http://www.germology.com/air_filters.htm 09/23/06
- [63] <http://www.airguard.com/industrynews.htm> 09/23/06
- [64] <http://www.imionline.org/oldarticles.html>, 09/26/06
- [65] http://www.knfilters.com/audio/audio_book_mp3.htm 09/26/06
- [66] Gustavsson, Jan, En 779:2002 - New European test method for air filters, *Filtration and Separation*, 40(2), March, 2003, p 22-26
- [67] Walsh, D.C.; Possibilities for the design of fibrous filter maters with enhanced dust holding capacity; *J. Aerosol SC*; Vol. 29, Suppl. I; 1998 pp S939-S940
- [68] <http://www.amsoil.com/StoreFront/eea.aspx>, 10/01/06

- [69] <http://www.eurovent-association.eu/web/eurovent/web/recommendations/REC10.pdf>
01/02/2007
- [70] http://www.ecompressedair.com/library/compressedairfiltersbasics_p3.shtml,
10/07/06
- [71] Kjell Folkesson & William Lawrance, FläktWoods Group, Calculate ventilation Life Cycle Cost and count on savings, *The Life Cycle Cost (LCC) of air handling units*,
http://www.touchbriefings.com/pdf/1140/Flakwood_tech.pdf, 10/07/06
- [72] <http://terrauniversal.com/products/measuring/airfiltergauge.php> 10/08/06
- [73] Alper, Hal; Novel surface modification which increases filter holding capacity at constant delta P; *the proceedings of American filtration and separation society*; 2003
- [74] Anderson, Bill; Air filters: Synthetic or glass based media, *Filtration and Separation*, 40(2); March, 2003, p 28-30
- [75] Kemp, P. C.; Neumeister-Kemp, H. G.; Lysek, G.; Murray, F. ; Survival and growth of micro-organisms on air filtration media during initial loading; *Atmospheric Environment* 35(28), 2001, p4739-4749
- [76] Sidney, C Stern; Dedham, Mass, Mechanisms and materials for fabric dust filtration, *3rd international fabric alternatives form: proceeding, phoenix, Arizon.*, 1978, p1-4
- [77] Schaefer, J.W., McDonald, B., and Gogins, M., “Nanofibers in Aerosol Filtration”, Nanotechnology for the Soldier System Conference, sponsored by the U.S. Army Soldier Systems Command (SSCOM), Army Research Office (ARO), Army Research Laboratory (ARL), and the National Science Foundation (NSF), Cambridge, MA, July 1998.

- [78] Brown, R.C., *Air Filtration*, Pergamon Press, Oxford, 1993.
- [79] Stechkina, I.B., A.A. Kirsch and N.A. Fuchs, "Studies on fibrous aerosol filter -- IV calculation of aerosol deposition in model filters in the range of maximum penetration," *Ann. Occup. Hyg.*; 12, 1969, p1-8
- [80] Pich, J. "Gas filtration theory," *Filtration -- Principles and Practices*, edited by M.J. Matteson and C. Orr, 1987, Chapter 1, 1-132
- [81] Kristine Graham, Ming Ouyang, Tom Raether, Tim Grafe, Bruce McDonald, Paul Knauf; Polymeric Nanofibers in Air Filtration Applications, the *Fifteenth Annual Technical Conference & Expo of the American Filtration & Separations Society*, Galveston, Texas, April 9-12, 2002.
- [82] Anon, Air filtration media for transportation application, *filtration and separation*, March 1998, p124-129
- [83] Schaefer, J. W., "Automotive and Turbine Air Cleaning," Air and Gas Filtration Short Course, University of Minnesota, August, (1995)
- [84] Pasanen, P., Pasanen, A.L. and Jantunen, M. Water condensation promotes fungal growth in ventilation ducts. *Indoor Air* 3, 1993, p106-112.
- [85] Maus, R.; Goppelsroeder, A.; Umhauer, H., Viability of bacteria in unused air filter media, *Atmospheric Environment*, 31(15), Aug, 1997, p 2305-2310
- [86] Barnett, Tim; Fabric filter dry dust collection: Food industry experiences, *Filtration and Separation*, v 37, n 3, 2000, p 34-35
- [87] Maus, R.; Goppelsroeder, A.; Umhauer, H.; Survival of bacterial and mold spores in air filter media, *Atmospheric Environment*, 35(1), 2001, p 105-113
- [88] Kelly-Wintenberg, Kimberly et al, Air filter sterilization using a one atmosphere

uniform glow discharge plasma (the Volfilter), *IEEE Transactions on Plasma Science*, v 28, n 1, Feb, 2000, p 64-71

- [89] Foarde, Karin K.; Hanley, James T.; Hanley, James T.; Determine the Efficacy of Antimicrobial Treatments of Fibrous Air Filters, *ASHRAE Winter Meeting CD, ethnical and Symposium Papers, ASHRAE 2001 Winter Meeting CD, Technical and Symposium Papers*, 2001, p 217-231
- [90] Wirtanen, Gun.; Miettinen, Hanna.; Pahkala, Satu.; Enbom, Seppo.; Vanne, Liisa. Clean air solutions in food processing, *VTT Publications*, (482), 2002, p94
- [91] Lee, Seong Hwan, et al; Air cleaning filter, PCT Int. Appl.; WO 2006009341A1, 2006, 23 pp
- [92] Anon, Air filter trends, *Filtration and Separation*, v 35, n 2, Mar, 1998, p130-133
- [93] McIlvaine, Bob. *Filtration and Separation*, 34(10), Dec, 1997, p1029-1032
- [94] Bergmann L., Nonwovens for filtration media, *TAPPI Journal*, 72(1); Jan. 1989, p77,
- [95] Petra Meinke and Joe Kiolbasa; Improve Dust Collection, *Plant engineering*, 57(10); 2003, p 54-56
- [96] [http://www.environmental-eexpert.com/resultteachpressrelease.asp?cid=5122](http://www.environmental-eexpert.com/resultteachpressrelease.asp?cid=5122&codi=5730)
[8/12/06](http://www.environmental-eexpert.com/resultteachpressrelease.asp?cid=5122&codi=5730)
- [97] Reddy, Narendra.; Yang, Yiqi.; Novel protein fibers from wheat gluten; *Biomacromolecules*, 8(2), February, 2007, p638-643

CHAPTER 2

PREPARATION OF FEATHER FIBER FOR USE IN FIBROUS PRODUCTS

2.1 Introduction

Chicken feathers (CF) directly collected from a chicken processing plant are always dirty and contain various foreign materials, such as skin, blood, feces and flesh, so they need washing by soap. On untreated feathers there are many kinds of bacteria such as aerobic, anaerobic and enteric bacteria. If they grow on the feathers, they will use feather keratin and decompose it, finally degrade CF and make CF very weak. Therefore, before using CF fiber, it is necessary to sterilize CF to inhibit bacteria. In this chapter, sterilization results of CF are discussed by using four different agents 10% peroxide, a mixture of acetone and water, 5% household bleach (Clorox ®) with pH adjusted to 8 and 95% ethanol. In the sterilization the standard plate count method was used for determination of bacterial numbers.

Since bacteria on feathers occur both singly and in aggregates, the feathers must be washed with sterile saline so that the aggregates are broken up and a suspension of single cells is achieved to estimate the number of bacteria in a gram of feathers. The bacteria cell suspension is then serially diluted and the dilution is dispensed onto the sterile, solidified agar medium in the Petri plate until in the final plate there are 30 to 300 cells. This method is based on an assumption that each viable bacterial cell is separate from all

others and will develop into a single colony on solid media. Each colony is referred to as a Colony Forming Unit or **CFU** for short. The total number is obtained by multiplying the number of CFU by its dilution factor.

In this bacteria study, three classes of bacteria were studied. They were aerobic (incubation requires oxygen), anaerobic (incubation does not require oxygen), and enteric. Finally, separation of feather fibers from CF is also discussed.

2.2 Equipments

2.2.1 Stripping machine

The stripping machine was used to strip feather fibers from chicken feather. It was built at Auburn University by using the main part of Fehrer DREF 2000 Friction Spinning Unit--friction unit with some modification. Its mechanism sketch is shown in Figure 2-1. In it there are two feed roller, two small cylinders, one of which is smooth covered with a piece of rubber and the other is fluted. They push feathers onto two much higher speed, larger wire-covered friction combing rollers. The combing roller is a hollow metal roll with a spirally-grooved surface containing a special saw-toothed wire. It tends to grab the feather from the feed roller, but the feed roller feeds much more slowly than the combing roller turns. Barbs are stripped from the quill by the wire of the combing roller. The mixture of chicken feather quill and barbs is collected by a vacuum cleaner.

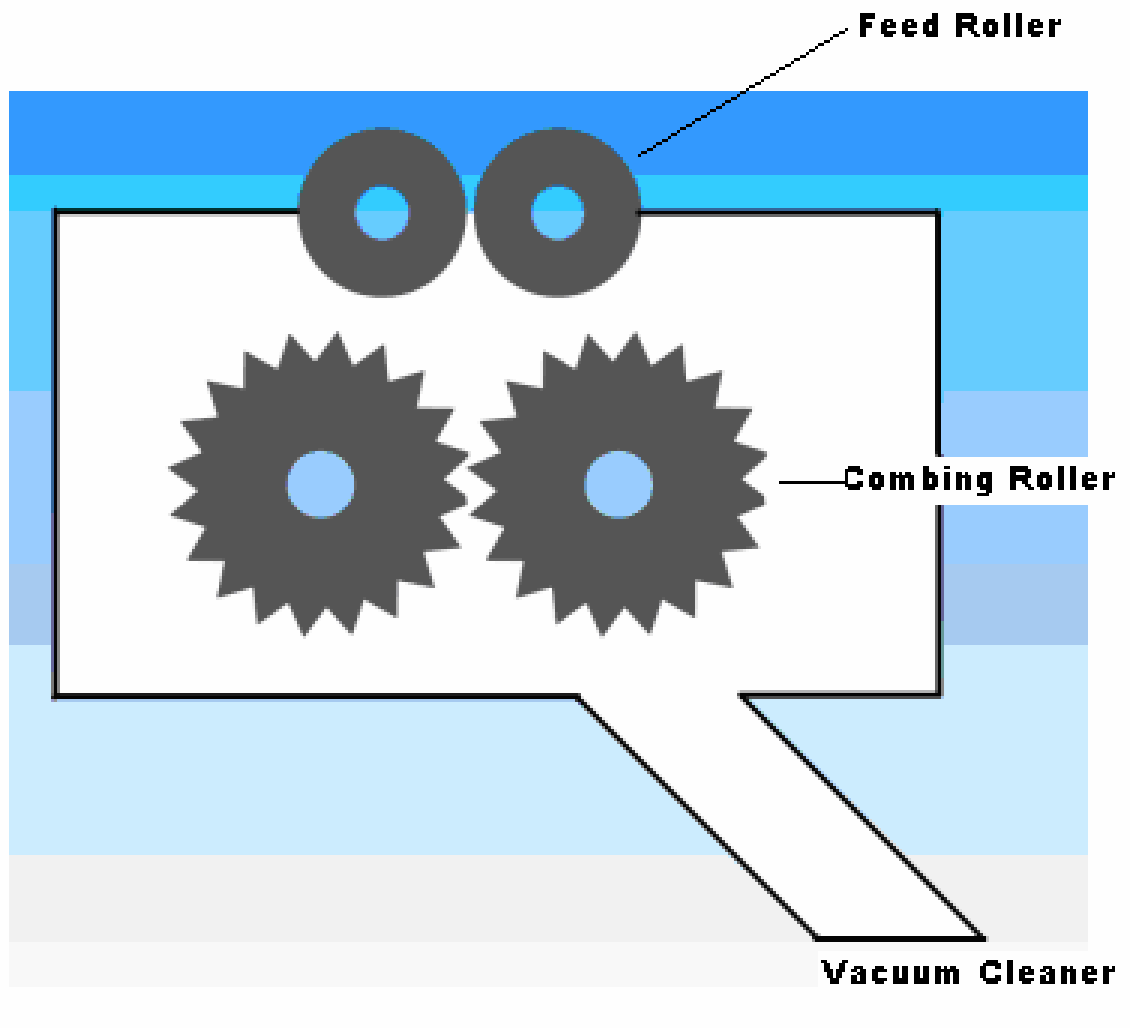


Figure 2-1 Mechanism sketch of Stripping Machine

2.2.2 Blender

After feather fibers were stripped from quills, the blender was used to separate the feather fibers from quills. Its basic structure is shown in Figure 2-2. It contains a cup and two couples of blades which can turn at high speed. Quills have higher real density than apparent density of feather fibers because feather fibers are thin and have tree-like structure and bigger surface area. When the blades turned at high speed, the mechanical agitation, caused by the blades, and a gravimetric process allowed their separation,

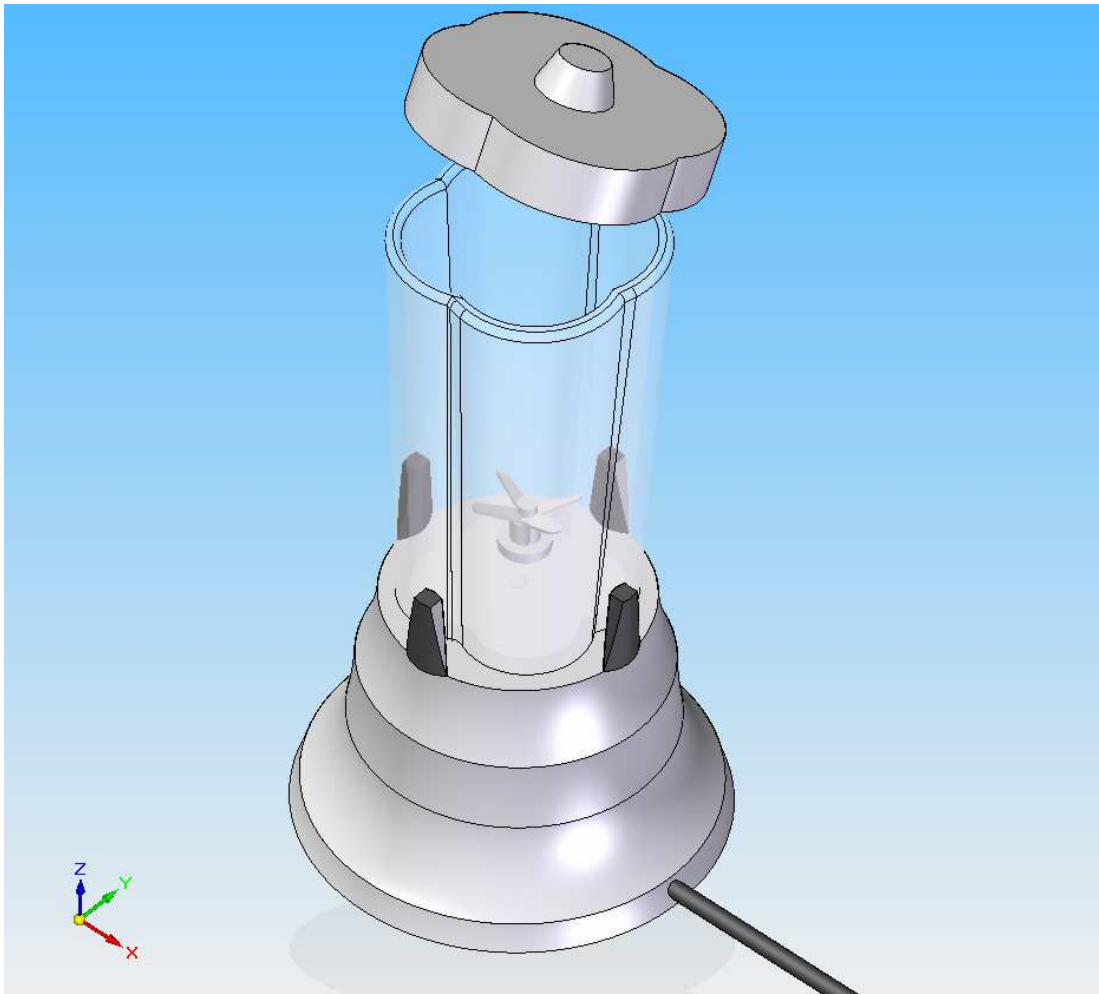


Figure 2-2 Blender sketch

2.3 Experimental [1]

2.3.1 Materials

The CF was obtained from the poultry processing plant at Auburn. The soap to wash CF was household product bought from Wal-Mart. Peroxide, acetone and ethanol to sterilize CF were from Fisher Scientific, New Jersey and household bleach (Clorox[®]) was from Mfd for the Clorox Company, California.

2.3.2 Procedure

2.3.2.1 Washing and sterilization

1. Washing

The untreated CF was washed with the 5% soap solution followed by rinsing. The wet washed CF was dried in a home dryer on moderate heat.

2. Sterilization

- **Treatment**

Four set of samples of washed CF were dipped at room temperature (21°C) for 30 minutes respectively in (1) 10% peroxide, (2) a mixture of acetone and water, (3) 5% household bleach (Clorox[®]) with pH adjusted to 8 and (4) 95% ethanol, then rinsed with water and air-dried.

- **Storage**

Every set of the dried treated CF was divided into three sets of samples again. One set of sample was not stored and tested. One set of sample was stored at room temperature (RT) and relative humidity (RH) of 65% for 3 months. One set of sample was stored at room temperature and relative humidity of 85% for 3 months.

- **Bacterial Testing**

---1g CF and 10 ml of sterile physiological saline (0.75% NaCl) were mixed together to make a 1:10 (w/v) dilution, then more saline was added to create 1:1,000,000 dilution. These dilutions were then spiral plated in duplicate onto the media: Plate-Count-Agar (PCA) media and MacConkey Agar (MA) (incubated aerobically at 37 °C), as well as Reduced Blood Agar (RBA) (incubated anaerobically at 37 °C). After 18 hours, colonies were quantified on a digital plate reader.

2.3.2.2 Separation of feather fibers and quills

After the dirty CFs were cleaned and dried, the clean feather fibers were separated using two successive steps as follows:

Step1: Strip fibers from feather and collect fibers and quills using the stripping machine (shown in Figure 2-1);

Step2: After the feather fibers were stripped from the quills, separate fibers and quills using a blender (shown in Figure 2-2).

2.4 Results and Discussions

2.4.1 Bacterial testing results

The following Table 2-1 shows the testing results for the growth of bacteria on feathers with different sterilization treatments.

As seen from the table, different sterilization agent produced significantly different sterilization results. From a mixture of acetone and water to 5% household bleach the sterilization results were improved.

Table 2-1 Bacteria recovered on feathers (Average count - CFU/g) [2]

Samples		A mix. of acetone and water treated	10% peroxide treated	95% ethanol treated	5% household bleach treated
PCA <i>(for aerobic bacteria)</i>	Pre-storage	2.05×10^7	2.89×10^5	1.30×10^3	0
	3 months RH = 65%	3.83×10^7	3.70×10^5	1.60×10^4	0
	3 months RH = 85%	7.55×10^7	1.18×10^5	0	0
RBA <i>(for anaerobic bacterial)</i>	Pre-storage	5.07×10^6	2.50×10^4	0	0
	3 months RH = 65%	5.93×10^7	8.21×10^5	0	0
	3 months RH = 85%	1.18×10^8	1.48×10^5	0	0
MA <i>(for enteric bacterial)</i>	Pre-storage	7.28×10^6	3.70×10^4	0	0
	3 months RH = 65%	7.84×10^5	0	0	0
	3 months RH = 85%	8.00×10^4	0	0	0

The mixture of acetone and water did not sterilize the feathers well. After the treatment there were still a lot of bacteria on it, 2.05×10^7 CFU aerobic bacteria, 5.07×10^6 CFU anaerobic bacteria and 7.28×10^6 CFU enteric bacteria. In this treatment, the numbers of all kinds of bacteria increased after storage of 3 months, the storage RH did not have much effect on aerobic bacteria, but had much on anaerobic and enteric bacteria. Higher humidity increased the number of anaerobic bacteria, but decreased enteric bacteria faster.

Peroxide did not sterilize the feathers well, either, and only a little better than the mixture of acetone and water. After this treatment, there were fewer bacteria left than the treatment of the mixture of acetone and water. Similar to acetone-and-water-mixture treated samples, the storage humidity did not impact much on aerobic bacteria but did on both anaerobic and enteric bacteria. Stored at these two different RH conditions, the number of the anaerobic bacteria increased but the enteric bacteria all died.

95% ethanol killed nearly all bacteria and only a small number of aerobic bacteria were isolated, which were much less than that found in a new feather pillow (see Table 2-2). Stored for three months at RH 65%, the number of aerobic bacteria increased and one log aerobic bacterial number increase was observed. Though the one log increase was seemingly large, it was probably nothing to be concerned about compared to 10% peroxide treated and a mixture of acetone and water treated feathers. The aerobic bacteria died at RH 85% after 3 months. With this treatment all of the anaerobic and enteric bacteria were killed. Even after storage for three months at different RH, neither of these two kinds of bacteria recovered.

Household bleach (5%) sterilized feathers very well and killed all of the three kinds of bacteria. After storing for 3 months at two different RH conditions no bacteria recovered. The RH of storage did not have effect on the recovery of these bacteria.

The following table (Table 2-2) showed the comparison of treated feathers before storage with commercial products and processed feather barbs. These commercial products and processed feather barbs specimens were not either sterilized or stored under any special conditions, but were used as found. From Table 2-2 it can be seen that on the all of commercial products, there were various kinds of bacteria, even though on some there were one or two kinds. On the processed feather barbs the three kinds of bacteria were found and the numbers of these three of bacteria were higher than on the commercial products. This may be because the processed barbs were very dirty and foreign materials on them made bacteria grow well on them. From the table, it can also be seen that the treatment of the mixture of water and acetone was ineffective at reducing the number of bacteria, compared to the other treatments. For this, the mixture of water and acetone could not be used as sterilization agent for chicken feathers at all. Ethanol (95%) was able to be used as sterilization agent for chicken feathers and eliminated anaerobic and enteric bacteria and some aerobic bacteria survived for a time, depending on storing conditions. Household bleach (5%) killed all the bacteria on feathers.

From above, it is seen that 5% household bleach treatment is the best. We were able to use the treated feathers immediately, but the feathers treated by household bleach would turn yellow after storage for some time, indicating degradation, which was not good for later use. Therefore, the feathers used in later experiments were all treated by 95% alcohol.

Table 2-2 Comparison of bacteria of commercials to feather products [2]

Bacteria counts	Average Count (CFU/g) pre-storage		
	PCA <i>(for aerobic bacteria)</i>	RBA <i>(for anaerobic bacterial)</i>	MA <i>(for enteric bacterial)</i>
Cotton	0	5.00×10^1	2.50×10^2
Wool	0	5.00×10^1	0
pillow-outer	1.66×10^4	1.04×10^4	0
pillow-inner	3.84×10^4	1.58×10^4	5.00×10^1
Processed feather barbs	2.58×10^6	2.88×10^6	2.90×10^3
A mixture of water and acetone treated feather	2.05×10^7	5.07×10^6	7.28×10^6
Peroxide treated feather	2.89×10^5	2.50×10^4	3.70×10^4
95% ethanol treated feather	1.30×10^3	0	0
Household Bleach treated feather	0	0	0

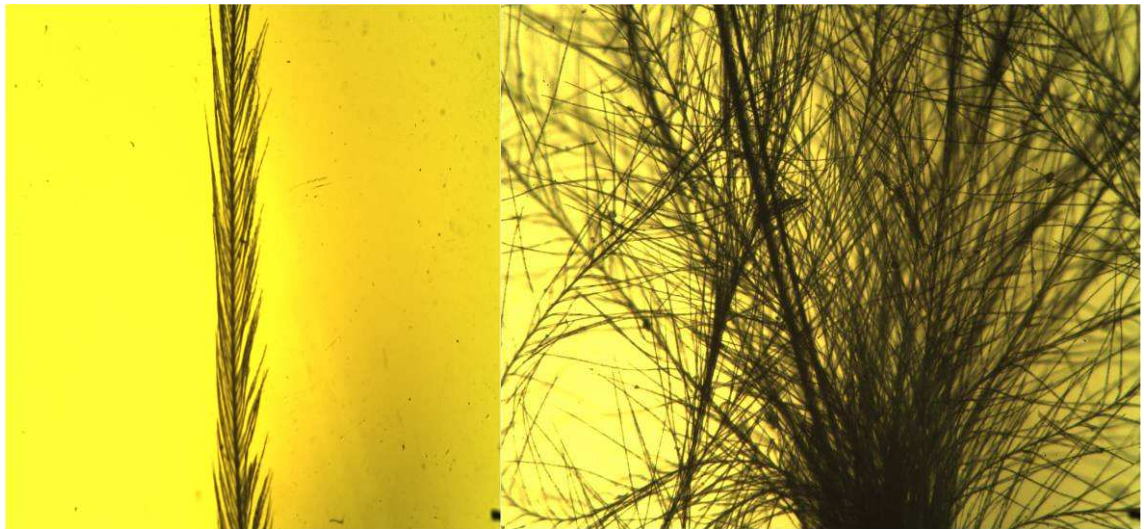
2.4.2 Feather fiber (barb) separation

The 95% alcohol treated chicken feathers were processed with the two separation steps for CF fibers. In the first step, the feather fibers were stripped from quills. In this step, not only feather fibers were produced but also some quill powders because the wires of the machine also worked on quills, scraped quill and made powders. Most part of quills of flying feathers is very hard and feather barbs were stripped very well from the hard part. Similarly, feather fibers were stripped from any hard quill very well. Feather fibers were not able to be stripped from soft quills. The top of flying feather quills is soft and its feather fibers were not stripped from it so the top of flying feather quill with a small fan of fibers and a long quill tail was left (Figure 2-3 (a)). In separation step two, almost half height of the blender cup was filled with CF having passed step one. The CF was processed for about ½ minutes in the blender and taken out by hand. In the blender the quill was cut into pieces and powder and fell down onto the bottom of the blender cup; the feather fibers were not cut and suspended in the middle of the blender cup. Not all the hard coarse quills were cut into powder and there were still some left connected with some feather fiber (see Figure 2-3 (b)). Some fibers were still tree-like.

After the two processing steps one pound CF gave about half pound of feather fiber and half pound of quill powder



(a) Feather fibers after stripped from quills



(b) Feather fibers after separation

Figure 2-3 Feather fibers

2.5 Conclusion

Chicken feathers collected from poultry processing plants were dirty and it was necessary for them to be washed by soap. There are kinds of bacteria growing on feathers, which would weaken feather fibers. Four kinds of sterilization agent were used to sterilize CF and they were a mixture of acetone and water, 10% peroxide, 95% ethanol and 5% household bleach (Clorox[®]) with pH adjusted to 8. The number of bacteria was measured after chicken feathers were sterilized and stored for 3 months at two different RH (65% and 85%) conditions. The measurement showed the household bleach treatment was the best. It killed all three classes of bacteria and no bacteria recovered after being stored for 3 months at two different RH conditions. 95% ethanol produced the similar results but it did not kill the aerobic bacteria completely and it was necessary to wait for the aerobic bacteria to die before the treated feathers could be used.

Using the device constructed at Auburn University, feather fibers were separated from hard feather quills but some still connected with soft quills. The blender used the quickly turning blades to cut quills into powders and employed mechanical agitation and a gravimetric process to separate fibers and quills powder. In the middle of the blender, the feather fibers were picked up by hand. Not all feather fibers were separated from quills and there were a small percentage of feather fibers still connected with quills, but their separation was enough for later research.

CFs were sterilized by 95% ethanol for later use of nonwovens and half pound of feather fibers was obtained from one pound of feather fibers for later research.

2.6 Reference

[1] Shen, Guanglin; Fan, Xiuling; Personal communications, 02/01/2004

[2] Macklin, Ken; personal communication, 12/04/2003

CHAPTER 3

NEEDLEPUNCHED NONWOVEN AIR FILTERS FROM CHICKEN FEATHER FIBERS

3.1 Introduction

As stated in Chapter 1, feather “waste” as a potential source of fibers is gradually being recognized; and studies have been begun to use chicken feather fibers to make commercial products. The current project not only provides novel products from chicken feathers, but also solves an environmentally sensitive problem of waste disposal. Two types of nonwoven fabrics had been made: needlepunched and thermal bonded. In this chapter needlepunched nonwovens are discussed.

Since feather fibers are short and stiff, and carding is difficult, an air-lay process was employed for mat formation. Needle punched fabric was made as follows: opening and mixing → mat formation → needlepunching.

Feather fibers mixed with polyester fibers were used to make needlepunched nonwovens. Feather fibers alone could not be entangled with each other during the needlepunching process - also because they were stiff and short. A certain percentage of polyester fibers were added to entangle with feather fibers. In addition, a scrim was used above and below the fiber mixtures, primarily to prevent feather fiber loss during handling.

3.2 Experimental

3.2.1 Material

Chicken feather fibers were obtained according to the method discussed in Chapter 2. Polyester staple fibers with denier 1.5 and length 2.50 inch for this study were from Wellman Industries Inc. (T0310). A point-bonded nonwoven polyester scrim having an areal weight of 31.5 g/m^2 was donated by V2 Composites Reinforcing Fabrics.

3.2.2 Equipment

3.2.2.1 Spinlab 338 (Fiber opener/blender)

Spinlab 338 is a machine primely used for opening and blending fibers. Figure 3-1 shows its mechanism. Its important function parts are a feed roller which is a small cylinder covered with saw-toothed wire, a liker-in roller which is a hollow metal roll with a spirally-grooved surface containing a large special saw-toothed wire and a vacuum box. The feed roller pushes the fibers to the liker-in. The liker-in turns at higher speed and tends to grab the fibers from the feed roller which restrains the fibers. Fibers are combed from the feed, opened in an air stream, mixed and collected on a screen by suction. Fibers were blended and opened well by three or more passes through the Spinlab338.

3.2.2.2 Vacuum box

The vacuum box is used to prepare mat. Its sketch is shown in Figure 3-2. There is a pipe between Spinlab 338 and the vacuum box. The fibers from the Spinlab, and through

the inlet, were sprayed into the top of a hollow pyramid and then pulled onto the screen of the vacuum to form a piece of mat.

3.2.2.3 Needlepunch machine

The needlepunch machine was used to produce needlepunched nonwovens. The needlepunch process is sketched in Figure 3-3. Barbed felting needles repeatedly passing into and out of the mat causes the mechanical interlocking (Figure 3-4).

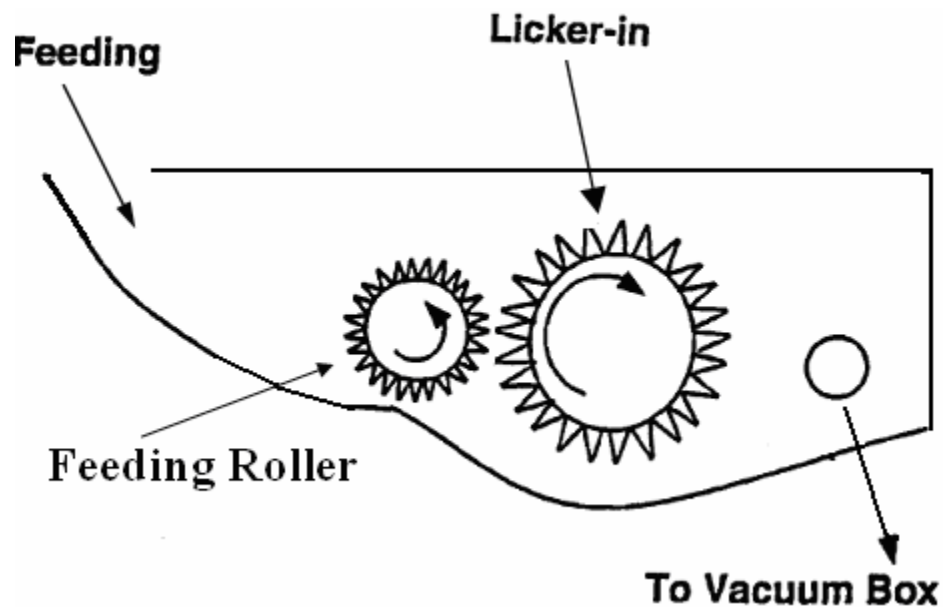


Figure 3-1 Mechanism sketch of Spinlab 338

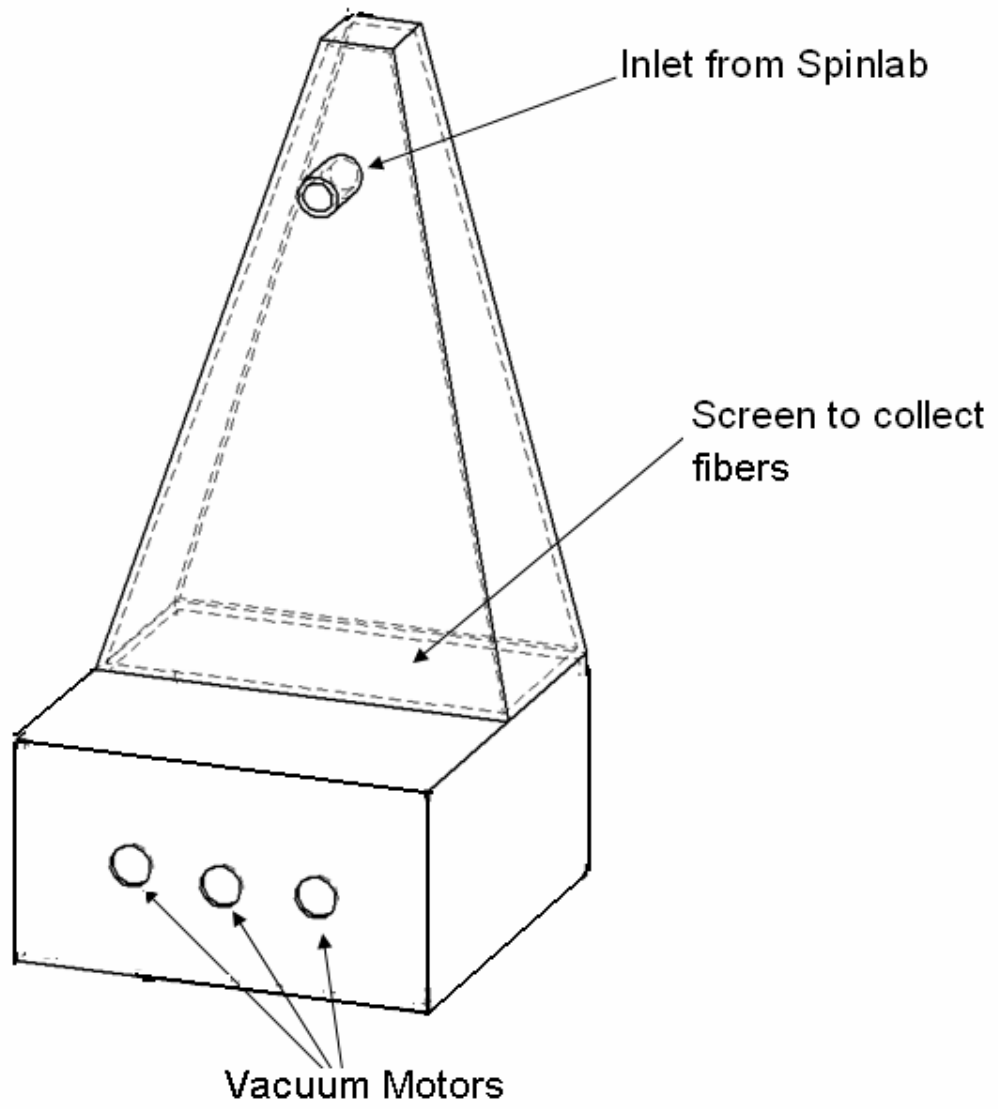


Figure 3-2 Sketch of Vacuum box

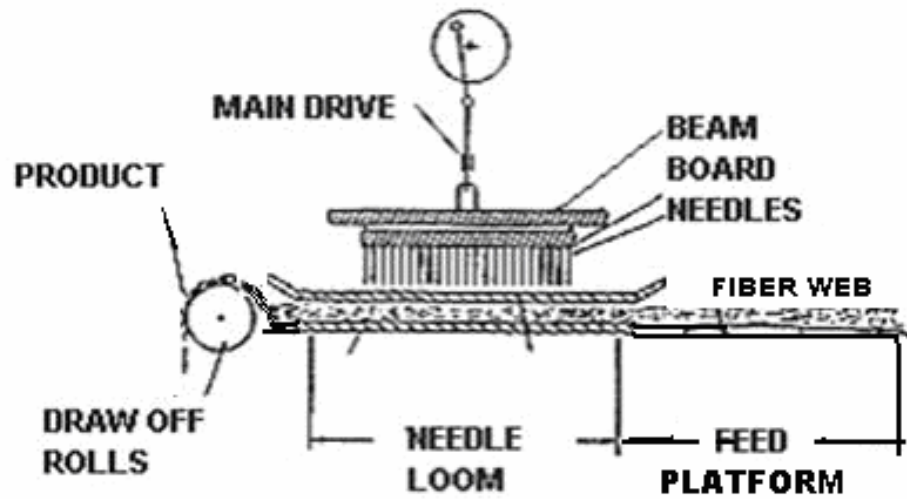


Figure 3-3 Needlepunch process sketch [1]

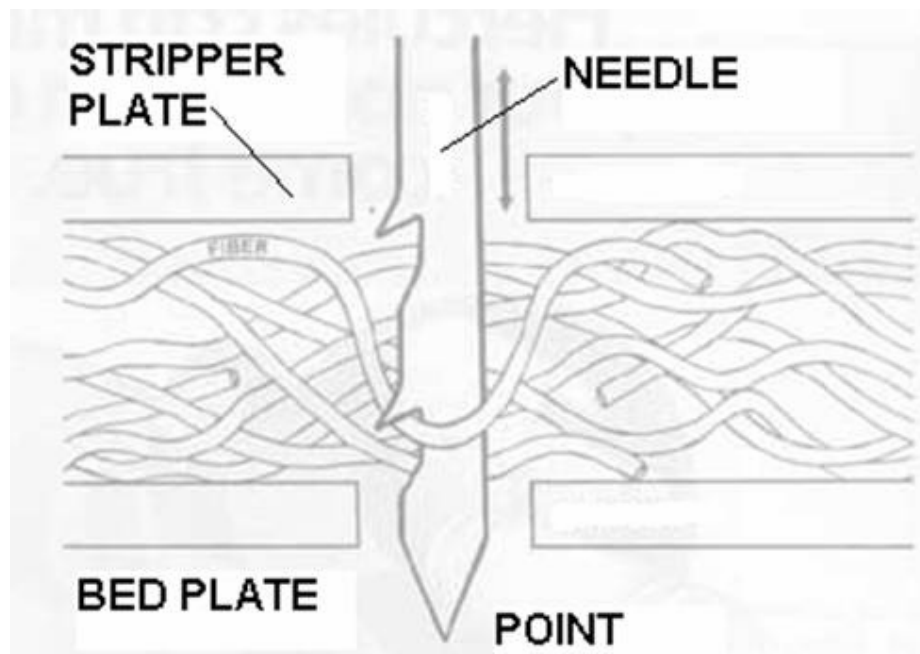


Figure 3-4 Needle Action – Schematic [1]

3.3.3 Procedure to produce needlepunch nonwovens

3.3.3.1 Opening and mixing of fiber mixtures

The polyester staple fibers directly from the manufacturing factory appeared as tangled clusters of fibers. After being opened four times with Spinlab 338, tangled fibers became separated, resulting in an accumulation of singular fibers. The opened polyester staple fibers and a percentage of feather fibers were blended 3 times to make the feather fibers distribute evenly in the polyester fibers. The samples were produced with the various combinations of fibers mixed ratio, and mixtures fibers area density. The experiment design about these factors is shown as following Table 3-1.

3.3.3.2 Preparation of PET and feather fiber mat

To prepare the PET and feather fiber mat by air-laying, two pieces of scrim were used to cover one piece of mat; otherwise, fibers would fly everywhere during needlepunching process. A piece of polyester scrim was laid on the screen of the vacuum box first; next, a pipe connected Spinlab 338 with the vacuum box; and then the PET and feather fiber mixtures were sprayed onto the scrim on the screen of the vacuum; finally, the other piece of polyester scrim covered the fibers.

3.3.3.3 Needlepunching PET and feather fiber mat

The needles 15×18×36×35PB-A from Foster 20 6-22-4B were used. The samples experiment design with various needle densities was shown in Table 3-1.

Table 3-1 Experiment design for needlepunched nonwovens

Areal Density (g/m ²)	Feather fiber% /PET%	Times of experiencing Needle punching process for each side (Nd*)		
		1/1	2/2	3/3
100	75/25	√	√	√
	67/33	√	√	√
	50/50	√	√	√
125	75/25	-	√	-
	67/33	-	√	-
	50/50	-	√	-
150	75/25	-	√	-
	67/33	-	√	-
	50/50	-	√	-
175	75/25	-	√	-
	67/33	-	√	-
	50/50	-	√	-
200	75/25	-	√	-
	67/33	-	√	-
	50/50	-	√	-

(*Note:

Nd1/1 –needlepunched once for each side

Nd 2/2 – needlepunched twice for each side

Nd 3/3 – needlepunched three times for each side

“√” means “having been done”. The needle density Nd1/1 of experiencing needle punching process once was 232.5 needles/ in². That of twice Nd 2/2 was 465.0 needles/ in², that of three times Nd 3/3 was 697.5 needles/ in². “Areal density” included only expected density of mixture of feather and polyester fibers and did not include that of scrim and same as follows.)

3.3.4 Property testing of the needle punched nonwoven for filtration

Air permeability was tested on the Frazier instrument according to Test Method D 737. The pressure drop and penetration testing was performed on 8110 Automated Filter Tester in the Nonwoven center of Tennessee University in Knoxville. (Particles used in the test were sodium chloride solid whose weight average diameter was 0.2 μm and number average number diameter was 0.075 μm .)

Tensile properties were also tested on a universal testing machine (Instron Model 1122) according to D 5035-95. The width of samples was one inch. A gauge length of 75mm (3 inch) and a crosshead speed of 150 mm (6inch)/min were used for tensile testing. The data were obtained from averages of 10 tests.

3.4 Results and Discussion

3.4.1 Properties of first set of needlepunched nonwovens with thick scrim

3.4.1.1 Filtration properties of needlepunched nonwovens with thick scrim

The following discussion concerns the first set of chicken feather needlepunched nonwovens. In them, we used a thick scrim (31 g/m^2) to cover the mat. Filtration and tensile properties are discussed as follows.

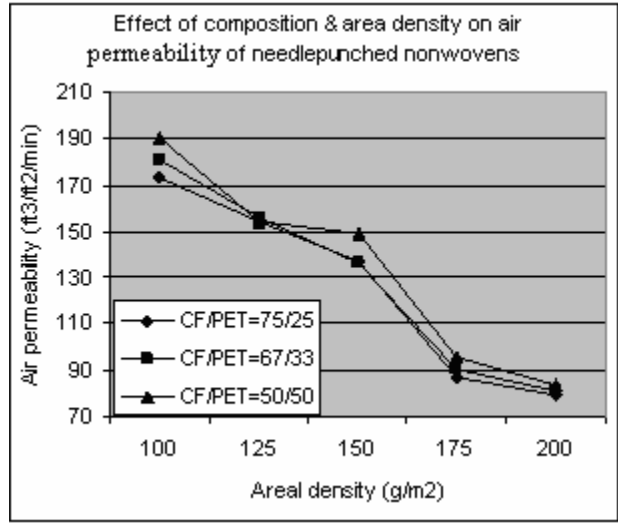
The air permeability results are in Table 3-2 and Figure 3-5. In them and following tables and Figures the ratio CF/PET is that of weight percentage of chicken feather fiber and polyester staples. From Table 3-2 and Figure 3-5 it can be seen that the air permeability decreased with the increase of areal density, and decreased a small amount with an increase in the percentage of feather fibers. The number of passes through the

Table 3-2 Air permeability of first set of needlepunched nonwovens

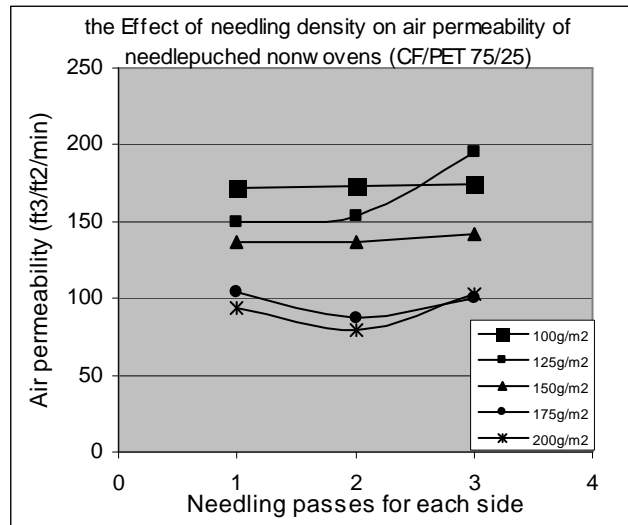
Areal density (g/m ²)	Feather fiber /PET(CF/PET)	Passes through needlepunched medium (Nd)		
		1/1	2/2	3/3
100	75/25	171.3	172.7	174.9
	67/33	-	180.7	-
	50/50	-	190.1	-
125	75/25	149.8	153.8	194.9
	67/33	-	155.7	-
	50/50	-	154.4	-
150	75/25	136.5	136.7	141.7
	67/33	-	135.7	-
	50/50	-	149.1	-
175	75/25	104.8	87.1	100.5
	67/33	-	91.0	-
	50/50	-	95.8	-
200	75/25	93.5	79.7	102.9
	67/33	-	81.2	-
	50/50	-	83.3	-

(Note: air permeability is the rate of air in cubic feet, per square foot of fabric per minute at 30" of mercury, 70°F., and 65% relative humidity and pressure drop 0.5 inch water. The following air permeability has the same definition. Feather fiber/PET (CF/PET) is the ratio of weight of feather fiber and polyester staple fibers and the following CF/PET has the same meaning.)

needlepunching process had no obvious effect on the air permeability. So Nd 2/2 (passes each side) was used for all other samples of this set.



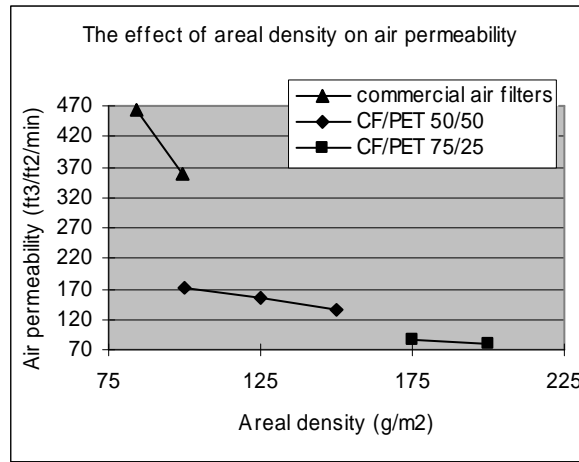
(a)



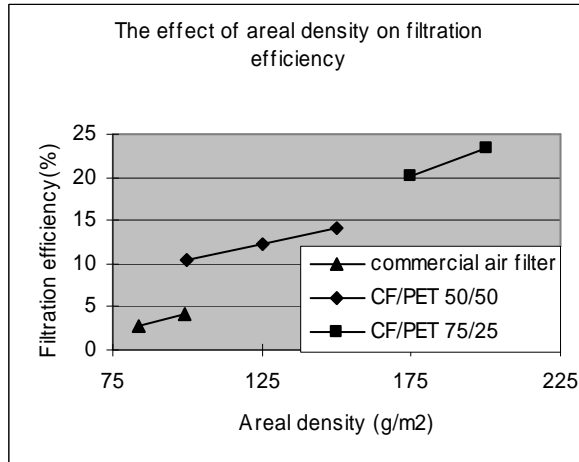
(b)

Figure 3-5 Effect of areal density, mixed ratio and times of experiencing needle punching process on air permeability (first set)

The filtration properties of some chosen needlepunching nonwovens compared to some commercial air filters are shown in Figure 3-6 (data in Table 3-3). The effect of adding feather fibers on air permeability and on filtration efficiency seems more likely related to the change in areal density rather than the structure of the feathers or the nonwovens containing feathers. The commercial air filters also follow the same trends.



(a)



(b)

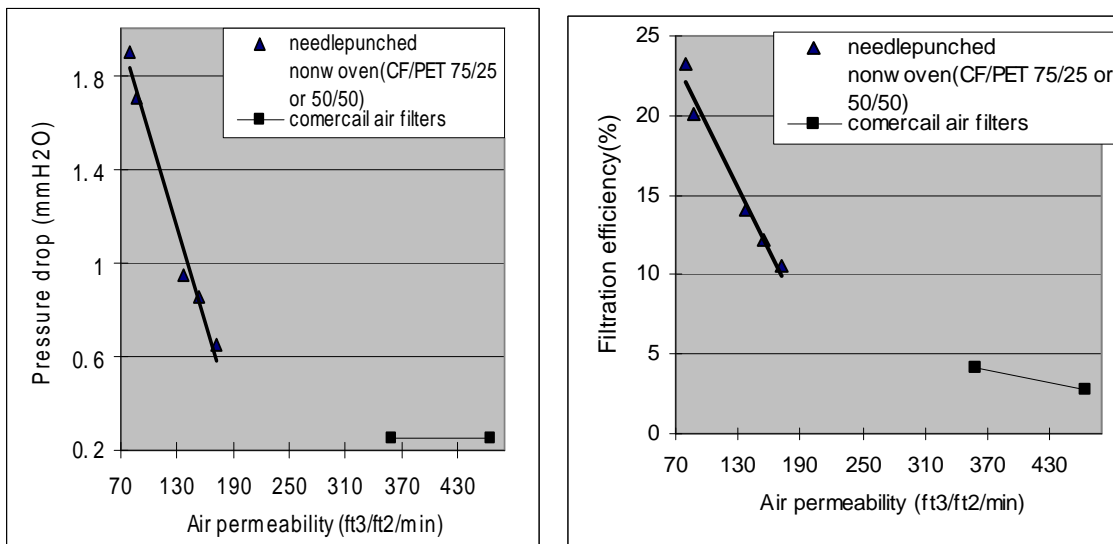
Figure 3-6 Filtration properties of needlepunched nonwovens (firs set) compared to some commercial air filters

Table 3-3 Filtration properties of commercial air-filters

Name	Areal density (g/m ²)	Air permeability (ft ³ /ft ² /min)	Pressure drop(mm H ₂ O)	Filtration efficiency (%)
Filter 1	84	456.24	0.25	2.8
Filter 2	99.3	359	0.25	4.2

(Note: Filter 1 was Dust guard, made in USA by Precisionaire, Inc., Filter 2 was Flanders which was classified UL Class 11 5442L.)

The relationship between air permeability and the values of pressure drop and filtration efficiency is shown in Figure 3-7 (a) and (b) respectively (data from Table 3-4). The pressure drop decreased linearly with the air permeability. Filtration efficiency decreased linearly with the air permeability. It seems that reducing air permeability could increase filtration efficiency.



(a)

(b)

Figure 3-7 Relationship of air permeability with pressure drop and filtration efficiency of needle punched nonwovens (first set) compared to the commercial air filters.

Table 3-4 Filtration properties of needlepunched nonwovens (first set, CF/PET 75/25)

Areal density (g/m ²)	Air permeability	Pressure drop (mm H ₂ O)	Filtration efficiency (%)
100	172.7	0.65	10.5
125	153.8	0.85	12.2
150	136.7	0.95	14.1
175	87.1	1.7	20.1
200	79.7	1.9	23.3

(*Note: The mix ratio of feather fibers and PET fibers was 75%/25%. The times of experiencing needle punching process was 2/2. “Areal density” included only that of mixture of feather and polyester fibers and did not include that of scrims. Pressure drop was measured at 70°F., and 65% relative humidity and 32L/min.)

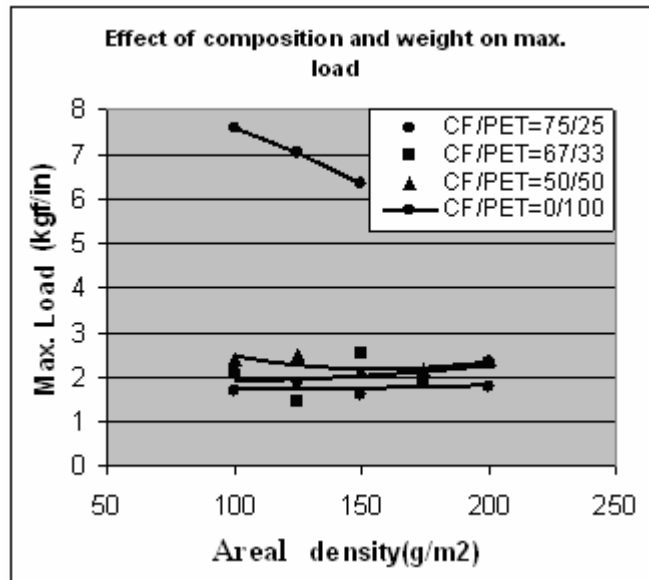
From Table 3-4, it is also can be seen that filtration efficiency and pressure drop increased with increasing the areal density. Compared to those of commercial air filters in Table 3-3), it can be seen that filtration of feather fibers/PET fibers 75/25 nonwovens had higher filtration efficiency than those commercial air filters, but had higher pressure drop.

3.4.1.2 Tensile property of needlepunched nonwoven with thick scrim

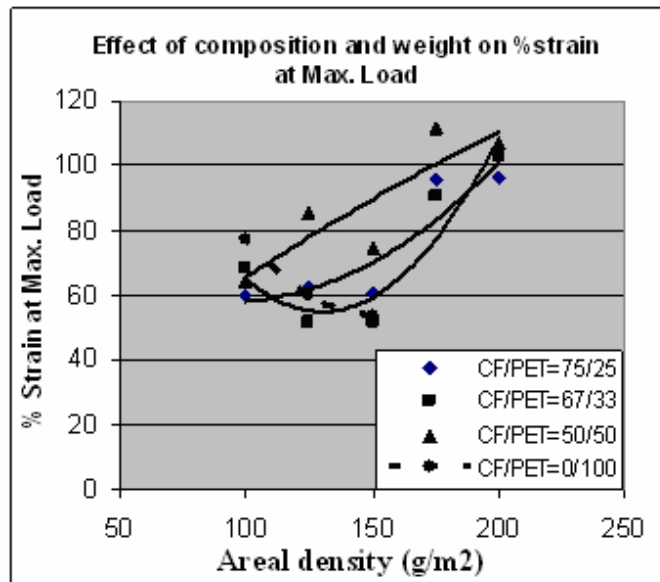
The tensile properties of the first set of needlepunched nonwovens at different areal densities and mix ratios were tested. The results are shown in Table 3-5 and Figure 3-8. The feather fiber component reduced the tensile strength of the needlepunched nonwovens, but within the mix ratios tested, the level of feather fiber had little effect. The data for %strain at maximum load were more scattered, but seemed to increase with increasing areal weight.

Table 3-5 Tensile Properties of Needlepunched Nonwovens with thick scrim

Ration of Component	CF/PET=75/25		CF/PET=67/33		CF/PET=50/50		Pure PET	
	Max. load (kgf/in)	%strain at max. load	Max. load (kgf/in)	%strain at max. load	Max. load (kgf/in)	%strain at max. load	Max. load (kgf/in)	%strain at max. load
100	1.712	59.7	2.081	68	2.411	64.2	7.593	77.039
125	1.88	62.3	1.494	52	2.483	85.8	7.019	59.961
150	1.588	60.4	2.531	51.5	2.106	75	6.334	53.742
175	1.887	95.6	1.954	90.9	2.155	112	-	-
200	1.808	96.4	2.3	103	2.409	107.3	-	-



(a)



(b)

Figure 3-8 Tensile properties of needlepunched nonwovens (first set)

3.4.2 Properties of needlepunched nonwovens produced by adjusted needle height and with new light scrim

3.4.2.1 Introduction

Everybody wishes to achieve high filtration efficiency and low pressure drop on the air filter [2], so does this research.

Since the first set of needlepunched nonwovens with heavy scrim had low filtration efficiency and became weaker with the number of passes, the needle height was adjusted and new light scrim was used for the next set of new nonwovens. Because in the needlepunching process some of the weight of nonwoven might be lost, but in the first set of needlepunched nonwoven the areal density was not the real one and only that of fiber mixtures, in the next set the density of nonwovens was measured. At the same time, the properties of two sets of nonwovens were compared.

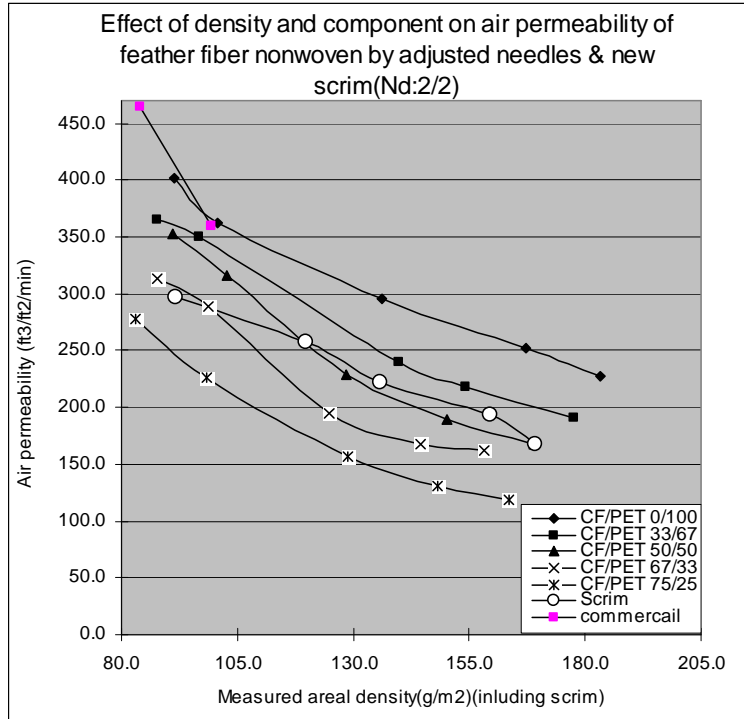
New nonwovens were produced by needlepunching process with adjusted needle height, which made needles pass just through the CF mat made by air-laying process. The new nonwovens were covered by two layers of new light scrim ($18\text{g/m}^2/\text{layer}$). The samples were produced with the various combinations of materials mixed ratio of chicken feather fibers to polyester staple fibers (CF/PET) 0/100, 33/67, 50/50, 67/33, and 75/25, and mixture fiber areal density. After the nonwovens were produced, their air permeability, filtration efficiency, pressure and tensile strength were measured using the same apparatus as in above part.

3.4.2.2 Properties of new needlepunched nonwovens (Nd 2/2)

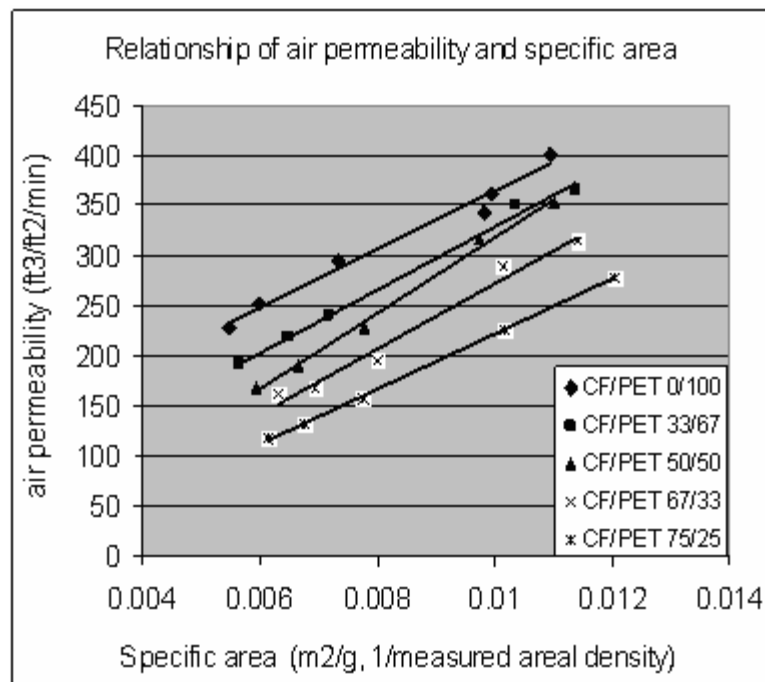
In this part all nonwovens were produced with the same needlepunching density, in which each of both sides of all passed through needles twice with the appropriate slow speed (Nd: 2/2, needle density 465.0 needles/in² for each side). Different layers of scrim nonwovens were also needlepunched in the same way.

3.4.2.2.1 The effect of areal density and component on air permeability

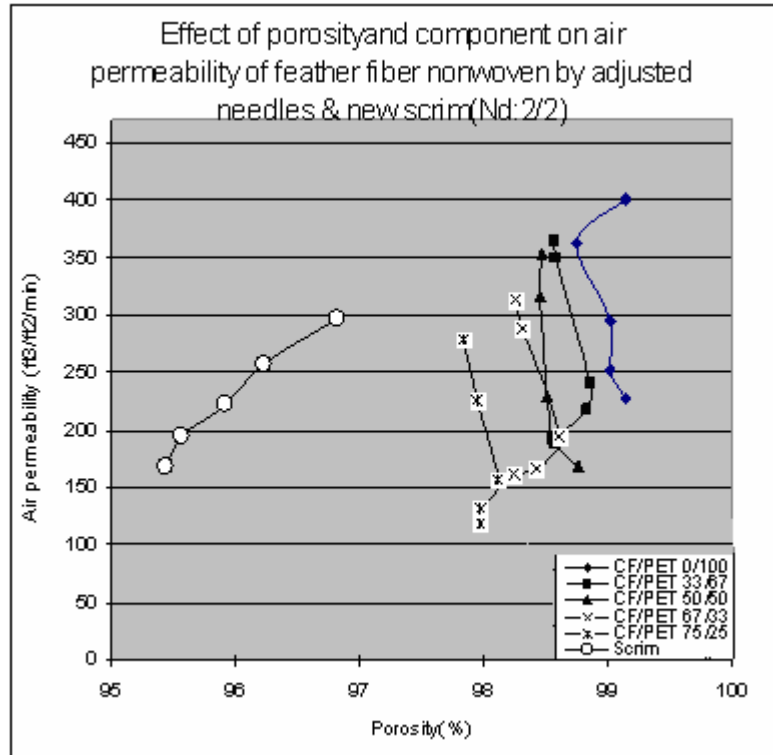
The effect of areal density and component on air permeability of the nonwovens compared to commercial air filters is shown in Figure 3-9. Figure 3-9(a) shows that the air permeability decreased with the measured areal density for every composition. At the same measured areal density, the higher percentage of chicken feather fiber (CF), the lower the air permeability of CF nonwovens, that is, the presence of CF reduced the air permeability. Most of the nonwovens had lower air permeability than the commercial air filters. The higher areal density and the higher CF percentage, the higher their air permeability difference between CF nonwovens and commercial air filter was. The air permeability of different layers of scrim nonwovens was in the middle of graphs of CF nonwovens at different measured density. At lower density (six layers of scrim), their air permeability was even lower than that of the CF/PET 63/33 nonwovens. At higher density, their air permeability was higher than that of the 50/50 nonwovens.



(a)



(b)



(c)

Figure 3-9 Effect of areal density and component on air permeability of new nonwovens

(a) Effect of areal density and component on air permeability of layers of scrim

nonwovens and feather fiber nonwovens by adjusted needles and new scrim

(b) Relationship between air permeability and specific areal density

(c) Effect of porosity and composition on the air permeability of scrim layers and feather

fiber nonwovens with adjusted needles and new scrim

(Note: Data are from Table 3-6 – Table 3-11, Nd: 2/2 means that each side of nonwovens was needlepunched twice.)

Table 3-6 Filtration and tensile properties of new CF/PET 0/100 nonwovens

Measured Areal Density (g/m ²)	Thickness (mm)	Volumetric Density (g/(dm) ³)	Porosity (%)	Air Permeability (ft ³ /ft ² /min)	Filtration Efficiency (%)	Pressure Drop (mm H ₂ O)	Max. Load At PD (lbf/in)	Max. Load At CD (lbf/in)	% Strain at Max. Load (%) at PD	% Strain at Max. Load (%) at CD
91.34	7.71	11.84	98.2	401.4	6.17	0.2	2.15	6.12	27.37	20.11
100.7	5.84	17.25	98.25	362.0	5.78	0.275	1.65	4.13	24.86	14.48
136.2	10.06	13.54	98.17	295.2	5.05	0.35	1.09	4.32	28.99	14.48
167.2	14.04	11.91	98.27	251.5	6.00	0.4	1.58	4.95	24.77	15.41
183.1	16.94	10.81	99.22	227.8	7.25	0.4	1.77	5.56	28.38	18.31

(Note: these nonwovens were produced by adjusted needle height and with new light scrim (Nd 2/2); PD is needlepunching

process direction, CD is cross needlepunching process direction)

Table 3-7 Filtration and tensile properties of new CF/PET 33/67 nonwovens

Measured Areal Density (g/m ²)	Thickness (mm)	Volumetric Density (g/(dm) ³)	Porosity (%)	Air Permeability (ft ³ /ft ² /min)	Filtration Efficiency (%)	Pressure Drop (mmH ₂ O)	Max. Load At PD (lbf/in)	Max. Load At CD (lbf/in)	%Strain at Max. Load (%) at PD	%Strain at Max. Load (%) at CD
87.81	4.94	17.78	98.62	337.4	5.2	0.3	1.80	5.12	26.78	12.30
96.8	5.56	17.41	98.64	302.1	6.15	0.3	1.42	4.76	26.56	20.98
139.7	10.08	13.86	98.88	221.7	10.5	0.45	2.00	6.31	27.37	18.13
154.1	10.75	14.33	98.85	198.5	10.75	0.6	1.27	3.52	26.33	13.58
177.5	10.98	16.17	98.59	194.8	10.15	0.55	1.23	4.47	23.57	12.79

(Note: these nonwovens were produced by adjusted needle height and with new light scrim (Nd 2/2); PD is needlepunching process direction, CD is cross needlepunching process direction)

Table 3-8 Filtration and tensile properties of new CF/PET 50/50 nonwovens

Measured Areal Density (g/m^2)	Thickness (mm)	Volumetric Density ($g/(dm)^3$)	Porosity (%)	Air Permeability ($ft^3/ft^2/min$)	Filtration Efficiency (%)	Pressure Drop (mm H ₂ O)	Max. Load At PD (lbf/in)	Max. Load At CD (lbf/in)	%Strain at Max. Load (%) at PD	%Strain at Max. Load (%) at CD
90.93	5.08	17.90	98.53	353.0	2	0.25	1.53	5.24	26.41	14.53
102.6	5.73	17.91	98.51	316.2	2	0.3	1.85	5.91	26.02	13.99
128.5	7.58	16.95	98.56	228.5	7.85	0.45	1.38	4.61	28.06	13.43
150.2	9.26	16.22	98.60	189.0	10.35	0.55	1.65	5.87	29.08	17.62
169	12.16	13.90	98.79	168.0	10.65	0.6	2.08	8.24	25.00	20.84

(Note: these nonwovens were produced by adjusted needle height and with new light scrim (Nd 2/2); PD is needlepunching process direction, CD is cross needlepunching process direction)

Table 3-9 Filtration and tensile properties of new CF/PET 67/33 nonwovens

Measured Areal Density (g/m^2)	Thickness (mm)	Volumetric Density ($g/(dm)^3$)	Porosity (%)	Air Permeability ($ft^3/ft^2/min$)	Filtration Efficiency (%)	Pressure Drop (mmH ₂ O)	Max. Load At PD (lbf/in)	Max. Load At CD (lbf/in)	%Strain at Max. Load (%) at PD	%Strain at Max. Load (%) at CD
87.72	4.51	19.45	98.33	313.7	6.3	0.45	1.83	6.17	30.83	16.83
98.76	5.32	18.56	98.38	288.4	4.0	0.3	1.62	7.25	26.58	21.12
124.9	8.33	14.99	98.65	194.7	9.3	0.5	1.64	5.25	23.64	13.68
144.4	8.57	16.85	98.47	167.3	10.55	0.6	1.55	5.55	28.52	18.66
158.3	8.46	18.71	98.28	162.1	11.3	0.55	1.18	4.27	20.04	14.88

(Note: these nonwovens were produced by adjusted needle height and with new light scrim (Nd 2/2); PD is needlepunching process direction, CD is cross needlepunching process direction)

Table 3-10 Filtration and tensile properties of new CF/PET 75/25 nonwovens

Measured Areal Density (g/m^2)	Thickness (mm)	Volumetric Density ($\text{g}/(\text{dm})^3$)	Porosity (%)	Air Permeability ($\text{ft}^3/\text{ft}^2/\text{min}$)	Filtration Efficiency (%)	Pressure Drop (mmH_2O)	Max. Load At PD (lbf/in)	Max. Load At CD (lbf/in)	%Strain at Max. Load (%) at PD	%Strain at Max. Load (%) at CD
83.04	3.50	23.73	97.86	278.4	4.9	0.35	1.40	3.32	24.60	11.64
98.38	4.45	22.11	97.97	226.3	6.3	0.45	1.80	6.32	22.98	20.57
128.9	6.51	19.80	98.13	156.5	11.05	0.6	2.26	7.12	29.70	18.37
148.1	7.03	21.07	97.99	131.2	14.7	0.8	2.26	7.25	28.70	19.49
163.4	7.82	20.90	97.99	118.1	15.9	0.85	2.29	6.94	31.56	20.87

(Note: these nonwovens were produced by adjusted needle height and with new light scrim (Nd 2/2); PD is needlepunching process direction, CD is cross needlepunching process direction)

Table 3-11 Filtration and tensile properties of needlepunched scrim layers

Layers of scrim	Measured Areal Density (g/m ²)	Thickness (mm)	Volume-Density (g/(dm ³))	Porosity (%)	Air Permeability (ft ³ /ft ² /min)	Filtration Efficiency (%)	Pressure Drop (mmH ₂ O)	Max. Load At PD (lbf/in)	Max. Load At CD (lbf/in)	%Strain at Max. Load at PD (%)	%Strain at Max. Load at CD (%)
2	33.87	1.50	22.58	-	649	3.02	0.1	2.23	8.20	28.63	23.30
4	55.65	1.81	30.75	-	406	12.85	0.2	14.4	3.57	21.47	25.48
6	91.74	2.08	44.11	96.81	296.4	34.60	0.25	4.63	14.03	27.10	18.31
7	119.70	2.30	52.04	96.23	257.0	48.85	0.4	6.20	20.48	31.12	17.34
8	135.85	2.41	56.37	95.92	221.9	56.60	0.55	7.24	30.83	29.49	21.17
9	159.62	2.61	61.16	95.57	193.9	66.00	0.6	7.99	31.15	28.93	18.96
10	169.38	2.69	62.97	95.43	167.9	67.40	0.7	8.80	30.80	29.86	13.81
2*	36.00	1.49	24.00	-	Too high	1.450	0.1	2.87	8.84	19.87	16.70

(Note: these nonwovens were produced by adjusted needle height and with new light scrim (Nd 2/2); PD is needlepunching process direction, CD is cross needlepunching process direction; 2* is two layers of original scrim and not needlepunched.)

The relationship between air permeability and specific area (1/areal density) can be seen in Figure 3-9 (b). Within the ranges of measurements made, it was found that the factor most closely related to the air permeability was the fabric areal density. The air permeability was found to be almost directly proportional to the specific area (the reciprocal of the fabric areal density), which is very close to Kothari's finding [3]. From this figure it can be seen that the slopes of all different composite nonwovens were very close. The air permeability of needlepunched scrim layers was also proportional to the specific area but its slope was different from that of CF nonwovens.

Air passes the nonwoven through void space. Porosity is the percentage of void space in the apparent volume of a nonwoven containing that void space. It can be expressed as a percentage of pore volume in an apparent volume of the nonwoven and calculated by 100% eliminated with the percentage of the real volume of fibers in the volume of the nonwoven. The effect of porosity on the air permeability was shown in Figure 3-9 (c). From this figure, it can be said that the porosity was not related to air permeability. It can also be seen that within the ranges of measurement made, the main tendency of CF nonwovens was that the presence of polyester fibers increases their porosity. This could also be seen from the outward appearances of CF nonwovens. For the same areal density of CF nonwovens, the higher feather fiber percentage or lower polyester percentage, the smaller the thickness was, that is, the presence of feather fiber reduced the thickness of CF nonwovens. (CF/PET 75/25 nonwovens had the smallest thickness for the same areal density among these CF nonwovens. Data is in Table 3-6 to Table 3-11.) The thickness was measured with an electrical digital caliper under zero pressure.

3.4.2.2.2 Effect of areal density and component on the filtration efficiency

The effect of areal density and component on the filtration efficiency of the new nonwovens compared to commercial air filters is shown in Figure 3-10.

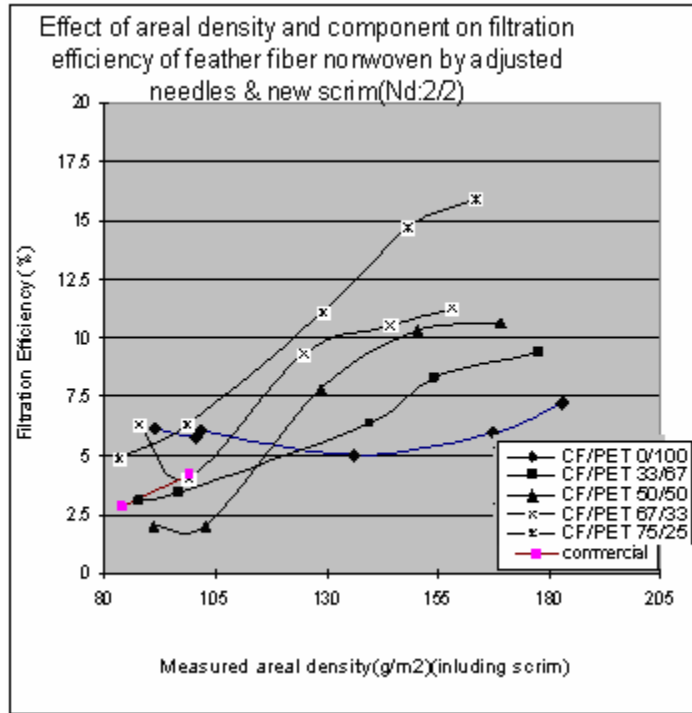


Figure 3-10 Effect of areal density and component on filtration efficiency of feather fiber nonwovens by adjusted needles and new scrim

(Note: data are from Table 3-6 –Table 3-11)

From Figure 3-10 it can be seen that, in general, for a given composition the filtration efficiency of CF nonwovens increased with their measured areal density. Also, in general, the bigger CF percentage in the nonwovens, the higher the filtration efficiency the nonwovens had at the same areal density. At lower areal density, the filtration of

these nonwovens had similar filtration efficiency to commercial air filters. But at higher areal density, these nonwovens had much higher filtration efficiency.

Different layers of new scrim were also needlepunched and their filtration properties were measured (data in Table 3-11). Since their filtration efficiency was much higher than that of CF nonwovens and even six layers of scrim had efficiency 34.6%, their filtration efficiency was graphed alone in Figure 3-11. From the figure, it also can be seen that with layers of scrim (areal density), their filtration efficiency increased. At similar areal density, needlepunched scrim layer had much higher filtration efficiency than commercials.

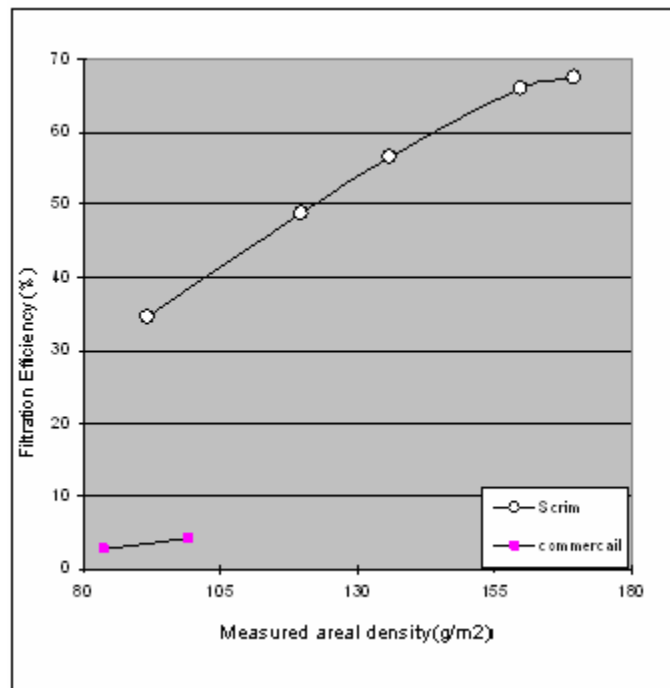


Figure 3-11 Effect of areal density on filtration efficiency of needlepunched scrim layers nonwovens (Nd: 2/2) (Data are in Table 3-11, layers of scrim was from 6 to 10)

Since over 6 needlepunched layers of scrim had so high filtration efficiency, we wanted to know how much filtration efficiency two layers of needlepunched scrim could have. First, we tried to predict it. Using their first four points at lower measured density (layers of scrim from 6 to 9) in the graph and zero filtration efficiency at zero density to make a straight line and extend it, the assumed straight line is showed in Figure 3-12.

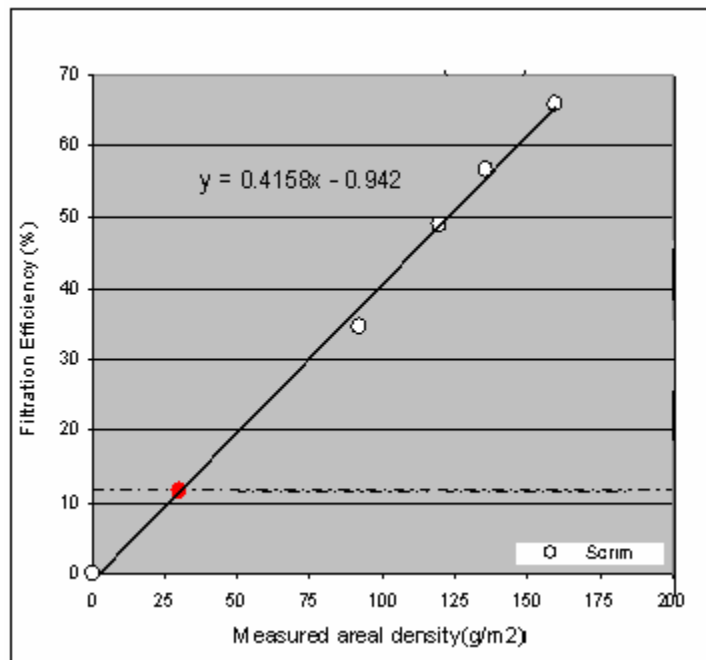


Figure 3-12 Assumed filtration efficiency straight line of needlepunched layers of scrim nonwovens

By using the measured areal density of two needlepunched layers of scrim (33.87 g/m²) and the equation formula in Figure 3-12, the calculation result is 11.58%. It seems that even the two needlepunched layers of scrim had bigger filtration efficiency than most CF nonwovens and commercial air filters. Could the two layers of needlepunched scrim

solve the filtration problem so that new air filters did not need to develop? No, of course they could not. One important point is that all of above filtration efficiency data was measured when the nonwovens were first used. The data were initial efficiency. Layers of scrim were very compact and had low porosity, but CF nonwovens were very lofty and have high porosity which makes the filter produce low filtration efficiency [4] and then the initial efficiency of layers of scrim was higher than that of CF nonwovens. Barris (1995) showed the mass efficiency of air filters is at the lowest point when the filter is new and improves in efficiency as the dust cake forms and porosity decreases, which then becomes the primary filtration media [5]. Furthermore, retention is also an important characteristic of air filters. It seems that thick nonwovens can hold a lot of particles but two layers of PET scrim cannot. Two layers of PET scrim only can be a surface loading media and a majority of particles stored on its surface with minimal depth penetration. Others layers of scrim nonwovens were similar because they did not have much depth to hold dust cakes. However, CF nonwovens can be a depth loading media and they can have minimal surface storage with particles stored throughout the depth [6]. Maybe filtration efficiency needs to be tested after CF nonwovens are used at different life time to see what would happen when dust cakes are formed.

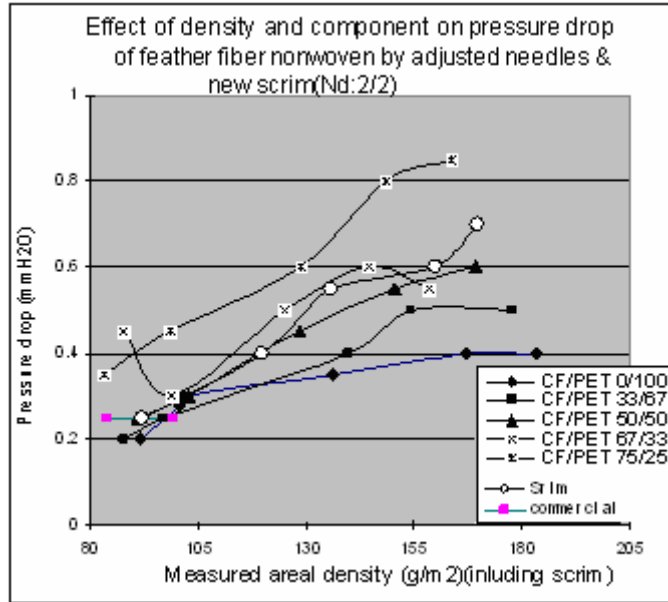
The filtration properties of two layers of needlepunched scrim were measured. Its filtration efficiency was 3.55%, a little higher than some CF nonwovens with lower areal density. It can be understandable because the needlepunched scrim layers were entangled together and their entangle fibers easily caught more particles, but in the CF nonwovens the two layers were separated by vertical fibers. In the vertical fibers there were a lot of

void space, and then particles maybe easily found ways to pass through the separated scrim.

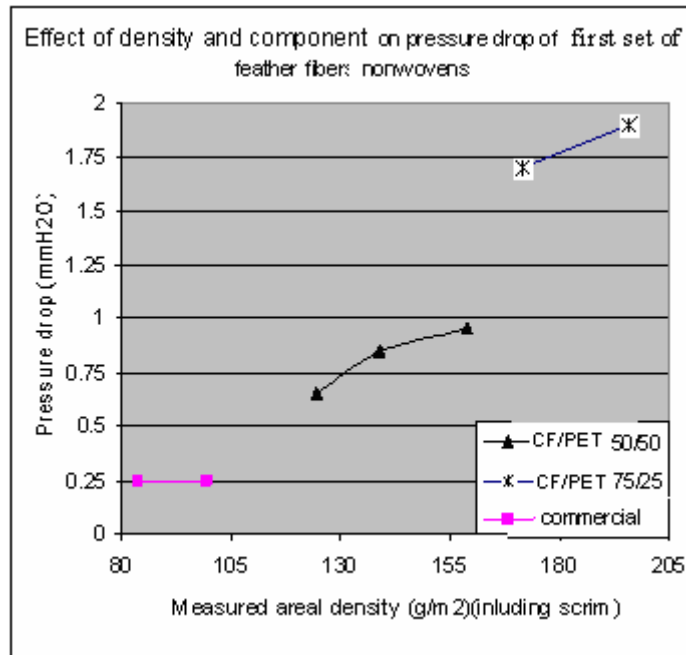
3.4.2.2.3 Effect of areal density and component on pressure drop

Pressure drop is the driving force for filtration. The effect of areal density and component on pressure drop of feather fiber and scrim nonwovens is shown in Figure 3-13.

From Figure 3-13 (a) it can be seen that the needed pressure drop for almost all CF and scrim nonwovens increased with the measured areal density. For most CF nonwovens, the higher the feather fiber percentage, the higher their pressure drop was at the same areal density. 0/100 nonwovens needed lowest and almost all 75/25 nonwovens needed highest pressure drop at the same measured density. Similarly, 0/100 nonwovens' pressure drop did not change much with the increase of their areal density and 75/25 nonwovens' pressure drop increased a lot with the areal density within the measured range. At high areal density the pressure drop difference was bigger for different component CF nonwovens. At the low areal density the pressure drop for 0/100, 33/67, and 50/50 nonwovens was very close and close to the commercial air filters. The regularity of properties of 67/33 nonwovens was poor. Similarly to the filtration efficiency, at the lowest density, the 67/33 nonwoven even needed bigger pressure drop than the 75/25 nonwoven. However, at the highest density the pressure for the 67/33 nonwovens was smaller than the 50/50 nonwovens, instead. Maybe we need to check this again. The pressure drop needed by scrim layers nonwovens was higher than 50/50 nonwovens and smaller than 33/67 nonwovens in some areal density range.



(a) Nonwovens produced by new ways



(b) First set of nonwovens

Figure 3-13 Effect of density and component on pressure drop of new feather fiber and scrim nonwovens compared to that of first set of nonwovens

Compared to that of new nonwovens made this time (showed in Figure 3-13), it is obvious that the needed pressure drop of nonwovens produced with original needle height and heavy scrim was higher than that of nonwovens made this time. Especially, old 75/25 nonwovens needed much higher pressure drop than commercial air filters; but the nonwovens made by new ways needed pressure drop similar to or a little bigger than that of the commercial air filters. This could be understandable because the nonwovens made by the new way were loose, while those produced with original ways were much more compact. The compact nonwovens did not have many vacant pathways for air to pass through, and then needed higher pressure drop. Running the new nonwovens maybe would not need much energy.

3.4.2.2.4 Relationships among filtration efficiency, air permeability and pressure drop

Figure 3-14 shows that the expected relationship between flow at ΔP 5 mmH₂O and ΔP at constant flow 32 L/min for the different media. All of the media appeared to fall on a single curve including scrim.

Relationship of filtration efficiency of CF and scrim nonwovens to air permeability is shown in Figure 3-15. The figure shows that multiple layers of scrim gave much higher filtration efficiency than air-laid nonwovens at the same permeability. The results suggest that, while depth may improve capacity, perhaps it does not improve initial filtration.

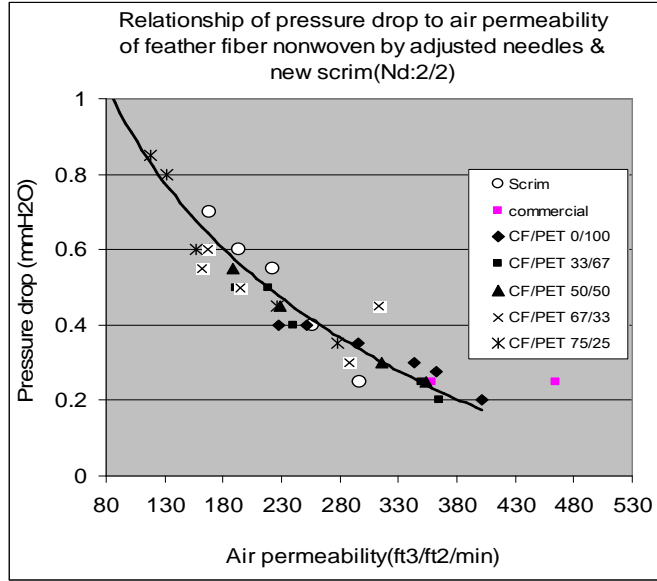


Figure 3-14 Relationship of the pressure drop of new CF and scrim nonwovens to air permeability (Note: data are from Table 3-6 – Table 3-11.)

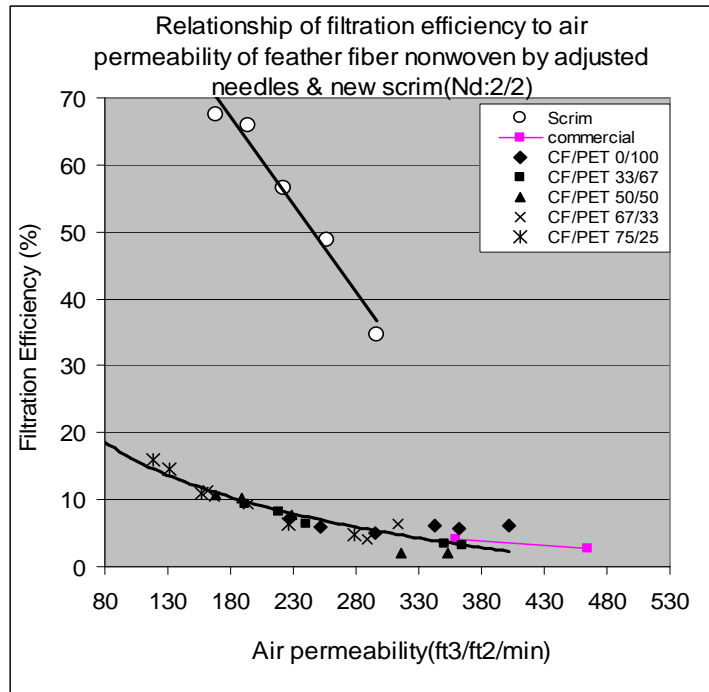


Figure 3-15 Relationship of filtration efficiency to air permeability of feather fiber nonwovens by adjusted needles & new scrim (Note: data are from Table 3-6 – Table 3-11.)

A better representation of the filtration efficiency is shown in Figure 3-16 which indicates that the needlepunched scrim was more efficient than the nonwoven filters in this study and the commercial filters at any given pressure drop. An important filter criteria, however, is how efficiency changes after using for some time and may decrease rapidly for a rather flat media without depth.

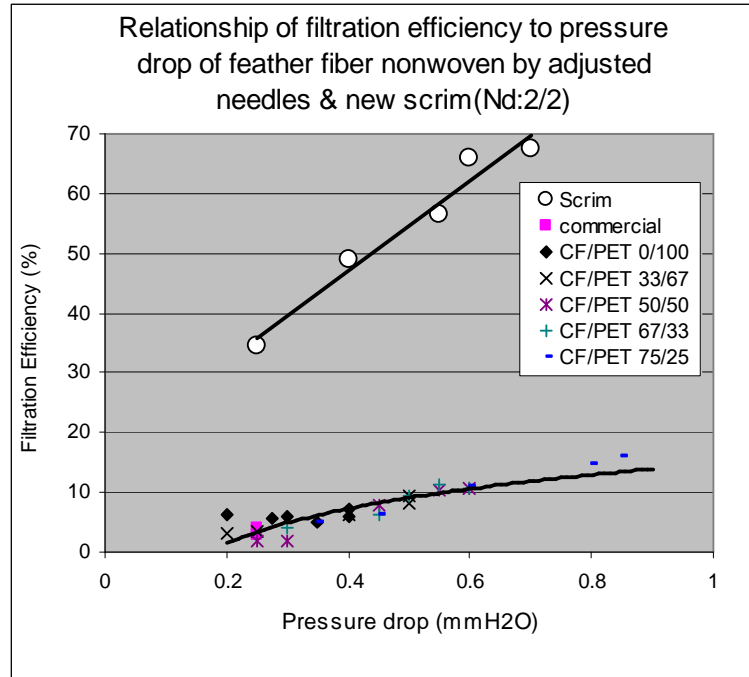


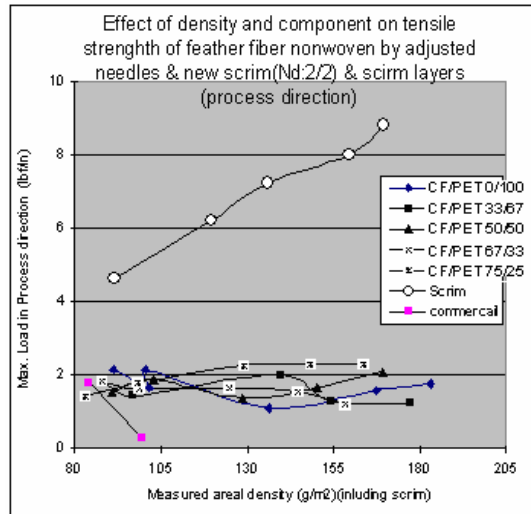
Figure 3-16 Relationship of the filtration efficiency of new CF and scrim nonwovens to pressure drop

(Note: data are from Table 3-6 – Table 3-11.)

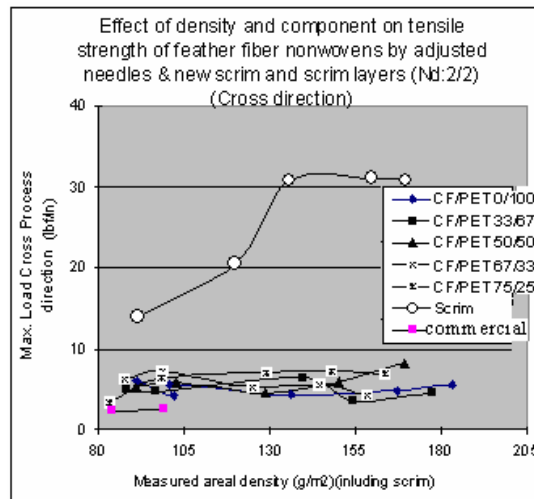
3.4.2.2.5 Tensile properties

The tensile strength of these nonwovens was also measured. The tensile strength of CF nonwovens had differences in (needlepunching) process direction and cross (needlepunching process) direction. The process direction refers only to the direction of

travel through the needlepunching machine as there is no sample movement during air-laying; the cross direction is one that is vertical to (/cross) the needlepunching process direction. The supporting scrim did have a machine and cross direction. Their maximum load in process direction was much smaller than in the cross direction (in Figure 3-17), so the maximum loads as well as the percent strain at maximum loads in different direction are described separately.



(a) in Process direction

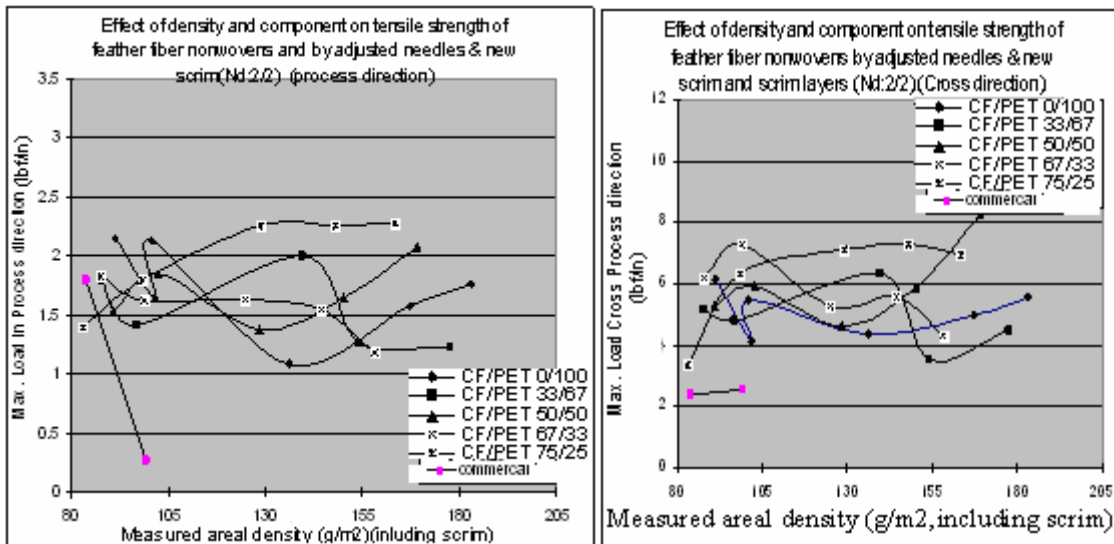


(b) in cross direction

Figure 3-17 Effect of density and component on tensile strength of new CF needlepunched nonwovens and scrim layers (from 6 to 10 layers)

(Note: data are from Table 3-6 – Table 3-11.)

Figure 3-17(a) shows that in the process direction needlepunched scrim layers were much stronger than CF nonwovens, so the maximum load of CF nonwovens is showed in Figure 3-18 (a) separately. In Figure 3-17, the horizontal line likely indicates that most (all) of the load was born by the scrim; if not all, this may indicate that the scrim was cut cross ways of its machine direction. From Figure 3-18(a) it can be seen that the effect of areal density and component on the maximum load of CF nonwovens was basically insignificant. Figure 3-18(b) is similar to Figure 3-18 (a).



(a) in the process direction

(b) in the cross direction

Figure 3-18 Effect of density and component on tensile strength of feather fiber nonwovens and by adjusted needles & new scrim (Nd: 2/2)

(Note: data are from Table 3-6 – Table 3-11.)

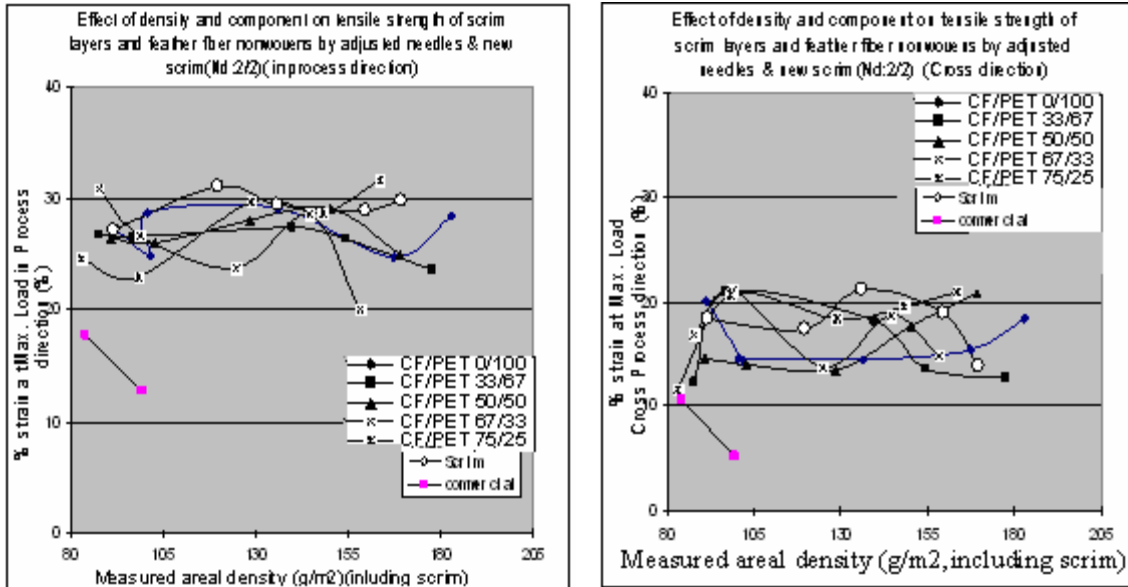


Figure 3-19 Effect of density and component on %strain at maximum load of scrim layers nonwovens and feather fiber nonwovens by adjusted needles & new scrim in both directions

(Note: data are from Table 3-6 – Table 3-11.)

The effect of density and component on %strain at maximum load of the new nonwovens was in Figure 3-19. From the figure it can be seen that the nonwoven had larger %strain at maximum load in process direction than in the cross direction. In each direction, %strain at maximum load of all the CF nonwovens and scrim layers nonwovens were very close to each other and did not change much with the density and composition. However, for old CF nonwovens made by original methods, the %strain at maximum load increased with the density while only that of 0/100 nonwoven decreased (in Figure 3-8 (b)). Furthermore, the tendency was that more feather fibers reduced the %strain at maximum load.

With the maximum load, the failure strain was relatively unaffected by composition and was the same magnitude as the needlepunched scrim tested alone. This further supported the conclusion that the strength properties being measured were of the scrim only. The fact that the measured maximum load and strain of the composition fabric was lower again indicates that scrim maximum load was crossed with the final fabric maximum load.

3.4.2.3 Effect of needling density on properties of the CF nonwovens produced by adjusted needle height and with new light scrim

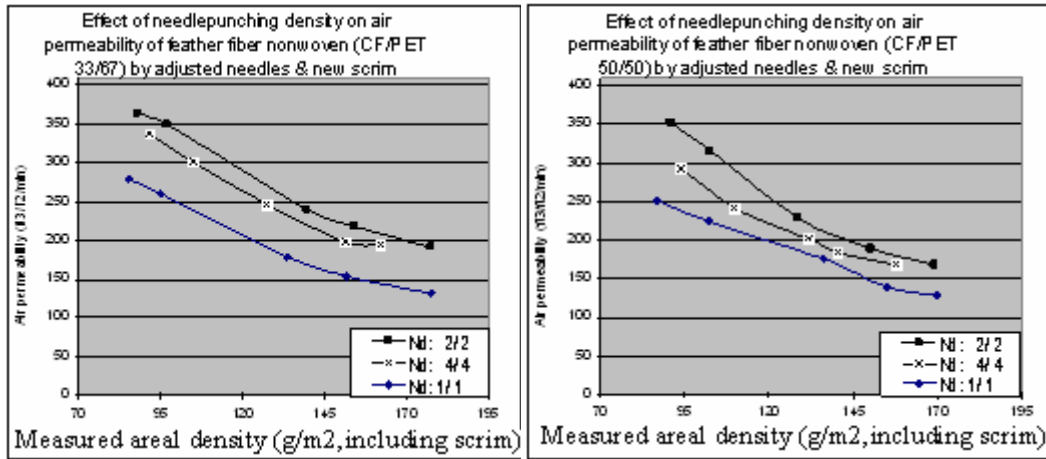
§3.4.2.2 only discusses the properties of new nonwovens produced at Nd 2/2, the only one needlepunching density. In §3.4.1 the measurement result shows that the needlepunching density did not have effect on the filtration properties of CF needlepunched nonwovens. This is unreasonable because different needlepunching density produced different pore properties in needle felt which affect their filtration properties. Therefore, this part §3.4.2.3 will discuss the effect of needlepunching density on the properties of needlepunched CF nonwovens. CF/PET 33/67, 50/50 and 67/33 nonwovens were produced for this study.

The different needling density in different range had different effects on the fabric thickness, air permeability, pressure drop and filtration efficiency.

The fabric specifications i.e. composition, used fiber weight, expected fibers weight and needling density have been indicated before in this chapter. The results of various tests are discussed with the plotted graphs under the following heading.

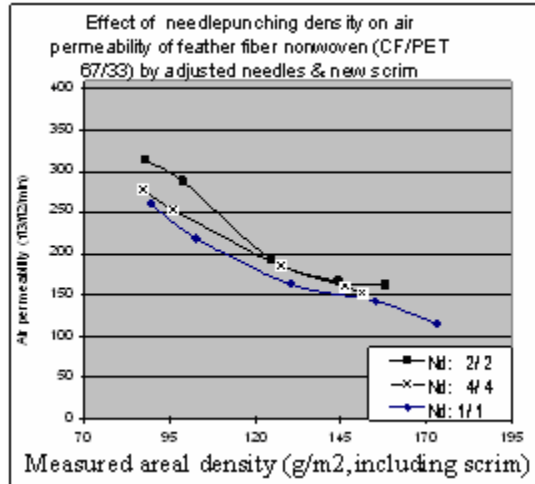
3.4.2.3.1 Air permeability

From Figure 3-20, Table 3-7 – Table 3-9 and Table 3-12 – Table 3-17 it can be seen that needlepunching density had different effect on the air permeability of different composition CF nonwovens, although the effect had one common tendency. The common tendency was that, for all the three compositions CF/PET 33/67, 50/50 and 67/33 nonwovens, at Nd 2/2 (needling punched twice for each of both sides of nonwovens), the nonwovens had highest air permeability. Then, both increasing and decreasing the needlepunching density reduced air permeability of the nonwovens. It is reasonable that decreasing needlepunching caused less vertical holes and increasing needlepunching density made the nonwovens more compact and both caused less vacancy for air to pass through.



(a)

(b)



(c)

Figure 3-20 Effect of needling density on air permeability of new CF nonwovens

For different composition CF nonwovens, the effect of needlepunching density on their air permeability was a little different. Figure 3-20 (a) shows that for CF/PET 33/67 nonwovens, decreasing the needlepunching density (Nd: 1/1) decreased much air permeability, several times more than increasing needlepunching density (Nd: 4/4). Figure 3-20 (b) shows that for CF/PET 50/50 nonwovens, Nd 4/4 nonwovens had the air permeability in the middle of Nd 2/2 and 1/1. For CF/PET 67/33 nonwovens, the effect tendency of needlepunching was similar to the above two, but only at low areal density, the effect tendency was a little large. At the high areal density, the air permeability of the nonwovens with different needlepunching density was very close and there were no big differences. From Figure 3-20 it also can be seen that needlepunching density had more obvious effects on the air permeability of low feather fiber content nonwovens than that of high feather fiber content nonwovens.

Table 3-12 Filtration and tensile properties of new CE/PET 33/67 nonwovens needlepunched with Nd 4/4

Measured Areal Density (g/m^2)	Thickness (mm)	Volumetric Density ($g/(dm)^3$)	Air Permeability ($ft^3/ft^2/min$)	Filtration Efficiency (%)	Pressure Drop (mmH_2O)	Max. Load		%Strain at Max. Load	
						At PD (lbf/in)	At CD (lbf/in)	at PD (%)	at CD (%)
91.8	5.03	18.25	337.4	5.2	0.3	4.27	1.56	17.52	26.50
104.7	5.35	19.57	302.1	6.15	0.3	4.22	1.20	17.70	23.13
150.4	6.48	23.21	221.7	10.5	0.45	3.18	1.34	16.68	23.78
151.4	7.75	19.54	206.7	10.75	0.6	2.98	1.05	16.08	25.81
161.9	7.81	20.73	194.8	10.15	0.55	2.90	0.94	15.41	23.91

(Note: these nonwovens were produced with adjusted needle height and new light scrim (Nd 4/4); PD is needlepunching process direction, CD is cross needlepunching process direction)

Table 3-13 Filtration and tensile properties of new CF/PET 33/67 nonwovens needlepunched with Nd 1/1

Measured	Thickness (mm)	Volumetric Density (g/(dm) ³)	Air Permeability (ft ³ /ft ² /min)	Filtration Efficiency (%)	Pressure Drop (mmH ₂ O)	Max.		%Strain	
						Load At PD (lbf/in)	Load At CD (lbf/in)	Load at Max.	%Strain at Max.
85.14	5.77	14.76	279.0	6.05	0.3	6.84	2.09	17.91	25.14
94.83	5.99	15.83	261.4	7.35	0.4	9.59	2.26	27.00	29.59
133.74	8.19	16.33	179.4	11.35	0.65	25.33	1.89	16.43	22.12
151.86	10.87	13.97	153.2	13.65	0.75	6.55	1.87	19.48	20.54
177.66	12.33	14.41	131.9	16.45	0.9	6.20	2.72	19.14	25.63

(Note: these nonwovens were produced with adjusted needle height and new light scrim (Nd 1/1); PD is needlepunching process direction, CD is cross needlepunching process direction.)

Table 3-14 Filtration and tensile properties of new CF/PET 50/50 nonwovens needlepunched with Nd 4/4

Measured Areal Density (g/m^2)	Thickness (mm)	Volumetric Density ($g/(dm)^3$)	Air Permeability ($ft^3/ft^2/min$)	Filtration Efficiency (%)	Pressure Drop (mmH_2O)	Max. Load	Max. Load	%Strain at Max. Load	%Strain at Max. Load
						At PD (lbf/in)	At CD (lbf/in)	(%) at PD	(%) at CD
93.7	4.80	19.52	292.4	5.35	0.4	2.85	0.86	13.87	23.59
109.6	5.34	20.52	242.3	8.15	0.45	2.24	0.90	13.82	26.02
131.7	6.31	20.87	201.2	10.9	0.5	4.82	1.64	19.30	27.43
140.3	7.04	19.93	184.5	11.45	0.6	4.10	1.14	19.92	26.43
157.8	9.31	16.95	168.3	10.6	0.65	3.69	1.09	17.72	25.46

(Note: these nonwovens were produced with adjusted needle height and new light scrim (Nd 4/4); PD is needlepunching process direction, CD is cross needlepunching process direction.)

Table 3-15 Filtration and tensile properties of new CE/PET 50/50 nonwovens needlepunched with Nd 1/1

Measured	Thickness (mm)	Volumetric Density (g/(dm) ³)	Air Permeability (ft ³ /ft ² /min)	Filtration Efficiency (%)	Pressure Drop (mmH ₂ O)	Max.		%Strain	
						Load At PD (lbf/in)	Load At CD (lbf/in)	at Max. Load (%) at PD	at Max. Load (%) at CD
86.7	5.97	14.52	251.8	7.25	0.45	7.42	1.83	13.83	15.81
102.1	6.75	15.13	224.6	9.4	0.5	6.58	1.86	16.68	17.67
136.0	8.78	15.49	175.5	12.4	0.7	7.55	2.73	20.02	26.12
154.9	10.51	14.74	139.1	14.8	0.9	6.47	2.37	18.77	28.61
169.6	10.68	15.88	128.9	17.3	0.95	7.79	1.82	22.59	22.97

(Note: these nonwovens were produced with adjusted needle height and new light scrim (Nd 1/1); PD is needlepunching process direction, CD is cross needlepunching process direction)

Table 3-16 Filtration and tensile properties of new CF/PET 67/33 nonwovens
 needlepunched with Nd 4/4

Measure	Thicknes	Volumetri	Air	Max.	Max.	%Strai	%Strai
d	s	c	Permeabilit	Load	Load	n at	n at
Areal	(mm)	Density	y	At PD	At CD	Max.	Max.
Density		(g/(dm) ³)	(ft ³ /ft ² /min)	(lbf/in	(lbf/in	Load	Load
(g/m ²)))	(%)	(%)
						at PD	at CD
87.1	3.11	28.01	278.6	5.24	1.44	21.23	30.57
95.7	3.62	26.44	253.4	3.29	0.99	12.13	29.68
126.0	4.79	26.30	206.6	3.31	1.35	18.13	27.07
146.5	5.69	25.75	160.8	3.23	1.30	15.33	28.84
151.4	5.99	25.28	153.5	3.98	1.42	19.53	28.69

(Note: these nonwovens were produced with adjusted needle height and new light scrim (Nd 4/4); PD is needlepunching process direction, CD is cross needlepunching process direction)

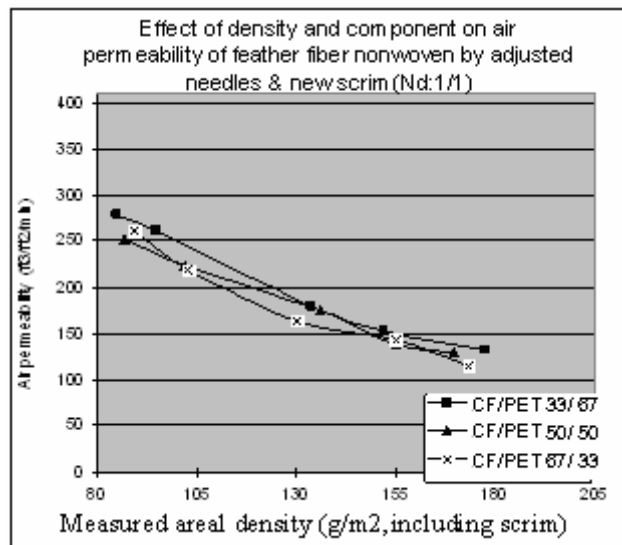
Table 3-17 Filtration and tensile properties of new CF/PET 67/33 nonwovens
 needlepunched with Nd 1/1

Measure d Areal Density (g/m ²)	Thicknes s (mm)	Volumetri c Density (g/(dm) ³)	Air Permeabilit y (ft ³ /ft ² /min)	Max. Load At PD (Ibf/in)	Max. Load At CD (Ibf/in)	%Strai n at Max. Load (%) at PD	%Strai n at Max. Load (%) at CD
89.5	4.85	18.45	261.4	6.39	2.08	15.90	19.27
102.7	5.70	18.02	218.7	8.10	2.28	17.73	26.27
130.3	6.98	18.67	163.6	7.61	2.36	18.37	24.13
162.0	9.13	17.74	141.4	6.63	2.54	19.57	22.13
173.5	9.81	17.69	115.6	6.10	2.22	22.63	24.07

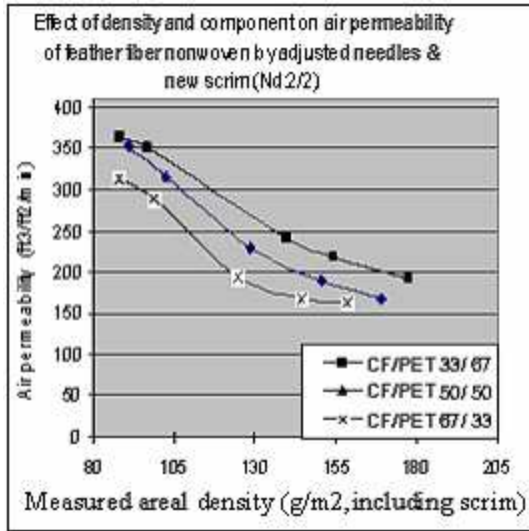
(Note: these nonwovens were produced with adjusted needle height and new light scrim (Nd 1/1); PD is needlepunching process direction, CD is cross needlepunching process direction)

Figure 3-21 (data in Table 3-7 – Table 3-9 and Table 3-12 – Table 3-17) shows the effect of the composition of CF nonwovens on their air permeability at the same needle punching density. At low needlepunching density (Nd 1/1) (Figure 3-21(a)), the air permeability of different composition of CF nonwovens at the same density was close, that is, composition had little effect on the air permeability. However, at higher

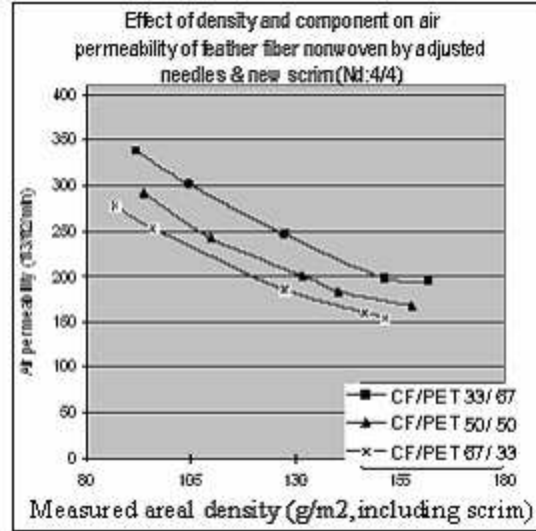
needlepunching density (Nd 2/2 and 4/4) (Figure 3-21 (b) and (c)), the CF fiber composition decreased the air permeability. At Nd 2/2 (Figure 3-21 (b)) the areal density decreased the air permeability of the fiber composition nonwovens more quickly than at Nd 4/4 (Figure 3-21 (c)). At Nd 4/4, for almost every same composition nonwoven, its air permeability decreased linearly with the measured areal density.



(a)



(b)

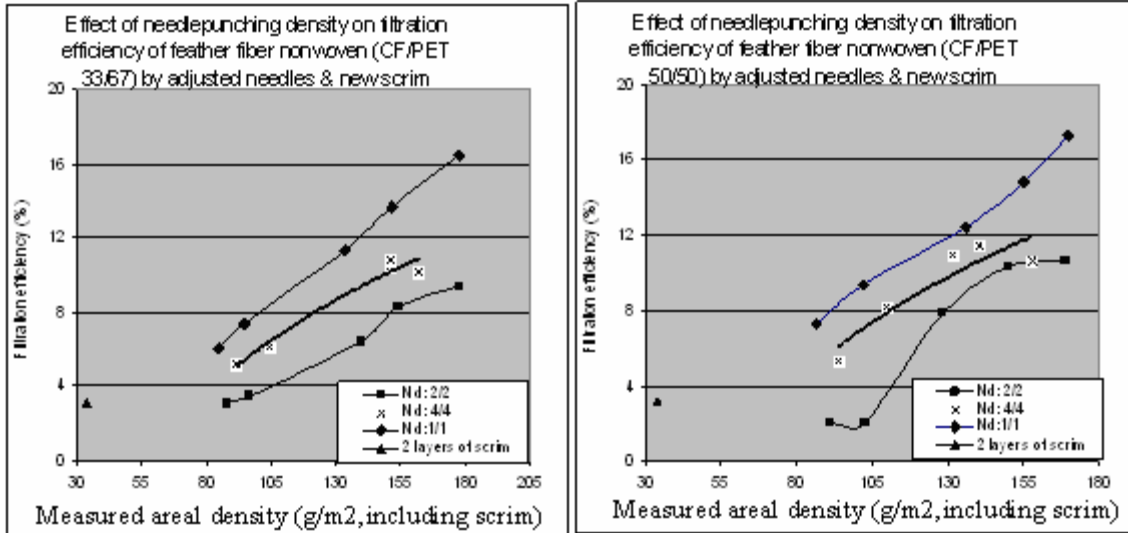


(c)

Figure 3-21 Effect of composition of new CF nonwovens on the air permeability at different same needlepunching density

3.4.2.3.2 Filtration Efficiency

Because the air permeability of CF/PET 67/33 at different needlepunching density was very close, the filtration efficiency of CF/PET 67/33 nonwovens was not tested and only that of CF/PET 33/67 and 50/50 was tested. As seen from Figure 3-22 (data in Table 3-7 – Table 3-9 and Table 3-12 – Table 3-17), it is clear that for these two compositions CF nonwovens needlepunching density had similar effect on their filtration efficiency. First of all, almost all nonwovens had higher filtration efficiency than that of two layers of Nd 2/2 scrim except two low density CF/PET 50/50 Nd 2/2 samples.



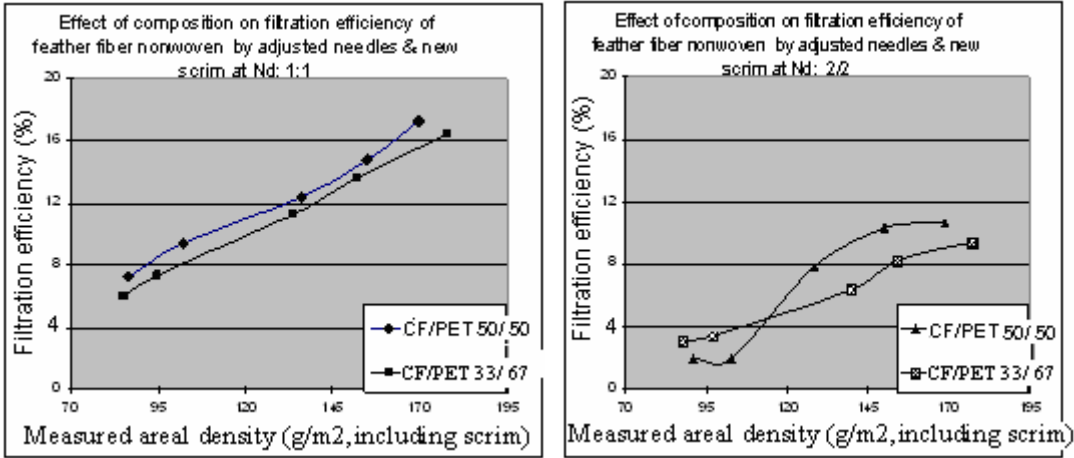
(a)

(b)

Figure 3-22 Effect of different needlepunching density on the filtration efficiency of new CF nonwovens (Note: 2 layers of scrim nonwovens were Nd 2/2 needlepunched.)

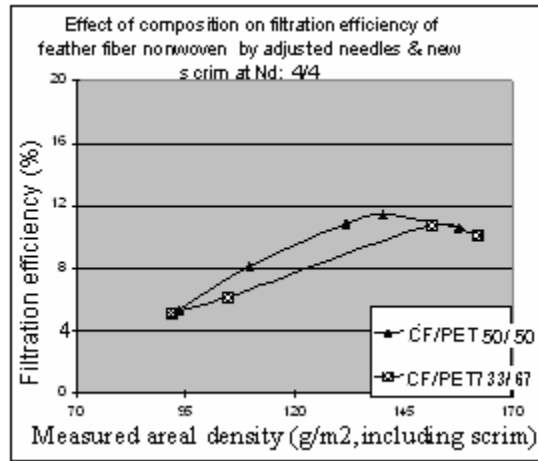
In the two different composition nonwovens (CF/PET 33/67 and 50/50), the lowest needlepunching density nonwovens (Nd 1/1) had highest filtration efficiency. However, the highest needlepunching density nonwovens did not get the lowest filtration efficiency and theirs was in the middle of that of the highest and second highest needlepunching density (Nd 2/2) nonwovens. Nd 2/2 nonwovens had the lowest filtration efficiency. For every different highest needlepunching density nonwovens, their filtration efficiency generally increased at the beginning with the measured areal density.

Figure 3-23 shows the filtration efficiency tendency of different composition nonwovens at the different same needlepunching density.



(a)

(b)



(c)

Figure 3-23 Filtration efficiency tendencies of new nonwovens at the same needlepunching density

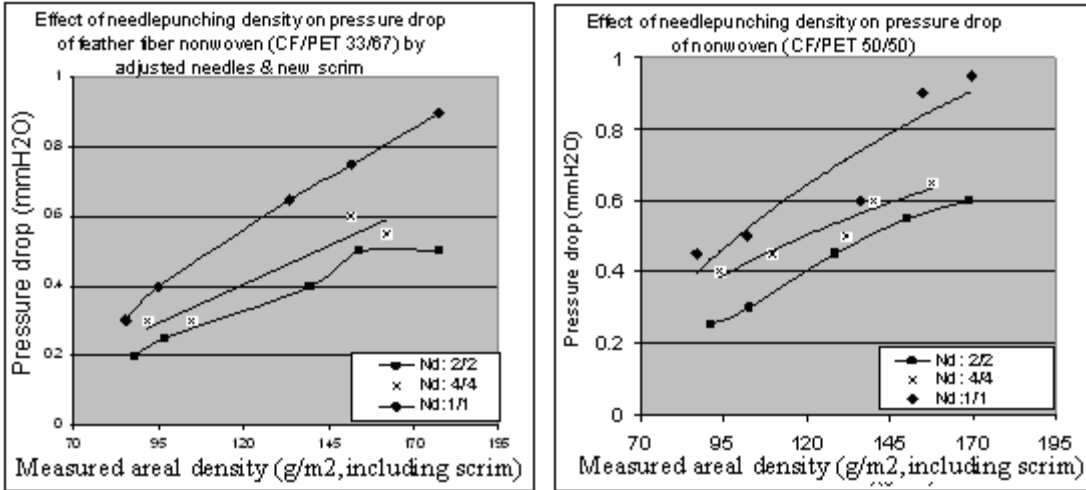
(Note: data in Table 3-7 – Table 3-9 and Table 3-12 – Table 3-17)

From Figure 3-23 (a) it can be seen that at the lowest needlepunching density (Nd 1/1), the two different composition nonwovens almost had the similar filtration efficiency tendency along with the measured areal density. Their filtration efficiency increased almost linearly with measured areal density and was improved by chicken feather fiber. Figure 3-23 (b) shows at needlepunching density Nd 2/2 different composition

nonwovens had different regular filtration efficiency action. At low density high PET percentage nonwovens had higher filtration efficiency, but at higher density high chicken feather fiber percentage nonwovens had higher filtration efficiency. Figure 3-23 (c) shows a complex filtration efficiency rule of high needlepunching density (Nd 4/4) nonwovens because of different composition. At low and high density CF/PET 50/50 and 33/67 nonwovens had the same filtration efficiency but the middle density high CF percentage nonwovens had higher filtration efficiency.

3.4.2.3.3 Pressure drop

It can be seen from Figure 3-24 (data in Table 3-7 – Table 3-9 and Table 3-12 – Table 3-17) all of the tested CF nonwovens needed higher pressure drop than two layers of needlepunched scrim and the pressure drop increased with the measured areal density. The effects of needlepunching density in different composition nonwovens were also shown in this Figure 3-24. For both composition CF nonwovens, lowest needlepunching density nonwovens (Nd 1/1) had the highest pressure drop and second highest needlepunching density nonwovens (Nd 2/2) had the lowest pressure drop, while the nonwovens with the highest needlepunching density had the pressure drop between them.



(a)

(b)

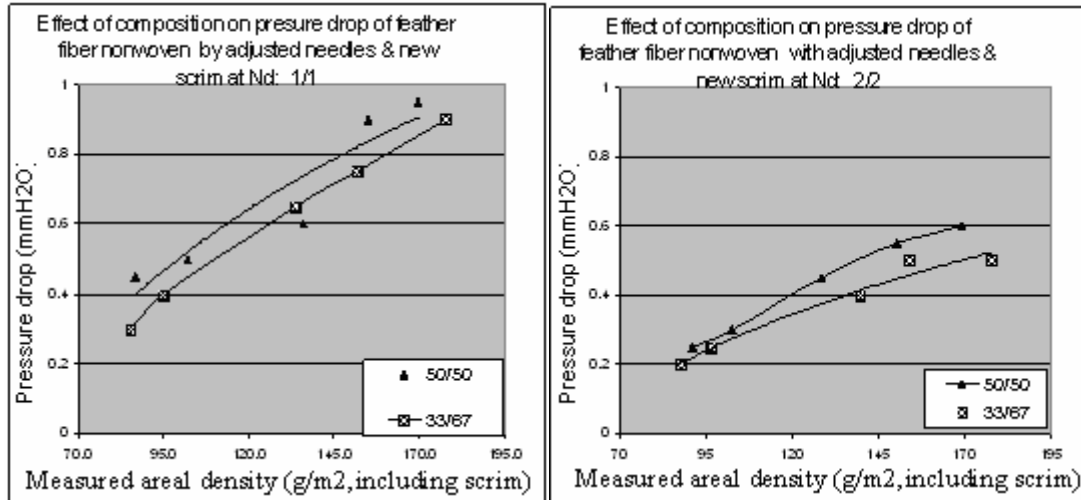
Figure 3-24 Effects of needlepunching density on the pressure drop of new CF nonwovens

(Note: (a) Effect of needlepunching density on pressure drop of feather fiber nonwoven (CF/PET33/67 by adjusted needles and with new scrim

(b) Effect of needlepunching density on pressure drop of feather fiber nonwoven (CF/PET50/50 by adjusted needles and with new scrim

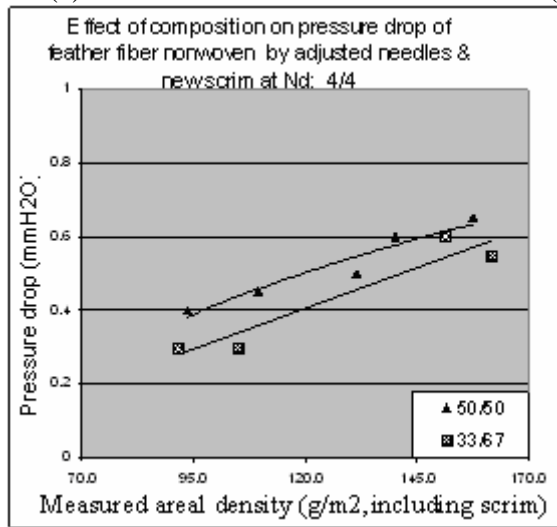
Data are from Table 3-7 – Table 3-9 and Table 3-12 – Table 3-17.)

Figure 3-25 shows the effect of CF nonwoven composition on their pressure drop at different same needlepunching density. From Figure 3-25 (a), (b) and (c), Table 3-7 – Table 3-9 and Table 3-12 – Table 3-17, it can be seen that at any needlepunching density CF/PET 50/50 nonwovens generally had higher pressure drop than CF/PET 33/67 nonwovens.



(a)

(b)



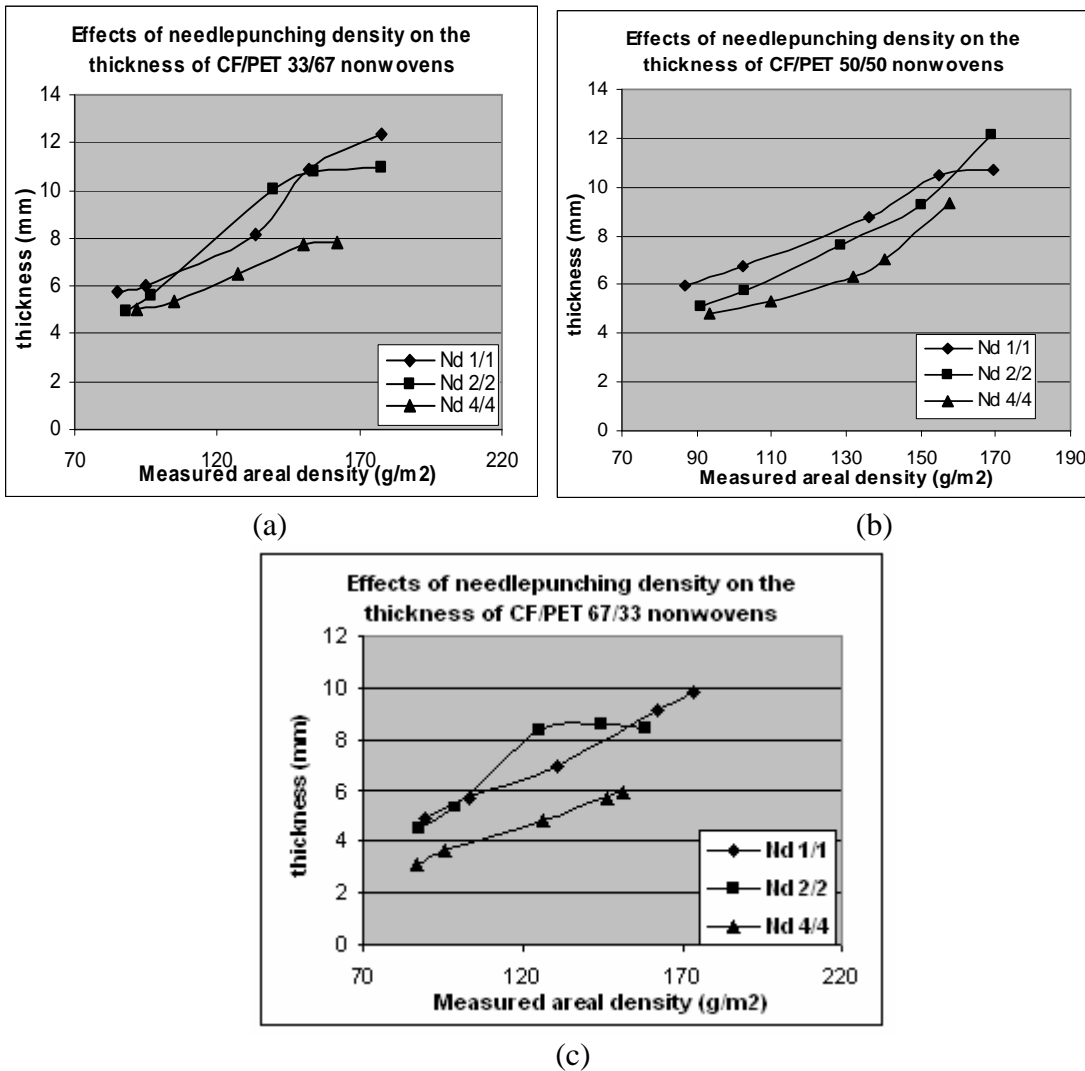
(c)

Figure 3-25 Effect of composition on the pressure drop of new CF nonwoven

3.4.2.3.4 Thickness:

Figure 3-26 (data in Table 3-7 – Table 3-9 and Table 3-12 – Table 3-17) shows the effects of areal density and needlepunching density on the thickness of different composition of CF nonwovens. From this figure, it can be seen that the thickness of CF nonwovens increased with the areal density, which is in agreement with the findings of Hearie and Sultan [7]. For all the three kinds of different composition CF nonwovens the

Nd 4/4 nonwovens had the smallest thickness at any areal density level. This is due to the fact that with the increase of needlepunching density by repeated needlepunching there will be lesser chance of fibers to bounce back to their original positions and, thus, fiber locking increased. According to the work of Gradmare and Martenssopn [8], increasing needling decrease the thickness, and then, Nd1/1 nonwovens should have larger thickness than Nd 2/2 nonwovens.

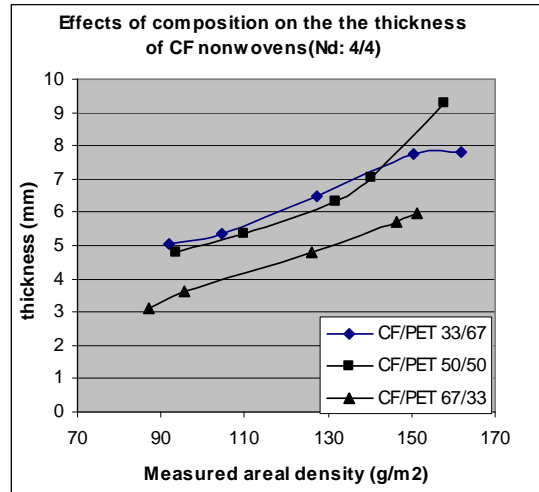
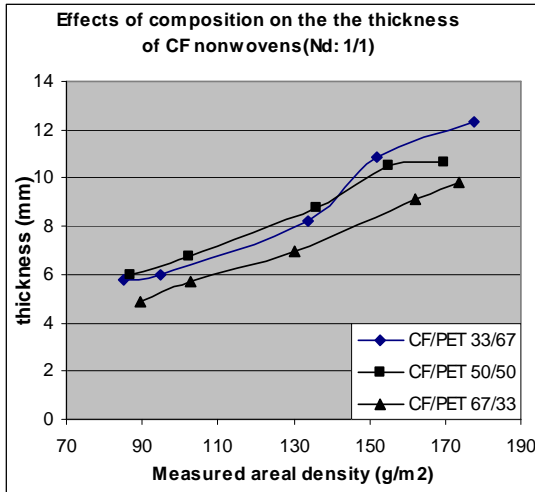


Figur3-27 Effects of areal density and needlepunching density on the thickness of new CF nonwovens (data in Table 3-7 – Table 3-9 and Table 3-12 – Table 3-17)

Figure 3-27 shows the effects of the composition of CF nonwovens on the thickness at different needlepunching density. It can be seen that highest CF component nonwovens had lowest thickness among all the samples at any needlepunching density. Figure 3-27 (c) indicates that the CF/PET 0/100 nonwovens had the biggest thickness. These two facts are in agreement with the finding of Igwe and Smith [9]. These may be due to the fact that feather fibers had smaller diameter than PET fibers, higher feather fiber percentage made the average diameter of fiber mixtures smaller and finer fiber were more easily contacted by needling. Increasing the amount of CF seems to make a more dense structure. CF/PET 67/33 nonwovens had lower thickness.

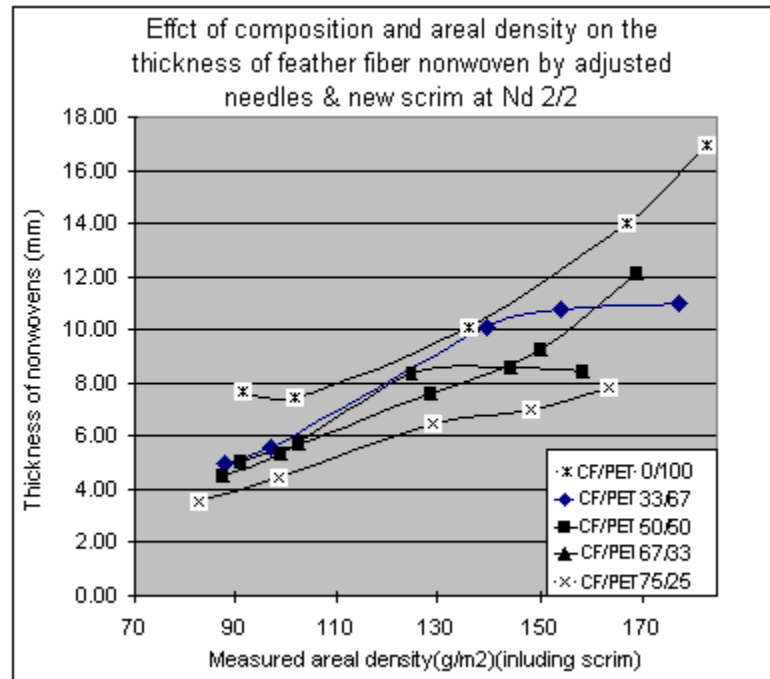
3.4.2.3.5 Comparison of commercial air filters to needlepunched CF nonwovens

Figure 3-28 shows that commercial air filters had higher filtration efficiency than needlepunched CF nonwovens. However, the commercial air filters with high filtration efficiency was tested under static electricity. Static electricity greatly improves filtration efficiency. Maybe CF nonwovens can also improve their filtration efficiency by static electricity. The commercial air filter with higher filtration efficiency had very low air permeability, which was only one fifth of that of CF nonwovens while low air permeability increase filtration efficiency.



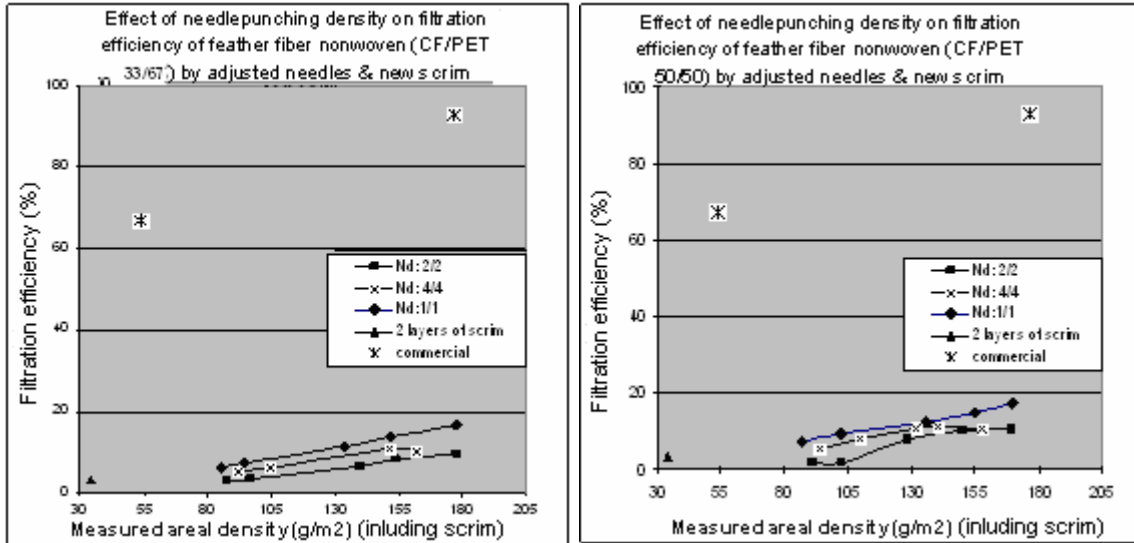
(a)

(b)



(c)

Figure 3-27 Effects of composition on the thickness of new CF nonwoven at different needlepunching density (Note: data are from Table 3-6 – Table 3-11.)



(a)

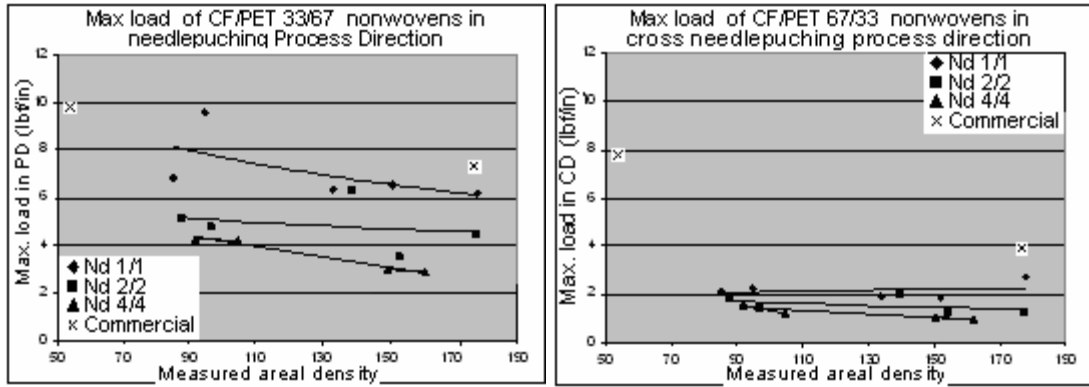
(b)

Figure 3-28 Comparison of filtration efficiency of commercial air filters to needlepunched new CF nonwovens (Note: data are from Table 3-7 – Table 3-9 and Table 3-12 – Table 3-17.)

3.4.2.3.6 Mechanic properties- maximum load

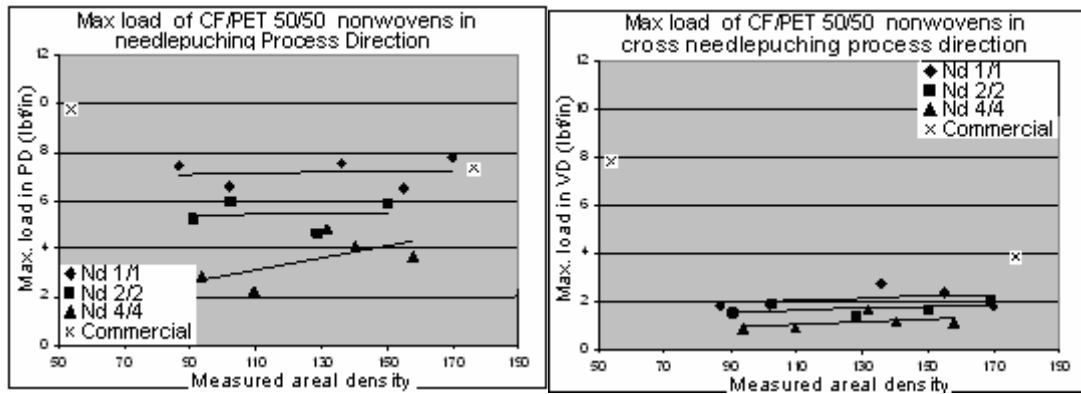
For these nonwovens, one of mechanical properties-maximum load was measured. Figure 3-29 shows that the effects of the needlepunching density on the maximum load of different composition CF nonwovens.

From Figure 3-29 it can be seen that, for every different composition CF nonwovens, the maximum load at different direction, needlepunching process direction and its vertical direction (cross direction) were different. The maximum load at the needlepunching process direction was much bigger than that at cross needlepunching process direction for all these samples. Larger needlepunching density reduced the maximum load at both directions. Figure 3-29 (a) and (e) show that the tendency of the maximum load at



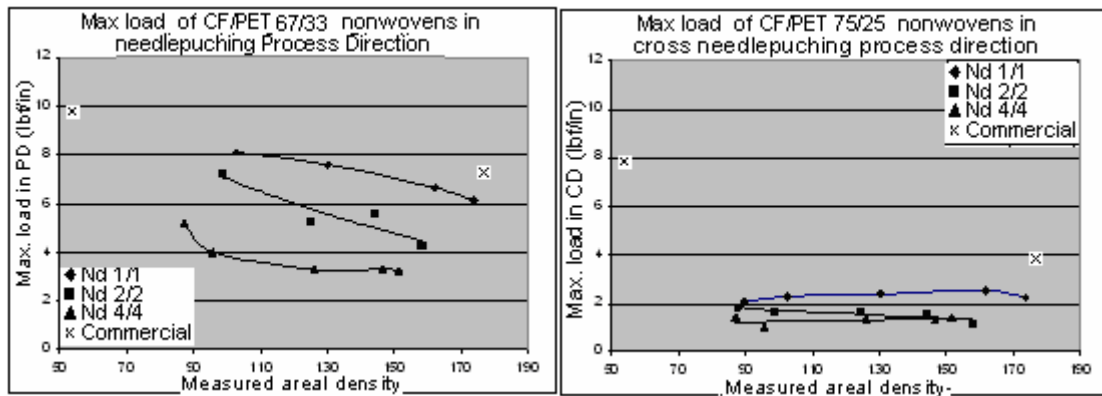
(a)

(b)



(c)

(d)



(e)

(f)

Figure 3-29 Effects of needlepunching density on the maximum load of new CF nonwovens

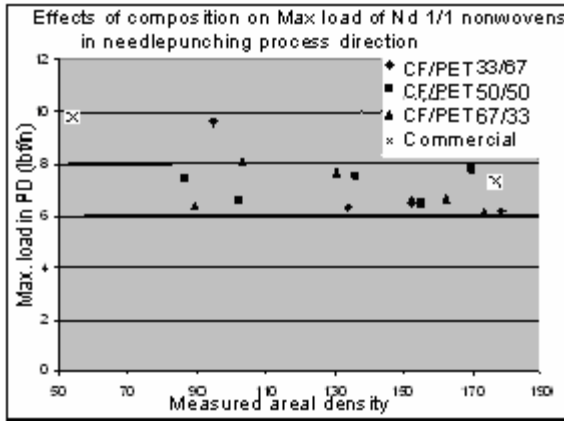
(Note: Measured density is measured areal density; and data are from Table 3-7- Table 3-9 and Table 3-12 – Table 3-17.)

needlepunching process direction was that it decreased obviously with the areal density for CF nonwovens who had bigger either feather fiber or PET percentage at any needlepunching density. However, Figure 3-29 (c) shows that the maximum load at needlepunching process increased a little with the areal density for CF/PET 50/50 nonwovens.

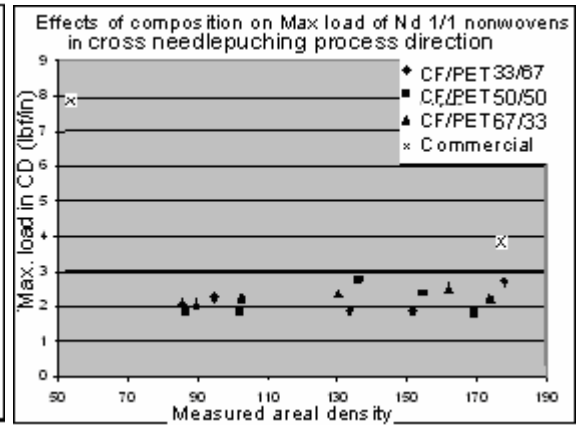
From Figure 3-29 (b), (d) and (f) it can be seen that the maximum load at the cross direction vertical to the needlepunching process also increased or decreased with the areal density of CF nonwovens. The degree of increase or decrease was very small.

Figure 3-30 shows the effect of composition of CF nonwovens on their maximum load at the same needlepunching density. It can be seen that at same needlepunching density different composition CF nonwovens had the similar maximum load at the same the direction.

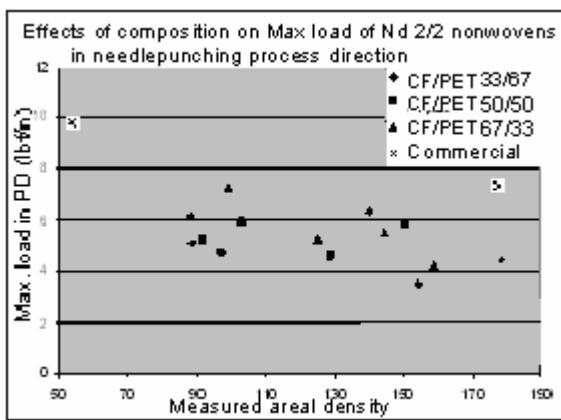
Since at the same needlepunching density, different composition CF nonwovens had the similar maximum load at the same direction, the CF/PET 33/67 nonwovens were chosen to compare maximum load with the two layers of scrim (Figure 3-31). Some low areal density CF nonwovens had higher maximum load than that of two layers of needlepunched scrim, but most other CF nonwovens had lower maximum load. That CF nonwovens had different maximum load at different direction was because of scrim. Since entangled feather and PET fibers do not form the needed strength, scrim was used to improve the tensile strength for CF nonwovens. The distribution of tensile strength of scrims affects that of CF nonwovens.



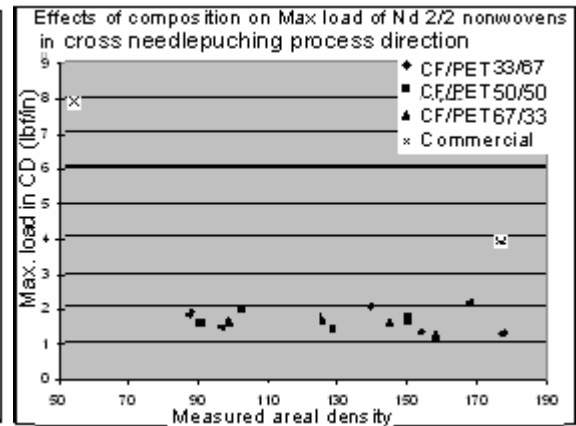
(a)



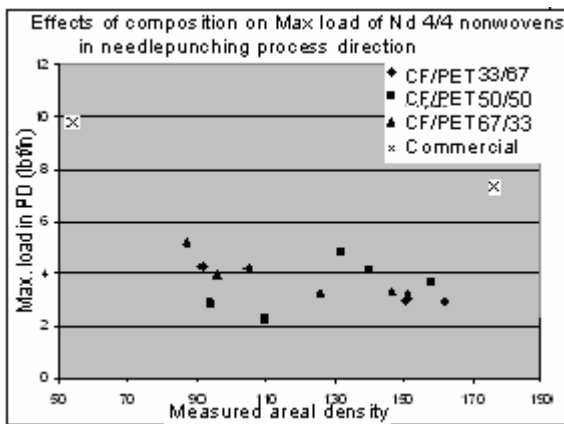
(b)



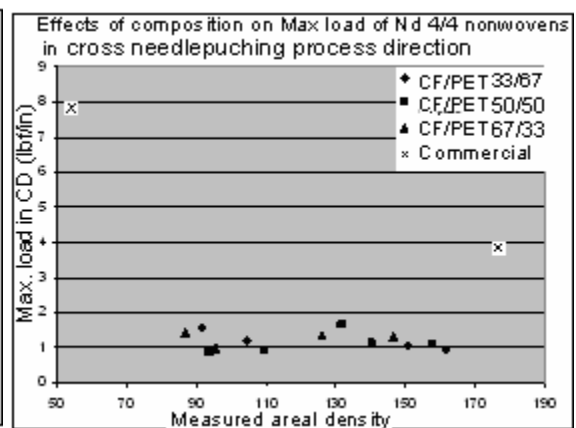
(c)



(d)



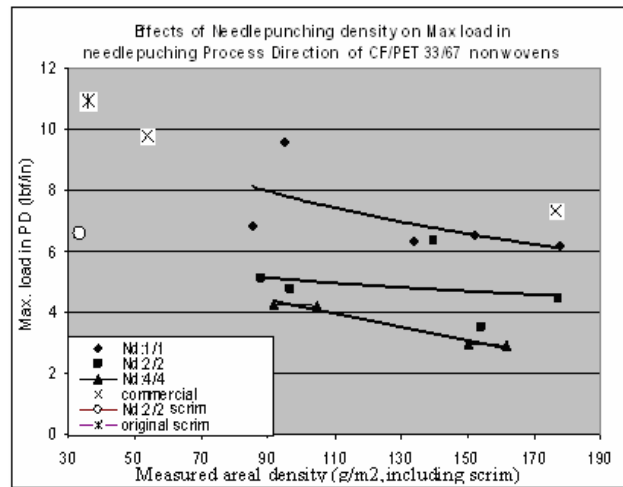
(e)



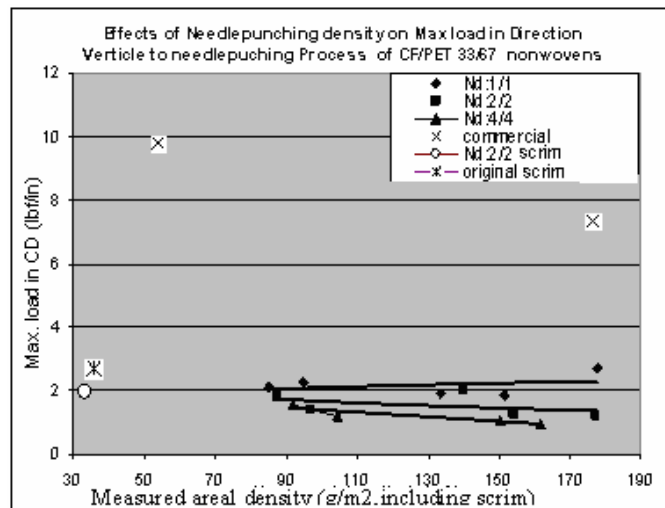
(f)

Figure 3-30 Effects of composition of new CF nonwovens on the maximum load at different needlepunching (Note: measured areal density includes scrim, and data are from Table 3-7 – Table 3-9 and Table 3-12 – Table 3-17.)

From Figure 3-31 it can also be seen that comparison of the maximum load of CF nonwovens to that of commercial air filters. In the commercial air filter the direction did not affect the maximum load much. At needlepunching process direction low needlepunching density (Nd 1/1) made the have similar maximum load to that of commercial air filters, but high needlepunching density (Nd 2/2 and 4/4) forced CF nonwovens have lower than commercial air filters.



(a) In needlepunching process direction



(b) In cross needlepunching process direction

Figur3-31 Comparison of maximum load of CF nonwovens with that of two layers of scrim and commercial air filter

3.4.2.3.7 Relationship between filtration efficiency and air permeability

Figure 3-32 shows the relationship between filtration efficiency and air permeability at different needlepunching density (the data are from CF/PET 33/67, 50/50 and 67/33 nonwovens for every needlepunching density and put together). It can be seen that needlepunching density did not affect their relationship much and their relationship at different had only a little different. At low needlepunching density (Nd: 1/1) the filtration efficiency increased a little fast with the decrease of air permeability; while at other two needlepunching density (Nd: 2/2, and 4/4) the filtration efficiency increase slowly and straightly with the decrease of air permeability and their trend line were almost the same to each other.

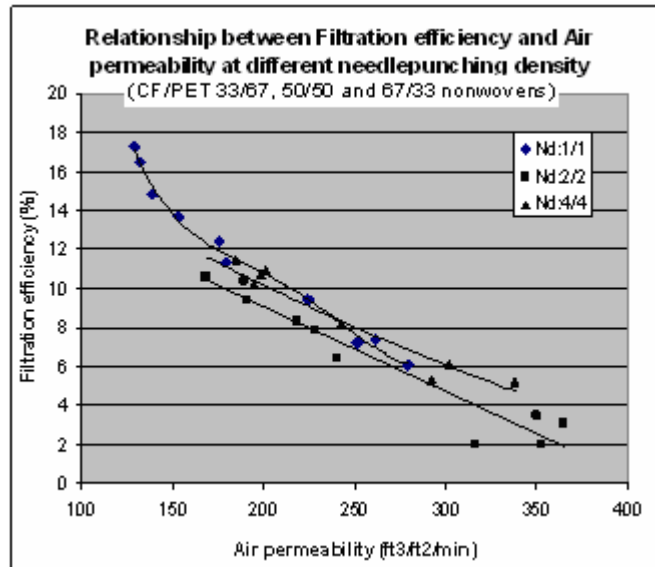


Figure 3-32 Relationship between filtration efficiency and air permeability of new CF nonwovens (Note: data are from Table 3-7- Table 3-9 and Table 3-12 – Table 3-17.)

3.4.2.3.8 Relationship between filtration efficiency and pressure drop

Figure 3-33 shows the relationship between filtration and pressure drop at different needlepunching density for CF nonwovens. It can be seen that needlepunching density did not affect the relationship much and it was almost in the same trend at different needlepunching density. At low and high needlepunching density (Nd 1/1 and 4/4) filtration efficiency increased slowly with the pressure drop while at middle needlepunching density (Nd 2/2) the filtration efficiency increased a little faster, but probably not significantly.

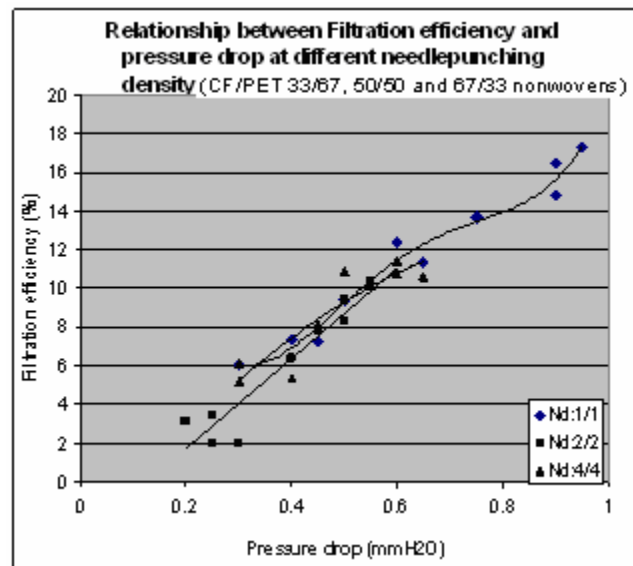


Figure 3-33 Relationship between filtration efficiency and pressure drop of new CF nonwovens at different needlepunching density

(Note: data are from Table 3-7– Table 3-9 and Table 3-12 – Table 3-17.)

3.5 Conclusion

In this chapter the chicken feather fiber was used in combination with polyester staple fibers by the processes of opening and mixing, mat formation (air-laying) and

needlepunching to produce needlepunched nonwoven fabrics for air-filtration. A layer of scrim placed above and below the fiber mixtures. With two kinds of different areal density scrim and different needle height, two sets of needlepunched nonwoven fabrics were produced. Their filtration properties such as air-permeability, filtration efficiency and pressure drop and mechanical properties such as tensile strength and % strain at break were measured.

The CF needlepunched nonwovens produced with adjusted needle height which just made needles pass through the mat and covered by light PET scrim had better regularity than first set of CF needlepunched nonwovens produced with heavy PET scrim and original needle height which made the whole needles pass through the mat. The second set of new nonwovens had higher air permeability. With an increase of areal density and feather fiber composition, the air permeability of nonwovens decreased, and filtration efficiency and pressure drop both increased. The case can be made that CF fiber gave fabrics better filtration at the same fabric weight, but the addition of CF fiber improves the filtration efficiency at the expense of air permeability and pressure drop.

In the second set of needlepunched CF nonwovens, needlepunching density in different range had different effects on the fabric thickness, density, air permeability, pressure drop and filtration efficiency. In this set Nd 2/2 nonwovens had highest air permeability, lowest filtration efficiency and lowest pressure drop among the three different needlepunching density nonwovens. The scrim and needlepunching process could improve the filtration efficiency, but this improvement was also at the expense of air permeability and pressure drop. Filtration efficiency directly related to pressure drop and inversely related to air permeability, regardless how these effects were obtained,

either by increase in CF content or by increased needling. Strength of the nonwovens was directly dependent on scrim and decreased with needling because needling breaks fibers of scrim and then weakens scrim. The conclusion is that, although feather fiber recycled into air filter fabrics, its fineness and the tree/fan-like structure of the feather does not offer a high level of performance advantages over conventional fibers. The use of feather fiber in air filtration applications must rely primarily on a favorable cost and weight differential in favor of the feather fiber.

3.6 Reference:

- [1] web.utk.edu/.../Needle%20Punched%20Nonwovens.htm, 05/01/07
- [2] Ciach, Tomasz; Gradon, Leon, Highly efficient filtering materials, *Journal of Aerosol Science*, 27(Suppl 1), Sep, 1996, p S613-S614
- [3] Kothari, V. K.; Newton, A. Air permeability of nonwovens fabrics, *Journal of the Textile Institute*, 65(10), Oct, 1974, p 525-531
- [4] Al-Otoom, Awni Y, Prediction of the collection efficiency, the porosity, and the pressure drop across filter cakes in particulate air filtration, *Atmospheric Environment*, 39(1), January, 2005, p 51-57
- [5] Barris, M. A., Total Filtration, The Influence of Filter Selection on Engine Wear, Emissions and Performance, SAE 952557, 1995
- [6] Anon, Air filtration media for transportation applications, *Filtration and separation*, 35(2), March, 1998, p 124-129

- [7] Hearle, J. W. S., Sultan, M. A. I.; A study of needled fabrics Part I: experimental methods and properties; *Journal of the textile institute*; 58(6); p251-265, 1967
- [8] Gardmark, L. and Martinso, L.; An Experimental Investigation of Fiber Orientation and Some Properties of Needled Felts; *Textile Research Journal*, 36(12), p1037-42, 1966,
- [9] Igwe, G. J. I.; Smith, P. A.; The influence of some production parameters on the characteristics of needlefelts for gas filtration; *Journal of the Textile Institute*; 77(4), p263-6; 1986

CHAPTER 4

THERMOBONDED NONWOVEN AIR FILTERS FROM CHICKEN FEATHER FIBERS

4.1 Introduction

In this chapter, CF thermobonded nonwoven fabric for air filtration is discussed. Thermal bonded nonwovens for filtration were made as follows: opening and mixing → mat formation → hot pressing.

Bonded nonwovens are widely used and well-known in the world [1]. Thermal bonding is one of the most widely used bonding technologies in the nonwoven industry. From its definition, bonded nonwoven fabric is prepared from a combination of fibers and a bonding agent which works as 'glue' to firmly bind the mat together to form the nonwoven fabric. The bonding agent has a significant effect on the properties of the fabric. There are many kinds of the binding agent, for example, dispersion foam, paste, powder and so on. In this research, binding fibers were used so the bonding of the mat was called Fiber Bonding (Thermofusion). In this method, the mat is heated to the temperature at which part or whole bonding fibers melt. The molten mass binds the matrix fibers which do not melt at their intersection points.

In Fiber Bonding method, low energy is needed during the process; the produced nonwoven fabric is high-bulking, but still fairly strong. The mat is not affected by pressure during heat treatment; and the produced nonwovens have high air permeability.

In this research, among kinds of bonding fibers were chosen Celbond™ (254) bi-component bonding fibers (4 den., 2 inch). Celbond™ is the brand name of the family of dual-polymer (bi-component) fibers [2]. This binder has a distinguishing sheath/core structure. Its sheath is co-polyester with a low melting point of 140°C. When heated, the sheath polymer melts and when it cools down, it turns into a solid bond with adjacent fibers, so that strength is added to the final product.

Bonding with Celbond™ fibers as binders produces many good results [2]. First, their chemical content is simple and there is little emission during bonding so their thermal bonding is very clean, much cleaner than resin bonding; second, these fibers are thermoplastic and the mat made from them can be molded to any shape, and heat-sealed to themselves or to other fibers; third, Celbond™ fibers have uniform shell thickness, and this uniformity produces durable bonding and high bond strength throughout the mat and improves processing, which causes nonwoven fabrics to have high abrasion resistance and fabric strength. Since then, they can be applied to a wide range of natural and synthetic fibers, such as polyester, nylon, cellulose, wool, and down. Therefore, Celbond™ fibers were tried in feather fibers

Thermal bonding can be taken in many ways such as through-air bonding, infrared bonding, ultrasonic bonding, and thermal point bonding, hot calendering [3], belt calendering and so on. In this research, we used thermal plate bonding, that is, hot-pressing, in which two hot plates were used and the required equipment are very simple

and easy to control. A uniform fabric requires uniform pressure, uniform temperature, besides uniform input mat, all of which the heated plate can supply because smooth plates provide uniform pressure and heat from hot plates makes thin mat uniformly hot.

In this thermal plate bonding, after the mat is formed, it is placed in between the plates. Between the plates, thermal bonding proceeds through three stages: (1) compressing and heating the mat, (2) bonding the mat, and (3) cooling the bonded mat.

During compression, minimal pressure is demanded at the nip to produce fiber-to-fiber contact [3]. Sufficient pressure is required to compress the mat and decrease its thickness. In this way, efficient heat transfer through conduction can happen. Over the range of pressures commercially applied, higher nip pressures do not necessarily produce higher performance [3].

At the same time of compression, both of the plates are heated. Since heating the mat begins when the mat first touches the hot plate and continues until it leaves the plate, the time spent in the nip is also the time available for heating the mat. The heating occurs primarily through conduction, the fibers placed between two plates get heated very quickly. To form a bond, the binding fibers in the middle of the nip must reach a certain temperature. The plate temperature must stay below the melting points of fibers; otherwise the web will fuse to the plates. If the time in the nip is greater than the time to reach the temperature, the bond is strong. However, the too long heating time cannot guarantee strong bond because long time heating maybe produces over-bonding and this makes bond spot fiber lose their orientation, then some strength would be lost. In this research the effect of heating time on the strength of nonwovens was tested.

In this chapter, the thermobonding process parameters were fixed at required points such as sufficient pressure, time and temperature. The thermobonded nonwovens were tested for their filtration and mechanical properties.

4.2 Experimental

4.2.1 Preparation of thermobonded chicken feather fiber nonwovens

4.2.1.1 Materials

The chicken feather fibers used in these experiments were obtained using the method in Chapter two.

CelBond™ sheath/core bicomponent polyester fibers (4den, 2in) used as binders for thermobonded nonwoven were from Hoechst Celanese.

4.2.1.2 Procedure and Equipments

4.2.1.2.1 Opening and mixing fibers

The CelBond™ bonding fibers directly from the manufacturing factory were very coarse, often uneven, crumpled, even wiry, and there were even some bundles of strands that appear as tangled clusters of fibers. These coarse fibers were opened with Spinlab 338. Spinlab 338 was the same as used in Chapter 3 and shown in Figure 3-1. After opened for 4 times, tangled fibers became more separated, resulting in an accumulation of singular fibers. The opened binder fibers and a percentage of feather fibers were opened 3 times again to make the feather fibers distribute evenly in the binder fibers. The samples were produced with the various combinations of fibers mixed ratio, and mixtures fibers areal density.

4.2.1.2.2 Preparation of binder and feather fiber mat

Binder and feather fiber mat was prepared by air-laying in the vacuum box (the same as used in Chapter 3 and shown in Figure 3-2). During the preparation, a piece of scrim was placed on the screen of the vacuum box first; next, a pipe was connected Spinlab 338 and the vacuum box; and then the binder and feather fiber mixtures were sprayed onto the scrim on the screen of the vacuum; finally, this piece of mat was moved onto a piece of paper.

4.2.1.2.3 Preparation of CelBond™ binder and feather fiber thermobonded nonwovens by Hot-pressing

The mechanism of hot pressing is sketched in Figure 4-1. A piece of mat and two pieces of shim (with the same thickness and placed to two opposite sides of the mat) were put into between the two plates. The temperature of two plates, top and bottom, was set to 130 °C. The mat was kept between two hot plates for 2 minutes. The pressure on between the top and bottom of shim was 0.5 lbf/in². The thickness of the heat-press nonwoven was controlled by the thickness of the shims. The hot nonwovens cooled down in air. Experiments were designed based on the combinations of mat areal density, mix ratio, and control thickness (CT).

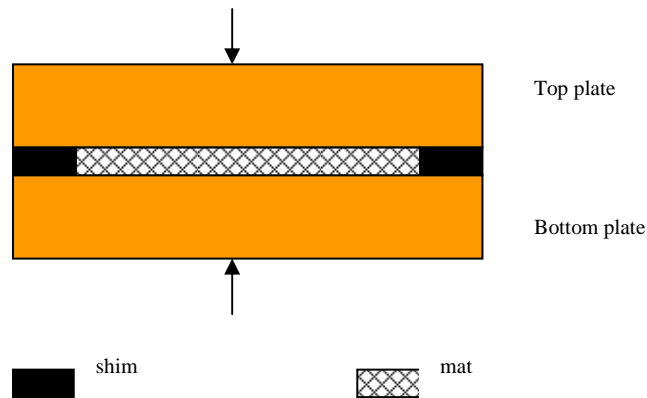


Figure 4-1 Mechanism sketch of hot pressing

4.2.2 Property testing of the thermobonded nonwovens for filtration

4.2.2.1 Filtration property testing

Air permeability was tested on the Frazier in Auburn University according to Test Method D 737. The pressure drop and penetration testing was performed on 8110 Automated Filter Tester in the Nonwoven center of Tennessee University in Knoxville. (Particles used in the test were sodium chloride whose weight average diameter was 0.2 μm and number average number diameter was 0.075 μm .)

4.2.2.2 Tensile property testing

Tensile strength was also tested on a universal testing machine (Instron Model 1122) according to D 5035-95. The width of samples was one inch. A gauge length of 75mm (3 inch) and a crosshead speed of 150mm (6inch)/min were used for tensile testing. The data were obtained from averages of 10 tests.

4.3 Results and Discussion

4.3.1 Filtration properties of thermal bonded nonwovens

The effect of areal density on the filtration property of thermal bonded nonwovens compared to some commercial air filters was shown Figure 4-2 (data in Table 4-1, 4-2 and 3-3). This figure shows the air permeability decreased and filtration efficiency increased with the increase of areal density of the thermal bonded nonwovens. Figure 4-2 (b) shows thermal bonded feather nonwoven had greater filtration efficiency than the commercial air filters but the difference seems to be the result of differences in areal density and air permeability.

Table 4-1 Filtration properties of thermal bond nonwovens in different density

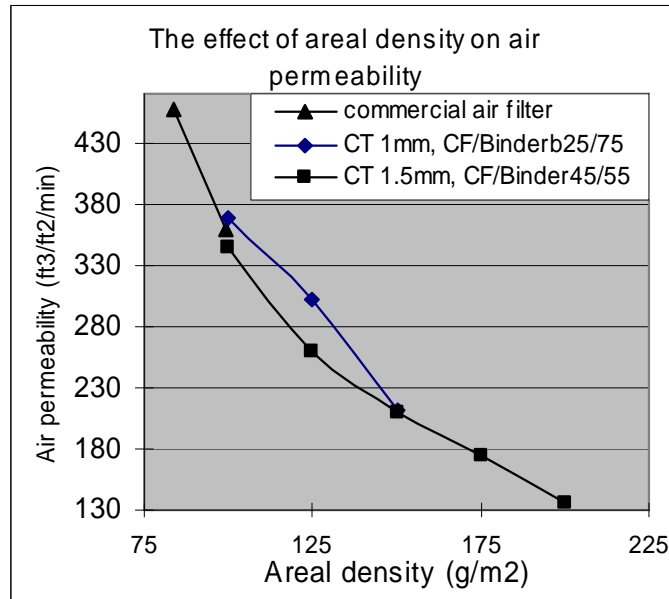
(Control thickness: 1.5mm, Feather fiber%/ binders%: 45/55)

Areal density (g/m ²)	Air permeability	Pressure drop (mm H ₂ O)	Filtration efficiency (%)
100	343.5	0.3	3.4
125	259.8	0.5	5.3
150	209.8	0.5	7.6
175	174.7	0.8	10.4
200	135.5	0.8	12.5

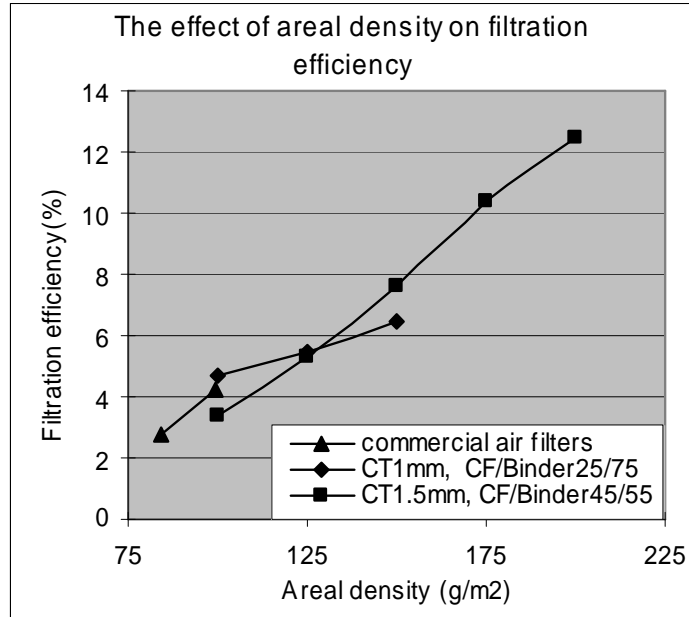
Table 4-2 Filtration properties of thermal bond nonwovens in different density

(Control thickness: 1.0mm, Feather fiber%/ binders%: 25/75)

Areal density (g/m ²)	Air permeability	Pressure drop (mm H ₂ O)	Filtration efficiency (%)
100	368.1	0.2	4.8
125	301.5	0.52	5.5
150	211.3	0.5	6.4



(a)

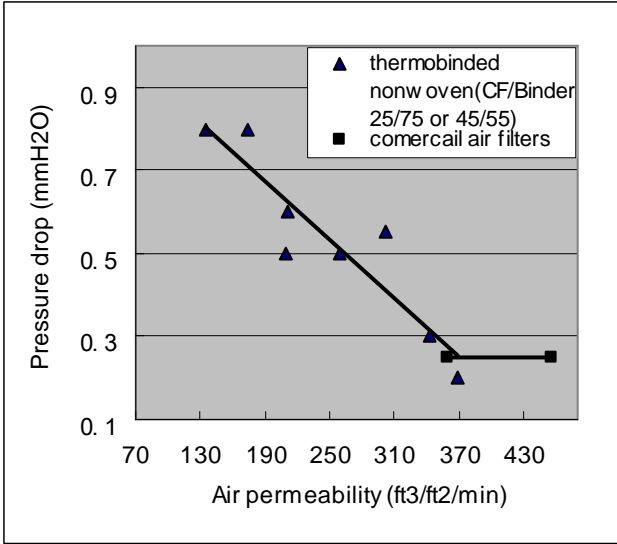


(b)

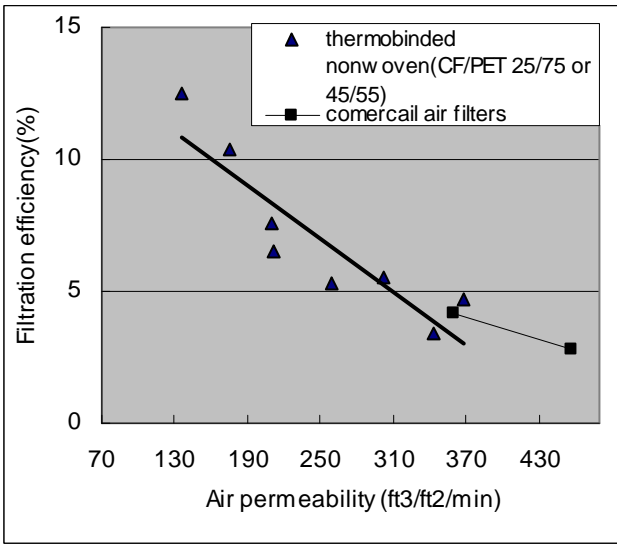
Figure 4-2 Filtration property of the thermobonded nonwovens compared to some commercial air filters

(Note: data in Table 4-1, 4-2 and 3-3)

Figure 4-3 (a) shows the relationship between air permeability and pressure drop. Most likely it was also linear to feather nonwovens. Figure 4-3(b) shows the relationship between filtration efficiency and pressure for the thermal bonded nonwovens. It can be seen that filtration efficiency decreased linearly with pressure drop. Feather fiber nonwovens have higher filtration efficiency than the commercial filters.



(a) Relationship between pressure drop and air permeability



(b) Relationship between filtration efficiency and air permeability

Figure 4-3 Relationship between pressure drop and air permeability of CF thermobonded nonwovens compared to the commercial air filters

(Note: data in Table 4-1, 4-2 and 3-3)

Table 4-3 Filtration properties of thermal bond nonwoven in different mix ratio
(Control thickness: 1mm)

Area density (g/m ²)	CF%/ Binder%	Air permeability	Pressure drop (mm H ₂ O)	Filtration efficiency (%)
125	45/55	219.6	0.2	4.7
	35/65	240.6	0.5	5.2
	25/75	301.5	0.6	6.5

From Table 4-3 it could be seen that the filtration efficiency increased with the ratio of chicken feather fiber. The filtration efficiency of the CF%/ Binder% 45/55 filter was similar to that of commercial air-filters (Table 3-3).

Table 4-4 shows that all the value of air permeability, pressure drop and filtration efficiency did not change much when the control thickness reached the certain value to a certain component and areal density thermal bonded nonwoven. The filtration efficiency of the CF/Binder 45/55 nonwovens was greater than that of commercial air-filters (Table 3-3), but again, the effect seems to be from the weight and permeability of the sample rather than from the fact that chicken feather fiber was added.

Table 4-4 Filtration properties of thermal bonded nonwovens in different volumetric density

Areal density (g/m ²)	CT (mm)	Air Permeability (ft ³ /ft ² /min)	Pressure drop (mm H ₂ O)	Filtration efficiency (%)
200	1.5	135.5	0.8	12.5
200	2.0	178.4	0.7	9.5
200	2.5	191.9	0.7	9.3

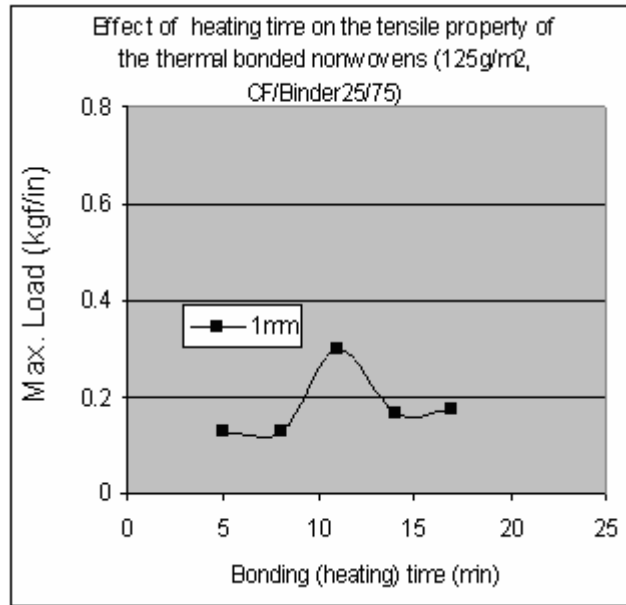
(Note: CF/Binder 45/55)

4.3.2 Tensile properties of thermal bonded nonwovens

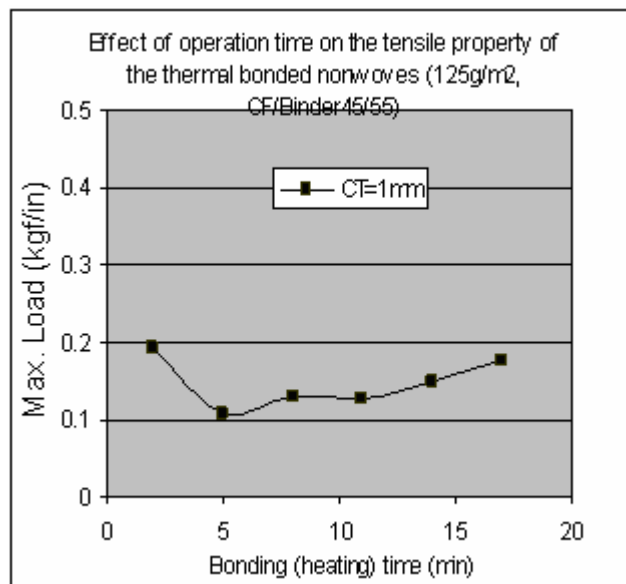
After hot-pressing, the loose and soft mat became a more compact stiff nonwoven. The effect of bonding (heating) time is shown in Figure 4-4. From these data, a bonding time of two minutes was selected and used throughout the study.

The tensile properties of thermal bonded nonwovens are shown in Figure 4-5 (data from Table 4-5). Generally, the presence of feather fibers reduced the maximum load. For these thermal bonded nonwovens the maximum load decreased with the increase of feather fibers. The more feather fiber the nonwovens had, the lower their maximum load was. Figure 4-5(b) shows that areal density did not have much effect on the maximum load of CF/Binder 45/55 nonwoven with high control thickness (1.5 mm). The change of %strain at the maximum load was complex, shown in Figure 4-6 (data from Table 4-5). For the control thickness 1 mm nonwovens, the %strain at maximum load increased with the presence of feather fiber, decreased with the increase of the areal density and CF/Bind 45/55 had the biggest for the same areal density. At the same control thickness, 1.5mm

nonwovens of CF/Binder 45/55, the %strain at maximum load was also greater than that of CF/Binder 0/100 along most of areal density range.

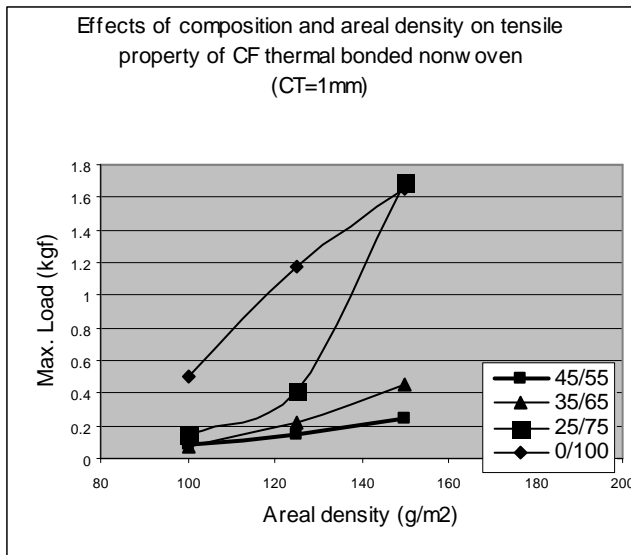


(a)

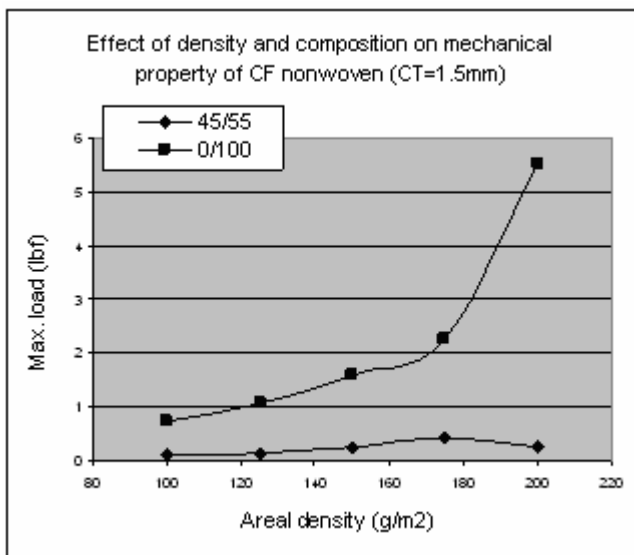


(b)

Figure 4-4 Effect of the bonding time on the tensile property of CF thermal bonded nonwovens



(a) Effect of composition and areal density on Maximum load of CF thermobonded nonwovens (CT=1mm)

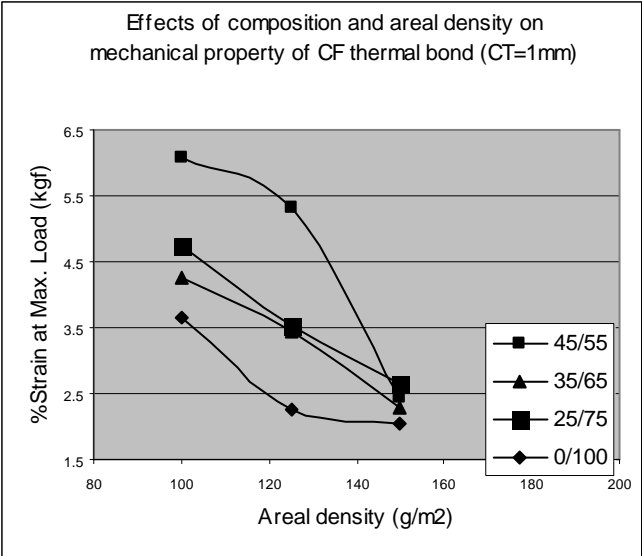


(b) Effect of composition and areal density on Maximum load of CF thermobonded nonwovens (CT=1.5mm)

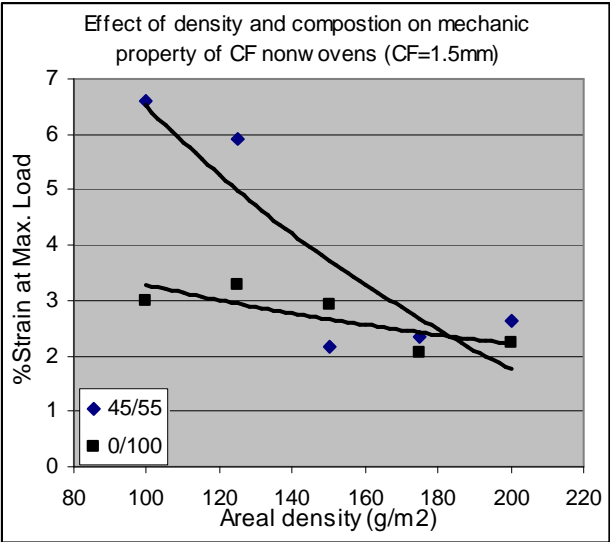
Figure 4-5 Tensile property of CF thermal bond nonwovens (a, and b)

(Note: the ration in figures was the CF/Binder)

(Note: data from Table 4-5)



(a) Effect of composition and areal density on %strain at Maximum load of CF thermobonded nonwovens (CT=1mm)



(b) Effect of composition and areal density on %strain at Maximum load of CF thermobonded nonwovens (CT=1.5mm)

Figure 4-6 Tensile property of CF thermal bond nonwovens (a and b)

(Note: the ration in figures was the CF/Binder and data from Table 4-5).

Table 4-5 Air permeability and tensile property of thermal bond nonwoven

Area density (g/m ²)	Feather fiber/Binder (% / %)	Control thickness (mm)	Air Permeability (ft ³ /ft ² /min)	Max. load (kgf)	% strain at Max. Load
100	45/55	0.5	211.7	0.266	1.966
		1.0	319.9	0.182	6.062
		1.5	380.9	0.100	6.600
	35/65	0.5	228.6	0.339	2.590
		1.0	346.9	0.069	4.266
	25/75	0.5	241.0	0.529	2.317
1.0		368.1	0.144	4.755	
125	45/55	0.5	138.0	0.212	3.379
		1.0	219.6	0.145	5.304
		1.5	316.6	0.144	5.923
	35/65	0.5	211.8	0.513	3.340
		1.0	240.6	0.223	3.431
	25/75	0.5	217.9	0.832	3.254
1.0		301.5	0.411	2.020	
150	45/55	0.5	94.3	0.157	3.177
		1.0	183.4	0.240	2.445
		1.5	243.1	0.251	2.153
	35/65	0.5	111.3	0.703	2.825
		1.0	189.5	0.448	2.277
	25/75	0.5	138	1.692	2.662
1.0		211.3	1.692	2.662	

4.4 Thermal bond nonwoven for heat transfer study

A thermal bonded nonwoven was also prepared for thermal insulation. The processing procedure was as follows:

Opening and mixing → Mat formation → hot-air bonding

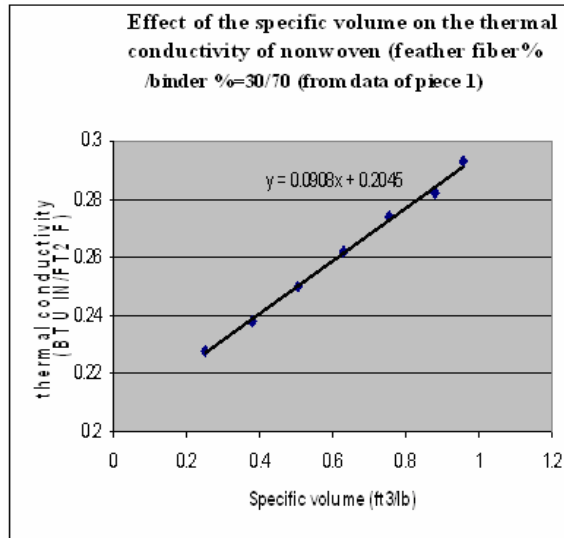
4.4.1 Manufacturing of thermal bonded nonwovens for heat transfer study

Feather fibers and CelBond™ fibers (bicomponent polyester fiber, 4den, 2in) were opened and mixed first using Spinlab 338 same as in Chapter 3; and formed into mat by air-lay in the Vacuum box same as in Chapter 3. The CelBond™ binder fibers were served as binder. Then the mat was heated by hot-air and bound naturally without any pressure. Since chicken feather fiber always flew out from the high feather fiber percentage thermal bond nonwoven, low feather fiber content mat feather fiber%/binder% 30/70 was chosen.

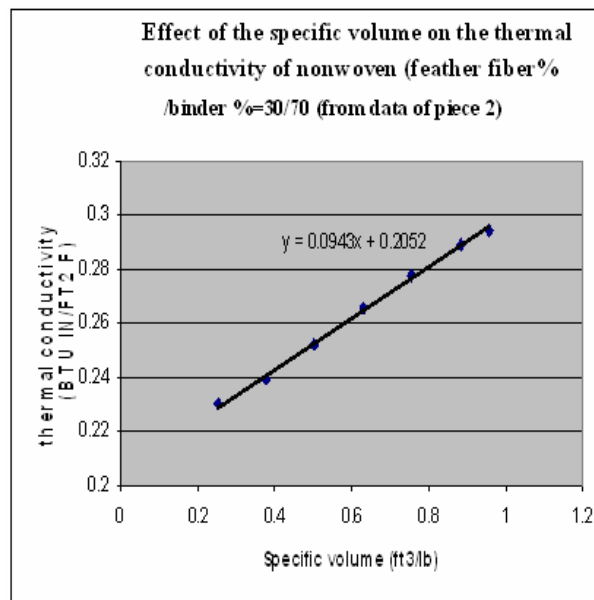
4.4.2 Thermal conductivity of the thermal bonded nonwoven (CF%/binder% 30/70)

Thermal conductivity was tested in K-Matic thermal conductivity instrument in Auburn University. From Figure 4-7 (a) and (b), it could be seen that for both of the pieces of the feather fiber%/binder% 30/70 thermal bonded nonwoven the thermal conductivity changed linearly with specific volume (1/density). The data were in Table 4-6. In Figure 4-7 (a) the slope was 0.0908, while it was a little higher, 0.0943 in Figure 4-7 (b). The two sets of data were put together to make up the error, the linear relationship could better fit the real fact. The slope became between them, 0.0926 (Figure 4-8). This

figure indicates that the more compact thermal bonded CF nonwovens transfer heat faster. The result agrees well with the work of a previous graduate student [4].



(a)



(b)

Figure 4-7 Thermal conductivity of thermal bond nonwoven

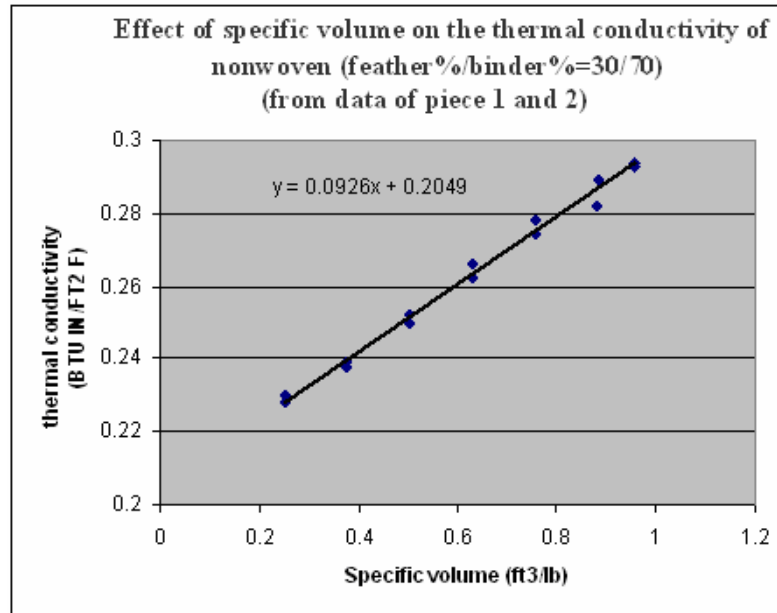


Figure 4-8 Thermal conductivity of thermal bond nonwovens

4.5 CONCLUSION

In this chapter the chicken feather fiber was used in combination with CelBondTM bi-component polyester as binder fibers by the processes of opening and mixing, mat formation (air-laying) and hot-pressing (2 minutes) to produce thermobonded nonwoven fabrics for air-filtration. Their filtration properties such as air-permeability, filtration efficiency and pressure drop and mechanical properties such as tensile strength and % strain at break were measured. The thermobonded CF nonwovens had high air permeability. With an increase of areal density and feather fiber composition, the air permeability of nonwovens decreased, and filtration efficiency and pressure drop both increased. There is an inverse relation between air permeability and either pressure drop

or filtration efficiency. Air filtration fabrics containing feather fiber seem to be equivalent to, or slightly better than commercial filtration products at the same permeability. Although we began the research with the hypothesis that the branched structure of feather fiber would allow better performance than typical fibers in air filtration applications, this does not seem to be the case. The use of feather fiber in air filtration applications must rely primarily on a favorable cost and weight differential in favor of the feather fiber.

4.6 Reference

- [1] The nonwovens handbook / INDA, Association of the Nonwoven Fabrics Industry, New York, N.Y.: The Association, 1988, p105
- [2] http://www.invista.com/page_product_celbond_en.shtml 11/08/06
- [3] Stephen Michielsen, Behnam Pourdeyhimi, Prashant Desai, Review of Thermally Point-Bonded Nonwovens: Materials, Processes, and Properties, *Journal of Applied Polymer Science*, 99, 2006, p2489–2496
- [4] [Ye, Weiqin](#); [Broughton, Roy M. Jr.](#); [Hess, Joseph B.](#) Chicken feather fiber: A new fiber for non-woven insulation materials, *Proceedings of the Largest International Nonwovens Technical Conference*, 1998, p 7.1-7.7

CHAPTER 5

PRODUCTION OF REGENERATED CHICKEN FEATHER PROTEIN FIBERS

5.1 Introduction

This chapter discusses the use of chicken feathers (CF) to produce regenerated fibers with satisfactory mechanical properties. The annual world fiber market is about 67 million tons, and includes about 2.3 million tons of the two natural protein fibers, wool and silk [2], but the demand for natural protein fibers remains high. As a result, the cost of these fibers remains expensive and their use is, therefore, limited [1]. After considerable research over years on the physical properties and chemical structure of CF protein, it is being recognized as a potential polymeric raw material for composites and regenerated fibers. Most of CF from chicken processing is a structural fibrous protein, keratin, which could potentially be used for protein fiber production as an alternative for natural protein fibers [2]. It has been found that wool keratin can be used for regenerated fibers [3]. Therefore, similarly, regenerated fibrous applications provide an opportunity to add high value and offer a large market to the huge amount of chicken feathers.

Originally, attempts to produce regenerated protein fibers were limited to protein of food materials such as soybean, corn, peanut and milk. The commercial scale production of fibers from these sources was reported during the 1930s and 1940s [2]. However, these artificial protein fiber productions have mostly ceased because their raw materials were

expensive, their production processes were not environmentally friendly and the regenerated protein fibers had worse properties than synthetic fiber. CF keratin had not been investigated to its regenerated fibrous production well.

CF keratin is similar to that of other outer coverings such as hair, wool, nail, and horns. From amino acid chemical structural, it is distinguished by the high Cysteine content (up to 7% the total molar amino acid residues). These Cysteine residues are oxidized to produce both inter- and intramolecular disulfide bonds, which causes the mechanically strong three-dimensionally cross-linked network of keratin fiber with limited conformational arrangement so feather fiber keratin has compact crystal structure. Generally, good strong fibers require high molecular weight polymers. Therefore, it is necessary to cleave the disulfide bonds without breaking the peptide linkage to dissolve the feather keratin for chicken feather regenerated keratin fiber production. Both reducing agents and oxidizing agents can be used to break the disulfide bonds. In this paper, the reducing agent bisulfide salt (shown in Figure 5-1), was used because this method produces reversible reduction of molecules and also produces keratin suitable for fiber production [1].

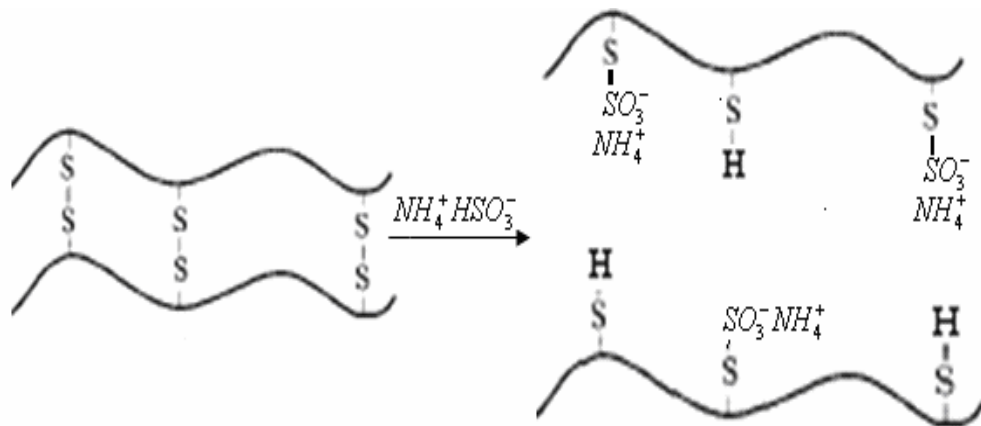


Figure 5-1 Breakage of disulfide bonds by reduction

In this chapter, an ionic liquid (IL) with reducing agent was used to dissolve protein. IL is a new kind of solvent, a salt with a melting point below 100°C and typically consists of a heterocyclic nitrogen-containing organic cation and an inorganic anion (shown in Figure 5-2).

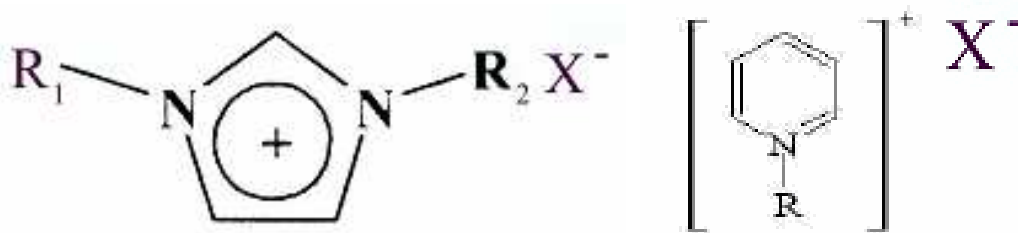


Figure 5-2 Basic chemical structure of an ionic liquid

Owing to its special structure compared to the traditional molecular solvents, IL has many unique solubility characteristics. IL is electrically conductive and non-flammable and has extremely low [vapor pressure](#) (its noticeable odors are possibly because of impurities.), excellent thermal stability, a wide liquid range, and favorable [solvating properties](#) for different compounds. Therefore, it becomes a route to volatile organic solvent replacement and acts as a green and designable solvent with the development of green chemistry and the requirement for environment protection. For this, IL has received a lot of attention. It has been found that IL is used already in organic synthesis and catalysis [3, 4].

In our research 1-butyl-3-methylimidazolium chloride (BMIM⁺Cl⁻) was used. Its chemical structure is shown in Figure 5-3. It has strong ability to disrupt hydrogen bonds under mild conditions and thus they can be used to dissolve biological

macromolecules that are linked by intermolecular hydrogen bonds such as carbohydrates (cellulose) and protein.

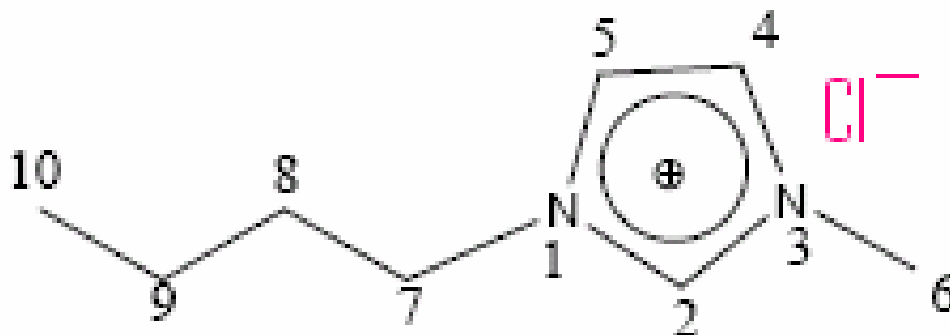


Figure 5-3 Chemical structure of BMIMCl

It was reported that BMIM^+Cl^- is an excellent solvent to dissolve cellulose and it was easy to prepare an up to 10 wt% solution by heating at 100°C [5]. Haibo Xie et al. reported that BMIM^+Cl^- is an excellent solvent for wool keratin and obtained 11%wt solution at 130°C by adding and dissolving 1 wt% wool keratin step by step [6].

From above, we tried to use BMIMCl to dissolve CF directly with reducing agent bisulfite salt, but the first trial experiments showed that this IL did not dissolve CF directly and only swelled it. We decided to obtain reduced keratin first and then dissolve it in BMIMCl . The process sketch is shown in Figure 5-4.

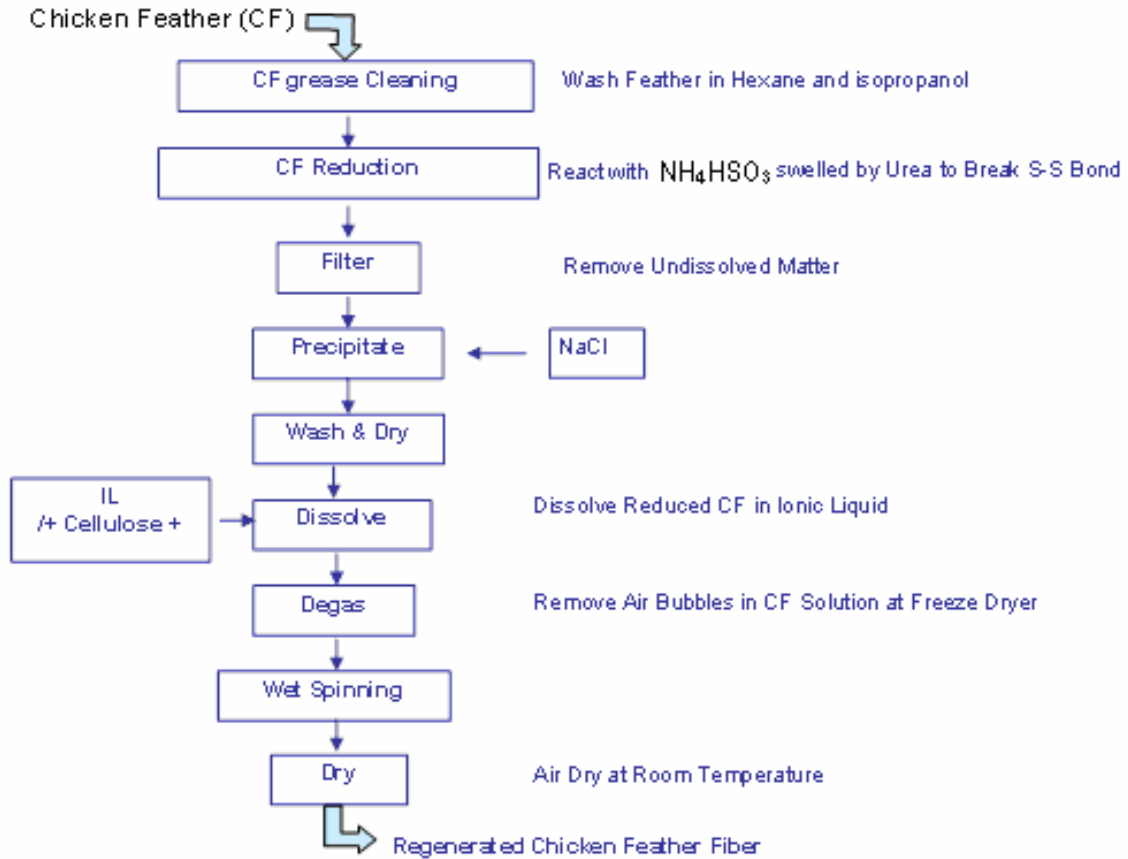


Figure 5-4 Diagram of production of regenerated CF fibers

5.2 Dissolution of CF

5.2.1 Introduction

5.2.1.1 Reduction of disulfide bonds

It was decided to break the –S-S- crosslinks in water solution by chemical reduction. In this chapter a reducing agent was used because disulfide bonds were wanted to become –SH groups and subsequently allow these –SH groups to form disulfide groups again. To break disulfide bonds easily, a swelling agent is used to denature the compact crystal structure of keratin. Urea was used as the swelling agent. After swelling, the crystal

becomes amorphous and the disulfide bond can be exposed to the reducing agent. This kind of disulfide bond is easily broken. Reduced keratin is dissolved in urea water solution or water. Although many reagents are capable of reducing disulfides in water solution, few have the required reactivity and specificity under conditions which do not cause protein damage. Only two classes of reducing agents are satisfactory – bisulfite salt and thiols. The thiol has frequently been used to break the disulfide bonds, but because of its vapor pressure, its unpleasant odor and high price, ammonium bisulfite was used instead. The -SH groups have high reactivity so the disulfide bonds are very easy to reform again when the solution is exposed to air at room temperature. Therefore, breaking disulfide bonds and dissolving reduced keratin was under nitrogen gas to protect -SH groups. Their reactions are shown in Figure 5-5.

Feather keratin denatures at about 78 °C. At around denaturation temperature, keratin is easy to swell and reduce.

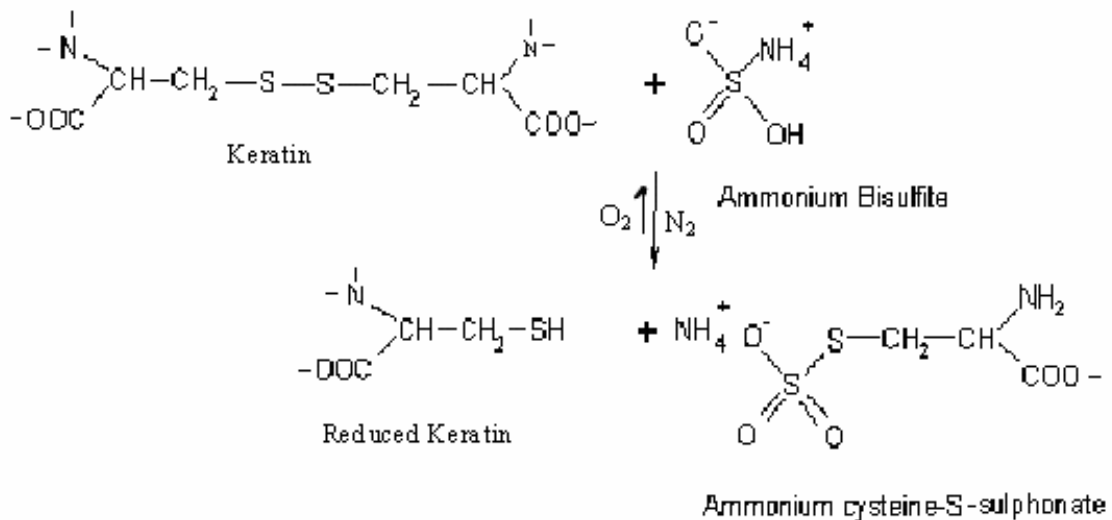


Figure 5-5 Reducing disulfide bonds of CF keratin

5.2.1.2 Salt precipitation of reduced keratin

After reduction of CF keratin, reduced chicken feather keratin is dissolved in water very easily because -COOH, -NH₂ and -OH groups in keratin molecules are hydrophilic. These groups and polar water molecules form hydrous film surrounding keratin molecules and become hydrosol particles – micelles with 1-10nm size which weaken the interaction between water and protein molecules. Generally, to separate protein from water, dialysis and freeze-dry are used, but both are time-consuming. Therefore, salt precipitation was used in our research to precipitate reduced keratin molecules from water. Because the hydrophilic ability of neutral salt is stronger than that of protein, when a large amount of neutral salt is added, water molecules are taken by salt, hydrophobic groups of protein molecules are exposed and at the same time the charges of protein are neutralized, hydrosol is destroyed, finally, protein molecules precipitate (see Figure5-6).

Neutral salt such as NaCl, (NH₄)₂SO₄, Na₂SO₄, and NaH₂PO₄ is always used for salt extraction of protein. In our research NaCl was used. Generally, to precipitate protein from its water solution, salt is added into the solution little by little while the solution container oscillates lightly [1]. This method was tried, but it took too long time. Therefore, reduced keratin solution was poured directly into salt water solution. It was found that the reduced keratin precipitated immediately as soon as the keratin solution was mixed with the salt solution.

During salt extraction, protein precipitated attached to salt. The attached salts need to be washed away. Otherwise, the salt ions affect the properties of regenerated keratin

fibers. During washing process, reduced keratin will not dissolve in water at room temperature because it has been denatured, aggregated and crystallized when precipitated by salt. Dissolving precipitated reduced keratin in water again also needs similar conditions to the reduction process under vigorous stir and at about 76 °C.

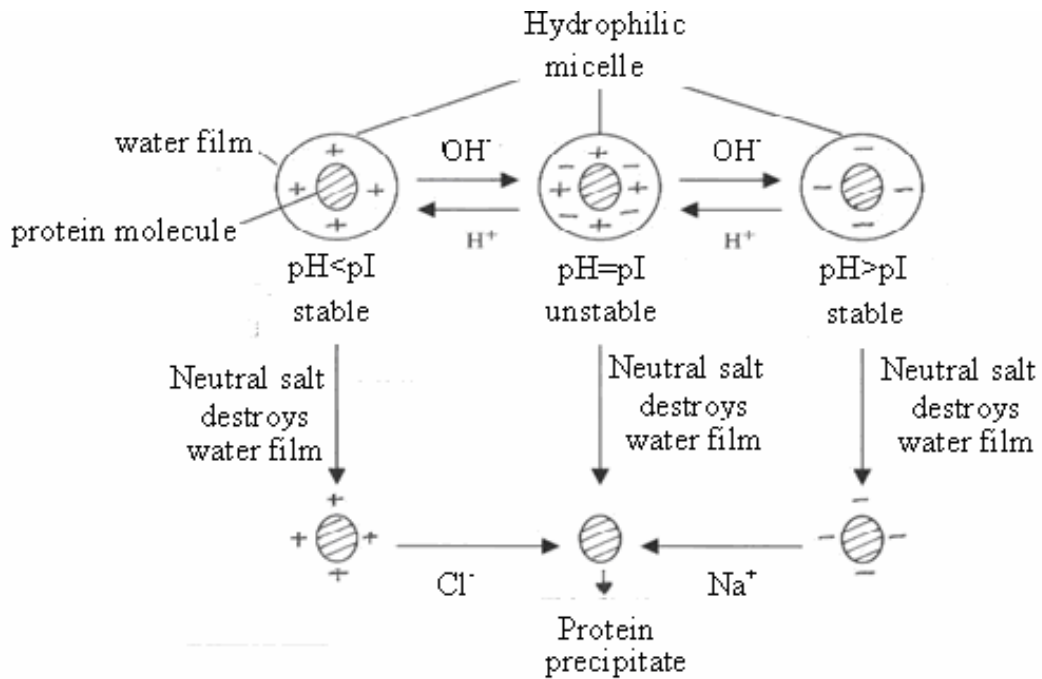


Figure 5-6 Salt precipitation diagram of protein

5.2.1.3 Dissolution of reduced keratin in an ionic liquid

Reduced CF keratin can be dissolved in water (PH7). Reduced CF keratin was tried to use its water solution to produce regenerated CF keratin fiber by wet spinning, but the viscosity of aqueous reduced keratin solution was too low to use in wet spinning. To solve this problem, Kazunori Katoh [7] combined poly (vinyl alcohol) with reduced keratin of wool to produce regenerated blend fibers, but in his article he did not discuss

their tenacity. The blend fibers readily shrank and dissolved in water, which is not good for washing in water. 1-butyl-3-methylimidazolium chloride (BMIMC, IL) was used to dissolve reduced CF keratin in this research. The solutions of IL and CF were easy to handle. Dissolution of wool keratin in IL has been patented [8].

In the reduced keratin to be dissolved there may be a small amount of disulfide bonds formed during filtration and drying because these processes were operated under air. NH_4HSO_4 could be used to break these disulfide bonds but NH_4HSO_4 do not dissolve well in IL. If using NH_4HSO_4 , a large amount of the salt solid would be needed and the remaining salt ions would affect the properties of the keratin fibers. Instead, Thiols such as Dithioerythritol or 1-thioglycerol $\text{HSCH}_2\text{CH}(\text{OH})\text{CH}_2\text{OH}$ can be used well (shown in Figure 5-7) because it is organic and dissolves well in this IL. Since there is no ion in it, it does not affect fibers much. To prevent the formation of disulfide bonds from $-\text{SH}$ groups during dissolution, this process was also protected by nitrogen gas. Since the 100% reduced CF keratin IL solution was not ideal for fibers and 100% keratin fibers were weak, bleached cotton was added into the solution.

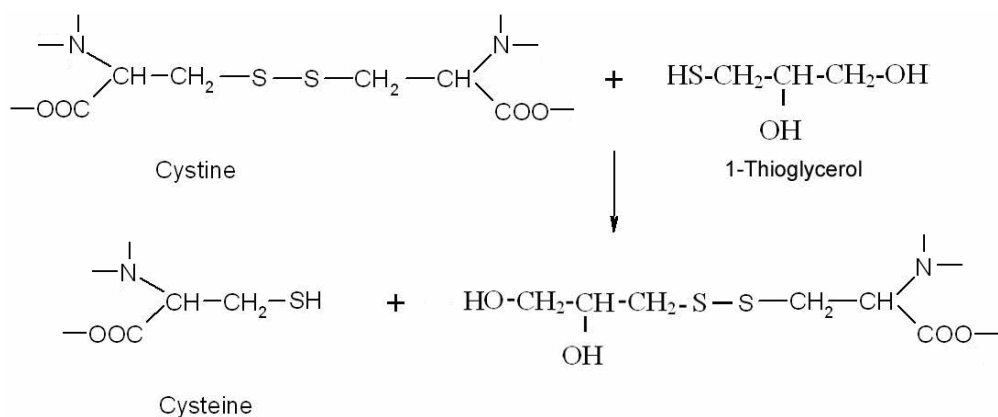


Figure 5-7 Breaking disulfide bonds of keratin during dissolving

5.2.1.4 Measurement of Molecular weight of reduced keratin by PAGE-SDS [9]

The molecular weight of protein can be measured with gel electrophoresis. Gel electrophoresis is a technique in which molecules having ionizable groups are forced across a span of gel, motivated by an electrical current and to diffuse through the gel material to separate the molecules by size. Polyacrylamide gels (PAGE's) are often used for electrophoresis of protein.

In electrophoresis, a detergent [sodium dodecyl sulfate (SDS)] is used to disrupt the tertiary and quaternary structure of the protein; and mercaptoethanol is used to reduce disulfide bonds (secondary structure), which cause the negative charges of protein to be masked. The electrophoretic mobility of the SDS-protein complex will be influenced primarily by molecular size (shape, charge, and chemical nature of the native protein do not play a role in the complex any more). Proteins can be observed after electrophoresis by treating the gel with a stain such as Coomassie Blue, which binds to the proteins but not to the gel itself. The separated molecules in each lane can be seen in a series of bands spread from one end of the gel to the other. Each band on the gel represents a different protein (or protein subunit).

5.2.2 Experimental

5.2.2.1 Materials

Chicken feathers used for this study were washed as used in nonwovens first, washed with detergent and dried in a home dryer on moderate heat. In addition, for this work these dried feathers were soaked in hexane for 1 hour and then in isopropanol for 1 hour

to remove the oil on them, and dried at temperature 50°C. The dried-twice feathers including fibers and quills together were ground into powder.

Ammonium bisulfite (45% solution) for reducing keratin in water solution was from Spectrum chemical MFG. Corp. Thiols, dithioerythritol for reducing disulfide bonds in ionic liquid were from ACROS Organic and 1-thioglycerol from SIGMA-Aldrich, Inc.. 1-butyl-3-methylimidazolium chloride (IL) for dissolving reduced keratin was from Aldrich (Milwaukee, WI). Sodium chloride for extracting keratin and urea for swelling feather powders were from Fisher Scientific Company. Sodium chloride was made into solution. Bleached cotton cellulose, with DP of 1900, was used. Distilled water was used for reduction of CF to prevent reduced CF keratin contaminated by impurity from tap water.

5.2.2.2 Procedure

5.2.2.2.1 Reduction of disulfide bonds of feather keratin in water solution

The reaction took place in a 250 ml flask, shown in Figure 5-8. Urea solutions were made using distilled water 150ml to concentrations of 4M, 5M, 6M, and 8M. Nine grams of chicken feathers powder was added into the urea solution. At 70-80 °C the mixture was stirred for 3-5 hrs at different stirring speed. Then, at this temperature, 45% ammonium bisulfite solution (15% weight of feather powder) was added to the mixture and stirring continued for 30-60mins (still at the same temperature). At the same time, Nitrogen gas was piped through the flask. To condense the water steam evaporating from the solution so as not to reduce the volume of water, a condenser tube was put into one of side necks of the flask. If 18 grams of chicken feather powders was used, all other

chemicals were doubled and a 500 ml flask was used to produce more keratin for experimentation.

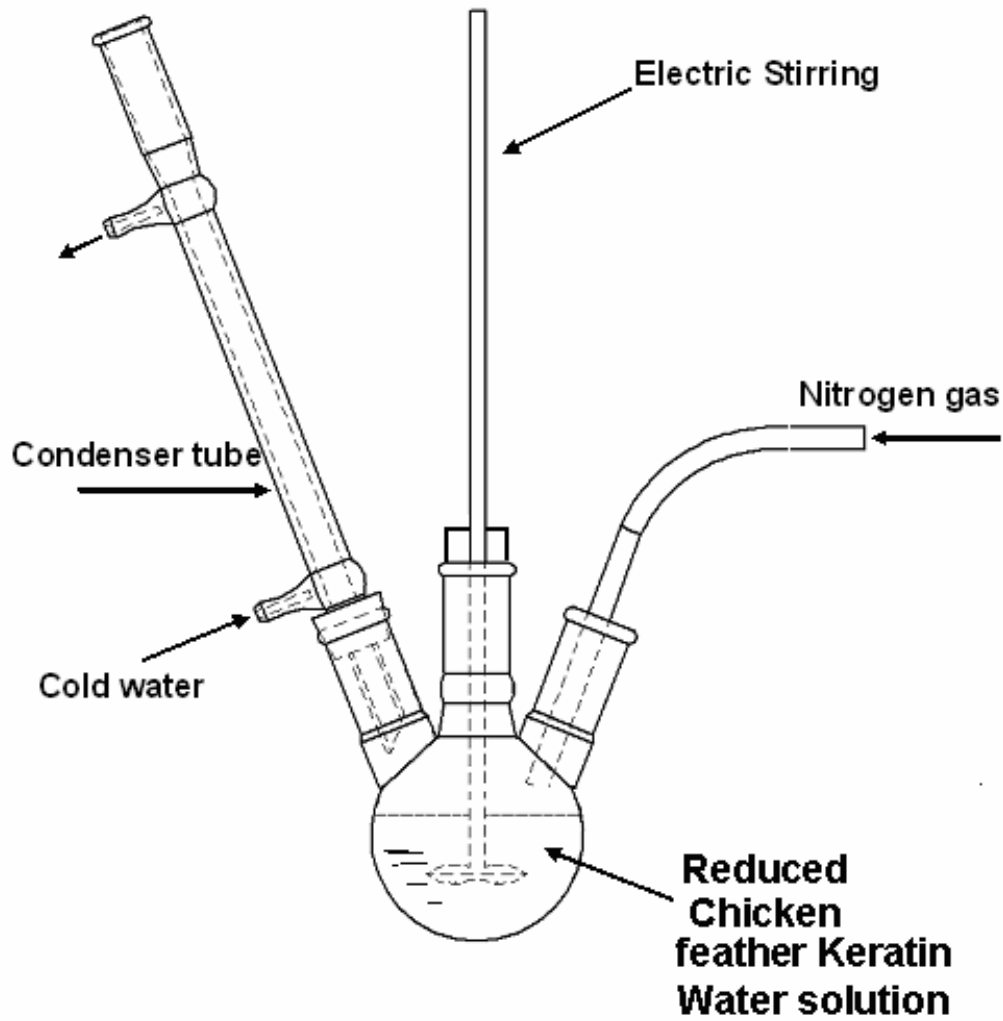


Figure 5-8 Diagram of reducing process

5.2.2.2.2 Salt precipitation of reduced keratin

After reduction, undissolved feather powder was removed by filtering through a piece of spunbonded nonwoven. The filtrate liquid was poured into sodium chloride solution. Reduced keratin particles precipitated and settled to the bottom part. The upper part clear liquid was decanted. Water was added to the precipitation and the mixture was stirred to wash away the remaining salt and urea. The precipitate was washed three times with distilled water. The reduced keratin was filtered under atmosphere and washed with ethanol three times, acetone twice and hexane once. Finally, it was dried in the freeze drier for two hours.

5.2.2.2.3 Measurement of undissolved CF weight

In above filtration process for the reduced keratin solution, the undissolved CF was left on the spunbonded nonwoven. The spunbonded nonwoven together with the undissolved CF on it was dipped in the 200 ml distilled water for 4 hours and the water was stirred occasionally for undissolved CF to release into water. The dipped water was filtered with another piece of spunbonded nonwoven whose weight had been measured. The undissolved CF was left on the spunbonded nonwoven. This piece of spunbonded nonwoven filter holding undissolved CF was dried in the oven at 105 °C for 1 hour. The total weight of the undissolved CF filtrate cake and filter was measured, and then the weight of undissolved CF was known.

5.2.2.2.4. Dissolution of reduce keratin

Reduced feather keratin and/or some bleached cotton were added into 40 g IL solvent with 1-thioglycerol of 5% or less of CF keratin weight to reduce disulfide bonds formed during filtration and drying. Dissolution was in a heated round-bottom flask and stirred by a glass rod under nitrogen atmosphere at about 70 °C. The recipe was designed in Table 5-1. The diagram of dissolution process is shown Figure 5-9. In the Figure the left opening of the flask was closed by a glass stopper which was occasionally removed to check how the solution was and if there was any solid left. At room temperature, IL is solid so, before used, IL was heated to liquid at 75 °C.

Table 5-1 Recipe of dissolution of CF in 40g IL (Cellulose. is bleached cotton.)

Ratio of Reduced CF keratin to Cellulose	(Reduced Keratin+ Cellulose) %	Reduced CF keratin %	Cellulose%	Reduced CF keratin (g)	Cellulose (g)	Reducing agent (g) (5% CF keatin)
20/0	20	20	0	10	0	0.50
4/1	4.5	6	1.5	6	1.5	0.125
3/1	6.4	4.8	1.6	1.92	0.64	0.096
2/1	4.5	3	1.5	1.2	0.6	0.03
2/1	5.25	3.5	1.75	1.4	0.7	0.07
1/1	4.0	2.0	2.0	0.8	0.8	0.04
1/4	3.0	0.6	2.4	0.24	0.96	0.012
0/1	4.0	0	4.0	0	1.6	0

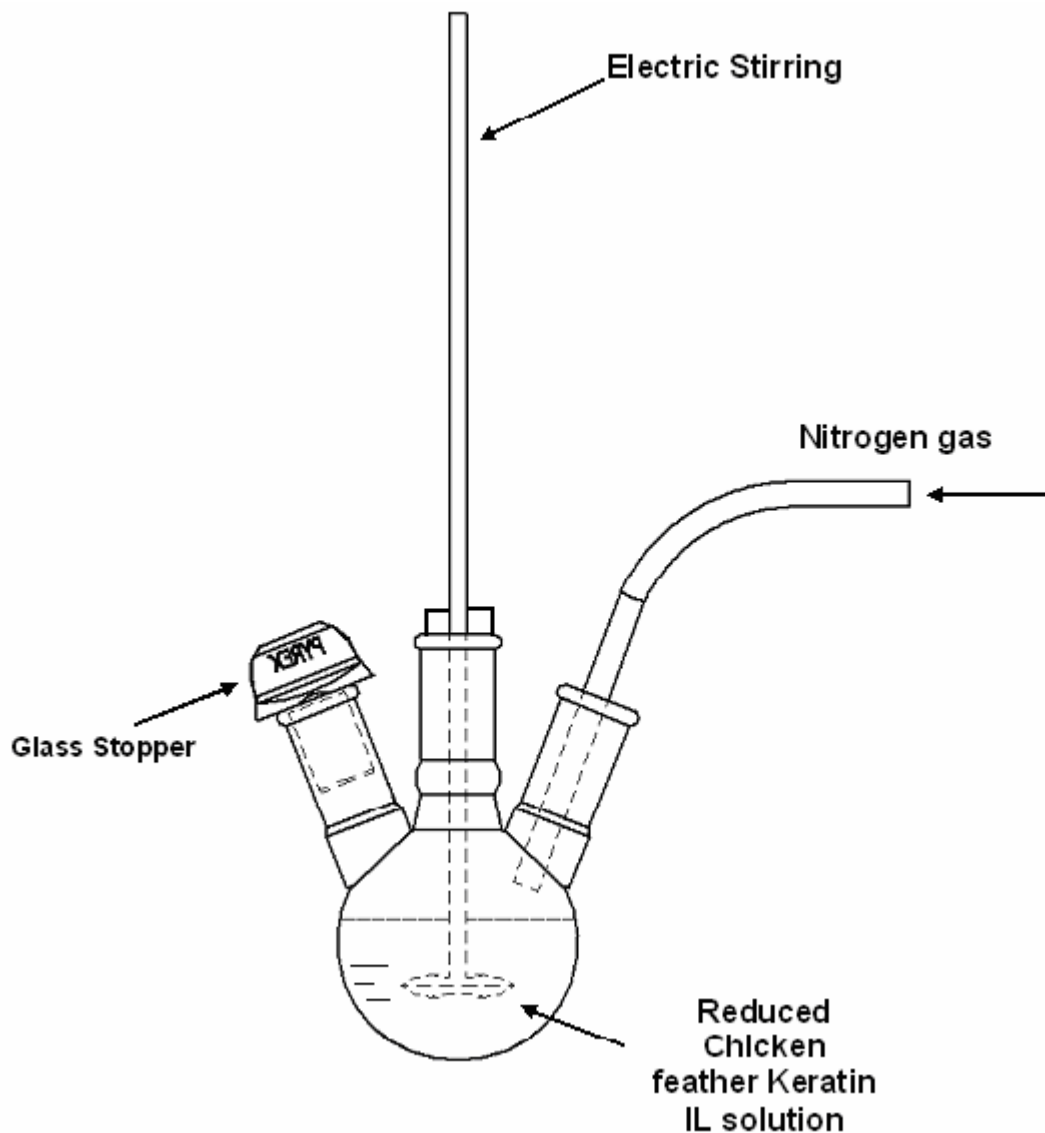


Figure 5-9 Diagram of dissolving process

5.2.2.2.5 Measurement of molecular weight of reduced keratin

For the measurement of molecular weight of reduced keratin, SDS–polyacrylamide gel electrophoresis (SDS-PAGE) was performed using a Bio-Rad Mini Protean Cell (Bio-Rad Laboratories, Hercules, CA) (shown in Figure 5-10.) and 12% gradient gel. The

separation gel was made for two pieces by mixing distilled water, 1.5 M Tris-HCl, 10% (w/v) SDS stock and 30% acrylamide/bis first, adding 10% APS and TEMED and polymerizing for 40mins between two glass plates. The reduced keratin was dissolved in IL and the IL solution was dispersed in distilled water and boiled with 2-mercaptoethanol for 2 mins. Reduced keratin was subjected to SDS-PAGE with molecular weight marker (PageRuler™ Prestained Protein Ladders, Fermentas) at 200 V. The proteins in the developed gel were stained by Coomassie brilliant blue G-250 (Bio-Rad Laboratories).

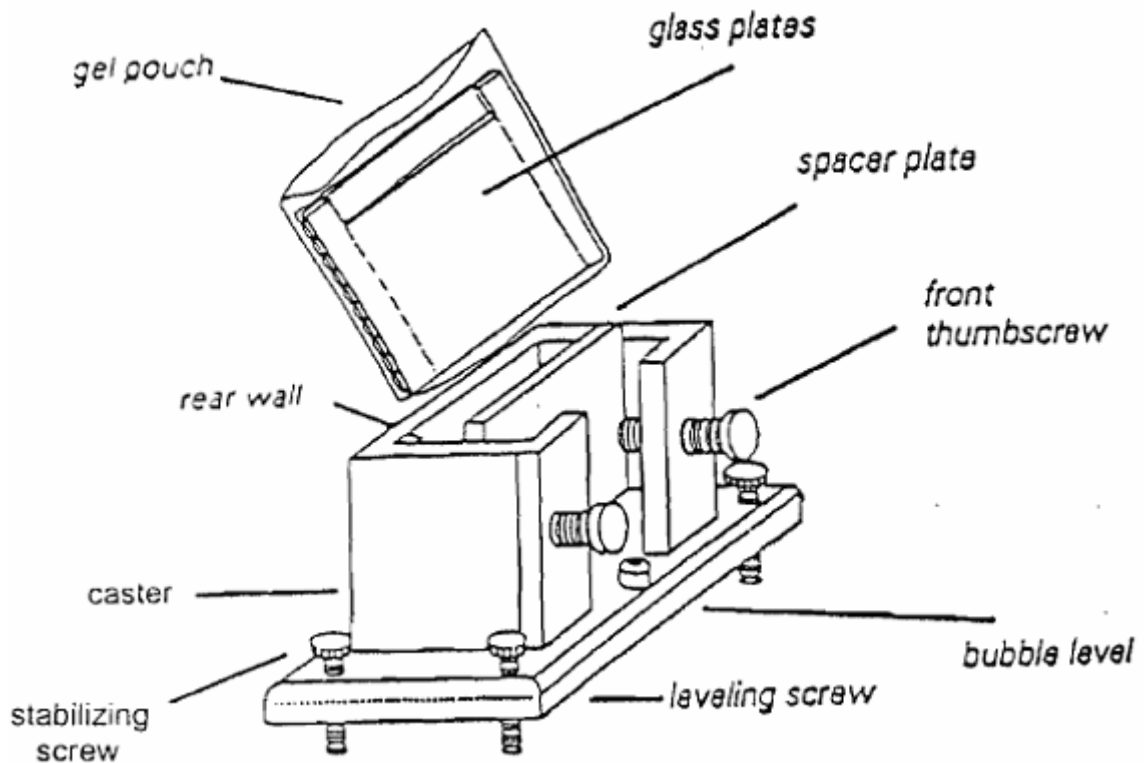


Figure 5-10 Sketch of a Bio-Rad Mini Protean Cell [9]

5.2.3 Results and discussion

5.2.3.1 Production of reduced feather keratin in water solution

To get reduced feather keratin, disulfide bonds must be broken to form thiol groups. However, thiol groups easily become disulfide bonds again under oxygen. Disulfide bonds form again very easily at room temperature, and then, at around 76 °C even a very small amount of oxygen can cause their formation much more quickly, which results in that CF powder become cross-linked, aggregated, and become one block with urea solution so no reduced keratin is obtained. Therefore, removing oxygen from the reaction flask is very important. Before adding ammonium bisulfite, oxygen gas must be removed first, that is, nitrogen gas was piped into the flask for a while first, and then ammonium bisulfite was added. The following production of reduced feather keratin was done after removing oxygen gas. Since percentage of cysteine of feather keratin is 7%, 15% of feather weight was chosen for the weight of the reducing agent to make sure reduce disulfide bonds fully. The weight of reducing agent kept constant in all reducing experiments. There are many other factors which had effect on the production of reduced CF keratin. In this chapter, the effects of stirring speed, swelling time, reduction time and temperature, and urea concentration on the production of reduced CF keratin were discussed.

5.2.3.1.1 Effect of swelling time and stirring speed on the production of reduced keratin

These experiments were the first trial to reduce CF keratin. 9 g chicken feathers were swelled by 4 M urea and reduced at 76 °C. Reduced keratin was precipitated by 150 g

NaCl/900 g water. In these experiments the effect of different swelling time and stirring speed on the keratin ready to spin was studied. The keratin ready to spin is that obtained after reduced keratin solution was precipitated, washed by ethanol, acetone, and hexane, and dried in the freeze dryer. It can be dissolved in IL to spin. The experiments results were shown in Table5-2.

Table 5-2 Effect of swelling time and stirring speed on the production of keratin ready to spin

Stirring speed (indicator/rpm)	Swelling time		
	2hrs	3hrs	5hrs
4/260	3g	-	-
5/315	3.3g	4.2g	5.4g
6/346	3.7	-	4.3g

From Table 5-2 it is can be seen that for CF swelled for 2hrs, with the increase of stirring speed the production of keratin ready to spin increased, which is reasonable because higher stirring speed improved the effect of urea swelling CF and more disulfide bonds exposed to the keratin surface to be reduced. At stirring speed 5, the production of keratin ready to spin also increased with the swelling time, which is understandable because organic reaction takes place slowly and more disulfide bonds exposed to be reduced with time. Using stirring speed 6 and swelling time 5 hrs the production of

reduced keratin ready to spin did not increased. From this point, for later reduced keratin production stirring speed 5 (rpm 315) and swelling time 5 hrs or longer were used.

5.2.3.1.2 Effects of reducing time and temperature on the production of reduced keratin

Because in later spinning experiments more reduced keratin would be used, in these reducing experiments 18 g chicken feather powders at 70 °C were reduced after being swelled by 4 M urea in 300 ml water for 5 hours. The effect of different reducing time on the production of reduced keratin was studied. In these experiments, undissolved CF besides the keratin ready to spin was measured. The dissolved CF and the keratin left in water were calculated. The results are shown in Table 5-3.

From Table 5-3 it can be seen that not all chicken feather could be reduced and not all dissolved reduced keratin could be precipitated. Only part of keratin was precipitated in salt solution, which is because only high molecular weight protein can be precipitated by salt, and low molecular weight reduced keratin was still left in water [3].

From Table 5-3 it is seen that at 70 °C with the increase of reducing time, the undissolved CF decreased only a little, that is, the reducing time almost had no effect on the reduction of CF keratin. From the table, it is also seen that the salt concentration had obvious effect on the production of the keratin ready to spin. With the salt concentration, more reduced keratin precipitated ready to spin. Since then, reducing time 30mins were used continuously in later reducing experiments.

Table 5-3 Effect of reducing time on the production of reduced keratin

Reducing time	30min	45min	1hr
Undissolved CF (g)	4.69	4.65	4.47
Dissolved CF (g)	13.31	13.35	13.53
Salt extraction solution (g NaCl/ 900g H ₂ O)	150	194	250
Keratin to spin (g)	7.56	11.7	10.23
Keratin left in water (g)	5.75	2.65	3.30

18 g CF reduced at 70 °C and precipitated by 150 g NaCl/ 900 g water was studied in above study and was not repeated for the next study and also put in Table 5-4 for next comparison. In other temperature the production of reduced keratin was studied. In these experiments 18 g CF was also swelled for 5 hours by 4M urea in 300 ml water and reduced in 30mins. The results are shown in Table 5-4. In higher temperature, we thought more keratin would be reduced so higher salt concentration solution was used. Even in 65 °C a little higher concentration salt solution was used to obtain more keratin to spin.

From Table 5-4, it can be seen that, generally, with the temperature more CF keratin was reduced and dissolved in urea water solution except at 80 °C. Even at 80 °C more keratin ready to spin were also obtained by using bigger volume salt solution with the same concentration used at 76 °C. For reducing more CF and not using too much salt,

reducing temperature 76 °C and less salt concentration was chosen for next study which focus on the effect of urea concentration on the production of reduced keratin .

Table 5-4 Effect of reducing temperature on the production of reduced keratin

Temperature	65°C	70°C	74°C	76°C	80°C
Undissolved CF (g)	8.30	4.69	2.85	1.65	2.22
Dissolved CF (g)	9.70	13.31	15.15	16.35	15.78
Salt extraction solution (g NaCl/900gH ₂ O)	262	150g	270	270	350*
Keratin to spin (g)	8.49	7.56	13.62	12.05	15.05
Keratin left in water (g)	1.21	5.75	1.53	4.30	0.73

(Note: * 1200g H₂O was used.)

5.2.3.1.3 Effects of urea concentration on the production of reduced keratin

The effect of Different urea concentration on the production of reduced feather keratin was studied. In these experiments, four different urea concentrations were used to swell 9 grams of chicken feather (CF) and the experiment using 4M urea to swell was repeated but using lower salt concentration solution to precipitate. The experiments were in oil bath. Maybe because the oil bath did not work well and the temperature did not actually reach 76 °C, the reduction of CF keratin was not as high as above. The results are shown in Table 5-5. Accompanying keratin production at different urea

concentration, different salt (NaCl) concentration was also used (also shown in Table 5-5). For higher reduction of CF keratin (8M urea swelling experiment) to precipitate more keratin to spin, bigger volume solution with higher salt concentration was used.

Table 5-5 Effect of urea concentration on the production of reduced keratin*

urea	4M	5M	6M	8M
Undissolved CF (g)	1.616 (18.0%)	1.250 (13.9%)	0.615 (6.8%)	0.443 (4.9%)
Dissolved CF (g)	7.384 (82.0%)	7.750 (86.1%)	8.385 (92.8%)	8.557 (95.1%)
Salt concentration (g NaCl/900 g H ₂ O)	194	250	250	350**
Keratin ready to spin	6.697 (74.4%)	6.000 (67.0%)	6.671 (74.1%)	8.25 (91.7%)
Keratin left in water	0.687 (7.63%)	1.750 (19.4%)	1.714 (19.0%)	0.307 (3.4%)

(Note: *: the percentage is that of original CF weight; ** 1200g H₂O was used.)

From Table 5-5, it can be seen that, with the increase of urea concentration, undissolved chicken feather reduced, that is, the reduced dissolved keratin increased. CF swelled by 8M urea had the biggest yield of dissolved CF. It is reasonable because the more urea swelled keratin better, keratin became more amorphous, more disulfide bonds were exposed outside and then more keratin was reduced and dissolved in water.

Reduction of feather keratin without urea swelling was also studied. The solution of this reduced feather keratin was added into NaCl salt extraction solution. There was no protein precipitating in the liquid. This shows that urea swelling during reduction of feather keratin was very important.

From above discussion it can be seen that, without urea swelling, reduced CF keratin ready to spin could not be obtained. Generally, high urea concentration, high stirring speed, long swelling time, high reducing time and high reducing temperature increased the production of reduced CF keratin. Therefore, CF reduction was chosen under urea concentration 6M to swell for 5 hrs and carry out for 30mins at 76°.

5.2.3.2 Dissolution of reduced keratin in ionic liquid

The first spinning trial was for 100% CF keratin. Subsequently, mixtures with cellulose were used. The viscosity of solution is very important for spinning. With too high viscosity, bubbles created during mixing are difficult to remove. Low viscosity makes filaments break easily. To produce solution with appropriate viscosity, different concentration solutions were tried. The 15% CF keratin solution was very difficult to coagulate. This solution did not coagulate immediately and took time to precipitate in the coagulation bath, which was not practical for the coagulation bath which cannot be made limitless long. For 25% CF keratin solution, complete dissolution of all reduced keratin was difficult as it was mixing (because of the stirrer climbing phenomenon). A concentration of 20% CF concentration was chosen to spin.

The bleached cotton formed into balls after grinding. If IL was directly added onto these ground balls and began to be stirred, the balls would become beads and could not

be spun. Since reduced CF keratin powder was always separated, we used reduced CF keratin powder to break these balls and mixed these two kinds of powder even, then removed the mixture powder into the flask, added IL liquid onto it.

Before the mixture was stirred by the rod, we used hand to mix it even first. The mixture looked grey or white. During dissolving, the solution was stirred very quickly at first. When the mixture began to climb the rod, the stirring speed was slowed down immediately to the smallest; otherwise, the mixture would climb the rod to the stopper of the flask. The final solution of all recipes looked similar, slightly orange similar to the color of IL (shown in Figure 5-11).

Generally, it took two days to dissolve the reduced keratin and/or using the general flask and glass rod under N_2 gas. If dissolved in longer time three or four days, the reduced keratin solution became inappropriate to spin.

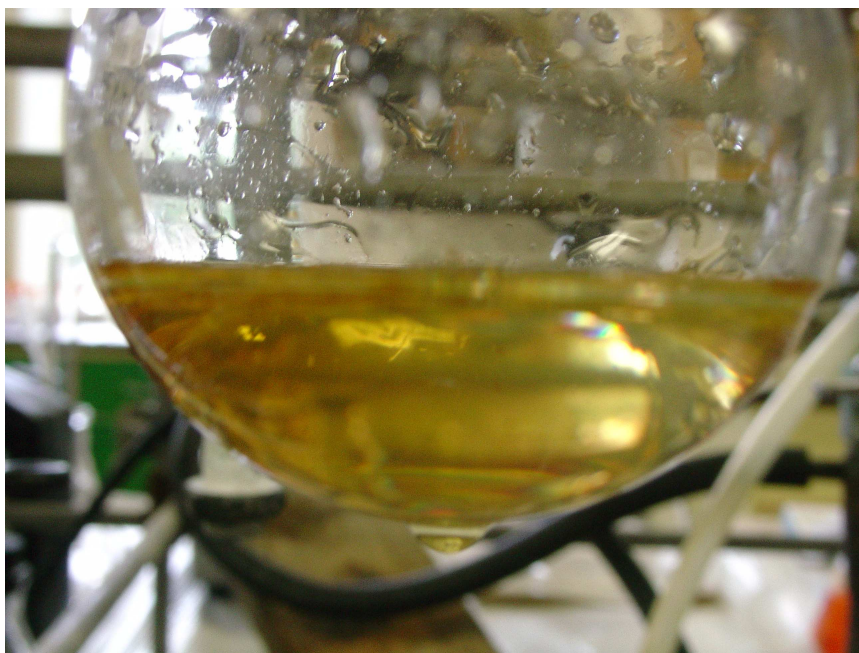


Figure 5-11 IL Solution of Reduced CF keratin

5.2.3.3 Molecular weight of reduced CF keratin

Precipitated reduced CF keratin was used for spinning but it does not easily dissolve in water, so, to measure its molecular weight, its IL solution was used. Then, the obtained reduced keratin was subjected to SDS-GAGE analysis, shown in Figure 5-12.

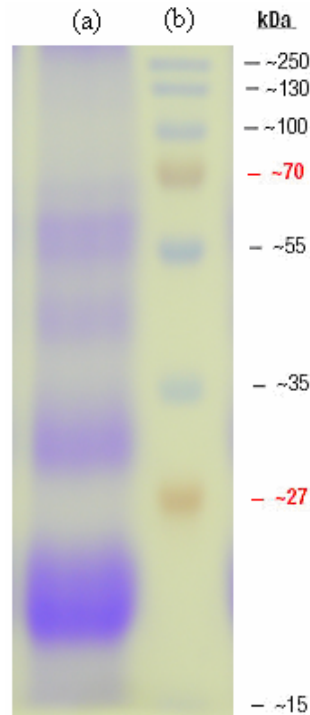


Figure 5-12 SDS-PAGE of precipitated reduced CF keratin in IL solution (a) reduced by 2-mercaptoethanol for 2 min and (b) the molecular weight marker

From Figure 5-12 it can be seen that the molecular weight of precipitated reduced keratin dissolved in IL had several ranges. It had major weight fraction at 23,000 to 18,000 Da and three minor fractions at 32,000 to 29,000, 42,000 to 38,000 and 60,000 to 55,000 Da. They were smaller than a previous literature report [13]. This may be because the molecules were reduced or hydrolyzed during reduction and dissolution but the

reported was not. Nevertheless, the CF blend fibers were still strong, which was not affected by the low molecular weight of reduced keratin but maybe by others factors such as orientation. As known, polyester fibers are very strong because of orientation of polyester molecules even though their molecular weight is small. Since then, the fibers are weak perhaps because their fiber molecules are porous or globular rather than extended.

5.3 Production of Regenerated CF fiber

5.3.1 Introduction

Regenerated CF keratin fibers were developed by wet spinning. Solutions of 100% CF keratin in IL dispersed rather than precipitated in water. For ethanol and acetone, 100% CF keratin solution dispersed in these solvents very rapidly as well and no fiber precipitated. From the literature it was known that protein in water solution was precipitated by salt. Salt Na_2SO_4 precipitation was tried for 100% CF keratin IL solution and it worked very well maybe because it has high solubility and can precipitate protein well in the solution. Therefore, in this chapter the salt Na_2SO_4 bath was used for 100% CF reduced keratin solution spinning. Mixed solutions of cellulose and keratin precipitated well in water so water bath was used for cellulose and keratin blend solution spinning. Tap water was tried to precipitate cellulose and keratin blend solution, but it made the fibers yellowish so distilled water was chosen. After the fibers were spun and dried, their properties were also measured and we evaluated them with compared to other protein and common fibers

5.3.2 Experiments

5.3.2.1 Materials

Reduced CF keratin solution was prepared according to above procedure. Before it was used for spinning, it was degassed in the freeze drier to remove the bubble produced during dissolution to improve the continuity of the fiber spinning process. The bubbles in the solution made the solution and fibers break easily. Salt sodium sulfate to precipitate 100% CF reduced keratin solution was from Fisher Scientific Company. Twenty percent sodium sulfate solution was prepared. Distilled water was used to precipitate CF reduced keratin and cellulose blend solution.

5.3.2.2 Wet spinning process

A dry-jet wet spinning technique was used to spin fibers from reduced CF keratin solutions. Its sketch is shown in Figure 5-13.

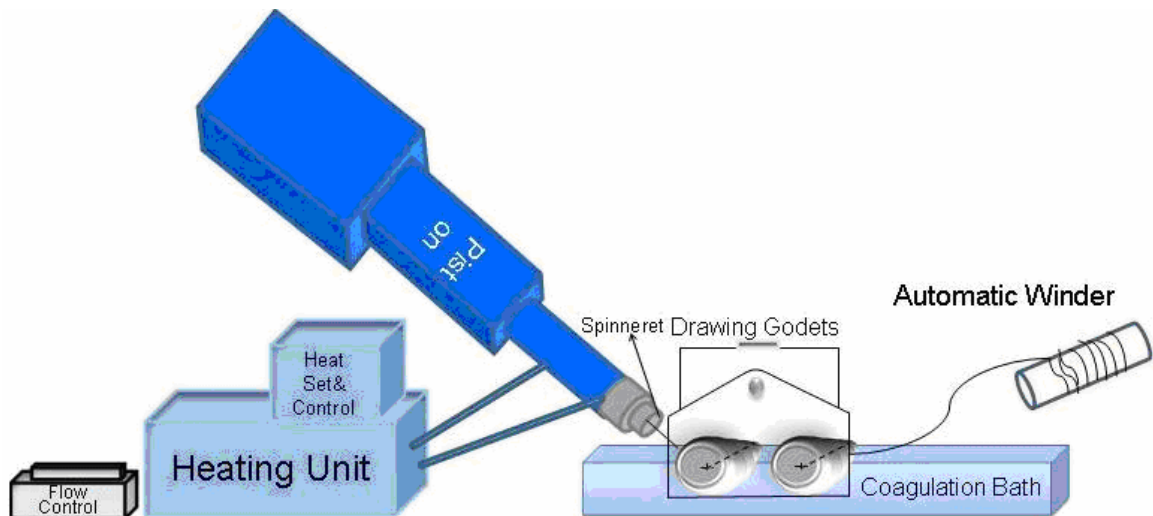


Figure 5-13 Sketch of dry-jet wet spinning [10]

The solution was then poured into a piston wet spinning apparatus (ISCO, Series D piston pump) which was fitted with a single hole (0.368mm diameter circular) spinneret. In the spin pack, the blended solutions were maintained a certain temperature and forced through the spinneret fitted with four layers of 325 mesh wire screen filter and a layer of coarse support screen to filter the solid which had not been dissolved. The set-up consisted of extruder, a coagulating bath, a stepped godet with four levels to stretch fibers (Figure 5-14) and a take-up winder. The extruded solution passed from the single of spinneret, through a short distance of air and into the coagulation bath and coagulated. The coagulated filament was wrapped around several levels in the godet and

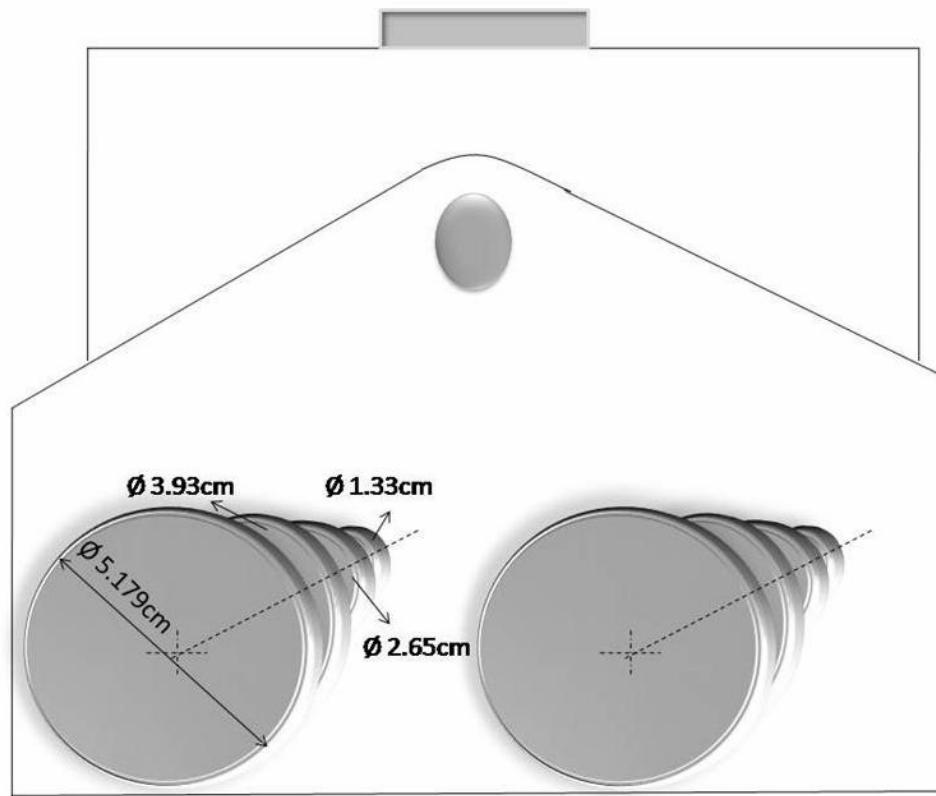


Figure 5-14 Stepped godets [10]

subsequently passed using minimal tension through the one-meter-long coagulation bath, finally, was picked up by a take-up spool-automatic winder. Extrusion conditions were as follows:

Process:	dry-jet wet spinning
Extrusion temperature:	20-70 °C
Throughput:	0.05-0.2 ml/min
Coagulation bath:	20% Na ₂ SO ₄ solution or distilled water
Godet speed:	10-40 RPM
Drawing:	3 stage or less, steps 1, 2, 3, and 4
Draw ratio:	step 1-2=1.99, 1-2-3=2.95, 1-2-3-4=3.89
Take-up speed:	3.09 – 4.07 m/min

100% CF solution was coagulated in 20% sodium sulfate solution and cellulose and CF solution in distilled water. After dry-jet wet spinning, 100% CF keratin fibers were soaked in 4% Na₂SO₄ for 24 hrs at ambient temperature followed by water soaked for 24 hrs and then, dried in air. Blend fibers were soaked in distilled water at ambient temperature for 3 hours to extract the remaining solvent and salt, dried in air to allow cross-link in air.

5.3.2.3 Measurement of Physical Properties

The fibers were conditioned for 24 hrs at 65% RH and 72 °F for testing fineness and tensile properties. The fiber fineness was measured on a vibroscope (Vibromat M)

according to ASTM D1577 (07.01) at 72 °F and 65% relative humidity. Tensile properties were measured on a universal testing machine (Instron Model 1122) according to ASTM D1774-94. A gauge length of 15 mm and a crosshead speed of 25.4 mm/min were used for tensile testing. The data were obtained from averages of 10 tests. The moisture regain of the fibers was investigated according to ASTM method 2654 under standard atmospheric conditions of 65% and 72 °F.

5.3.3 Results and Discussion

5.3.3.1 Production of 100% reduced CF keratin regenerated fibers

The 100% reduced CF keratin solution offered a very poor continuity of fiber extrusion. These problems might be caused by three factors. The first was the residual bubbles in the solution and the non-uniformity of the solution. Residual bubbles in the solution were entrapped in the fluid filament and generated weak spots and discontinuity in the fluid. The second was highly swollen polymer gel in the solution, which was produced when the reduction reaction only broke part of the -S-S- bonds of CF keratin. These gels were sometimes visible in the stirring solution. They might pass the filter screens with the solution, and progressed into the filament where they would impede draw down of the fluid filament and thus cause breaks. The third was low MW keratin created by degradation of protein during the previous chemical treatment.

Regenerated 100% CF keratin fibers were produced when the corresponding solution coagulated in 20% sodium sulfate solution. The studied regenerated keratin fibers could not be stretched and were wound at the circumferential speed of the godet at 18.8 rpm. Pump speed was varied and a smaller extrusion rate produced thinner fibers. The

extrusion rate had effects on their tenacity. The results are shown in Figure 5-15 and Table 5-6. From the figure it can be seen that, generally, the tenacity decreased with the increase of extrusion rate. When the extrusion rate increased from 0.05 ml/min to 0.2 ml/min, the tenacity reduced from 0.232 to 0.136 g/den. It should be pointed out that decreasing the extrusion rate while maintaining godet speed causes an increase in the draw-down between the spinneret and godet. Draw down is a processing factor. It is the ratio of the godet's circumferential speed to the fluid velocity exiting the spinneret. It describes the degree of stretching fibers before coagulation begins. With increasing draw down, the tenacity of CF fibers increased, which was reasonable because stretching process forces the molecule chains to align with each other along the stretching direction, forming an oriented structure and the oriented structure tends to increase the strength of fibers.

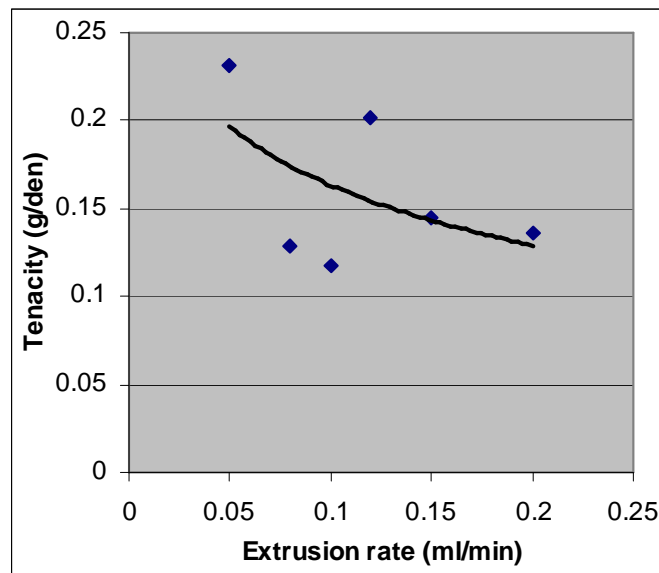


Figure 5-15 Effect of the extrusion rate on the tenacity of regenerated 100% reduced CF keratin fibers (data in Table 5-6)

Table 5-6 Mechanical properties of regenerated 100% CF keratin fibers (not stretched and kept on their godet speed 18.8rpm)

Extrusion rate (ml/min)	Linear density (den)	Tenacity (g/den)	Strain at break (%)
0.2	312.2±72.6	0.136±0.059	1.44±0.33
0.15	291.8±93.4	0.145±0.051	2.57±1.01
0.12	316.2±78.2	0.202±0.081	2.87±1.21
0.10	319.9±36.8	0.117±0.064	2.42±1.21
0.08	248.6±9.8	0.129±.070	2.11±0.84
0.05	204.2±32.2	0.232±0.040	2.31±0.84

5.3.3.2 Production of regenerated CF keratin and cellulose blend fibers

The 100% reduced CF keratin regenerated fibers had very low tenacity and the tenacity even did not reach the lowest requirement for general cloth fibers so cellulose from bleached cotton was added into the solution. A small percentage of bleached cotton made a low concentration CF keratin solution suitable to spin; for example, 1.5% of bleached cotton made 6.0% CF keratin solution appropriate to spin. During spinning CF and cellulose blend fiber, the spinning process showed that the blend fiber solution gave a very good continuity of fiber extrusion even in case of being stretched; and it was able to be extruded continuously until it was used up. This phenomenon happens maybe because the cellulose forms a strong molarity in which the CF can precipitate.

The cellulose component improved the tenacity of CF fibers greatly, which is shown in Figure 5-16 and data in Table 5-7 to Table 5-10. The figure shows that, with the cellulose content, the tenacity of CF blend fibers increased significantly. Fifty percent cellulose CF blend fibers had the similar tenacity to that of 100% cellulose fibers. Low cellulose content improved the tenacity of CF keratin blend fibers a lot and high cellulose content did it dramatically. At 20% cellulose, the blend fibers had tenacity 1.6g/den, but at 80% cellulose the blend fibers had tenacity 3.9g/den, much higher than 100% cellulose fibers. This is maybe because, in the blend fibers, the crosslinking of keratin in small percentage CF was formed very well and crosslinking improved tenacity, but for big percentage CF fibers, there were not many crosslinkages formed.

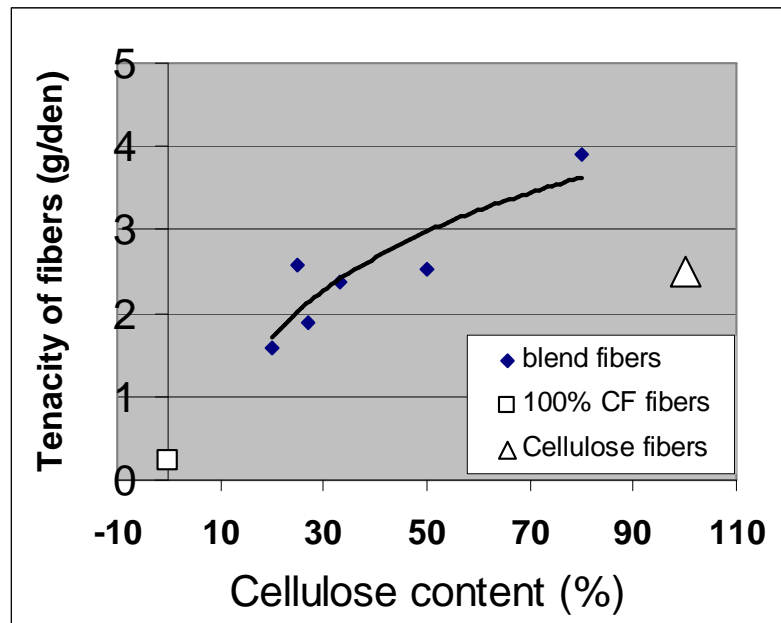


Figure 5-16 Effect of cellulose content on the tenacity of regenerated CF fibers
 (Note: the linear density of all fibers was around 10 denier, except that of the 100% CF fiber was 204 den. The tenacity of 100% cellulose fibers is from reference [10].)

Table 5-7 Mechanical properties of regenerated CF keratin fibers (80%CF, 20%
Cellulose, Cellulose/CF 1/4, extrusion solution Cellulose 1.5%, CF 6%)

Draw down	Linear density (den)	Tenacity (g/den)	Strain at Break (%)
4.64	19.3±6.1	1.42±0.42	4.50±1.96
5.45	15.9±2.1	1.41±0.25	5.89±2.05
5.90	16.7±2.9	1.59±0.34	6.09±2.20
6.81	15.1±1.9	1.43±0.20	6.19±1.77
9.08	14.1±1.9	1.48±0.23	6.00±1.82
14.07	10.5±1.5	1.62±0.28	6.43±2.30
14.07	14.8±4.9	1.16±0.48	5.93±2.88
18.54	18.2±4.8	1.59±0.42	7.44±1.54

Table 5-8 Mechanical properties of regenerated CF keratin fibers (25%CF, 75% Cellulose, Cellulose/CF 1/, extrusion solution Cellulose 1.6%, CF 4.8%)

Draw down	Linear density(den)	Tenacity(g/den)	Strain at Break (%)
0.89	25.5±3.7	1.47±0.27	7.88±1.88
0.89*	31.4±4.7	1.47±0.20	15.2±1.8
1.19	23.5±1.6	1.74±0.20	6.44±1.22
1.19*	23.7±1.7	1.86±0.17	11.2±1.7
1.79	16.7±3.7	2.07±0.23	11.5±2.9
1.79*	14.4±1.4	2.29±0.14	14.2±1.7
3.58	10.3±0.9	2.57±0.21	9.04±2.58
3.58*	11.4±1.0	2.30±0.22	15.3±3.86
1.79	12.8±5.7	2.33±0.37	7.88±1.34
2.39	19.2±3.6	1.82±0.18	7.95±1.67
3.58	12.4±2.4	2.04±0.38	6.59±1.39
3.58*	10.5±1.5	2.16±0.41	12.2±1.0
7.16	10.7±2.9	2.29±0.13	8.17±1.10
7.16*	7.62±1.6	2.18±0.34	8.77±2.41
1.31	21.4±3.7	1.78±0.40	6.75±1.14
1.75	21.1±2.8	1.59±0.35	7.43±1.41
2.62	16.2±2.5	1.95±0.29	14.8±6.3
2.62*	12.9±2.0	2.30±0.27	10.8±2.2

(*: Fibers were dried in air when wet fibers were wound off the spindle to prevent sticking to each other.)

Table 5-9 Mechanical properties of regenerated CF keratin fibers (66.7%CF, 33.3%

Cellulose, Cellulose/CF 1/2, extrusion solution Cellulose 1.75%, CF 3.5%)

Draw down	Linear density (den)	Tenacity (g/den)	Strain at Break (%)
0.89	19.7±1.7	1.77±0.87	5.45±0.87
1.19	18.8±2.1	1.91±0.23	6.62±1.31
1.79	13.0±1.0	2.38±0.22	6.96±0.59
3.58	9.23±2.6	2.37±0.40	7.00±1.32
1.79	20.7±2.2	1.86±0.23	8.31±2.30
2.39	18.2±1.3	1.95±0.21	8.39±2.25
3.58	11.3±1.1	2.17±0.26	6.77±1.36
7.16	7.91±1.7	2.21±0.29	5.87±1.20
2.68	17.7±1.7	1.90±0.28	6.97±1.58
3.58	11.5±1.6	1.80±0.27	3.90±0.90
5.37	8.72±0.83	1.92±0.45	5.28v1.11

Table 5-10 Mechanical properties of regenerated CF keratin fibers (66.7% CF, 33.3% Cellulose, Cellulose/CF 1/2, extrusion solution Cellulose 1.5%, CF 3.0%)

draw down	Linear density (den)	Tenacity (g/den)	Strain at Break (%)
1.79	10.9±1.50	1.72±0.39	4.74±1.09
2.39	10.3±1.10	1.64±0.24	4.93±1.05
3.58	8.83±0.61	1.67±0.64	4.25±1.75
7.16	7.97±1.85	2.03±0.45	6.45±1.93
2.68	12.3±1.40	1.50±0.24	5.02±1.83
3.58	9.47±0.58	2.05±0.51	5.52±2.39
5.37	7.98±1.53	1.67±0.31	4.26±1.49
10.74	6.44±1.38	2.01±0.42	5.75±0.93

Table 5-11 Mechanical properties of regenerated CF keratin fibers (50% CF, 50% Cellulose, Cellulose/CF 1/1, 1extrusion solution Cellulose 2.0%, CF2.0%)

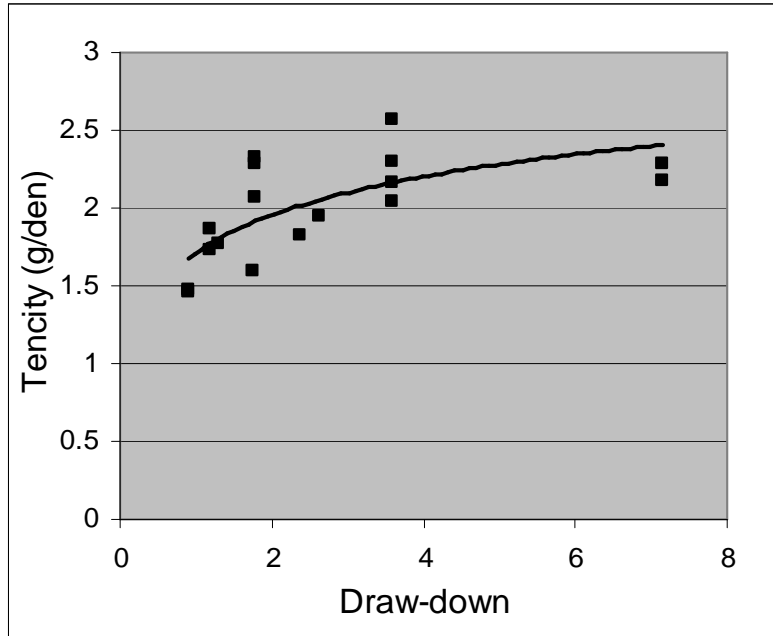
Draw down	Linear density (den)	Tenacity (g/den)	Strain at Break(%)
0.89	18.6±6.1	2.21±0.69	6.50±2.77
1.19	17.8±2.4	2.46±0.39	9.99±2.15
1.79	15.2±1.7	2.47±0.25	10.2±2.0
3.58	9.20±2.00	2.53±0.34	8.90±2.64
1.79	18.6±2.5	2.08±0.30	6.77±2.05
2.39	15.3±2.2	2.39±0.20	10.6±3.2
3.58	16.0±1.4	2.39±0.25	11.2±2.1

Table 5-12 Mechanical properties of regenerated CF keratin fibers (20%CF, 80%

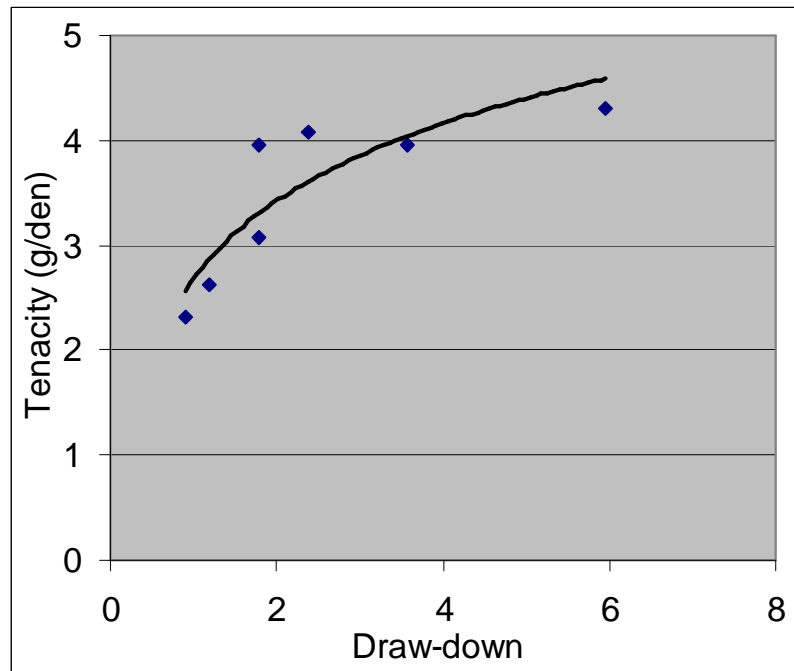
Cellulose, Cellulose/CF 4/1, extrusion solution Cellulose 4.8%, CF 0.6%)

Draw down	Linear density (den)	Tenacity(g/den)	Strain at Break (%)
0.89	36.3±5.1	2.32±0.44	7.74±2.06
1.19	22.8±4.7	2.61±0.52	6.69±1.70
1.79	13.9±1.1	3.06±0.46	6.30±1.68
3.58	7.68±0.89	3.95±0.21	6.74±0.78
5.96	6.03±1.41	4.31±0.50	6.47±1.15
1.79	9.37±0.88	3.95±0.33	7.31±2.11
2.39	7.04±0.57	4.07±0.24	6.37±0.60

Draw down also had effect on the tenacity of CF blend fibers, shown in Figure 5-17 and data in Table 5-8 and 5-12. The figures shows that, with the draw-down, the tenacity of CF blend fibers increased, which shows that spinning variables can be used to improve CF blend fibers' tensile properties.



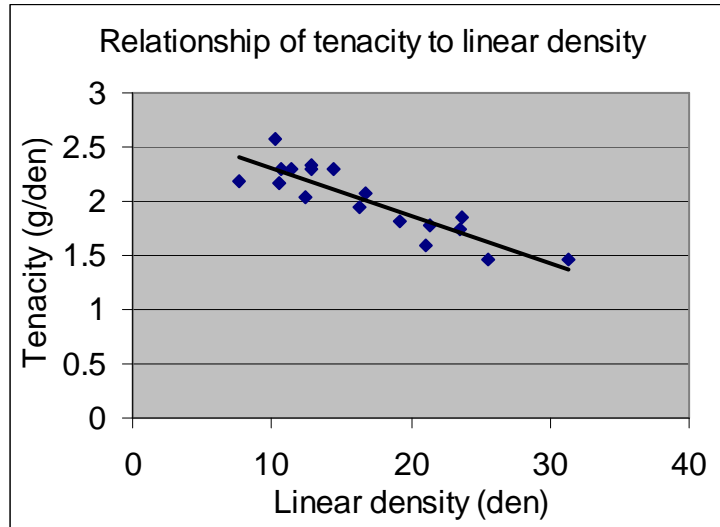
(a)



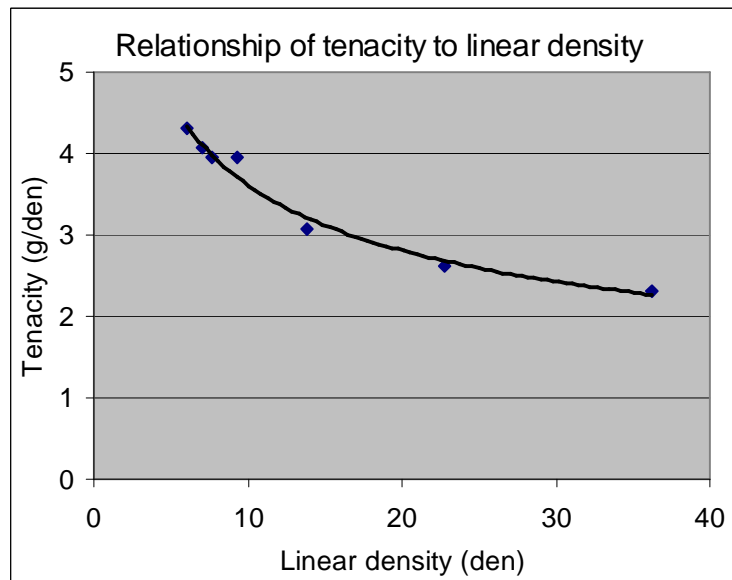
(b)

Figure 5-17 Effect of draw-down on tenacity of regenerated CF fibers
 (a) 75% CF and 25% cellulose blend fibers
 (b) 20% CF and 80% cellulose blend fibers

The relationship of linear density to tenacity of regenerated CF keratin fibers was also studied (shown in Figure 5-18 and data in Table 5-8 and 5-12). The figure shows that with linear density, the tenacity decreased. It is reasonable to assume that with a decrease of linear density, the regenerated fibers had better and better orientation, which improves tenacity of fibers.



(a) 75% CF and 25% cellulose blend fibers



(b) 20% CF and 80% cellulose blend fibers

Figure 5-18 Relationship of linear density to tenacity of regenerated CF keratin fibers

5.3.3.3 Physical structures of regenerated CF keratin fibers

The as-spun 100% chicken feather fibers experienced different post-treatment, which produced various surface appearances as shown in Figure 5-19. This figure shows that only drying in air immediately after removal from the salt coagulation bath produced a rough surface for 100 % CF regenerated fibers (perhaps from salt) and dipping in water helped “clean” the fiber surface. The CF and cellulose blend fibers were all dipped in water for 3 hrs as a last washing step after coagulation. Figure 5-20 shows the blended fibers had a smooth even surface. The blend fibers obtained in this chapter had an irregular cross-section, which is evident in the micrographs.

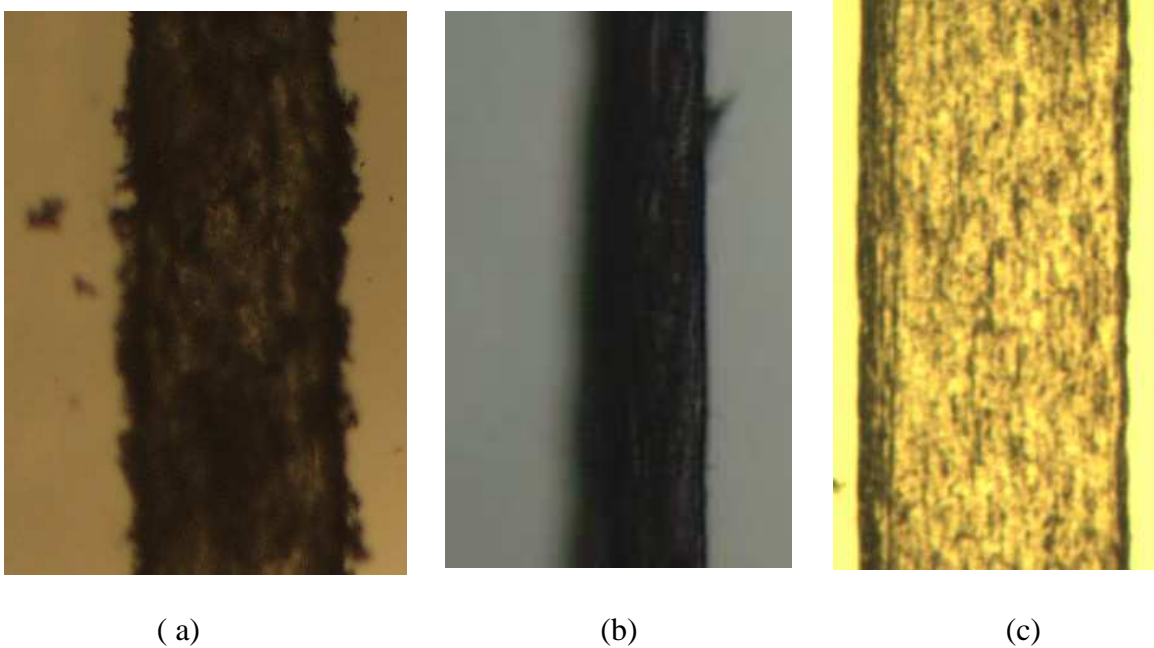


Figure 5-19 Regenerated 100% chicken feather fibers after different posttreatment

(a) Dried in air only after take-up

(b) Dipped in 4% Na_2SO_4 one day and then dried in air after take-up

(c) Dipped in 4% Na_2SO_4 and water 1 day respectively and successively,
finally dried in air after take-up.

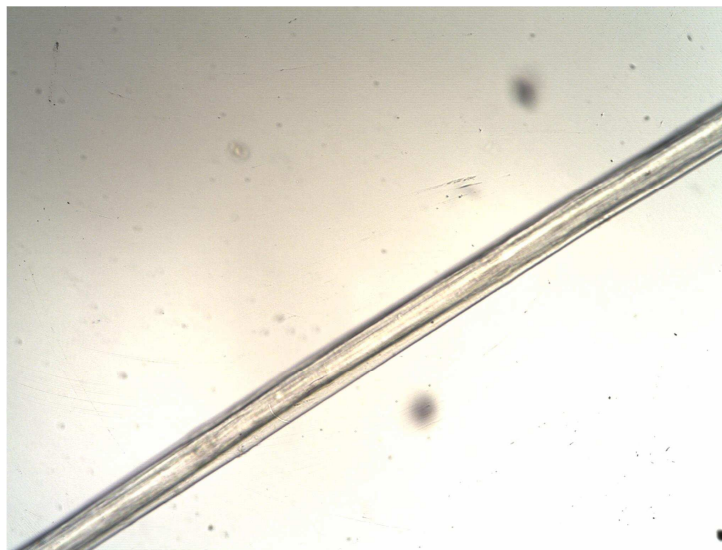


Figure 5-20 CF and Cellulose blend fiber

When wet blend fibers on spindles were dried in air, the adjacent fibers often stuck to each other and the wound fibers formed nets. It was not easy to separate a single fiber from the nets. This happened perhaps because crosslinking took place between the adjacent surfaces of different fibers. To solve this problem, we unwound the wet fibers and dried single wet fiber in air while it was unwound from the wet spindle just after being dipped in water for 3 hours. The single fibers appeared to dry very fast in air and sticking/crosslinking did not happen between separate dry surfaces when wound again on spindles.

5.3.3.4 Properties of CF fibers compared to other protein and some common fibers

The fineness, tensile properties and moisture regain of regenerated CF fibers are compared to those of protein fibers such as soyprotein, zein, wool and silk and some common fibers such as cotton and polyester in Table 5-13. The table shows that the

fineness of regenerated 100% CF protein fibers was very high, but CF blend fibers had fineness similar to that of wool and were produced as filaments, same as silk.

Table5-13 Tensile Properties of regenerated CF Fibers compared to some protein and common fibers *

Fiber	denier	tenacity g/den	break strain%	modulus ** g/den	moisture regain (%)	water absorption (%)
100%CF	204 ±32	0.232±0.29	5.8±8.4			
75%CF	10±3	2.3 ±0.3	15±3.8	34±8	15	125
50%CF	9.2±2.0	2.5±0.3	8.9±2.6	61±19	13	206
20%CF	6.0±1.4	4.3±0.5	6.5±1.1	87±14	8	95
soyprotein		0.32-0.91	0.4-5.9			
Zein		0.31-0.02	1.8-5.0			
Wool	8-15	1.0-1.7	25-35	43-65	18	100
Silk	0.9-2.5	1.7-2.2	14-25	53	11	42
Cotton	1.4-1.9	2.4-2.9	3-7	55	8	50
Polyester	1.53	4.8-6.0	25-30	103	0.4	3

*Data for soyprotein, zein, wool and silk are from ref [11] and [12] and for cotton and polyester from [14] and [15].

** modulus is Young's modulus.

From Table 5-13, it also can be seen that the tenacity of regenerated 100% CF fibers was only about 20% of that of wool and similar to that soyprotein and Zein, but 75% CF blend fibers had tenacity twice that of wool and similar to that of silk. The breaking strain of regenerated 100% CF fiber was 20% of that of wool and silk but much higher than that of soyprotein and zein. The breaking strain of the 75% CF blend fiber was about 70% of wool and similar to that of silk and much higher than that of 100%CF, soyprotein and Zein. The Young's Modulus and moisture of 75% CF fibers was similar to that of

wool and silk so the products made from 75% CF blend fibers would be expected to be soft and flexible as wool and silk if similar denier fibers were used. These regenerated CF fibers were able to hold as much water as wool. The Young's modulus of 100% CF was not shown in the measurement results. No report is found about the Young's modulus of 100% soyprotein and zein fibers.

From the table, it can also be seen that, 50% CF fibers had tenacity and moisture regain close to cotton but their Young's modulus was larger than that of cotton so 50% CF fibers was able to be produced as strong as, but softer and more creaseresistant than cotton if similar denier fibers are used. 20% CF fibers had similar tenacity to polyester, but their Young's modulus was smaller and moisture regain and water absorption were larger than that of polyester fibers so 20%CF fibers should be as strong as polyester but softer and more flexible and hold more water than polyester fibers. Therefore, 20%CF fibers should be produced as strong and crease resistant as, but softer and more flexible than polyester fibers if similar denier fibers are used.

Compared to the common fibers in Table 5-13, the raw materials of regenerated CF fibers was very inexpensive but the production process was expensive because of using expensive IL. Maybe in the near future, when the production of IL is not expensive and a good way to recover used IL is found, the regenerated CF fibers will be promising.

5.4 Conclusions

Protein blend fibers with mechanical properties better than those of wool, much better than those of 100% soyprotein and zein fibers and close to those of silk have been produced from chicken feather combined with cellulose. It has been found that, only after

chicken feather keratin was reduced, could it dissolve well in IL. Reduced keratin production increased with urea concentration and temperature. Only CF keratin did not produce high tenacity fibers; CF keratin and cellulose blend produced high quality fiber and the mechanical properties of the blend fibers were improved with draw-down. The tenacity of the blend fibers increased with the content of cellulose.

Based on the properties of the CF blend fibers, it can be proposed that CF gives the potential to produce higher quality fibers than zein and soyproteins; and based on the percentage of CF, the regenerated CF fibers will be produced not only having advantages of common commercial fibers such as silk, cotton, and polyester but also making up their disadvantages. Moreover, chemically reforming crosslinks might improve mechanical properties and the stability of the fibers to water and make them suitable for most fibrous applications. Using chicken feather for fiber production maybe is a good way to add value to the poultry industry and utilize the large amount of by-product “waste” of that industry. The availability of chicken feather “waste” provides an opportunity for the development of inexpensive and environmentally friendly protein-based bioproducts for most fibrous application. This is attractive because the CF protein does not compete with the food supply for humans.

5.5 Reference

[1] Katoh, Kazunori; Shibayama, Miki; Tanabe, Toshizumi; Yamauchi, Kiyoshi;

Journal of Applied Polymer Science, v 91, n 2, Jan 15, 2004, p 756-762

[23] Wasserscheid, P.; Welton, T.; Editors. Ionic Liquids in Synthesis, Germany.

- (2003), p364, Publisher: (Wiley-VCH Verlag GmbH & Co. KGaA, Weinheim, Germany)
- [31] Yao, Jinpo; He, Tianhong; Preparation of wool's keratin solution, *maofang keji*, (4), 2003, p16-19
- [4] Smith, P. J.; Sethi, A.; Welton, T.. Synthesis and catalysis in room-temperature ionic liquids, NATO Science Series, II: Mathematics, Physics and Chemistry (2002), 52(Molten Salts: From Fundamentals to Applications), p345-355.
- [5] R. P. Swatloski, S. K. Spear, I. D. Holbrey and R. D. Rogers, 1. *Am Chem. Soc.*, 124, 2002, p 4974
- [6] Xie, Haibo; Li, Shenghai and Zhang, Suobo; Ionic liquids as novel solvents for the dissolution and blending of wool keratin fibers, *Green chemistry*, 7, 2005, p606-608,
- [7] Kato, Kazunori; Shibayama, Mikio; Tanabe, Toshizumi; Yamauchi, Kiyoshi, Preparation and Properties of Keratin-Poly(vinyl alcohol) Blend Fiber, *Journal of Applied Polymer Science*, 91(2), Jan 15, 2004, p 756-762
- [8] Xie, Haibo; Zhang, Suobo; Method for preparing keratin solution; Faming Zhuanli Shenqing Gongkai Shuomingshu (2005), p9; CN 1660901 A 20050831
- [9] Voet, Donald; Voet, Judith G; Biochemistry; John Wiley & Sons, Inc., 1990
- [10] Fama S. Kilinc-Balci, Xiuling Fan, Kansan Kocer, Roy M. Broughton, Extrusion of composite fibers, INTC 2007, Atlanta, Sept 24-26
- [11] Blakey, P. R.; Happey, F. Protein fibers, *Rept. Progr. Appl. Chem.* 47, 1962, p245-52
- [12] Mathur, Manisha; Hira, Manisha. Speciality fibres - I: Soybean protein fibre. *Man-Made Textiles in India*, 47(10), 2004, p365-369.

- [13] Schmidt WF, Line MJ. Physical and chemical structures of poultry feather fiber fractions in fiber process development. In: TAPPI Proceedings: 1996 Nonwovens Conference, 135–140.
- [14] http://www.2008red.com/member_pic_357/files/xjtjnongye/html/article_3901_1.shtml 12/18/2007
- [15] <http://www.sccvtc.cn/wlxy/xwwlyhx/html/00.intro.fm17.html> 12/18/2007

CHAPTER 6
PREDICTION OF AIR PERMEABILITY OF FEATHER FIBER
NEEDLEPUNCHED NONWOVENS FOR AIR FILTRATION

6.1 Introduction

As indicated in literature, air filters are porous media. Under a pressure differential, air passes through the air filter. Both air permeability and pressure drop describe its porosity. As air permeability becomes small, the needed pressure drop (driven energy) becomes large. Since then, air permeability is one of their most important properties that determine their quality. There are standard methods to measure it. To direct and check experimental results, air permeability is calculated and predicted. In this study, air permeability was measured in standard conditions, so the prediction of air permeability of chicken feather nonwovens was carried out in standard conditions in this chapter.

6.2. Analytical Models

Darcy's law describes the laminar flow of a single gas flowing through a porous medium filled with gas as:

$$V = \frac{K(P_1 - P_2)}{\mu L} \quad (1)$$

where V: flow velocity,

K: permeability of the medium,

μ : gas viscosity,

P_1 and P_2 : pressures at the inlet and outlet ends of the filter.

L : thickness of the medium

Permeability K of the medium was calculated [2,3,4] as

$$K = \frac{C' \phi^3}{S^2 (1 - \phi)^2} \quad (2)$$

where ϕ : porosity, i.e. the ratio of the free volume in the medium to the total volume of the medium,

S : specific surface area or surface area per unit volume of media

C' : is the ratio between an orientation factor and a shape factor

From equation (1) and (2), equation (3) was obtained as

$$V = \frac{C' \phi (P_1 - P_2)}{\mu S^2 L (1 - \phi)^3} \quad (3)$$

A similar analytical model that refers the relationship between fabric parameters and flow properties [5] was achieved as follows:

$$V = \frac{K'' d^2 (P_1 - P_2) \epsilon}{16c\mu L} \quad (4)$$

where d: fiber diameter.

c: packing density (1- ϕ) in previous equations,

ε : inhomogeneity factor, and

K" is the Kuwabara factor $[-0.5 \ln(c)-0.75 + c - (c^2/4)]$ where $c = w / \rho L$ (where w is weight per unit area and ρ is the density of fibers)

From these two equations (3) and (4), two analytical approaches relating pressure drop to flow rate and fabric parameters were gained as follows:

Kozeny/Carman/Sullivan [6]

$$V = 5405405\Delta PC FL\rho \left(1 - \frac{0.001335}{\rho L}\right) / W^2 \quad (5)$$

Liu/Rubow [8, 9]:

$$V = 700.28\Delta P \left[-0.5 \ln\left(\frac{0.001336W}{L\rho}\right) - 0.75 + \frac{0.001002W}{L\rho} \right] F\varepsilon / W \quad (6)$$

where $\Delta P=P_1-P_2$, in inches of water, W is the nonwoven's areal density in oz/yd², V is air permeability in ft³/ft²/min, L is the nonwoven's thickness in inches, F is fibers' denier in gram per 9000 m, and ρ is fibers' density in g/m³.

6.3 Comparison with Experiments

The air permeability (AP) of CF nonwovens was measured at pressure drop 0.5 inch water according to Test Method D 737. All of the following calculations were based on the second set of new needlepunched Nd 2/2 nonwovens produced with adjust needle height and light scrim to make comparison.

From sample (1) (data in Table 6-1) as a calculation standard and for equation (5) and (6), C' was calculated C'=0.02745 and $\epsilon=0.15$. Using these two constants, the AP of other samples was calculated by using these two equations (5) and (6). The calculation was as follows:

Measured condition: $\Delta P=0.5$ inch in water

Fiber condition: PET density = 1.38g/cm³,

CF density = 0.89g/cm³,

Scrim areal density of two layers = 33.87g/m²,

PET fiber diameter = 14.2 μ m

Scrim diameter = 15.6 μ m

CF diameter = 7.49 μ m

Sample (1) had CF/PET 50/50, and measured and calculated data as follows:

Table 6-1 Measured and calculated data of new 50/50 nonwoven sample (1)

Thickness (mm)	Thickness (in)	Nonwoven wt(real)(g)	Nonwoven Size(m ²)	Measured Areal Density (g/m ²)	Measured Areal Density (oz/yd ²)	Scrim Wt (g)	Staple fiber Wt (g)
7.581	0.298	13.940	0.108	128.500	3.79	3.673	10.267

CF fiber Wt (g)	PET staple fiber Wt (g)	Fibers' Wt ave df (μ m)	Fibers' Wt average density (g/m ³)	Fibers' denier	Measured AP (ft ³ /ft ² /min)
5.133	5.133	12.098	1.200	1.240	228.5

(Note: Scrim Wt = Nonwoven Size \times Scrim areal density of two layers;

Staple fibers Wt = Nonwoven Wt - Scrim Wt;

CF fiber Wt = Staple fiber Wt × percentage of CF in staple fibers

PET staple fiber Wt = Staple fiber Wt × percentage of PET staple fibers in staple fibers;

Fiber's Wt average d_f = (Scrim fiber Wt × its diameter+ CF fiber Wt × its diameter + PET fiber Wt × its diameter)/ nonwoven's Wt.

Fibers' Wt average density (g/m^3) = (Scrim fiber Wt × its density+ CF fiber Wt × its density + PET fiber Wt × its density)/ nonwoven's Wt.

Fiber's Denier = $9000 \times 3.14/4 \times (\text{Fibers' Wt average } d_f)^2 \times \text{Fibers' Wt average density}$.

The calculating method in the following tables were calculated in the same way)

From data of Table 6-2, using equation (5) and (6), C' was calculated 0.02745 and ϵ was 0.15.

From $C' = 0.02745$ and $\epsilon = 0.15$, two equations were determined by substitution into equation (5) and (6) as follows:

$$\begin{aligned} V_1 &= 540540.5 \Delta P C' L \rho \left(1 - \frac{0.001335}{\rho L} \right) / W^2 \\ &= 540540.5 \times 0.5 \times 0.03 L \rho \left(1 - \frac{0.001335}{\rho L} \right) / W^2 \end{aligned} \quad (7)$$

$$\begin{aligned} V_2 &= 700.28 \Delta P \left[-0.5 \ln \left(\frac{0.001336W}{L\rho} \right) - 0.75 + \frac{0.001002W}{L\rho} \right] F \epsilon / W \\ &= 700.28 \times 0.5 \left[-0.5 \ln \left(\frac{0.001336W}{L\rho} \right) - 0.75 + \frac{0.001002W}{L \times \rho} \right] F \times 0.15 / W \end{aligned} \quad (8)$$

By using equation (7) and (8), for other composition CF nonwovens the calculation results were shown in Table 6- 3, 4, 5, 6.

Table 6- 2 Measured and calculated data of new CF/PET 75/25 nonwovens

CF/PET 75/25	Sample (26)	Sample (25)	Sample(7)	Sample(8)	Sample(9)
Thickness (mm)	3.503	4.455	6.508	7.030	7.819
Thickness (in)	0.138	0.175	0.256	0.277	0.308
Nonwoven wt (g)	8.650	9.630	14.250	16.010	18.010
Nonwoven Size(m ²)	0.104	0.098	0.111	0.108	0.110
Measured areal density(g/m ²)	83.040	98.380	128.900	148.100	163.400
Measured areal density(oz/yd ²)	2.45	2.90	3.80	4.37	4.82
Scrim Wt(g)	3.528	3.315	3.745	3.661	3.733
Staple fiber Wt (g)	5.122	6.315	10.505	12.349	14.277
CF fiber Wt (g)	3.842	4.736	7.879	9.262	10.708
PET staple fiber Wt (g)	1.281	1.579	2.626	3.087	3.569
Fiber's Wt ave df (μm)	11.791	11.382	10.858	10.638	10.501
Fiber's Wt average density g/cm ³	1.162	1.139	1.109	1.097	1.089
Fiber's Denier	1.142	1.043	0.924	0.877	0.848
Measured AP (ft ³ /ft ² /min)	278.4	226.3	156.5	131.2	118.1
V1	224.47	182.28	134.12	103.01	90.42
V1 relative error%	-19.37	-19.45	-14.30	-21.49	-23.43
V2	296.53	233.17	162.80	130.73	114.65
V2 relative error%	6.51	3.04	4.02	-0.36	-2.92

(Note: V1 relative error% = (V1-Measured AP)/Measured AP×100%

V2 relative error% = (V2-Measured AP)/Measured AP×100%, same as follows.)

Table 6- 3 Measured and calculated data of new CF/PET 67/33 nonwovens

CF/PET 67/33	Sample (24)	Sample (23)	Sample(4)	Sample(5)	Sample(6)
Thickness (mm)	4.511	5.319	8.330	8.567	8.458
Thickness (in)	0.178	0.209	0.328	0.337	0.333
Nonwoven wt (g)	8.430	9.420	13.880	15.910	17.770
Nonwoven Size(m ²)	0.096	0.095	0.111	0.110	0.112
Measured areal density(g/m ²)	87.720	98.760	124.900	144.400	158.300
Measured areal density(oz/yd ²)	2.59	2.91	3.68	4.26	4.67
Scrim Wt(g)	3.255	3.230	3.765	3.733	3.803
Staple fiber Wt (g)	5.175	6.190	10.115	12.177	13.967
CF fiber Wt (g)	3.467	4.147	6.777	8.159	9.358
PET staple fiber Wt (g)	1.708	2.043	3.338	4.019	9.358
Fiber's Wt ave df (μm)	11.981	11.726	11.303	11.087	10.966
Fiber's Wt average density g/cm ³	1.178	1.164	1.141	1.129	1.491
Fiber's Denier	1.195	1.131	1.030	0.980	1.267
Measured AP (ft ³ /ft ² /min)	313.7	288.4	194.7	167.3	162.1
V1	275.43	239.83	209.86	152.12	213.40
V1 error%	-12.20	-16.84	7.79	-9.07	31.65
V2	318.80	271.41	209.26	164.76	206.28
V2 error%	1.62	-5.89	7.48	-1.52	27.25

Table 6- 4 Measured and calculated data of new CF/PET50/50 nonwovens

CF/PET 50/50	Sample (22)	Sample (21)	Sample(1)	Sample(2)	Sample(3)
Thickness (mm)	5.076	5.735	7.581	9.257	12.158
Thickness (in)	0.200	0.226	0.298	0.364	0.479
Nonwoven wt (g)	8.210	10.330	13.940	16.100	18.900
Nonwoven size(m ²)	0.090	0.101	0.108	0.107	0.112
Measured areal density(g/m ²)	90.93	102.60	128.50	150.20	169.00
Measured areal density(oz/yd ²)	2.68	3.03	3.79	4.43	4.98
Scrim Wt(g)	3.058	3.410	3.673	3.630	3.789
Staple fiber Wt (g)	5.152	6.920	10.267	12.470	15.111
CF fiber Wt (g)	2.576	3.460	5.133	6.235	7.556
PET staple fiber Wt (g)	2.576	3.460	5.133	6.235	7.556
Fiber's Wt ave df (μm)	12.616	12.415	12.098	11.917	11.798
Fiber's Wt average density g/cm ³	1.226	1.216	1.200	1.190	1.184
Fiber's Denier	1.379	1.324	1.240	1.194	1.164
Measured AP (ft ³ /ft ² /min)	353	316.2	228.5	189	168
V1	346.68	293.04	228.53	195.23	196.63
V1 error%	-1.79	-7.33	0.02	3.30	17.04
V2	370.96	314.84	238.92	199.28	181.70
V2 error%	5.09	-0.43	4.56	5.44	8.15

Table 6- 5 Measured and calculated data of new CF/PET 33/67 nonwovens

CF/PET 33/67	Sample (20)	Sample (19)	Sample(10)	Sample(11)	Sample(12)
Thickness (mm)	4.939	5.560	10.247	10.887	10.080
Thickness (in)	0.194	0.219	0.403	0.429	0.397
Nonwoven wt (g)	9.080	10.460	14.880	16.750	20.320
Nonwoven Size(m ²)	0.103	0.108	0.106	0.109	0.114
Measured areal density(g/m ²)	87.810	96.800	139.700	154.100	177.500
Measured areal density(oz/yd ²)	2.59	2.85	4.12	4.54	5.24
Scrim Wt(g)	3.502	3.660	3.607	3.681	3.877
Staple fiber Wt (g)	5.578	6.800	11.273	13.069	16.443
CF fiber Wt (g)	1.841	2.244	3.720	4.313	5.426
PET staple fiber Wt (g)	3.737	4.556	7.553	8.756	11.017
Fiber's Wt ave df (μm)	13.380	13.250	12.862	12.780	12.675
Fiber's Wt average density g/cm ³	1.281	1.275	1.257	1.254	1.249
Fiber's Denier	1.620	1.581	1.470	1.447	1.418
Measured AP (ft ³ /ft ² /min)	364.5	349.9	240.2	218.2	191.1
V1	443.79	399.76	324.96	278.57	189.76
V1 error%	21.75	14.25	35.29	27.67	-0.70
V2	459.41	409.21	284.73	250.79	197.88
V2 error%	26.04	16.95	18.54	14.94	3.55

Table 6-6 Measured and calculated data of new CF/PET 0/100 nonwovens

CF/PET 0/100	Sample (18)	Sample (31)	Sample (17)	Sample (13)	Sample (14)	Sample (15)
Thickness (mm)	7.713	5.836	7.458	10.059	14.042	16.938
Thickness (in)	0.304	0.230	0.294	0.396	0.553	0.667
Nonwoven wt (g)	9.080	10.550	10.620	15.040	19.140	20.530
Nonwoven Size(m ²)	0.099	0.105	0.104	0.110	0.114	0.112
Measured areal density(g/m ²)	91.340	100.700	101.700	136.200	167.200	183.100
Measured areal density(oz/yd ²)	2.69	2.97	3.00	4.02	4.93	5.40
Scrim Wt(g)	0.099	0.105	0.104	0.110	0.114	0.112
Staple fiber Wt (g)	3.367	3.548	3.535	3.741	3.877	3.797
CF fiber Wt (g)	5.713	7.002	7.085	11.299	15.263	16.733
PET staple fiber Wt (g)	14.719	14.671	14.666	14.548	14.484	14.459
Fiber's Wt ave df (μm)	1.380	1.380	1.380	1.380	1.380	1.380
Fiber's Wt average density g/cm ³	2.112	2.098	2.097	2.064	2.045	2.038
Fiber's Denier	2.112	2.098	2.097	2.064	2.045	2.038
Measured AP (ft ³ /ft ² /min)	401.4	362	342.9	295.2	251.5	227.8
V1	902.00	557.26	698.38	517.22	475.19	476.48
V1 error%	124.71	53.94	103.67	75.21	88.94	109.17
V2	673.36	538.02	574.87	423.32	355.58	333.06
V2 error%	67.75	48.62	67.65	43.40	41.38	46.91

From Table 6-2 – 6-6, it can be seen that, when the composition was CF/PET mixture, the mixture is close to the calculation standard and its d_f was smaller than that of the standard, the error was small. However, when the fiber mixture was 100% PET fiber, the error was very large and maybe it needed to use its own constants and be calculated again.

Sample (1) was chosen as calculation standard to calculate constants. The calculation process was similar to above and for equation (5) and (6), C' was calculated $C' = 0.02745$ and $\varepsilon = 0.15$. All of the other nonwovens used the same constants.

6.4 Conclusion

An analytical model to calculate air permeability of porous air filter was developed. Constants for two equations were derived from experimental results and used to calculate air permeability for CF remaining nonwovens. When the fiber composition was close to the nonwoven to calculate the constants, the calculation error was small; otherwise, the calculation error was large.

It is uncertain whether errors result from the theory used to derive the equation or from the errors in measurements of fibers or fabric properties, or the process of averaging fiber dimensions and density.

6.5 Reference

- [1] Alper, Hal; Novel surface modification which increases filter holding capacity at constant delta P; *the proceedings of American filtration and separation society*; 2003

- [2]. Hertel, K. L., and Craven. C. J., Cotton Fineness and Immaturity as Measured by the Arealometer, *Textile Research Journal*, 21(11), 1951, p765-774.
- [3]. Sullivan. R. R.. and Hertel, K. L., The Flow of Air Through Porous Media. *Journal of Applied Physics*, 12, 1940, p76 1-765.
- [6]. Fowler, J. L. and Hertel. K. L., Flow of a Gas Through Porous Media, *Journal of Applied Physics*, 11, 1940, p 496-502.
- [7] Liu, B. Y. H. and Rubow, K. L.; Air Filtration by Fibrous Media, in *Fluid Filtration: Gas, Volume 1* ASTM Special Technical Publication 975. Ed. Robert R. Raber. ASTM, Philadelphia. PA, 1986.
- [8]. Duckett. K. E.. Cain. J. and Krowicki. R. S.; Automating the Arealometer: Examination of the Kozeny Equation, *Textile Research Journal*, 61(6), 1991, p309-318.
- [9] Sullivan, R. R., Further Study of the Row of Air through Porous Media, *Journal of Applied Physics*, 12, 1941, p503-509.

CHAPTER 7

PREDICTION OF PENETRATION AND INITIAL FILTRATION EFFICIENCY OF FEATHER FIBER NONWOVENS FOR AIR FILTRATION

7.1 Introduction

The fibrous filter is simple widely-used equipment in which particle-holding gas passes through a permeable porous textile medium. Particle filtration efficiency of fibrous filter media is important for gas cleaning, sampling and production in industry and research. Therefore, the prediction of filtration efficiency for a fibrous filter has been an important research topic for a long time. Because particle collected on fibrous filters is a very complex problem, and real particles always have a complicated structure (which influences their deposition behaviors on filters), the particle shape is generally assumed to be spherical to avoid further complication.

For a new fibrous air filter, there are three mechanisms of particle caption. They are diffusion, interception and electrical forces. Interception takes place when a particle, for its momentum, crosses the fluid streamlines and strikes a fiber. Larger particles have more chances of impaction onto smaller diameter fibers by particle inertia. Diffusion is Brownian motion and is the primary filtration mechanism for particles below 0.1 micrometer. Since electrical forces are not used in this research, only diffusion and interception influences on filtration efficiency are discussed in this chapter

7.2 Analytical model

Spherical particle penetration through fibrous filter is discussed here for the analytical model. Generally, description of particle penetration through fibrous filters is in terms of the **single fiber efficiency E**. The relationship between the **penetration P** of particles through the whole filter and **E** is provided by [1]:

$$P = \exp\left[-\frac{4\alpha L}{\pi(1-\alpha)d_f} \mathbf{E}\right] \quad (1)$$

where

α is the **mean fiber volume fraction**,

L is the **mean thickness of the filter**

d_f is the **mean fiber diameter**

The factor in front of **E** depends on the filter structure, and **E** is on the particle properties and the face velocity of air filters.

7.2.1 Filtration including diffusion

The single fiber efficiency of pure diffusion, **E_D** is proportional to $(Pe)^{2/3}$ [2].

$$E_D \propto (Pe)^{2/3} \quad (2)$$

The Peclet number, given by

$$Pe = \frac{U_0 d_f}{D} \quad (3)$$

depends on the face velocity U_0 on the air filter, the fiber diameter d_f and D , the diffusion coefficient of the particles. D is given [3] by

$$D = \frac{k_B T C}{6\pi\eta d_D} \quad (4)$$

where d_D is equal to their geometrical diameter for particle spheres ;

k_B is Boltzmann's constant,

T is the absolute temperature,

C is the slip correction factor

η is the viscosity of the gas medium.

For this research, all the filtration efficiency measurement of nonwovens was taken at fixed conditions such as fixed temperature and flow field (face velocity) and used the same kind of particles so in this research D is constant.

Therefore, for this research the dependence of E_D on the filter property, fiber diameter d_f is given [4] by

$$E_D \propto P e^{\frac{2}{3}} = \left(\frac{U_o d_f}{D} \right)^{\frac{2}{3}} \propto d_f^{\frac{2}{3}} \quad (7)$$

that is,

$$E_D = k_1 (d_f)^{\frac{2}{3}} \quad (8)$$

where k_1 is a constant.

7.2.2 Filtration including interception

Interception takes place for the finite size of the particles. For pure interception, particle diffusion is not considered. Therefore, it is determined by the flow field. The single fiber **interception efficiency** E_R of direct interception is provided [5] by

$$E_R = \frac{1}{2\kappa} \left[2(1 + R) \ln(1 + R) - (1 + R) + \frac{1}{(1 + R)} \right] \quad (7)$$

where R is the interception parameter, given by

$$R = \frac{d_R}{d_f} \quad (8)$$

(d_R is equal to its geometrical diameter for spheres.)

κ is called the Kuwabara hydrodynamic factor, depends only on α , and can be expressed[6] by

$$\kappa = -\frac{\ln \alpha}{2} - \frac{3}{4} + \alpha - \frac{\alpha^2}{4} \quad (9)$$

For Chicken feather nonwoven, Equation (9) was used.

7.2.3 Filtration including diffusion and interception

The simplest way to combine the diffusion and interception mechanisms is to add the two individual efficiencies to obtain the combined efficiency E . This way is based on the assumption that only one mechanism is predominant, the contribution made by the other mechanism being small [7]. This is obtained by a combination term for diffusion and interception. The overall efficiency E is used as:

$$E = E_D + E_R \quad (10)$$

All above equations are used and Equation (6), (7), (8), (9), (10) are substituted into Equation (1) to get the penetration of the spheres through new filters, Equation (11)

$$P = \exp \left\{ - \frac{4\alpha L}{\pi(1-\alpha)d_f} \left[k_1 d_f^{\frac{2}{3}} + k_2 \frac{1+R}{\kappa} \ln(1+R) - k_2 \frac{1+R}{2\kappa} + k_2 \frac{1}{2\kappa(1+R)} + k_3 \right] \right\} \quad (11)$$

where k_1 , k_2 and k_3 are constants, and depends on the face velocity and experimental air flow.

7.3 Calculation method and comparison with experiments

7.3.1 Known conditions of penetration measurement

Equation (8) $R = \frac{d_R}{d_f}$ is used. d_R was chosen solid NaCl particle weight

average diameter $0.2\mu\text{m}$. d_f is calculated as weight average diameter of fibers

including polyester, scrim and chicken feather fibers.

Diameter of feather fiber d_{cf} was as measured as following:

$$d_{cf} = 7.49\mu\text{m}$$

Diameter of PET staple fiber was measured under a microscope meter and calculated at the average of 25 fiber samples as follows:

$$d_{PET} = 14.2 \mu\text{m}$$

Diameter of Scrim fiber diameter was measured under a microscope meter and calculated at the average of 25 fibers samples as following:

$$d_{scrim} = 15.6 \mu\text{m}$$

For face velocity to be determined the diameter of tube was 1.5in; the volume velocity was 32L/min.

The gas properties at 72 °F:

$$\mu = 1.826 \times 10^{-5} \text{ Nsm}^{-2}$$

$$\rho = 1.196 \text{ kg / m}^{-3}$$

For known fiber parameters,

Volumetric density of Chicken feather fiber: 0.89 g/cm³

Volumetric density of PET fiber: 1.38 g/cm³

Two layers of needlepunched scrim area density: 33.87 g/m²

To simplify the calculation of penetration of nonwovens, penetration calculation

Equation (11) is written as follows:

$$P = \exp \left\{ -B \left[k_1 d_f^{\frac{2}{3}} + k_2 A + k_3 \right] \right\} \quad (12)$$

where

$$B = \frac{4\alpha L}{\pi(1-\alpha)d_f} \quad (13)$$

$$A = \frac{1+R}{\kappa} \ln(1+R) - \frac{1+R}{2\kappa} + \frac{1}{2\kappa(1+R)} \quad (14)$$

7.3.2 Calculation of constants in the penetration equation

The data of the lightest CF/PET 0/100, heaviest CF/PET 75/25 and middle weight CF/PET 50/50 nonwovens [sample (18) in Table 7-1, sample (9) in Table 7-2 and sample (1) in Table 7-3] were used to calculate the constants k_1 , k_2 and k_3 , and then these constants were used to calculate other nonwovens' penetration. All of the calculations in this chapter are based on the second set of new needlepunched CF nonwovens (Nd 2/2) produced with adjusted needle height and light scrim.

Table7-1 Measured basic physical data of CF/PET 0/100 nonwovens

	CF/ PET	Areal density (g/m ²)	Nonwoven Wt (g)	Width (cm)	Length (cm)	Thickness (mm)
Sample(18)	0/100	91.34	9.08	23.50	42.3	7.713
Sample(31)	0/100	100.7	10.55	23.08	45.4	5.836
Sample(13)	0/100	136.2	15.04	23.75	46.5	10.059
Sample(14)	0/100	167.2	19.14	23.65	48.4	14.042
Sample(15)	0/100	183.1	20.53	23.85	47	16.938

[Note: above data are all measured except areal density, and

$$\text{Areal density} = \text{Nonwoven's wt} / (\text{its Width} \times \text{its Length})$$

The following areal density in tables uses the same definition.]

Table 7-2 Measured basic physical data of CF/PET 75/25 nonwovens

	CF/PET	Areal density (g/m ²)	Nonwoven Wt (g)	Width (cm)	Length (cm)	Thick- ness (mm)
Sample(26)	75/25	83.04	8.65	23.70	43.95	3.503
Sample(25)	75/25	98.38	9.63	23.25	42.10	4.455
Sample(7)	75/25	128.9	14.25	23.60	46.85	6.508
Sample(8)	75/25	148.1	16.01	23.65	45.70	7.030
Sample(9)	75/25	163.4	18.01	23.70	46.50	7.819

(Note: above data are all measured except areal density)

Table 7-3 Measured basic physical data of CF/PET 50/50 nonwovens

	CF/PET	Areal density (g/m ²)	Nonwoven Wt (g)	Width (cm)	Length(cm)	Thickness (mm)
Sample(22)	50/50	90.93	8.21	22.35	40.4	5.076
Sample(21)	50/50	102.6	10.33	23.2	43.4	5.735
Sample(1)	50/50	128.5	13.94	23.1	46.95	7.581
Sample(2)	50/50	150.2	16.1	22.9	46.8	9.257
Sample(3)	50/50	169	18.9	23.55	47.5	12.158

(Note: above data are all measured except areal density)

The calculation process of k_1 , k_2 and k_3 are calculated as following steps:

Step 1: Equation (15) was used to calculate the weight of scrim used for nonwovens, Equation (16) for weight of PET staple fibers and Equation (17) for weight of CF fibers in the nonwovens.

$$\text{Weight of scrim} = (\text{Length} \times \text{width}) \text{ of nonwoven} \times \text{areal density of two layers of needlepunched scrim} \quad (15)$$

$$\text{Weight of PET staple fibers} = (\text{weight of nonwoven} - \text{weight of scrim}) \times \text{percentage of PET staple fibers used in this nonwoven} \quad (16)$$

$$\text{Weight of CF fiber} = (\text{weight of nonwoven} - \text{weight of scrim}) \times \text{percentage of CF fibers used in this nonwoven} \quad (17)$$

The calculation results are as follows in Table 7-4:

Table 7-4 Weight of scrim, PET and CF fibers in Sample (18), (9) and (1)

	Weight of scrim(g)	Weight of PET staple fibers (g)	Weight of CF fibers (g)
Sample(18)	3.37	5.71	0
Sample(9)	3.73	4.65	9.63
Sample(1)	3.67	5.13	5.13

Step 2, Real volume of fibers in nonwovens was calculated according to Equation (18), apparent volume of the nonwovens to Equation (19), their volumetric percentage of fibers to Equation (20) and weight average diameter of nonwoven fiber, d_f to Equation (21). Calculation results are shown in Table 7-5.

real volume of fibers

$$= \frac{\text{weight of (PET scrim + PET staple fibers)}}{\text{volumetric density of PET}} + \frac{\text{weight of CF fibers}}{\text{volumetric density of CF}} \quad (18)$$

$$\text{apparent volume of the nonwoven} = \text{Length} \times \text{width} \times \text{thickness} \quad (19)$$

$$\text{Volumetric fraction of fibers } \%(\alpha\%) = \frac{\text{real volume of fibers}}{\text{apparent volume of nonwoven}} \quad (20)$$

Weight average diameter of nonwoven fibers

$$\begin{aligned} &= (\text{diameter of scrim PET fiber} \times \text{weight of needlepunched scrim} \\ &+ \text{diameter of batting PET fiber} \times \text{weight of PET staple fibers} \\ &+ \text{diameter of CF fiber} \times \text{weight of CF fibers}) / \text{measured weight of} \\ &\text{nonwoven} \end{aligned} \quad (21)$$

Table 7-5 Volume fraction of fibers and diameter of nonwovens fibers in Sample (18), (9) and (1)

	Real volume of fibers (cm ³)	apparent volume of fibers (cm ³)	Volume percentage of fibers (100 α , %)	Diameter of nonwoven fibers d _f (μm)
Sample(18)	6.580	766.7	0.858	14.719
Sample(9)	17.324	861.7	2.011	10.501
Sample(1)	12.149	822.2	1.440	12.098

Step3: From Equation (8) and d_R ($0.2\mu\text{m}$) to calculate interception parameter, results are as follows in Table 7-6,

Table 7-6 Interception parameter of Sample (18), (9) and (1)

	R
Sample(18)	0.013588
Sample(9)	0.019046
Sample(1)	0.016532

Step4: From Equation (13) and (14) the values of A and B are calculated. The calculation results of A and B in sample (18), (9) and (1) are as follows in Table 7-7:

Table 7-7 Values of A and B of Sample (18), (9) and (1)

	A	B
Sample(18)	0.0001117	0.5778
Sample(9)	0.0002928	1.9466
Sample(1)	0.0001953	1.1676

Step5: Using the data of the measured penetration of sample (18) and (9) in Table 7-8 and the value of A and B in Table 7-7 and substituting them in Equation (12), k_1 , k_2 and k_3 was calculated in Table 7-8.

Table 7-8 Measured penetration of sample (18), (9) and (1)

	Mmeasured Penetration
Sample(18)	0.93833
Sample(9)	0.8410
Sample(1)	0.9215

Table 7-9 Calculation results of constants of penetration equation

Constant	Value
k_1	1712.5
k_3	1027.7
k_3	-1.0332

7.3.3 Calculation of penetration of CF nonwovens and comparison with experiments

Using k_1 , k_2 and k_3 calculated in §7.3.2 and calculating A and B of every nonwoven at the same time, the penetration of all nonwovens can be calculated with Equation (12).

First, A and B were needed to be calculated. The calculation of A and B could be done the similar steps to **Step 1** to **Sep 4** in §7.3.2.

For CF/PET 0/100 nonwovens, their measured basic physical data has been shown in Table 7-1. The calculation process of penetration and filtration efficiency of CF/PET 0/100 nonwovens are shown as follows:

Step 1: Equation (15) was used to calculate the weight of scrim used for the nonwoven, Equation (16) for weight of PET staple fibers and Equation (17) for weight of CF fibers in the nonwoven. The calculation results are shown in Table 7-10.

Table 7-10 Weight of scrim, PET and CF fibers in CF/PET 0/100 nonwovens

	CF/PET	Weight of scrim (g)	Weight of PET staple fibers (g)	Weight of CF fibers (g)
Sample(18)	0/100	3.37	5.71	0
Sample(31)	0/100	3.55	7.00	0
Sample(13)	0/100	3.74	11.30	0
Sample(14)	0/100	3.88	15.26	0
Sample(15)	0/100	3.80	16.73	0

Step 2, real volume of fibers in the nonwoven was calculated according to Equation (18), its apparent volume to Equation (19), its volumetric fraction of fibers to Equation (20) and its eight average diameter of nonwoven fiber d_f to Equation (21). Calculation results are shown in Table 7-11.

Table 7-11 Volume fractions of fibers and average diameter of all fibers in CF/PET 0/100 nonwovens

	CF/PET	Real volume of fibers (cm ³)	apparent volume of fibers (cm ³)	Volume fraction of fibers 100 α (%)	Diameter of nonwoven fibers d_f (μ m)
Sample(18)	0/100	6.580	364.85	1.80	14.719
Sample(31)	0/100	7.645	436.04	1.75	14.671
Sample(13)	0/100	10.899	719.56	1.51	14.548
Sample(14)	0/100	13.870	759.81	1.83	14.484
Sample(15)	0/100	14.877	861.66	1.73	14.459

Step 3: From (8) and d_R (0.2 μ m) to calculate interception parameter of the nonwoven and correspondent values of d_f substituting into it, the results are shown in Table 7-12.

Table 7-12 Interception parameter of CF/PET 0/100 nonwovens

	R
Sample(18)	0.01359
Sample(31)	0.01363
Sample(13)	0.01375
Sample(14)	0.01381
Sample(15)	0.01383

Step 4: A was calculated according to Equation (13) and B to Equation (14). The values of R (in Table 7-12), L in Table 7-1 and α in Table 7-11 were substituted into Equation (13) and (14). The calculation results are shown in Table 7-13.

Table 7-13 Values of A and B in CF/PET 0/100 nonwovens.

	CF/PET	A	B
Sample(18)	0/100	0.0001117	0.5778
Sample(31)	0/100	0.0001267	0.6416
Sample(13)	0/100	0.0001191	0.8727
Sample(14)	0/100	0.0001156	1.0749
Sample(15)	0/100	0.0001127	1.1782

Step 5: Using $k_1 = 1712.5$, $k_2 = 1027.7$ and $k_3 = -1.0332$ and substituting of the values of A and B in Table 7-13 in Equation (12), the penetration of every CF/PET 0/100 nonwoven were calculated in Table 7-14 with measured penetration.

Table 7-14 Calculation results of the penetration of CF/PET 0/100 nonwovens

CF/PET 0/100	Calculated penetration	Measured Penetration (%)	Relative calculated penetration error (%)
Sample(18)	0.9383	93.833	0.00
Sample(31)	0.9239	94.225	-1.95
Sample(13)	0.9086	94.95	-4.31
Sample(14)	0.8951	94.00	-4.78
Sample(15)	0.8899	92.75	-4.05

Step 6: According to Equation (22), relative error of calculated penetration (%) was calculated and also shown in Table 7-14.

$$\begin{aligned}
 & \text{Relative error of calculated penetration}(\%) \\
 & = \frac{\text{calculated penetration} - \text{measured penetration}}{\text{measured penetration}} \times 100\%
 \end{aligned}
 \tag{22}$$

Step 7: For the following equations,

$$\text{Filtration efficiency} = 1 - \text{penetration}
 \tag{23}$$

$$\text{Relative error of calculated filtration efficiency (\%)} \quad (24)$$

$$= \frac{\text{calculated filtration efficiency} - \text{measured filtration efficiency}}{\text{measured filtration efficiency}} \times 100\%$$

The measured filtration efficiency and its relative error of calculated filtration efficiency of CF/PET 0/100 nonwovens were also calculated according to Equation (23) and (24) shown in 7-15.

Table 7-15 Calculation results of the filtration efficiency of CF/PET 0/100 nonwovens

	Calculated filtration efficiency	Measured filtration efficiency (%)	Relative Error of calculated filtration efficiency (%)
Sample(18)	0.0617	6.17	0
Sample(31)	0.0761	5.78	31.7
Sample(13)	0.0911	5.05	81.0
Sample(14)	0.1107	6.00	74.8
Sample(15)	0.1206	7.25	51.8

Similarly, the penetration and filtration efficiency of other CF nonwovens could also be calculated. For CF/PET 33/67 nonwovens their measured basic physical data are shown in Table 7-16.

Table 7-16 Measured basic physical data of CF/PET 33/67 nonwovens

	CF/PET	Areal density (g/m ²)	Nonwoven wt(g)	Width (cm)	Length(cm)	Thickness (mm)
Sample(20)	33/67	87.81	9.08	23.5	44	4.9393
Sample(19)	33/67	96.8	10.46	23.75	45.5	5.56
Sample(10)	33/67	139.7	14.88	23	46.3	10.08
Sample(11)	33/67	154.1	16.75	23	47.25	10.887
Sample(12)	33/67	177.5	20.32	23.8	48.1	10.247

(Note: above data are all measured except areal density)

The similar steps of calculations in above calculations of CF/PET 0/100 nonwovens are used in the calculation of CF/PET 33/67.

The weight of scrim, PET and CF fibers of these nonwovens were calculated according to Equation (15), (16), and (17) respectively, the correspondent values of variables were substituted into the equations and the calculation results are shown in Table 7-17.

Real volume of fibers, apparent volume, volumetric fraction of fibers and weight average diameter of fibers d_f of these nonwovens were calculated according to Equation

(18), (19), (20) and (21) respectively, the correspondent values of variables were substituted into the equations and the calculation are shown in Table 7-18.

Equation (8) and d_R ($0.2\mu\text{m}$) were used to calculate interception parameter, the correspondent values of variables were substituted into the equation and the calculation results are shown in Table 7-19.

A and B of these nonwovens were calculated according to Equation (13) Equation (14) respectively, the correspondent values of variables were substituted into the equation and the calculation results are shown in Table 7-20.

The penetration of these nonwovens, relative error of calculated penetration (%) were calculated according to Equation (12) and (22), the correspondent values of variables were substituted into the equations and the calculation results are shown in Table 7-21.

The measured filtration efficiency, calculated filtration efficiency and its relative error of calculated filtration efficiency of the nonwovens were calculated according to Equation (23) and (24), the correspondent values of variables were substituted into the equations and the calculation results are shown in Table 7-22

Table 7-17 Weight of scrim, PET and CF fibers of CF/PET 33/67 nonwovens

	CF/PET	Weight of scrim (g)	Weight of PET staple fibers (g)	Weight of CF fibers (g)
Sample(20)	33/67	3.50	3.74	1.84
Sample(19)	33/67	3.66	4.56	2.24
Sample(10)	33/67	3.61	7.55	3.72
Sample(11)	33/67	3.68	8.76	4.31
Sample(12)	33/67	3.88	11.01	5.43

Table 7-18 Volume fractions of fibers and average diameter of all fibers in CF/PET 33/67 nonwovens

	CF/PET	Real volume of fibers (cm ³)	Apparent volume of fibers (cm ³)	Volume fraction of fibers 100 α (%)	Diameter of nonwoven fibers d _f (μm)
Sample(20)	33/67	7.032	510.7	1.38	13.380
Sample(19)	33/67	8.180	600.8	1.36	13.250
Sample(10)	33/67	11.976	1073.4	1.12	12.862
Sample(11)	33/67	13.561	1183.1	1.15	12.780
Sample(12)	33/67	16.577	1173.1	1.41	12.675

Table 7-19 Interception parameters of CF/PET 33/67 nonwovens

	R
Sample(20)	0.01495
Sample(19)	0.01509
Sample(10)	0.01555
Sample(11)	0.01565
Sample(12)	0.01578

Table 7-20 Values of A and B in CF/PET 33/67 nonwovens.

	CF/PET	A	B
Sample(20)	33/67	0.0001573	0.6565
Sample(19)	33/67	0.0001598	0.7378
Sample(10)	33/67	0.0001586	1.1450
Sample(11)	33/67	0.0001620	1.2583
Sample(12)	33/67	0.0001768	1.4521

Table 7-21 Calculation results of the penetration and its relative error of CF/PET 33/67 nonwovens

	Calculated penetration	Measured Penetration (%)	Relative calculated penetration error (%)
Sample(20)	0.9404	96.9	-2.95
Sample(19)	0.9358	96.55	-3.07
Sample(10)	0.9231	93.6	-1.38
Sample(11)	0.9163	91.7	-0.07
Sample(12)	0.8910	90.6	-1.65

Table 7-22 Calculation results of the filtration efficiency of CF/PET 33/67 nonwovens

	Calculated filtration efficiency	Measured filtration efficiency (%)	Relative Error of calculated filtration efficiency (%)
Sample(20)	0.0596	3.1	92.3
Sample(19)	0.0642	3.45	86.0
Sample(10)	0.0769	6.4	20.2
Sample(11)	0.0837	8.3	0.8
Sample(12)	0.1090	9.4	15.9

Similarly, the measured basic physic data of CF/PET 50/50 nonwovens are shown in Table 7-3. Similar calculation steps to CF/PET 33/67 nonwovens were used to calculated for the weight of scrim, weight of PET staple and CF fibers, interception parameter, values of A and B, the calculated penetration and its relative error, and the calculated filtration efficiency and its relative error. The calculation results are shown in Table 7-23 to 7-28.

Table 7-23 Weight of scrim, PET and CF fibers of CF/PET 50/50 nonwovens

	CF/PET	Weight of scrim (g)	Weight of PET staple fibers (g)	Weight of CF fibers (g)
Sample(22)	50/50	3.06	2.57	2.58
Sample(21)	50/50	3.41	3.46	3.46
Sample(1)	50/50	3.67	5.14	5.13
Sample(2)	50/50	3.63	6.23	6.24
Sample(3)	50/50	3.79	7.55	7.56

Table 7-24 Volume fractions of fibers and average diameter of all fibers in CF/PET 50/50 nonwovens

	CF/PET	Real volume of fibers (cm ³)	apparent volume of fibers (cm ³)	Volume fraction of fibers 100 α (%)	Diameter of nonwoven fibers d _f (μm)
Sample(22)	50/50	6.730	458.332	1.47	12.616
Sample(21)	50/50	8.591	577.415	1.49	12.415
Sample(1)	50/50	11.853	822.226	1.44	12.098
Sample(2)	50/50	13.861	992.059	1.40	11.917
Sample(3)	50/50	16.404	1360.024	1.21	11.798

Table 7-25 Interception parameters of CF/PET 50/50 nonwovens

	R
Sample(22)	0.01585
Sample(21)	0.01611
Sample(1)	0.01653
Sample(2)	0.01678
Sample(3)	0.01695

Table 7-26 Values of A and B in CF/PET 50/50 nonwovens.

	A	B
Sample(22)	0.0001808	0.7638
Sample(21)	0.0001876	0.8887
Sample(1)	0.0001953	1.1676
Sample(2)	0.0001991	1.4022
Sample(3)	0.0001932	1.6027

Table 7-27 Calculation results of the penetration and its relative error of CF/PET 50/50 nonwovens

	Calculated penetration	Measured Penetration (%)	Relative calculated penetration error (%)
Sample(22)	0.9402	98.00	-4.06
Sample(21)	0.9332	98.00	-4.77
Sample(1)	0.9215	92.15	0.00
Sample(2)	0.9131	89.65	1.85
Sample(3)	0.9188	89.35	2.83

Table 7-28 Calculation results of the filtration efficiency of CF/PET 50/50 nonwovens

	Calculated filtration efficiency	Measured filtration efficiency (%)	Relative Error of calculated filtration efficiency (%)
Sample(22)	0.0598	2.00	199.0
Sample(21)	0.0668	2.00	233.9
Sample(1)	0.0785	7.85	0.0
Sample(2)	0.0869	10.35	-16.0
Sample(3)	0.0812	10.65	-23.7

The measured basic physical data of CF/PET 67/33 and 75/25 nonwovens are shown in Table 7-29 and 7-3. Similarly to CF/PET 0/100 nonwovens, their necessary parameters for calculated penetration were calculated and shown in Table 7-30 to 7-35 and Table 7-36 to 7-41.

Table 7-29 Measured basic physical data of CF/PET 67/33 nonwovens

	CF/PET	Areal density (g/m ²)	wt(real)(g)	Width (cm)	Length(cm)	Thickness (mm)
Sample(24)	67/33	87.72	8.43	23.1	41.6	4.5106
Sample(23)	67/33	98.76	9.42	23.15	41.2	5.3193
Sample(4)	67/33	124.9	13.88	23.65	47	8.33
Sample(5)	67/33	144.4	15.91	23.7	46.5	8.5673
Sample(6)	67/33	158.3	17.77	23.15	4835	8.458

(Note: above data are all measured except areal density)

Table 7-30 Weight of scrim, PET and CF fibers of CF/PET 67/33 nonwovens

	CF/PET	Weight of scrim (g)	Weight of PET staple fibers (g)	Weight of CF fibers (g)
Sample(24)	67/33	3.255	1.708	3.467
Sample(23)	67/33	3.230	2.043	4.147
Sample(4)	67/33	3.765	3.338	6.777
Sample(5)	67/33	3.733	4.018	8.159
Sample(6)	67/33	3.803	4.609	9.358

Table 7-31 Volume fractions of fibers and average diameter of all fibers in CF/PET 67/33 nonwovens

	CF/PET	Real volume of fibers (cm ³)	apparent volume of fibers (cm ³)	Volume fraction of fibers 100 α (%)	Diameter of nonwoven fibers d _f (μm)
Sample(24)	67/33	7.230	433.45	1.668	11.981
Sample(23)	67/33	8.220	507.34	1.620	11.726
Sample(4)	67/33	12.458	925.92	1.345	11.303
Sample(5)	67/33	14.483	944.16	1.534	11.087
Sample(6)	67/33	16.304	949.64	1.717	10.966

Table 7-32 Interception parameters of CF/PET 67/33 nonwovens

	R
Sample(24)	0.01696
Sample(23)	0.01757
Sample(4)	0.01842
Sample(5)	0.01880
Sample(6)	0.01905

Table 7-33 Values of A and B in CF/PET 67/33 nonwovens.

	A	B
Sample(24)	0.0002099	0.8135
Sample(23)	0.0002167	0.9517
Sample(4)	0.0002183	1.2803
Sample(5)	0.0002375	1.5334
Sample(6)	0.0002529	1.7163

Table 7-34 Calculation results of the penetration and its relative error of CF/PET 67/33 nonwovens

	Calculated penetration	Measured Penetration (%)	Relative calculated penetration error (%)
Sample(24)	0.9377	93.7	0.07
Sample(23)	0.9325	96.0	-2.86
Sample(4)	0.9336	90.7	2.93
Sample(5)	0.9088	89.45	1.60
Sample(6)	0.8838	88.7	-0.37

Table 7-35 Calculation results of the filtration efficiency of CF/PET 67/33 nonwovens

	Calculated filtration efficiency	Measured filtration efficiency (%)	Relative Error of calculated filtration efficiency (%)
Sample(24)	0.0623	6.30	-1.1
Sample(23)	0.0675	4.00	68.7
Sample(4)	0.0664	9.30	-28.6
Sample(5)	0.0912	10.55	-13.6
Sample(6)	0.1162	11.30	2.9

Table 7-36 Weight of scrim, PET and CF fibers in CF/PET 75/25 nonwovens

	CF/PET	Weight of scrim (g)	Weight of PET staple fibers (g)	Weight of CF fibers (g)
Sample(25)	75/25	3.53	1.28	3.84
Sample(26)	75/25	3.32	1.57	4.74
Sample(7)	75/25	3.74	2.63	7.88
Sample(8)	75/25	3.66	3.09	9.26
Sample(9)	75/25	3.73	3.57	10.71

Table 7-37 Volume fractions of fibers and average diameter of all fibers in CF/PET 75/25 nonwovens

	CF/PET	Real volume of fibers (cm ³)	apparent volume of fibers (cm ³)	Volume fraction of fibers 100 α (%)	Diameter of nonwoven fibers d _f (μm)
Sample(25)	75/25	7.800	364.846	2.138	11.791
Sample(26)	75/25	8.866	436.037	2.033	11.382
Sample(7)	75/25	13.471	719.564	1.872	10.858
Sample(8)	75/25	15.297	759.806	2.013	10.638
Sample(9)	75/25	17.324	861.660	2.011	10.501

Table 7-38 Interception parameters of CF/PET 75/25 nonwovens

	R
Sample(25)	0.01696
Sample(26)	0.01757
Sample(7)	0.01842
Sample(8)	0.01880
Sample(9)	0.01905

Table 7-39 Values of A and B in CF/PET 75/25 nonwovens.

	A	B
Sample(25)	0.0002383	0.8268
Sample(26)	0.0002506	1.0346
Sample(7)	0.0002665	1.4566
Sample(8)	0.0002855	1.7294
Sample(9)	0.0002928	1.9466

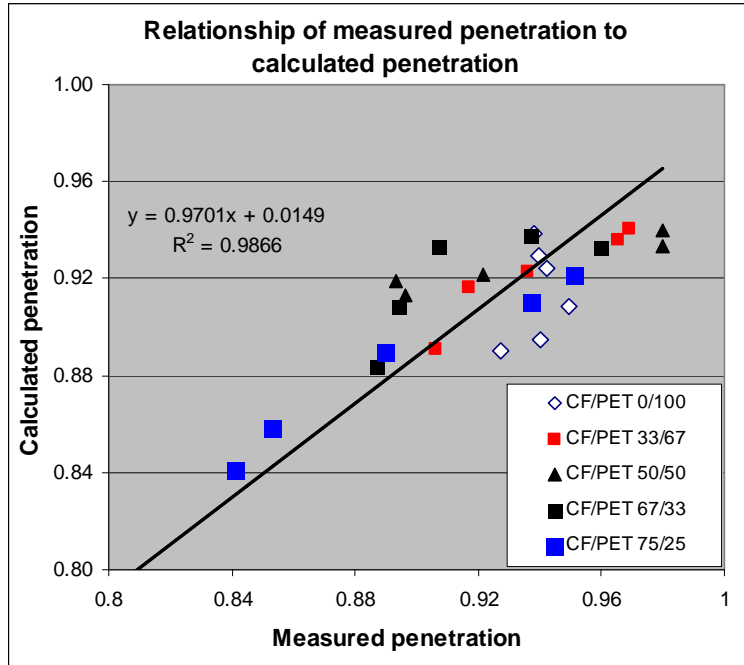
Table 7-40 Calculation results of the penetration and its relative error of CF/PET 75/25 nonwovens

	Calculated penetration	Measured Penetration (%)	Relative calculated penetration error (%)
Sample(25)	0.9215	95.1	-3.10
Sample(26)	0.9103	93.7	-2.85
Sample(7)	0.8895	88.95	0.00
Sample(8)	0.8580	85.3	0.59
Sample(9)	0.8410	84.1	0.00

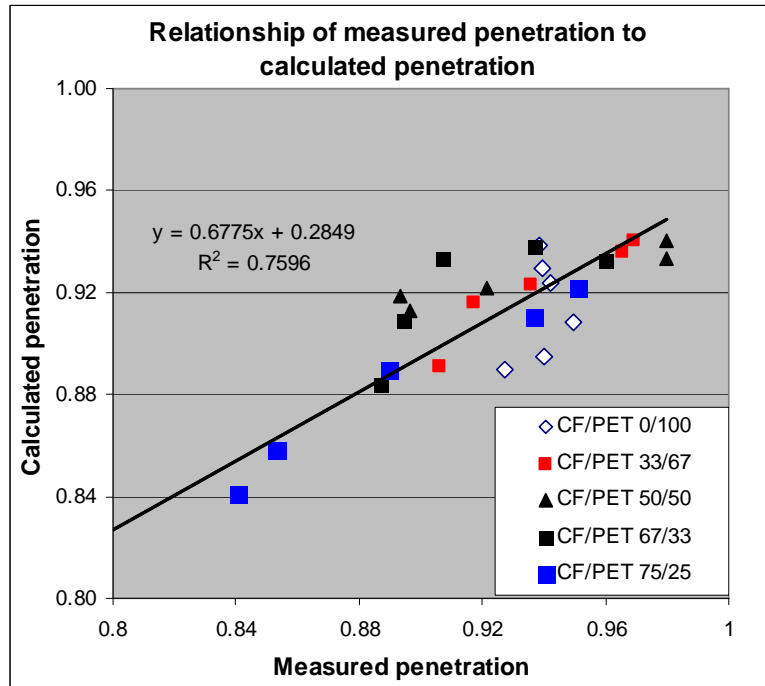
Table 7-41 Calculation results of the filtration efficiency of CF/PET 75/25 nonwovens

	Calculated filtration efficiency	Measured filtration efficiency (%)	Relative Error of calculated filtration efficiency (%)
Sample(25)	0.0785	4.9	60.2
Sample(26)	0.0897	6.3	42.4
Sample(7)	0.1105	11.05	0.0
Sample(8)	0.1420	14.7	-3.4
Sample(9)	0.1590	15.9	0.0

From all above, the penetration of all of the samples had been calculated; the relationship of the measured penetration to the calculated penetration is shown in Figure 7-1. Theoretically, if the calculated penetration of nonwovens matched the measured penetration well, the slope of the line should be 1. From the figure it can be seen that, if the trend line of the data included the penetration zero, the calculated penetration of nonwovens really matched the measured penetration very well. If the trend line was drawn only in the range of the measured penetration, from a thorough point of view, the calculated penetration was a little smaller than the measured.



(a) The trend line included (0, 0).



(b) The trend line included (0.8, 0.8).

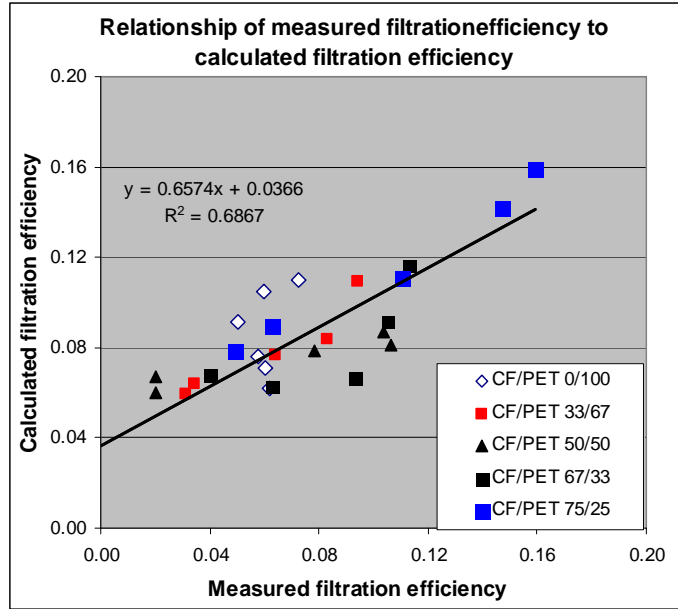
Figure 7-1 Relationship of measured penetration to calculated penetration

The relationship of the measured filtration efficiency to the calculated filtration efficiency of the nonwovens was also obtained and shown Figure 7-2. Similarly, if the calculated filtration efficiency of nonwovens matched the measured filtration efficiency well, the slope of the line should be 1. From the figure it can be seen that if the trend of the data was from the filtration efficiency 0, the calculated filtration efficiency of nonwovens matched the measured filtration efficiency well. If the trend was only studied in the range of the measured filtration efficiency, from the thorough point of view, the calculated filtration efficiency was a little smaller than the measured.

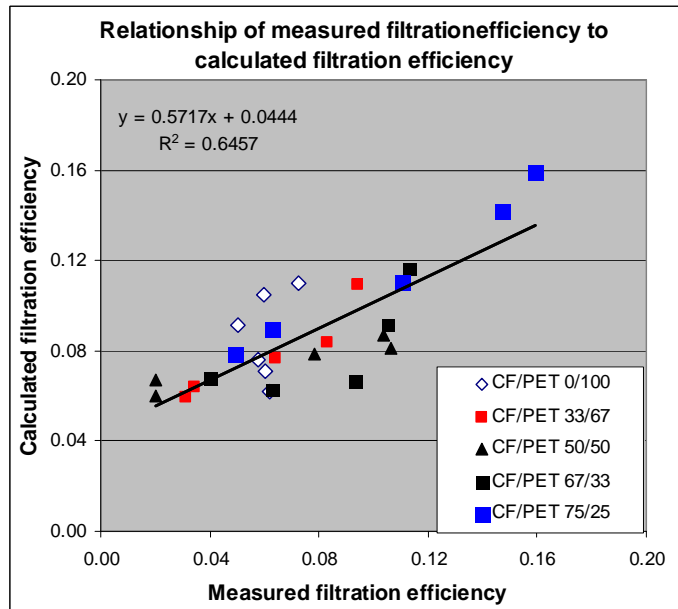
7.4 Conclusion

An analytical model to calculate penetration and initial filtration efficiency of CF air filter was developed. Constants for it were derived from experimental results and used to calculate penetration and initial filtration efficiency for remaining CF nonwovens.

From the calculated results, it can be seen that the calculated penetration of CF nonwoven was good and relative error was small but the calculated filtration efficiency was not good and their relative error was very large except those samples close to the samples that were used to calculate constants. It seems that the filtration efficiency needs a new way to calculate, but it is not true. The error is so big maybe because the calculated filtration efficiency was divided by a small number.



(a) The trend line included the point (0, 0)



(b) The trend line only included the measured data

Figure 7-2 Relationship of Measured filtration efficiency to calculated efficiency of CF nonwovens

7.5 Reference

- [1] N. C. Davies: Air Filtration. Academic Press, London 1973.
- [2] D. T. Shaw: Fundamentals of Aerosol Science, Wiley, New York, 1978.
- [3] R. C. Brown: An Integrated Approach to the Theory and Applications of Fibrous Filters, Pergamon Press, New York 1993
- [4] Lange, R. et al, Predicting the collection efficiency of agglomerates in fibrous filters, *Part. Part. Syst. Charact.*, 16(2), 1999, p60-65
- [5] Stechkin, I.B and Fuchs, N. A., Studies on fibrous aerosol filters-I. calculation of diffusional deposition of aerosols in fibrous filters, *Ann. Occup. Hyg.*, 9(1), 1966, p59-64
- [6] Wang, Q.; Maze, B; Vahedi Tafreshi, H.; Rourdeyhimi, B.; Approaches for Predicting Collection Efficiency of Fibrous Filters, *Journal of Textile and Apparel, technology and management*, 5(2), summer 2006, p1-6
- [7] Kirsch, A. A.; Stechkina, I. B.; The theory of aerosol filtration with fibrous filters, in D. T. Shaw (ed.): Fundamentals of Aerosol Science, Wiley, New York 1978, Chap. 4, p165-256.